Jacking Force Prediction: An Interface Friction Approach Based On Pipe Surface Roughness

A Dissertation
Presented to
The Academic Faculty

by

Kimberlie Staheli

In Partial Fulfillment
of the Requirements for the Degree
Doctor of Philosophy in the
School of Civil and Environmental Engineering

Georgia Institute of Technology
August, 2006

Jacking Force Prediction: An Interface Friction Approach
Based On Pipe Surface Roughness

Approved by:

Dr. J. David Frost, Advisor
School of Civil and Environmental Engineering
Georgia Institute of Technology

Dr. G. Wayne Clough
President
Georgia Institute of Technology

Dr. Paul W. Mayne
School of Civil and Environmental Engineering
Georgia Institute of Technology

Dr. William F. Marcuson, III
Director Emeritus
Geotechnical Laboratory
Engineer Research and Development Center, Waterways Experiment Station

Dr. Susan E. Burns
School of Civil and Environmental Engineering
Georgia Institute of Technology

Date Approved: June 29, 2006

To two people of paramount importance in my life: Harold Douglas Schultz, who was with me when I began this journey, and Allison Rose Louch, who was with me when I finished. The desire to begin, the drive to continue, and the strength to complete, are because of you.

ACKNOWLEDGMENTS

This research would not have been possible without the tremendous support of many kind people. I am very grateful to Dr. David Frost who provided me the opportunity to work on this topic that I have always loved and wanted to pursue. Your dedication, direction, and countless hours of work will not be forgotten. I appreciate your friendship and look forward to working with you in the future.

David Bennett is deserving of many thanks as he was the first to convince me that a PhD was an achievable goal. Your friendship, encouragement, and support ultimately lead to the completion of this journey. Thank you for sharing the long conversations about interface friction, total unit weight, Terzaghi, normal forces, jacking force as a function of the diameter squared (ok—you're right!) and the Ramblin Wreck vs. the Illinois Mafia. Thank you for never letting me give up on this dream—even when I though I couldn't make it, you knew I could.

I would like to thank Dr. William F. Marcuson III for adopting me as an honorary daughter and guiding me through this process. You will never know how much you have inspired me throughout these years. I appreciate every ounce of energy that you have given me. You are a very special person.

I would like to thank Dr. G. Wayne Clough for serving on my committee. I have tremendous respect for your work in the field of tunneling and know that your time is at a premium. I am honored that you would serve on my committee. You are truly an inspiration to the civil engineering community and one of my heroes.

I would like to thank the other members of my committee, Dr. Paul Mayne and Dr. Susan Burns. Your kindness, support, and willingness to serve on my committee are greatly appreciated.

I am indebted to Dave Mathy for providing the data, project notes, and geotechnical information for the Alvarado Boulevard projects containing case history information on microtunneling with Polycrete Pipe. My case history data would not have been complete without this information and I am truly appreciative.

I would like to thank all of the people who helped with the logistics of preparing my dissertation from the West Coast while attending school on the East Coast including Amy Hansen, Lynn Sexton, and Shelly Russell. Your kindness will not be forgotten.

I want to sincerely thank Sue Staheli for nursing me through the best and worst of times, Cason Adams for the strength I found through you, and Dr. Richard Ellenbogen for saving my life. Finishing my PhD would not have been possible without you. They say there are angels masquerading on this earth as people…

Finally, this would not have been possible without the support of my family. Steve, your unconditional support will forever hold a place in my heart. To my parents, Jan Staheli, Allen Staheli, and Merilyn Staheli; my sister and brother, Julie and Sean; my niece and nephew, Shelby and Derek; and my beautiful daughter, Allison Rose; thank you for your love, support, encouragement, and thank you for sharing my dreams.

TABLE OF CONTENTS

Page

LIST OF TABLES

Page

LIST OF FIGURES

LIST OF SYMBOLS AND ABBREVIATIONS

R_a	average roughness
R_n	normalized roughness factor
μ	coefficient of friction
δ	interface friction angle
σ_v	vertical stress
σ_h	horizontal stress
γ	total soil unit weight
φ	soil internal friction angle
D	diameter
r	radius
K	coefficient of earth pressure
c'	cohesion intercept
kPa	kilo-Pascals
u	pore pressure
ψ	soil dilation angle
h	height of soil over the pipeline
L	pipeline or tunnel length
JF_{fric}	frictional component of jacking force
μ_{int}	interface friction coefficient
$\mu_{int.lube}$	lubricated interface friction coefficient
φ_r	residual friction angle
φ_p	peak friction angle
psi	pounds per square inch
psf	pounds per square foot
tsf	tons per square foot

SUMMARY

This study focuses on the identification of the mechanisms that control interface shearing between pipes and granular materials and the development of a model to predict jacking forces. The surface roughness of six common jacking pipe materials, including Hobas (Centrifugally Cast Fiber Reinforced Polymer Mortar), Polycrete (Polymer Concrete), Permalok Steel (Rolled Steel with a Painted Surface), Wet Cast Concrete, Concrete manufactured with the Packerhead method, and Vitrified Clay pipe, have been characterized to determine the role of surface roughness on the mechanism of shearing at the soil-pipe interface.

Interface shear tests were performed between pipe materials and two characteristically different granular soils: Ottawa 20/30 sand and Atlanta Blasting sand. Shearing behavior between the sands and the pipe materials was evaluated to determine the mechanisms of shearing on materials with varied roughness values. Interface friction values were established for the pipe materials and soils.

Field research on fourteen case histories of microtunneling and pipe jacking projects was presented. Pertinent project details were provided including pipe materials, site geometry, geotechnical information, construction sequencing, lubrication injection, and jacking force records. Jacking force records for each project were separated into isolated segments along the alignment to analyze jacking stresses.

Unlubricated segments of the microtunneling drive records were analyzed to compare interface friction values measured in the laboratory and jacking force measurements collected in the field. From this information, normal stresses acting on the

pipelines in the field were back-calculated. A model was developed to predict normal stresses acting on the pipeline, based on Terzaghi's Arching Theory, which closely approximated the normal stresses in the field.

A predictive model for calculating jacking forces in unlubricated soil was presented. This model used interface friction coefficient values for different pipe materials based on laboratory values from interface shearing tests. This model was compared to other models currently available for predicting the frictional component of jacking forces.

An analysis of the effects of lubrication on jacking forces was presented. Segments of jacking records were back-analyzed to determine how the interface friction coefficient changed once lubrication was applied to the pipeline. Two types of lubrication strategies were identified and predicted lubricated jacking forces were shown.

A step-by-step guide for using the predictive model to calculate jacking forces was presented. Recommendations were made on applying the model for design applications and estimating lubricated interface friction values. Recommendations for further research were provided.

CHAPTER 1

INTRODUCTION

Microtunneling is a closed-face pipe jacking operation where positive face stabilization is provided to the excavation by pressurized slurry. This feature allows tunneling below groundwater or in unstable soil conditions without risk of soil settlement, soil heave, or loss of stability. Excavated material enters into the face of the microtunneling machine as the machine is advanced forward. The excavated material is mixed with clean slurry and is pumped to the surface for muck removal and soil separation. The microtunneling machine is operated from a control container located on the ground surface and all machine functions are operated by remote control. No personnel are required in the tunnel during pipe jacking operations. Microtunneling is steerable and guided with a laser or theodolite system. Pipe installation tolerances of plus or minus one inch over one thousand feet of length are achievable with microtunneling methods. Figure 1.1 shows two different microtunneling machine head configurations,

Figure 1.1. Microtunnel Cutterhead Configurations. Combination Rock Cutter (left); Soft Ground Head (right)

one equipped with rock cutting tools for cobble and boulder conditions, and the other equipped with picks and spades for soft ground soil conditions.

Microtunneling takes place from within a jacking or launch shaft constructed to the designed pipeline depth. A hydraulic jacking unit located in the jacking shaft propels the tunneling machine and pipe string from the jacking shaft to the reception or retrieval shaft, as shown in Figure 1.2.

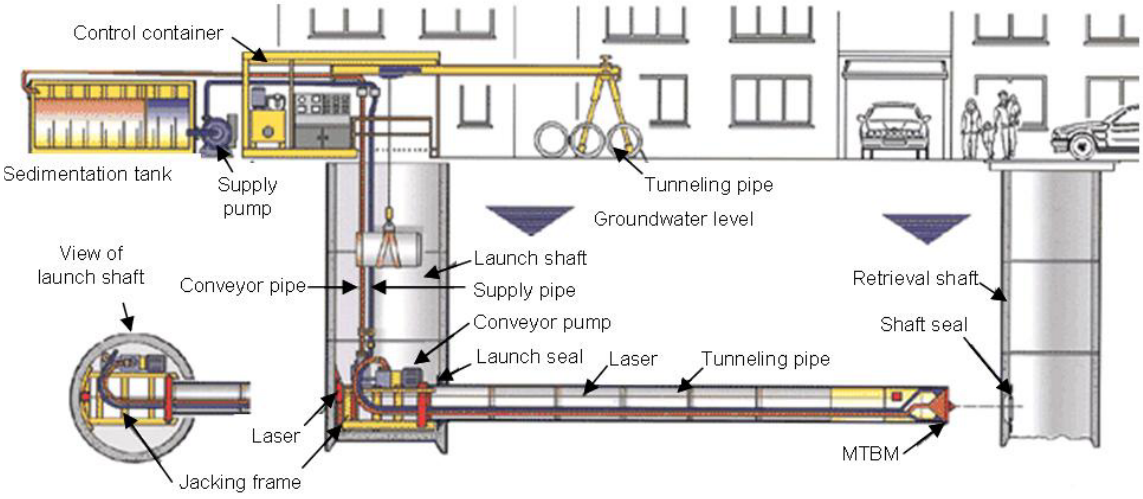

Figure 1.2. Schematic of Microtunneling Operation (Herrenknecht, 2006).

The total jacking force required to propel the tunneling machine and pipe sections forward must overcome forces associated with face pressure on the machine and friction on the machine and pipeline. The face pressure force acts at the front of the machine and originates from ground water and earth pressures. The frictional force develops between the surrounding soil and the exposed outer surface area of the tunneling machine and installed pipe sections. The face pressure component relates to the depth of burial and is estimated based on the soil and groundwater conditions at the site. The face pressure

component of the jacking force remains theoretically constant if the depth of soil over the pipeline is constant. However, the frictional force increases as the drive length increases. As a result, longer drives require greater jacking forces.

Microtunneling is a method of tunneling and is not limited by size. Typical microtunneling diameters range from 24 to 144 inches. The microtunnel machine excavates a slightly larger diameter hole than the diameter of the installed pipe sections. The distance between the maximum excavated diameter and the outer diameter of the installed pipe sections is referred to as the over cut or annular space. Over cuts of between 0.75 and 2.0 inches on the diameter (i.e. 0.375 and 1.0 inch on the radius) are typical. The over cut is necessary to reduce frictional forces, facilitate steering of the tunneling machine, and to allow injection of lubrication into the annular space if required.

Once the machine is jacked into the reception shaft, the microtunneling machine is removed, leaving the pipeline installed along the alignment. Any necessary pipe connections are made and the shafts are typically backfilled and properly abandoned.

1.1 Motivation for Study

A number of practitioners and researchers have analyzed jacking forces on microtunneling and pipe jacking projects in order to increase the understanding of the mechanisms that control these forces, and to establish a means of predicting jacking forces. These studies have been largely based on observations of ground behavior and empirical data and have taken place in Germany, Japan, the UK, and the US. The work completed to date has advanced the practice and led to a better understanding of jacking force behavior. However, the results of the previous studies have produced highly mixed results, and have yet to provide accurate jacking force predictions on projects with

varying parameters, such as different pipe materials, soil conditions, and installation depths.

Concurrent with jacking force studies, other practitioners and researchers have been investigating interface friction behavior. The surface roughness and hardness of different materials was shown to impact the interface friction between the material and soil at the interface. Many studies have focused on characterizing the surface roughness of a material and determining the interface strength mechanisms based on the surface topography of the material. Meanwhile, an interface shear device capable of performing direct shear tests on curved surfaces was developed at Georgia Institute of Technology (Iscimen, 2004).

Although jacking pipe materials have dramatically different surface roughness characteristics, the advances in interface friction and the effects of surface roughness have not been applied to pipe jacking. There is an opportunity for a better understanding of the mechanisms controlling frictional behavior during pipe jacking by examining the interface between pipes and soil and applying the advances in interface friction mechanisms to jacking force behavior. With an enhanced knowledge of the mechanism that controls shearing at the interface, the normal stresses developed during jacking operations can be evaluated. By determining the frictional mechanisms at the interface and understanding the normal stresses acting on the pipe during pipe jacking, a method to control and predict jacking forces can be developed.

1.1.1 Importance of Predicting Jacking Forces

Predicting jacking forces is important for planning, design, and construction phases of microtunneling projects. The construction of the microtunneling shafts has a

significant economic impact on the total cost of the pipeline installation project. For pipes with diameters less than 36-inches the maximum length of the tunneling drive is determined by the maximum jacking capacity and this, in turn, dictates shaft spacing. The engineer must predict the jacking forces to determine the maximum spacing of the jacking shafts during the design process. Often the microtunneling alternative will be compared to the open-cut alternative. The microtunneling alternative may be eliminated as a feasible construction alternative from a cost perspective if the number of shafts cannot be minimized.

In pipe diameters greater than 36-inches, intermediate jacking stations (IJS) can be used, as shown in Figure 1.3. An IJS is a series of hydraulic jacks that can be incorporated into the pipeline at a distance behind the microtunneling machine. The hydraulic jacks in the IJS propel the machine and the pipes between the machine and the IJS forward. The main jacks located in the jacking shaft are then activated to propel the pipes that have been installed after the IJS. In this fashion, the IJS serves to "inchworm" the pipe-string forward, effectively isolating the frictional component of the jacking force in particular sections of the pipeline.

IJS shells are fabricated to the exact outer diameter of the jacking pipe and are machined to exert the thrust from the hydraulic jacks to the load-bearing end of the jacking pipe. IJS's are long lead-time items and must be ordered well in advance of construction. The contractor must predict the jacking forces to determine the number of IJS's needed on any particular tunnel drive.

Figure 1.3. Intermediate Jacking Station (IJS)

Microtunneling jacking shafts must also be structurally designed to withstand the jacking forces. As the main jacks push the microtunneling machine and pipeline into the ground, a thrust wall, located behind the main jacking system, distributes the reactionary force into the walls of the shaft and the ground surrounding the shaft. If the shaft is not designed adequately to support the jacking forces, shaft failure can occur. Shaft failure is a serious and significant problem on microtunneling projects in the United States today that results in a large number of construction claims, which have significant monetary value. Jacking force predictions are therefore crucial to adequately design thrust blocks and jacking shafts to avoid shaft failures.

1.1.2 Understanding Mechanisms that Govern Jacking Forces

As previously noted, jacking forces are comprised of two components: the face pressure force and the frictional force, as schematically shown in Figure 1.4. The face pressure force is made up of the earth and fluid pressure acting on the face of the

machine. Microtunneling machines are designed with the intent to be operated in a "pressure-balance" fashion. The operator pumps pressurized slurry to the face of the machine to counterbalance the groundwater pressure. Further, the rate of advance of the machine theoretically balances the excavation rate so that neither settlement nor heave of the ground surface occurs. For these conditions to be met, the face pressure force acting on the machine remains between the active and passive earth pressure acting over the area of the face of the machine. However, in practice, the face pressure force is highly dependent on the operation of the machine. Operators tend to find a balance between maximizing production rates without expending all of the available torque required to turn the cutting wheel at the face of the machine.

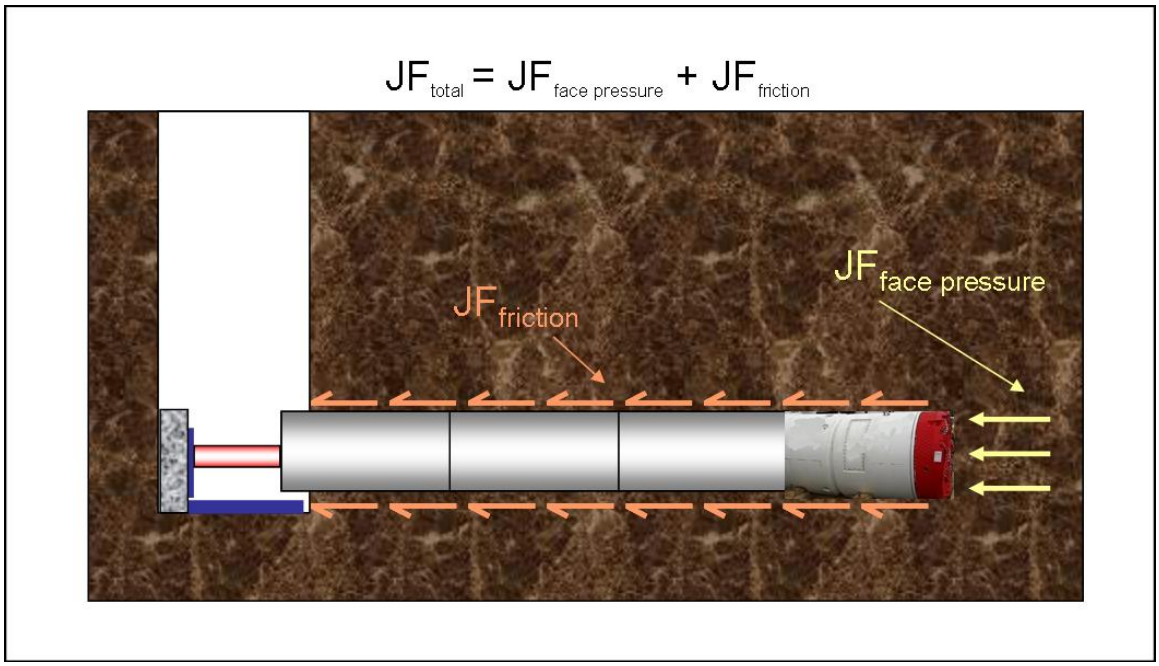

Figure 1.4. Microtunneling Machine and Pipe Jacking Operation Illustrating the Components of Jacking Forces.

If the operational speed is too fast, face pressure forces will increase, resulting in increased torque on the head causing the machine to stall. If the operational speed is too slow, torque readings will be low and material will tend to slough into the machine resulting in over-excavation. This has the potential to manifest as settlement at the ground surface, depending on ground conditions and depth of cover.

A great amount of effort has been spent trying to predict face pressure forces. In general, field experience shows that face pressure forces represent a very low percentage of the overall jacking force. They are also the primary indicator used by the machine operator to determine advance rates. As such, the operator has the ability, by adjusting the machine speed, to control the face pressure force. Therefore, it may not be worthwhile to further refine these predictions. It is noteworthy that on most projects in the United States, production goals drive the manner in which the project is conducted. Therefore, most operators tend to drive the machine as fast as possible without pushing the machine beyond the reasonable limits of the torque capacity, causing the machine to stall. As a result, the face pressure acting on the face of the machine is closer to the active than the passive earth pressure.

Frictional forces on the microtunneling machine and pipeline have been much less understood than face pressure forces, although there is general agreement that the frictional component of the jacking forces should follow the general formula,

$$JF_{friction} = \mu \cdot N \qquad (1.1)$$

where μ is the coefficient of friction and N is the normal force. There is debate over the appropriate values for the coefficient of friction and the method used to calculate the normal force. The vast majority of the work that has been performed on microtunneling

jacking forces has been at a macro-scale and has focused on evaluation of field data, taking an empirical approach to developing models to determine jacking forces.

To estimate the friction coefficients, the vast majority of the models focus on the friction angle of the soil (ϕ'), and use some type of reducing factor on the soil internal friction angle to develop the friction coefficient (from ¼ ϕ' to ¾ ϕ'). Others have published values for interface friction coefficients between specific pipe materials and specific soils. However, these published coefficients of friction are based on a limited number of field case history evaluations and do not identify the mechanism of shearing at the interface. Since soil internal friction angles have a relatively small range, values chosen in most of the models do not have a significant impact on the overall calculation of jacking force compared to the accuracy of the calculation method (on the order of 15 to 25 percent).

Significant variation in jacking force calculation models have existed in the calculation of the normal forces. Very little is understood about the mechanisms that control the arching in the soil when pipe jacking is occurring. As a result, there is a wide range of approaches used to calculate the normal force in jacking force models that have been developed to date. Most of the models have some base in Terzaghi's Arching Theory; however, some do not allow for soil arching at all, and base the normal force on the soil unit weight and the depth of cover.

Since the mechanisms surrounding both the friction and the normal force are not well understood, until one of these variables is better understood, the relative influence of the other will remain unknown.

1.2 Scope of Dissertation

This dissertation presents the results of a study focused on the identification of the mechanisms that control interface shearing between jacking pipes and granular materials and the subsequent development of a model for predict jacking forces. Granular materials were chosen as the focus of the study because in practice the problems that manifest as a result of high jacking forces generally occur in granular soils. Although many pipe jacking project occur in clay soils, jacking forces on projects in clay soils are typically much lower than in granular materials and as such, the need to accurately predict the jacking forces is much less critical.

Prior to performing the research, a review of previous work was conducted. This work, including studies on interface friction, normal stress distributions around tunnels, and the prediction and control of jacking forces is summarized in Chapter 2. Focus was placed on current research involving microtunneling projects and the development of models for predicting jacking forces.

The surface roughness of six common jacking pipe materials have been characterized and examined to determine the role of surface roughness on the mechanism of shearing at the soil-pipe interface in Chapter 3. Interface shear tests were performed between common jacking pipe materials and two characteristically different granular soils: Ottawa 20/30 sand and Atlanta Blasting sand. Shearing behavior between the sands and the pipe materials at the interface was evaluated to observe the mechanisms of shearing on materials with varied roughness values. Interface friction values were determined for a variety of jacking pipe materials including Hobas (CCFRPM, Centrifugally Cast Glass-Fiber Reinforced Polymer Mortar Pipe), Permalok Steel, Polycrete (polymer concrete),

Vitrified Clay, Wet Cast Concrete, and Packerhead Concrete (a dry casting method) for varying residual soil friction angles.

Chapter 4 introduced and described a number of case histories of microtunneling and pipe jacking projects. For each case history, pertinent project details were provided including geotechnical information, construction details, lubrication details, depth of the pipeline, pipe materials, and jacking force records. The projects included microtunneling and pipe jacking projects constructed with Hobas, Permalok Steel, Polycrete, Wet Cast Concrete, and Packerhead Concrete. Jacking force records for each project were separated into isolated segments along the alignment to further analyze jacking stresses.

Unlubricated segments of the microtunneling drive records were analyzed to compare interface friction values measured in the laboratory and jacking force measurements collected in the field in Chapter 5. From this information, normal stresses acting on the pipelines in the field were back-calculated

A predictive model for calculating jacking forces in unlubricated sections was presented in Chapter 5. This model used interface friction coefficient values for different pipe materials based on laboratory values from interface shearing tests. The model uses a normal force calculation method based on Terzaghi's Arching Theory and a comparison of laboratory and case history data. The new model which closely approximated the normal stresses that were back-calculated using the field data and the laboratory values of the interface friction coefficient measured between the pipe materials and the soils in the laboratory. This model was also compared to other models currently available. A parametric study was presented showing the relative effects of each input variable in the predictive model.

Chapter 6 presented an analysis of the effects of lubrication on jacking forces. Sections of jacking records were analyzed to determine how the interface friction coefficient changed once lubrication was applied to the pipeline. Two types of lubrication strategies were identified and resulting lubricated jacking forces identified.

Chapter 7 summarizes the results of the study, including a step-by-step guide for using the predictive model to calculate jacking forces. Recommendations were made for applying the model for future design applications and estimating lubricated interface friction values. Recommendations for further research were provided.

CHAPTER 2

MECHANISMS CONTROLING JACKING FORCES: CURRENT UNDERSTANDING

2.1 Introduction

A number of researchers have conducted both laboratory and field studies to further the understanding of the development of jacking forces during microtunneling and pipe jacking. Many of these studies have included in-depth evaluations of jacking forces in conjunction with a variety of other parameters including face pressure forces or cutting forces, steering corrections, pipe joint deflection, and the effects of lubrication. Other studies have involved statistical analyses of a large number of case histories where basic predictive models were used and empirical data were analyzed to propose factors for both the frictional and normal load components of the jacking force. These empirically-based factors were then multiplied by the friction and normal load components of the basic models to predict field behavior on microtunneling projects.

To date, few researchers have investigated to a limited extent the mechanism of shearing at the interface between the soil and the pipes to further isolate the friction that is developed during jacking. Studies on interface friction have shown that surface roughness can have a tremendous impact on whether the soil shears at the interface or whether the shearing occurs in the soil mass. Interface friction has received relatively little attention as it applies to microtunneling applications. This thesis seeks to exploit this opportunity and determine how an interface based approach may lead to a greater understanding of the mechanisms of shearing that control jacking forces.

2.2 Frictional Studies

Research on interface strength has been conducted since the early 1940's. Early research conducted by Potyondy (1961) concluded that three major factors had an effect on interface strength: the moisture content and composition of the soil, the continuum surface roughness, and the normal load. To analyze interface frictional behavior between sands and a variety of roughened surfaces, Brumund and Leonards (1973) developed a cylindrical apparatus that they filled with sand. They then pulled seven different textured rods from the cylinder and measured the interface strength. They were able to conclude that interface strength increased with surface roughness until the strength was equal to the internal friction angle of the sand. By testing two different types of sand, they were also able to conclude that the size, angularity, and surface texture of the sand have an effect on the interface friction angle.

Uesugi and Kishida (1986-a) made tremendous advances in relating interface friction to surface roughness when they tested five granular materials against a set of mild steel plates in a simple shear apparatus. Each of the mild steel plates had different surface roughness characteristics. Uesugi and Kishida found that the average soil particle diameter, roughness of the steel plate, density of the material, and the type of sand were significant factors affecting the interface friction. A statistical analysis of their data revealed a relationship between the average particle size of the particulate material and the roughness of the continuum that the particle was contacting, leading them to propose a normalized roughness factor R_n (1986-b). When the normalized roughness was analyzed, the relationship between normalized roughness and interface friction proved to be bilinear, revealing a "critical roughness" as can be seen in Figure 2.1. At values of

surface roughness below the critical roughness, the interface friction increased in a linear fashion up to the critical roughness value. However, once the continuum surface reached the critical roughness value, further increases in continuum roughness did not result in higher interface friction. This critical roughness represented an interface friction value that was equal to the internal friction angle of the soil that was being sheared against the interface.

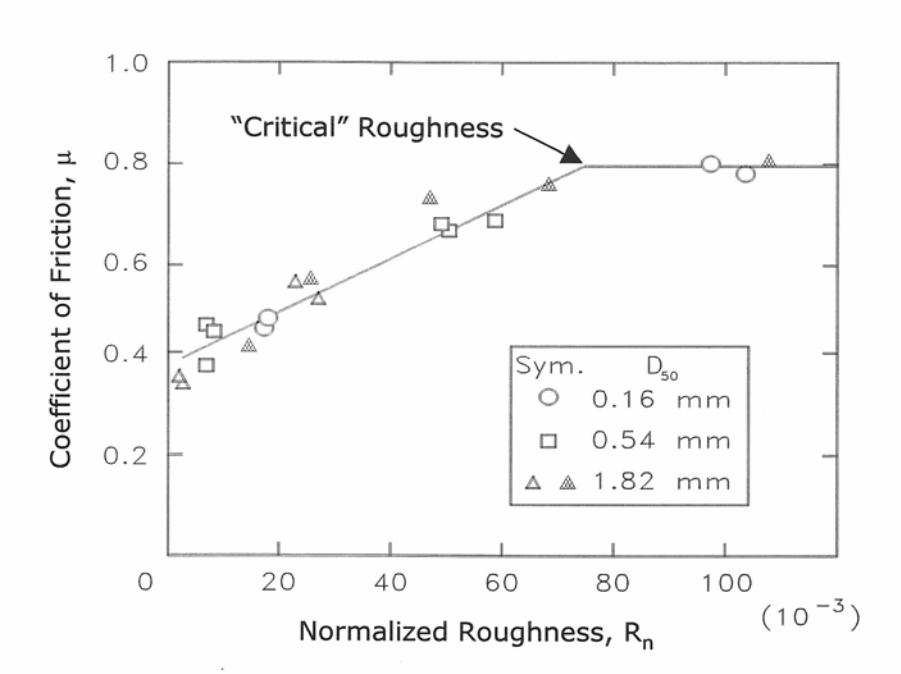

Figure 2.1 Normalized Surface Roughness vs. Friction Coefficient for Sand-Steel Interfaces (Uesugi and Kishida, 1986-b)

Dove and Frost (1999) conducted studies on interface shear behavior for granular materials and geomembranes of varying topography. They examined the shear mechanisms operating on smooth geomembranes and characterized the interface friction region with granular soils. A surface roughness parameter was used to develop a

classification scale for surface roughness for smooth and textured geomembranes. It was found that surface roughness has a first order effect on granular material-geomembrane interface strength. However, there is a limit to the beneficial effect with increasing degrees of surface texturing. Experimental and theoretical analyses showed that the shear mechanisms for smooth geomembranes-granular material interfaces are elastic-plastic sliding and plowing (Dove 1996). Interface shear testing at different normal stresses showed that in the region of sliding friction, at a normal stress value less than approximately 50kPa, the interface friction coefficient decreased with increasing normal load as shown in Figure 2.2.

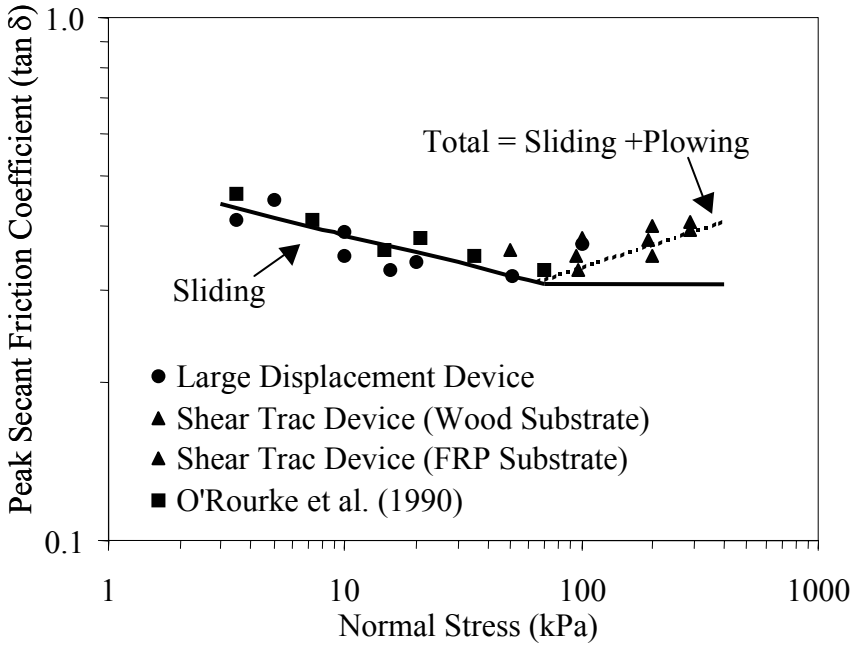

Figure 2.2. Smooth HDPE Geomembrane/Ottawa 20/30 Sand Interface Shear Mechanisms (Adapted from Dove and Frost, 1999).

At low values of normal stress, the maximum number of soil particles is not in contact with the surface area. As the normal stress increases, the number of soil particles in contact with the surface area increases, causing the interface friction coefficient to decrease. At approximately 50kPa, the maximum number of soil particles is in contact with the surface area. If the surface is hard, the interface friction coefficient remains stable at normal stresses above 50kPa, as depicted by the solid line in Figure 2.2. If the surface is softer, plowing of the soil grains will begin at normal stresses above 50kPa, causing the interface friction coefficient to increase.

DeJong and Frost (2000) performed a series of laboratory tests that measured the surface roughness and hardness of a variety of geomaterials. A modified large displacement interface direct shear device was used to determine the peak and residual interface friction angles. Ottawa 20/30, a sub-rounded quartz sand, was used as the granular medium at all of the interfaces. The primary mechanisms governing the interface friction, whether it be sliding or plowing, were investigated. DeJong and Frost demonstrated that for surface roughness values that varied over three orders of magnitude, the peak interface friction value increased with surface roughness more than 20 degrees between the surface with the lowest and the highest value of surface roughness. The hardness was also found to affect the interface strength with the materials with the lower hardness values having the larger interface friction angles.

DeJong further conducted extensive laboratory testing and discrete element modeling to show that an increase in surface roughness or a decrease in hardness was shown to increase the interface friction, provided the internal soil friction angle had not already been obtained. This coupled effect was clearly shown through mapping a three-

dimensional surface of surface roughness, hardness, and interface friction, as shown in Figure 2.3.

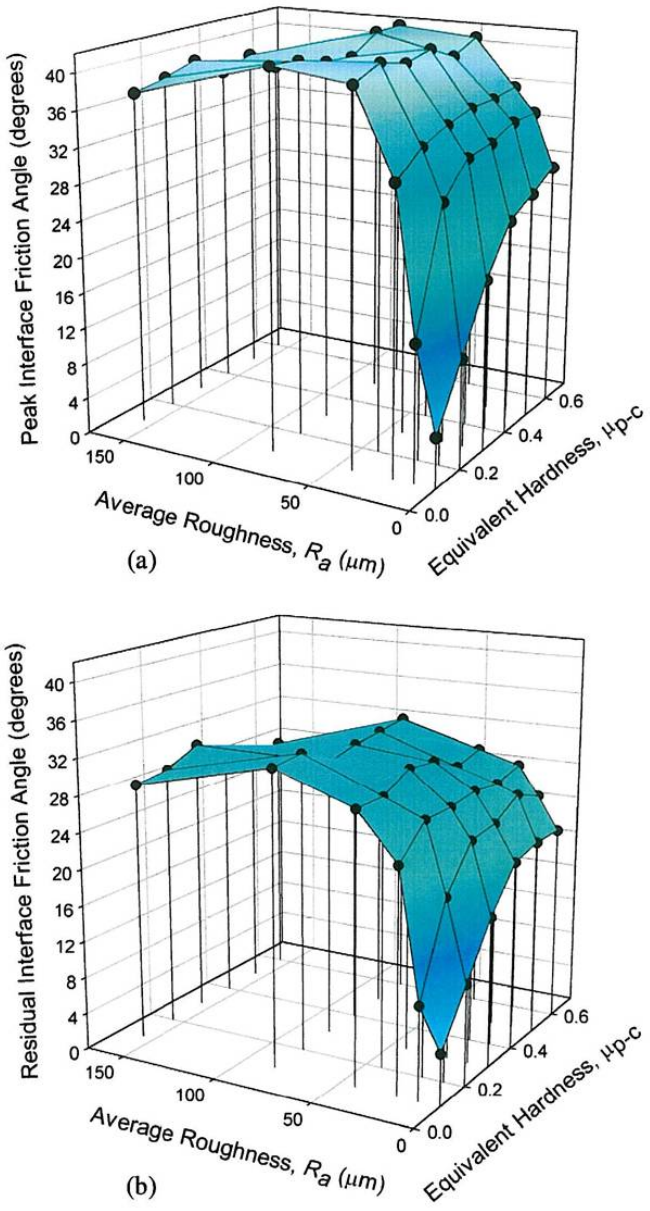

Figure 2.3. Relationship Between Surface Roughness, Hardness, and Interface Friction for DEM Modeling with Uniform Grain Size (a) Peak Internal Friction Angle, (b) Residual Friction Angle (DeJong, 2001).

2.3 Theories Governing Normal Stresses on the Pipeline

When determining the normal load acting on the pipeline during tunneling, microtunneling, or pipe jacking, the most widely accepted theory of how the soil stresses are distributed on the pipeline is that presented by Karl Terzaghi in his arching theory (Terzaghi, 1943). Terzaghi performed experiments in which he layered sands within a large box that contained a small trap door in the base of the box. He then slowly removed the trap door at the base and measured the stresses when the soil began to yield. Terzaghi found large decreases in the vertical stresses for very small displacements of the trap door. He attributed this phenomenon to arching in the soil mass above the door. The pressure decrease on the trap door was equal to the vertical component of the shearing resistance that acted on the boundaries. Figure 2.4 shows a representation of Terzaghi's Trap Door model.

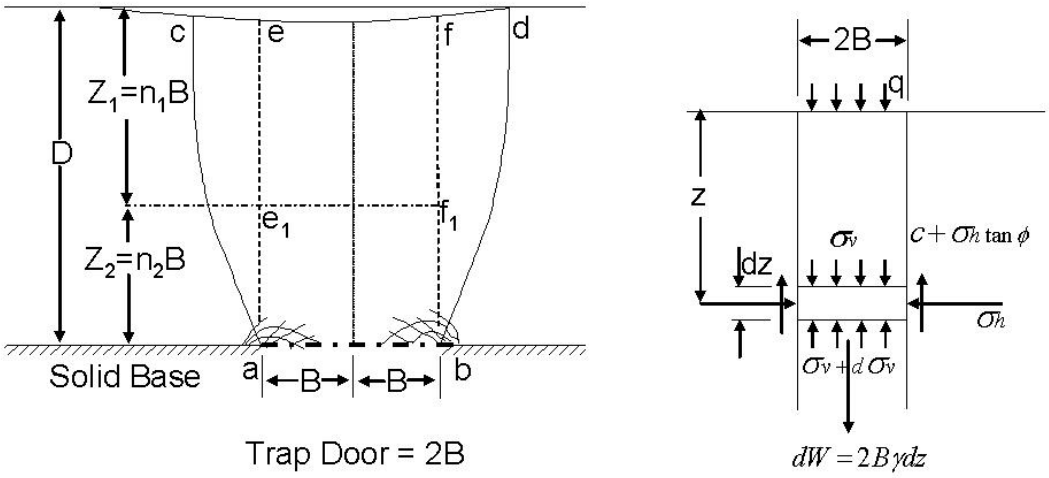

Figure 2.4. Terzaghi's Trap Door Model.

Terzaghi then developed equations for the vertical stress acting on the trap door at a depth of z, based on the width of the trap door, 2B. For ideal sand (cohesion equal to zero) without any surcharge loading, he found that as the vertical stress to be independent of the depth and derived the following equation:

$$\sigma_v = \sigma_{v\infty} = \frac{\gamma B}{K \tan \phi} \tag{2.1}$$

Experimental investigations performed by Terzaghi indicated that K=1 above the centerline of the trap door up to a maximum of 1.5 at a distance of 2B above the centerline. At a distance of 5B, lowering the trap door had no effect on the state of stress of the soil.

Many tunneling researchers have used this research performed by Terzaghi and applied it to calculating the normal stress acting on the pipe during pipe jacking operations. The variations in the methods are primarily in the choice of the width of Terzaghi's Trap Door, 2B, and how that is applied to pipe jacking, correlating the Trap Door width to the pipe diameter.

Auld (1982) presented a model for calculating normal stresses based on Terzaghi's Trap Door Model. Auld's model represents a pipe driven through cohesionless soils, and was based on the assumption that the soil would collapse onto the pipeline exerting a radial stress around the circumference of the pipeline. Figure 2.5 shows the basis for Auld's model. The model takes into account the arching of the soil above the pipeline and applies the Terzaghi's Arching Theory to a pipe diameter with the following equations:

$$\sigma_v = \frac{\gamma B}{K \tan \phi}\left(1 - e^{-k \tan \phi \, H/b}\right) \tag{2.2}$$

$$\sigma_H = 0.3\gamma \cdot (0.5D + D\sigma_v) \tag{2.3}$$

$$P_{Total} = \frac{\pi D}{2}(\sigma_v + \sigma_H) \tag{2.4}$$

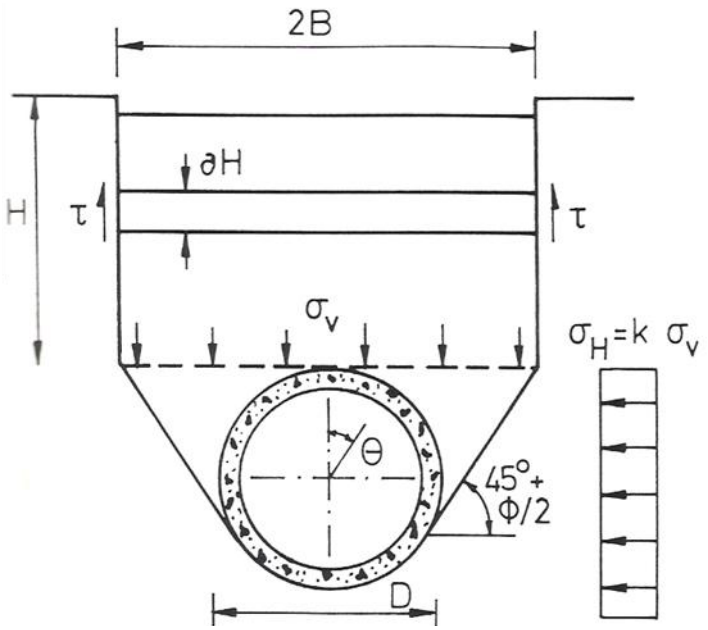

Figure 2.5. Distribution of Normal Stresses According to Auld (1982).

Standards have been established in Germany for calculating the normal load on pipes for microtunneling projects for pipe design purposes. These standards, similar to ASTM standards, are set forth specifically for microtunneling applications. The German standards covering microtunneling pipe design are found in ATV A 161. (Stein, et. al 1989) These standards recommend using a silo width (b) according to Figure 2.6, that is very similar to the model proposed by Auld.

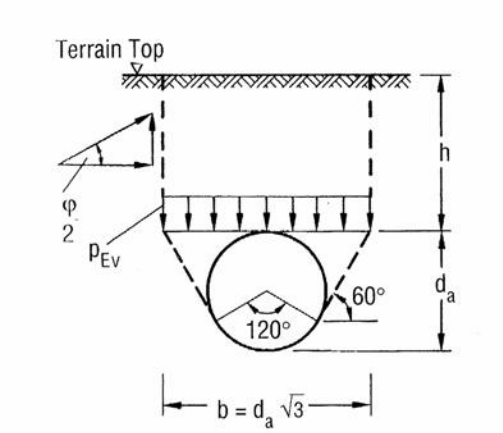

Figure 2.6 Recommended Area for Calculating Normal Stresses on Microtunneled Pipelines According to ATV A161 (Stein et al. 1989)

The German standard ATV A161 recommends using the following formula to calculate the vertical pressure P_{EV} acting on the pipeline.

$$P_{EV} = \frac{b \cdot \left(\gamma - \frac{2c}{b}\right)}{2K \tan\delta}\left(1 - e^{-2K \tan\delta \frac{h}{b}}\right) \qquad (2.5)$$

Where: d = pipe diameter
b = ideal silo width = $\sqrt{3}d$
h = depth of cover
K = coefficient of soil pressure above the pipe
δ = angle of wall friction in plane of shear
c = cohesion

Figure 2.7 shows a variety of interpretations and applications of Terzaghi's arching theory as it has been applied by various authors to calculate normal loads acting on microtunneled pipelines.

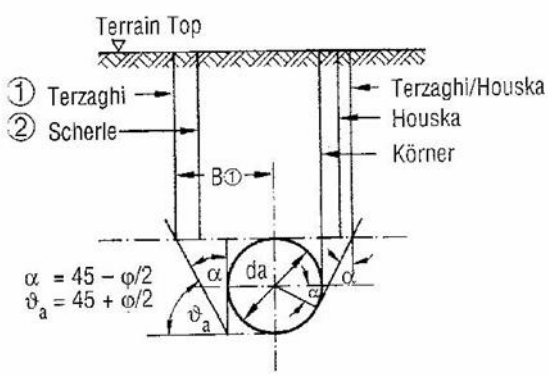

Figure 2.7 Applications of Terzaghi's Arching Theory by a Variety of Authors for the Calculation of Normal Stresses (Stein, 1989)

2.4 Research on Normal Stress Distributions Around Jacking Pipes

A number of practitioners and researchers have conducted studies on normal stress distribution around jacking pipes during pipe jacking operations. These have included field studies, numerical modeling studies, centrifuge modeling studies, and evaluations with critical state soil mechanics using the CAM-CLAY model for pipe jacking in cohesive materials. A significant amount of research was conducted at the University of Oxford under the direction of Dr. George Milligan. Results from three of his students, Norris (1992), Marshall (1998), and Zhou (1998) are discussed herein.

2.4.1 Field Studies Conducted by Norris

Milligan and Norris conducted field studies at the University of Oxford from the late 1980's through the 1990's that involved jacking an instrumented concrete jacking pipe on five (5) field projects (Norris and Milligan, 1991). Their studies focused on joint deflection, interface friction, normal stresses, the effects of misalignment, and the effects of time delays on jacking forces. The instrumented pipe was fitted with sensors to

measure joint deflection, contact stress transducers, pore pressure probes, and extensometers. Figure 2.8 shows the instrumented pipe used in the field tests.

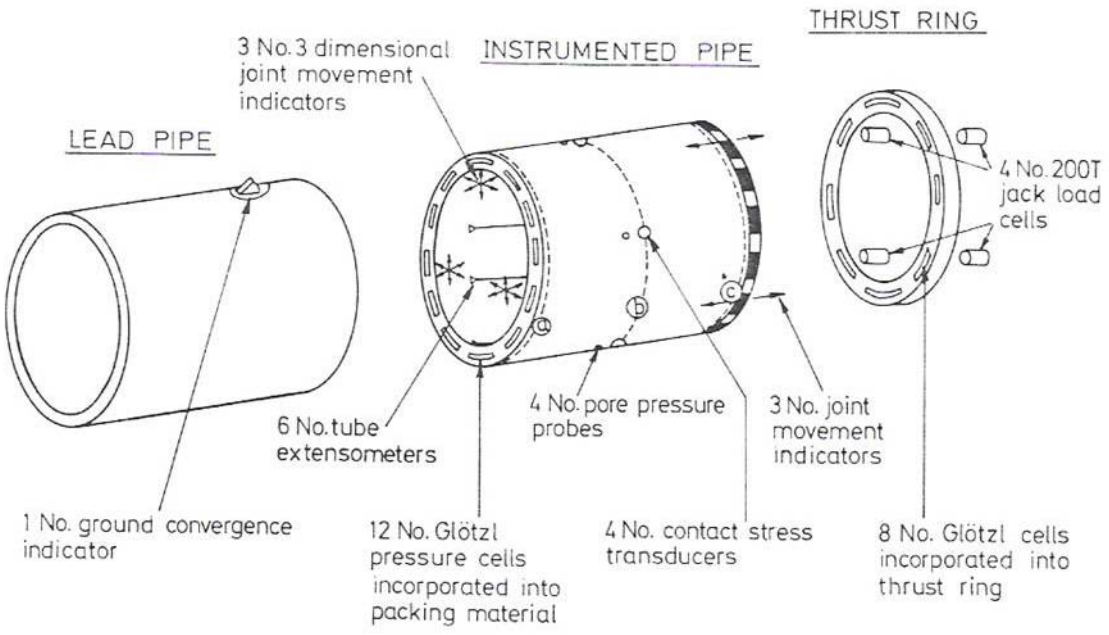

Figure 2.8. Instrumented Pipe Used in Field Tests at University of Oxford. (Norris and Milligan, 1991).

Of the five projects on which the instrumented pipe was jacked, two were in clay soils, one was in weathered mudstone, one was in dense silty sand, and one was in loose sand and gravel (Norris, 1992).

For the case history with silty sand, a 59.5-inch Spun Concrete pipe was jacked 514 feet at a depth ranging from 23 to 32 feet deep. Norris found that load cells measuring normal stresses around the pipe during jacking generally measured values between 20kPa and 40kPa on the top and right sensors, as shown in Figure 2.9. Values on the bottom sensor measured higher peak values, although it should be noted that

bentonite was pumped thorough a port on the bottom of the pipe inducing high pore pressures on the bottom of the pipe, as shown in Figure 2.9. Normal stress values generally measured below 50kPa for the left sensor. Values for the left sensor were greater than the right sensor due to steering corrections during the drive.

For the field case history in loose sands and gravel, a 47-inch Spun Concrete pipe was jacked 1,260 feet at a depth ranging from 13 to 23 feet. During microtunneling, steering corrections were excessive and even caused pipe joints to break (Norris, 1992). Norris found that normal stresses around the pipe were fairly evenly distributed and averaged approximately 50kPa at any given time. Norris concluded that bentonite injection into the annular space around the pipe caused the concrete pipe to float, resulting in equal normal stresses on the top and bottom of the pipeline. Figure 2.9 shows the total normal stress distribution around the pipeline during jacking between 91 and 131 meters of the drive at the main jack and interjack location.

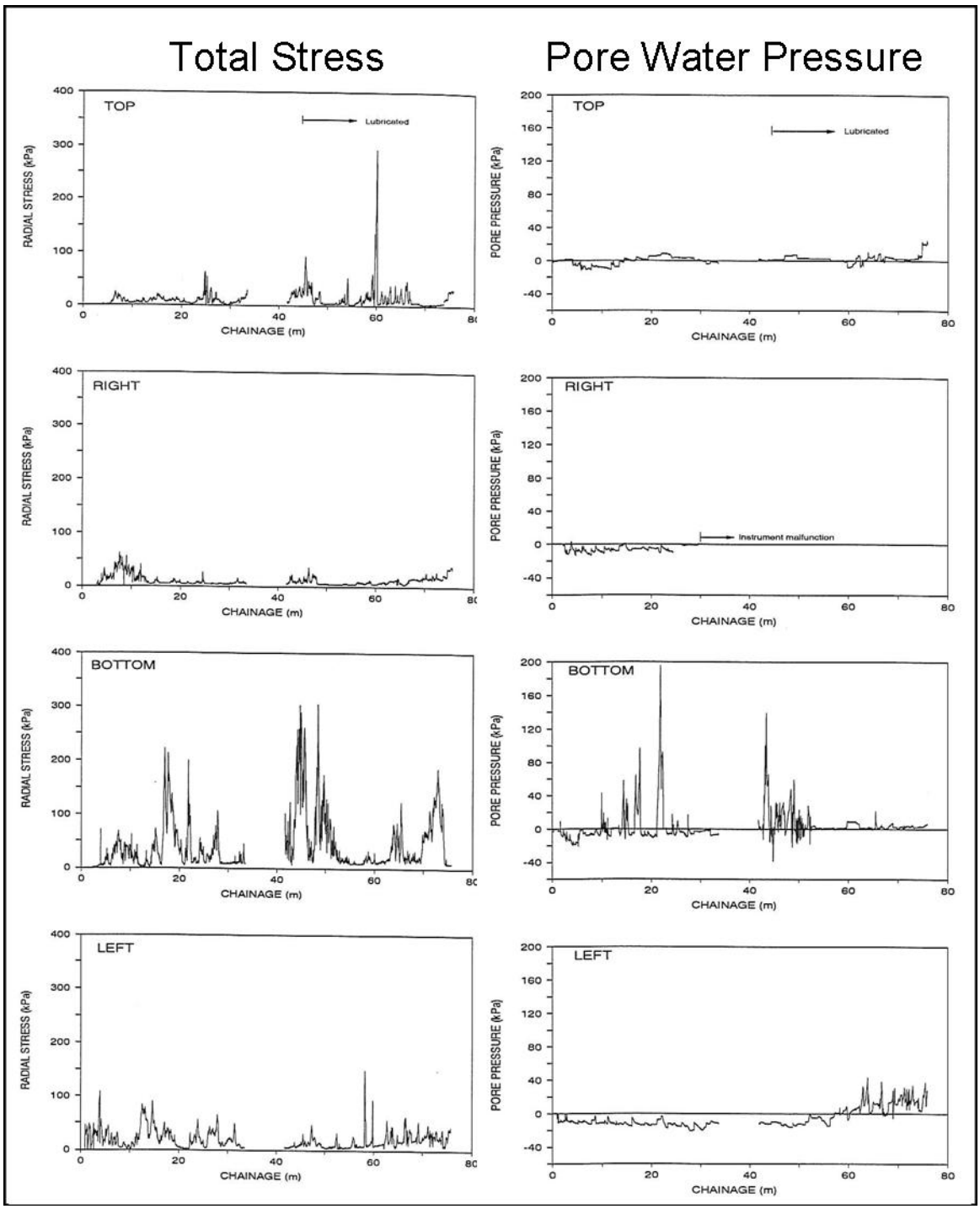

Figure 2.9. Total Normal Stress and Pore Water Pressure Measured by Norris Around Pipe While Jacking in Dense Silty Sand (Norris, 1992).

2.4.2 Continuation of Field Studies by Marshall

Marshall continued the work by Norris by completing four additional field studies. These included one test in London clay, one in glacial till, one in soft peaty clay, and a fourth test in sandy gravel. The test in sandy gravel consisted on a 39.4-inch Spun Concrete pipe that was jacked 524 feet approximately 18 feet deep in dense silty sand. The measurements of effective radial stress in the main and intermediate jacking stations are shown in Figure 2.10.

Marshall found that all pore pressure plots revealed excellent agreement with calculated pressures and indicated that hydrostatic pore pressure generally existed during jacking in the fine sand. Pore pressures increased above hydrostatic on the whole, corresponding with the pumping of lubrication. Pore pressure data, considered together with total radial stress data, provided very useful information on effective stress behavior (Marshall, 1998). Table 2.1 shows the sensor positions as well as peak and average measurements during the drive.

Table 2.1. Effective Radial Stress and Pore Pressures Measured by Marshall on Field Case History in Dense Silty Sand (after Marshall, 1998).

Sensor Position	Rear Set of Sensors				Center Set of Sensors				Front Set of Sensor			
	σ' [kPa]		u [kPa]		σ' [kPa]		u [kPa]		σ' [kPa]		u [kPa]	
	Peak	Avg	Peak	Avg	Peak	Avg	Peak	Avg	Peak	Avg	Peak	Avg
Bottom	49	4	86	48	41	6	83	50	51	22	89	54
Left	209	49	74	41	171	45	100	46	65	59	74	43
Top	122	44	47	38	67	16	70	38	-	-	-	-
Right	26	2	80	44	46	12	-	-	82	55	87	45
Average	101	25	72	43	81	20	84	45	66	45	83	47

Note: Right Pore Pressure Sensor not functioning in Center Set of Sensors. Top radial stress and pore pressure cell not functioning in front set of sensors.

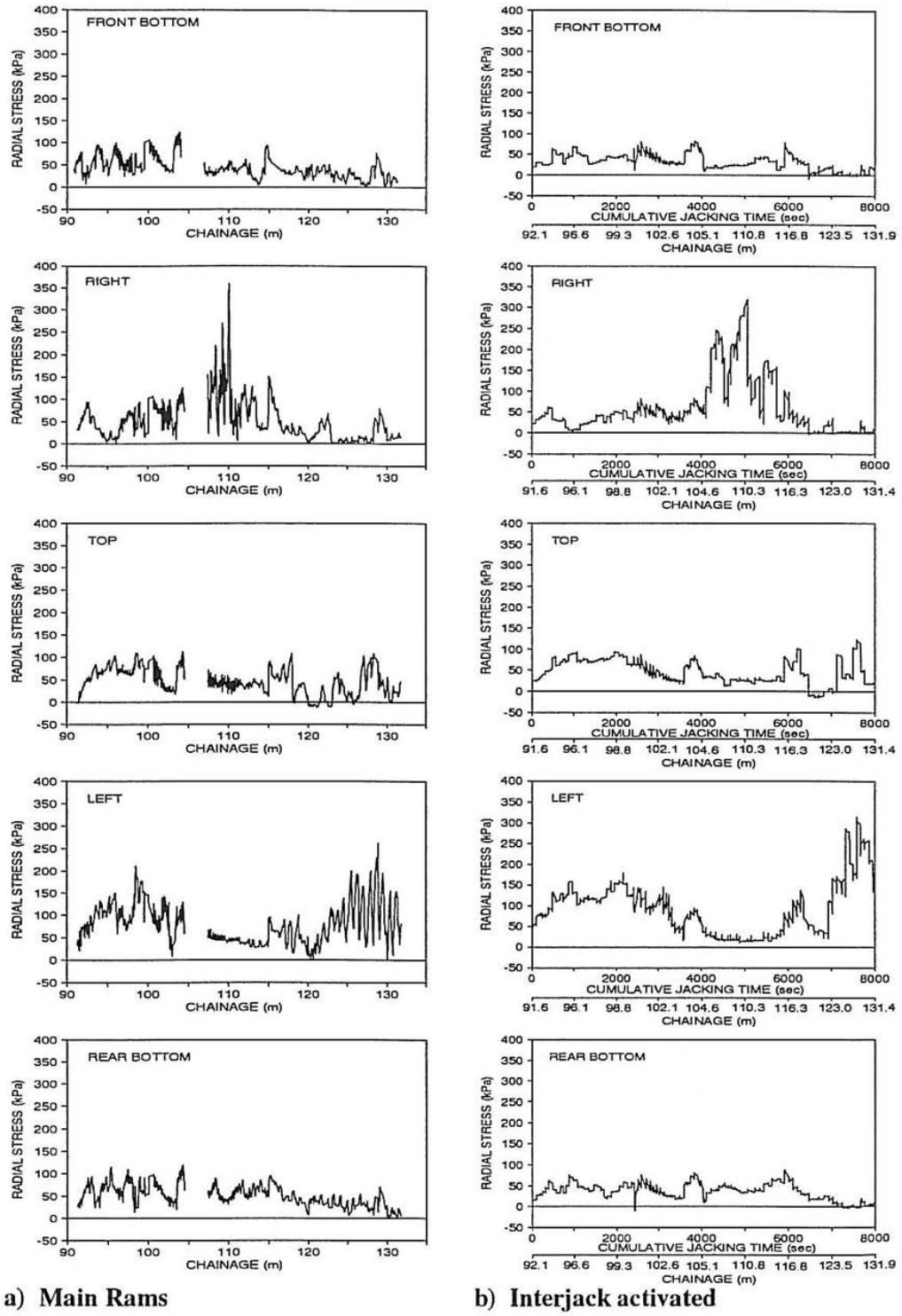

Figure 2.10. Total Normal Stress Measured by Norris While Jacking Through Loose Sand with Gravel. (Norris, 1992)

Based on these results, Marshall concluded that the pipeline was buoyant in the bentonite lubricant and that the pipe-soil contact was shown to be non-uniform along and around the instrumented pipe. He also concluded that the reason for the non-uniform contact between the pipe and the soil was due to the arrangement of the lubrication injection sockets and the position of the instrumented pipe relative to the microtunneling machine (inserted as the second pipe behind the shield) (Marshall, 1998).

2.4.3 Numerical Modeling Studies by Zhou

As Marshall was conducting field studies on concrete jacking pipes, Zhou was conducting numerical analysis of concrete jacking pipes with finite elements. Zhou used the mesh generation program DATAIN (Zhou, 1998) for his finite element model and examined stresses within the pipe and stresses at the boundary between the pipe and the soil by modeling interface elements. Zhou modeled normal stresses acting on the pipe due to soils of various stiffness.

In granular materials, Zhou found that the normal stresses between the pipe and the soil were very small. Zhou concluded that it was clear that the pipe separated or almost separated from the surrounding soil over most of the external surface of the pipeline. He further concluded that the effects of the distribution of the stresses from the surrounding soil on the stresses in the pipeline are small, since the magnitudes of the stresses on the interface are small. (Zhou, 1998). Zhou further concluded that the Australian model (Based on the work by Auld (1982) from the Terzaghi model) gives a "somewhat good" prediction for the maximum normal stress acting on the pipeline. (Zhou, 1998).

2.4.4 Centrifuge Modeling of Stress Changes above a Tunnel in Sand

At the University of Cambridge, Jacobsez, Standing and Mair (2004) investigated the changes in stresses in sand above a tunnel by developing a centrifuge model. They modeled the excavation at the tunnel face with the cavity contraction model after Atkinson and Potts (1977) and the radial equilibrium model. They found that during tunneling excavation, a considerable stress distribution occurred so that support pressures of relatively small magnitude were required, following the cavity contraction model. Figure 2.11 shows the failure mechanism proposed by Atkinson and Potts. In the model developed by Atkinson and Potts, the failure envelope is defined by the angle 2ψ, where ψ is the dilation angle of the soil. The model illustrated that the cavity contraction model is a good representation of actual conditions in granular material as the stress path at the tunnel crown reached failure at the predicted failure envelope. Figure 2.12 shows the vertical stress measurements on the pipe during the test.

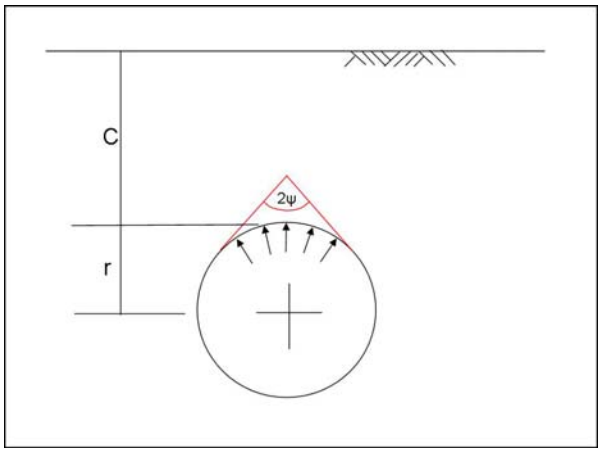

Figure 2.11. Predicted Failure Envelope based on Cavity Collapse Model (Atkinson and Potts, 1977).

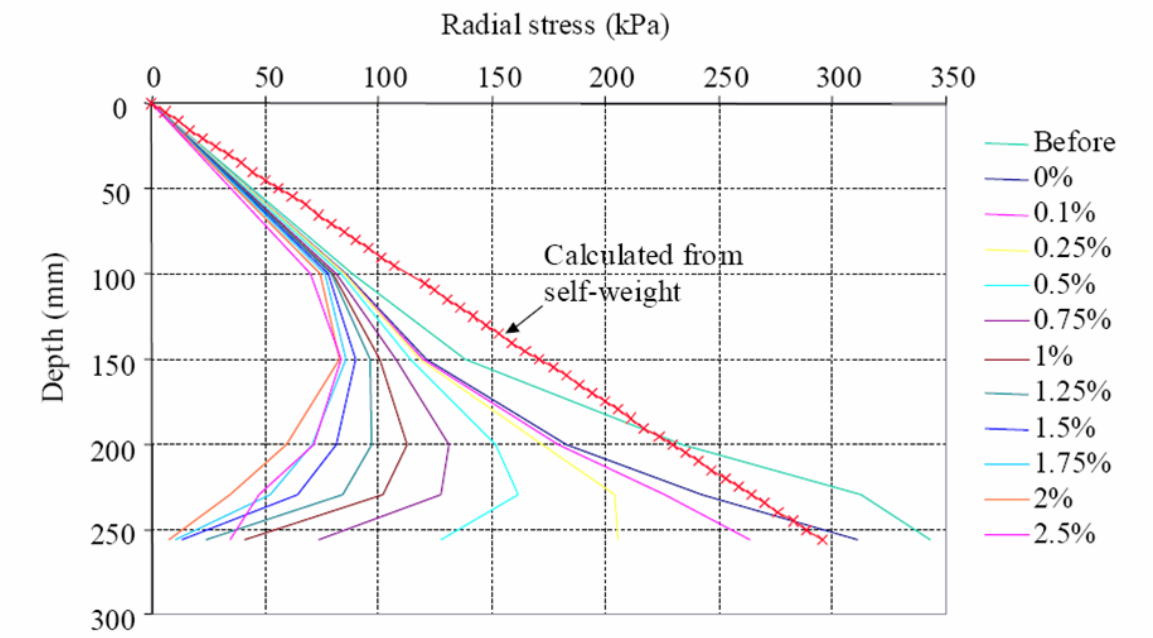

Figure 2.12. Vertical Stress Measurements during Centrifuge Tests (Jacobsz, et.al. 2004)

2.5 Research on Microtunneling and Jacking Forces

A number of practitioners and researchers have developed predictive models for the estimation of frictional jacking forces in the late 1970's and early 1980's. These methods are summarized in Stein (2005). A summary of the predictive models is presented in Table 2.2. Details of selected models are presented herein.

Table 2.2. Existing Predictive Models for Predicting the Frictional Component of Jacking Forces (Modified and Adapted from Stein 2005).

Author	**Predictive Model Frictional Component of Jacking Force**	**Symbols, Notes, Etc.**
Walendky / Möncke (1970)	$\gamma \cdot h \cdot \sqrt{\frac{K_o^2 + 1}{2}} \cdot \tan \delta$	$\delta = \varphi$ э / 2 δ= Wall friction angle K_o = Coefficient of lateral earth pressure at rest H = Cover depth
Helm (1964)	Circular Cross Section: $\mu \cdot \gamma \cdot h \cdot \frac{K_a + 1}{2}$ Rectangular Cross Section: $\mu \cdot \gamma \cdot h \cdot \frac{b_a + K_a \cdot d_a}{b_a + d_a}$	K_a = Active earth pressure coefficient b_a = External width of the microtunneling shield or machine d_a External height or diameter of microtunneling shield or machine
Szentandrasi (1981) Scherle (1977)	$\mu\left(H_w + \frac{d_a}{2} \cdot \frac{K_{Sch} + K_{K1} + K_{K2} + K_{So}}{4} + \frac{W_s - F_A}{4 d_a} \right)$	H_w = Effective cover depth W_s = Dead weight of pipe F_A = Buoyancy
Solomo (1979)	Circular Cross Section: $\gamma \cdot \left(h + \frac{d_a}{2} \right) \cdot \sqrt{K_m} \tan \delta$ Rectangular Cross Section: $\mu \cdot \gamma \cdot h \cdot \left(b_a + K_m \cdot d_a \right) \cdot \frac{1 + \frac{d_a}{2h}}{b_a + d_a}$	For a very dense compacted sand. K_m = Effective earth pressure coefficient
Weber (1981)	Circular Cross Section: $\mu \cdot \sqrt{p_v \cdot p_h}$ Rectangular Cross Section: $\mu \left(\left(\kappa \cdot b_a \right) + \left(K_o \cdot d_a \right) + K_o \cdot \frac{d_a^2 \diagup 2h}{b_a + d_a} \right)$	Slurry Boring Method μ = 0.46 p_v = Vertical earth pressure p_h = Horizontal earth pressure
Weber (1981)	$\mu \cdot E_s \cdot \frac{\Delta d_a}{d_a}$ With Stiff ness Modulus from Ohde: $E_s = \nu \cdot \left(\frac{\sigma}{\sigma_1} \right)^w$	Auger Boring Method with Steel Pipes (318, 508 and 711 mm diameter): ν,w = Stiffness coefficients Δd_a = Deformation dimension of the pipe string
Iseki (as Summarized in Stein 2005)	$\mu\left(q + W_s\right) + C$	q = Loading vertical to pipe axis [kN/m^2] $\mu = \tan \frac{\phi}{2}$

<table>
<tr><th>Author</th><th>Predictive Model
Frictional Component of Jacking Force</th><th>Symbols, Notes, Etc.</th></tr>
<tr><td>ATV-A 161E (1990)</td><td>Circular Cross Section:
$\mu \cdot \gamma \cdot h \cdot \kappa\left(b_a + \left(K_2 \cdot d_a\right)\right) + K_2 \cdot \frac{d_a^2 / 2h}{\left(b_a + d_a\right)}$</td><td>$\kappa = \frac{1 - e^{\tan(0.5\phi) \cdot h/b}}{\tan(0.5\phi) \cdot h/b}$
$b_a = \frac{2d_a}{\sqrt{3}}$</td></tr>
<tr><td>Hasan (1985)</td><td>$\tan\delta \cdot \left(\kappa_m \cdot \gamma \cdot \frac{h}{2} \cdot \left(1 + \frac{d_a}{2} \cdot \kappa_m \cdot h\right)\right) + \frac{W_s}{4d_a}$
<table>
<tr><th>Jacking Method</th><th>h/da</th><th>Overcut</th><th>Non-Cohesive</th><th>Cohesive</th></tr>
<tr><td rowspan="2">Open Shield</td><td>≤ 2</td><td>With or Without</td><td>κ_m =1</td><td>κ_m =1</td></tr>
<tr><td>≥ 2</td><td>With or Without</td><td>κ_m=(1+κ)/2</td><td>κ_m=(1+κ)/2</td></tr>
<tr><td rowspan="3">Closed Shield</td><td>≤ 2</td><td>With</td><td>κ_m =1</td><td>κ_m=(1+κ)/2</td></tr>
<tr><td>≤ 2</td><td>Without</td><td>κ_m =1</td><td>κ_m =1</td></tr>
<tr><td>≥ 2</td><td>With</td><td>κ_m=(1+κ)/2</td><td>κ_m=(1+κ)/2</td></tr>
</table></td><td>tanδ = Coefficient of friction
κ_m= Reduction factor</td></tr>
<tr><td>Ebert (1990)</td><td>$0.5\mu \cdot \left(a \cdot \gamma \cdot h + \left[\gamma \cdot \left(h + \frac{d_a}{2}\right) + P_a\right] \cdot K_e + W_S\right) \cdot \frac{10}{L_R}$</td><td>γ = Soil density
a = Active load coefficient
P_o = Surface loads
K_e = Earth pressure coefficient at rest
L_R = Pipe length</td></tr>
<tr><td>Herzog (1996)</td><td>$\mu \cdot \gamma \cdot \left(h + \frac{d_a}{2}\right) \cdot \frac{1 + K_o}{2}$</td><td>Note Similarities to Helm.</td></tr>
<tr><td>Paul
(as summarized in Stein 2005)</td><td>$\mu \cdot \left[2\left(\gamma \cdot \frac{h}{d_a} + P_{VR}\right) \cdot \left(1 + K_a^{'}\right) + W_s\right]$</td><td></td></tr>
<tr><td>Chapman (1999)</td><td>$a + 3.8d_a$

Details of Method found in Section 2.4.3</td><td>Based on Statistical Evaluation of 198 Slurry Microtunneling Projects.
a= 1.53 for clay
a= 2.43 for sand
a= 3.43 for sand/gravel</td></tr>
<tr><td>Bennett (1998)</td><td>$F_r = C_a \gamma^{'} d_p \tan(C_f \phi_r) A_p L$

Details of Method and Values for Friction Reduction Factor, C_f, and Arching Reduction Factor, C_a, found in Section 2.4.4.</td><td>γ’ = Effective soil unit weight,
d_p = Pipe diameter;
ϕ_r = Residual soil friction angle,
A_p = Pipe circumference,
L = Length of tunnel.</td></tr>
<tr><td>Osumi (2000)</td><td>$f_o = \beta(\pi B_c q + w)\mu' + \pi B_c C'$

C’ = Adhesion of Pipe and Earth (8kN/m^2 for N<10 and 5kN/m^2 for N>10)
Details of Method found in Section 2.4.5.</td><td>β= Jacking force reduction factor
B_c = Diameter of the pipe
Q = Normal force
W = Pipe weight</td></tr>
</table>

2.5.1 Predictive Model Developed by Scherle

Scherle (1977) established interface friction coefficients between concrete and asbestos cement pipes and various soil types based on data collected at field sites. He grouped the interface friction coefficients into three categories representing the state of motion of the pipeline: static friction, sliding friction, and fluid friction. The third category, fluid friction, represented the state of motion when bentonite was used as a "supporting and lubricating" fluid around the pipeline, and Scherle gave a range of friction coefficients for this state depending on the liquid limit of the bentonite suspension. Scherle asserted that the frictional component of the jacking force was a function of the interface friction coefficient, multiplied by the unit weight of the soil, multiplied by the depth of cover to the springline of the pipe, times a factor that was based on the state of stress in the soil. Values for the interface friction coefficient as established by Scherle are shown in Table 2.3.

Table 2.3. Interface Friction Coefficients According to Scherle (as summarized in Stein et al. 1989)

Pipe Material and Soil at Interface	Static Friction Interface Friction Coefficient, μ [-]	Sliding Friction Interface Friction Coefficient, μ [-]	Fluid Friction Interface Friction Coefficient, μ [-]
Concrete Pipe on Gravel or Sand	0.5 to 0.6	0.3 to 0.4	0.1 to 0.3
Concrete Pipe on Clay	0.3 to 0.4	0.2 to 0.3	0.1 to 0.3
Asbestos Cement Pipe on Gravel or Sand	0.3 to 0.4	0.2 to 0.3	0.1 to 0.3
Asbestos Cement Pipe on Clay	0.2 to 0.3	0.1 to 0.2	0.1 to 0.3

2.5.2 Predictive Model Developed by Weber

Weber conducted investigation of jacking forces of microtunneling pipes and found no relationship between depth of burial and jacking forces. Weber established a

calculation model that provided an upper bound for the interface friction value. Weber used an interface friction value of 0.46, corresponding to an interface friction angle of 24.7 degrees (as summarized in Stein et. al 1989). Weber uses this value regardless of pipe material or soil type in order to provide a conservative value for predicted jacking forces. Weber also published a table of jacking stresses related to skin friction that were categorized by soil type. These values for jacking stresses were calculated post-construction from several microtunneling projects as shown in Table 2.4.

Table 2.4. Frictional Jacking Stresses for Various Soil Types as Reported by Weber(1981)

Soil Type	Jacking Stress due to Skin Friction [kN/m^2]	Jacking Stress due to Skin Friction [tons/ft^2]
Gravel, sand	8.4 ± 2	0.087 ± 0.02
Loamy sand	9.3 ± 1	0.097 ± 0.01
Loam	7.3 ± 1	0.076 ± 0.01
Loam, stones	5.7 ± 4	0.060 ± 0.04

2.5.3 Investigations of Pipe-Soil Interactions with an Instrumented Jacking Pipe Conducted by Milligan and Norris

With the measurements of the normal loads on the pipes from the contact stress transducers, Milligan and Norris determined the soil-pipe interface friction angle at each of the sites. They attempted to isolate sections of the bore where lubrication was applied and compared those to sections where lubrication was not applied or poorly applied.

Milligan and Norris studied the pipe-soil interface for cohesive materials and developed a hypothesis regarding the asperities in the concrete pipe at the soil-pipe interface and the contact area with the cohesive soil. They found that much higher values of interface shear strength were measured at low normal stress levels. They hypothesized that the roughness of the concrete, and, more particularly, the soil surface caused the

surface area over which contact was made to be small, and that as the normal stress increased, the contact area between the pipe and the soil would increase. They assumed this trend would continue until the normal stress caused intimate contact at the surface, similar to the findings of Dove and Frost (1999). Milligan and Norris conducted a laboratory test with a standard direct shear Cassagrande apparatus to model shearing conditions in the field, replacing the upper portion of the shearing device with concrete and filling the lower portion with London Clay. However, difficulties were encountered in specimen preparation due to the fissured nature of the London Clay and modeling clay was used in its place. Testing with the shearing apparatus was found to be "somewhat inconclusive."

2.5.4 Statistical Evaluation of Jacking Force Data by the ISTT Working Group No. 3 and Chapman leading to Chapman's Predictive Model

The International Society for Trenchless Technology formed a working group in 1992 entitled Working Group No.3, which conducts technical research on microtunneling. The group focused their efforts on the analysis of jacking forces in order to "find a formula to calculate jacking forces by type." (ISTT WG No.3 1994) At the time the research statement was developed, the "type" was undetermined, and a statistical analysis of data from 398 projects was undertaken to find similarities in order to group the data by a "common variable." The variables included machine type, soil type, soil removal system type (auger vs. slurry), pipe diameter, earth cover, jacking distance, among others. However, because all of the projects were analyzed together, and none of the records were analyzed for construction problems or case history anomalies, the range of data scatter was extremely large and few conclusions could be drawn from the study. In addition, the parameters studied, such as the largest force at the completion of the

drive, were not necessarily indicative of the jacking behavior throughout the drive. The committee recommended that the data be further analyzed in smaller groups separated by categories such as geotechnical conditions along the tunnel, pipe diameter, etc. However, a follow-up report was not published.

In 1999, Chapman and Ichioka (1999) revisited the work done by the ISTT working group and re-evaluated the data. They separated the microtunneling case histories into three categories by soil type: clay, sand, and sand with gravel. For each category they plotted pipe diameter versus frictional resistance along the pipe (in tons per square meter) resulting in the graphs shown in Figure 2.13 through 2.15.

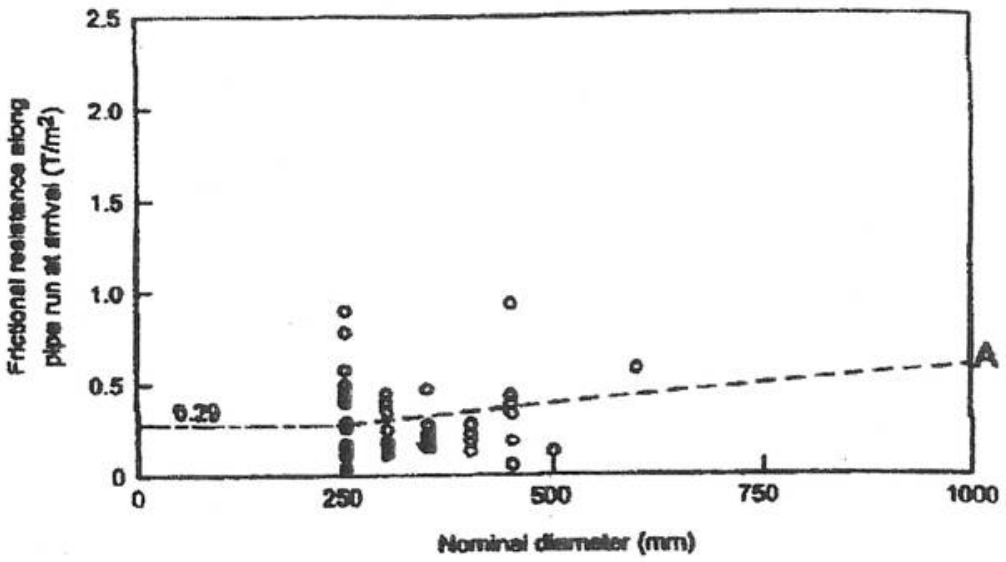

Figure 2.13. Pipe Diameter vs. Frictional Resistance in Clay
(Chapman and Ichioka, 1999)

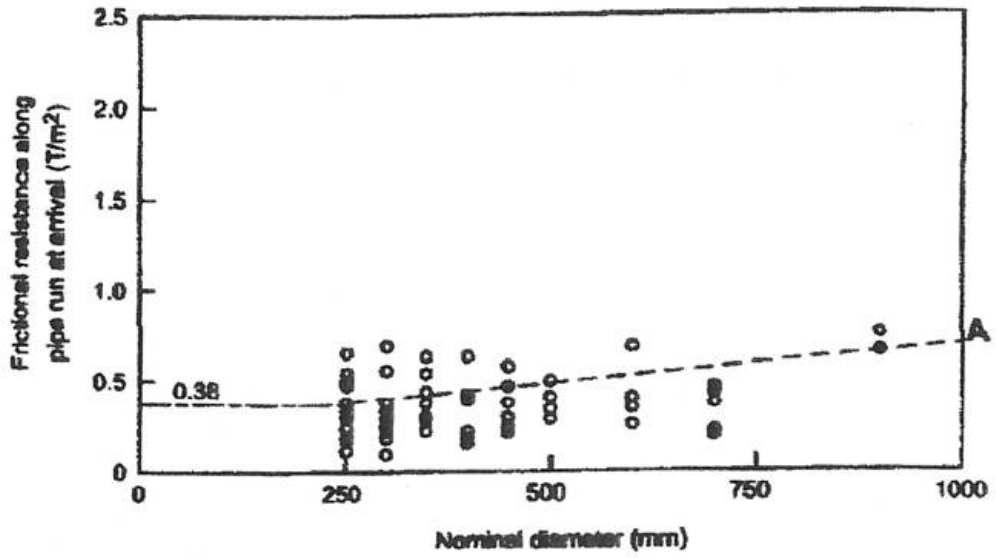

Figure 2.14. Pipe Diameter vs. Frictional Resistance in Sand
(Chapman and Ichioka, 1999)

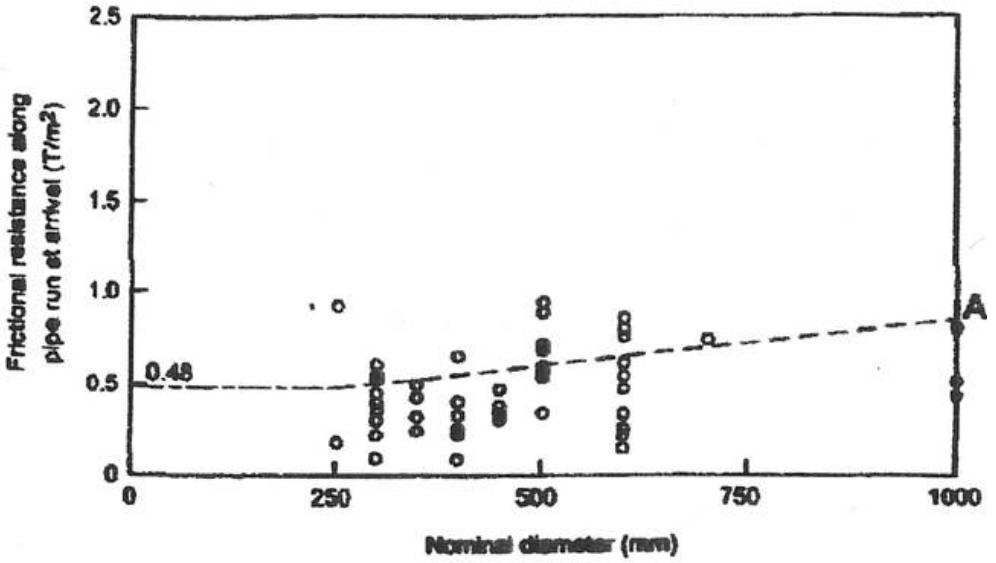

Figure 2.15. Pipe Diameter vs. Frictional Resistance in Sand and Gravel
(Chapman and Ichioka, 1999)

Chapman and Ichioka plotted all of the data contained in the three charts shown in Figures 2.13 through 2.15 on one chart and performed a linear regression on the data. For all of the soil types plotted on a single chart, they found the slope of the regression line to be 0.38 as shown in Figure 2.16, labeled A.

Linear regression lines were also carried out on the data when separated out by soil type in figures 2.13 through 2.15 and the slope of the linear regression was found to be similar to 0.38 but with a different intercept.

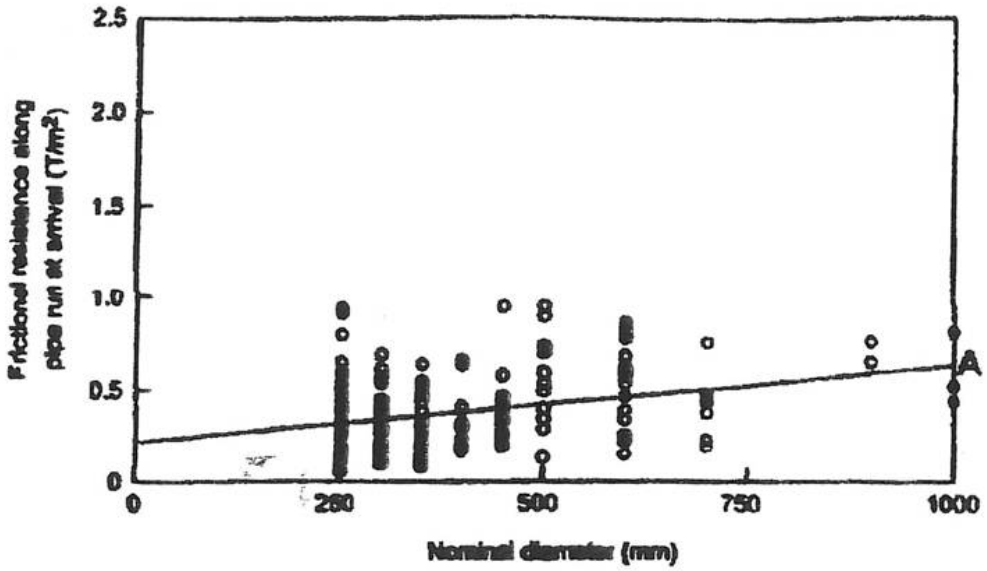

Figure 2.16. Pipe Diameter vs. Frictional Resistance for All Soil Types (Chapman and Ichioka, 1999)

Chapman and Ichioka then developed an equation for frictional resistance, P, which they related to the diameter of the pipe by the following equation:

$$P = a + 0.38D \qquad (2.6)$$

where P= frictional resistance [tons/m^2]
a = intercept value for each soil type (taken from figures 2.13 through 2.15)
D = pipe diameter

The intercept value, a, was found by using the smallest nominal diameter, 250 mm (outer diameter 360 mm). Chapman listed values for "a" as shown in Table 2.5.

Table 2.5. Intercept Values "a" for Chapman, Ichioka Predictive Model

Soil Type	Intercept Value "a" for Chapman, Ichioka predictive model.
Clay Soils	0.153
Sand	0.243
Sand and Gravel	0.343

2.5.5 Controlled Field Tests with Microtunneling Leading to Bennett's Predictive Model

A series of field tests were conducted by the US Army Corps of Engineers in which instrumented test beds were constructed of four soil types, and through which two microtunnels were constructed. Figure 2.17 shows test bed through which the microtunnels were driven.

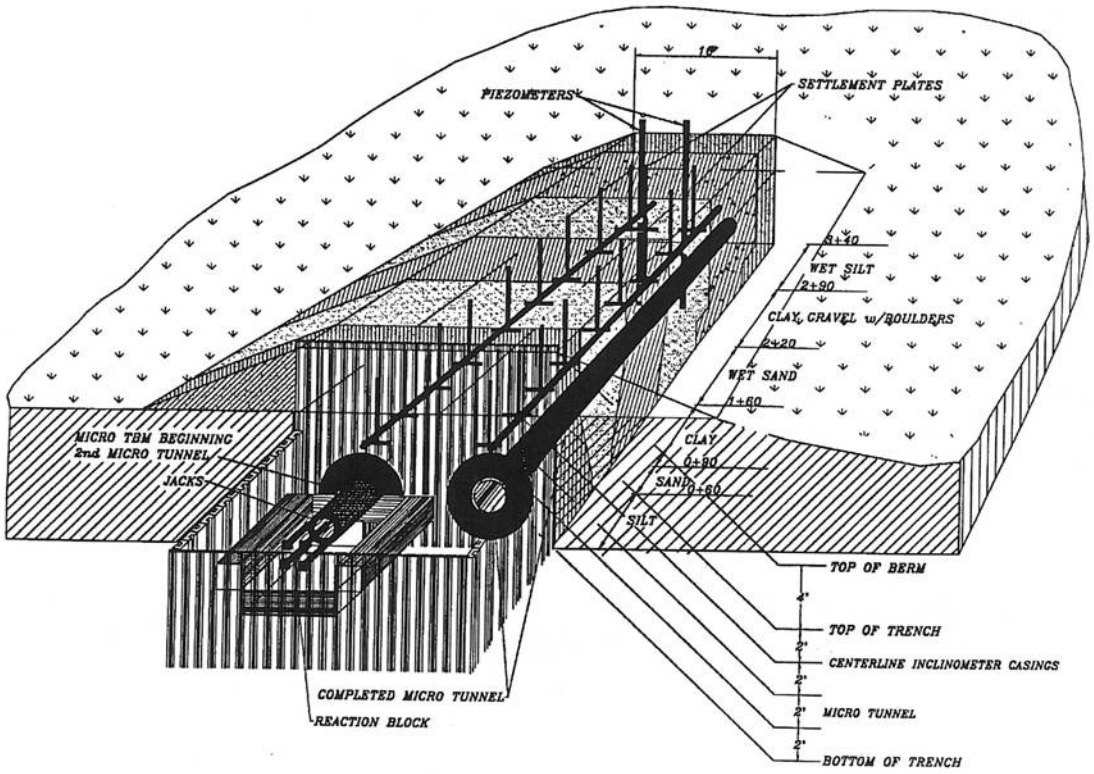

Figure 2.17. Microtunneling Test Bed for Controlled Field Test (Bennett, 1998)

The drive data from the microtunnels were collected and analyzed by Bennett (Bennett 1998), who then developed a model for predicting jacking forces in both cohesive and granular soils. Bennett also analyzed the effects of steering corrections, delays, face pressures, loss of face stability, over-cut and lubrication. In addition to the field testing performed at the Waterways Experiment Station, Bennett also analyzed case history data from five (5) projects that included 39 microtunnel drives. Of these 39 microtunnels, 37 of the tunnels ranged between 34 and 36 inches in diameter. The remaining two tunnels had 62.9 and 82.5-inch outer diameters.

Bennett's predictive model is based on the concept that the total jacking force is a function of the surface area of the pipe multiplied by a normal force and a friction coefficient. The normal force, however, is not based on depth, but rather on the diameter

of the pipe and the effective unit weight of the soil. Bennett then introduces an arching reduction factor that he terms C_a that is multiplied by the effective unit weight and the diameter.

Bennett's friction factor is based on the friction angle of the soil. Here Bennett introduces the friction reduction factor that he calls C_f that is multiplied by the residual friction angle of the soil. Bennett then establishes upper bound, best-fit, and lower bound values for the arching and friction reduction factors for use in his proposed model. Further, Bennett separates his recommendations for the arching and friction reduction factors based on whether the microtunnel is in sand or clay.

One final distinction that makes Bennett's model unique is that he separates the drive into two individual segments. The first segment of the microtunnel drive Bennett terms the "initial dewatered, non-lubricated interval" followed by the "lubricated non-dewatered interval." Each of these segments has different recommended values for the arching and friction reduction values. Table 2.6 provides the coefficients C_a and C_f for Bennett's predictive model where:

$$F_r = C_a \gamma' d_p \tan(C_f \phi_r) A_p L \qquad (2.7)$$

Where:

F_r = Frictional Jacking Force;
γ' = Effective soil unit weight,
d_p = Pipe Diameter;
ϕ_r = Residual Soil Friction Angle,
A_p = Pipe Circumference, and
L = Length of Tunnel.

Table 2.6 Arching and Friction Reduction Factors from Bennett (1998)

Bennett's Model for Calculation of Frictional Jacking Forces				
	Initial Dewatered, Non-Lubricated Interval		Lubricated Non-Dewatered Interval	
	Arching Reduction Factor C_a	Friction Reduction Factor C_f	Arching Reduction Factor C_a	Friction Reduction Factor C_f
SANDS				
Upper Bound	1.5	1.0	1.0	0.66
Best Fit	1.0	1.0	0.66	0.66
Lower Bound	0.75	1.0	0.5	0.5
STIFF TO HARD CLAY				
Upper Bound	1.0	1.0	0.66	0.66
Best Fit	0.66	1.0	0.5	0.5
Lower Bound	0.33	0.66	0.5	0.5
SOFT TO MEDIUM CLAY				
Upper Bound	1.0	1.0	3.0	1.0
Best Fit	0.66	1.0	1.5	1.0
Lower Bound	0.5	1.0	1.0	0.5

2.5.6 Osumi's Predictive Model using Jacking Force Reduction Factors

Osumi of the Japan Microtunneling Association studied 49 pipe jacking projects and developed a method for calculating the frictional component of jacking forces. (Osumi, 2000). Osumi based the interface friction coefficient between the pipe and the soil on the internal friction angle of the soil. He assumed that regardless of pipe material, the interface friction coefficient, μ', was equal to the tangent of half of the interface friction angle ($\tan(\frac{\phi}{2})$). Osumi bases the normal force on the depth of cover and the weight of the pipe. His jacking force equation also has a component for adhesion between the pipe and the earth which accounts for cohesive soils.

Osumi's equation for the frictional component of the jacking force is as follows:

$$f_o = \beta(\pi B_c q + w)\mu' + \pi B_c C' \quad (2.8)$$

Where: f_o = frictional component of jacking force
β= Jacking Force Reduction Factor
B_c = Outer Diameter of the Pipe
Q = Normal Force
W = Pipe Weight
C' = Adhesion of Pipe and Earth
($8kN/m^2$ for N<10 and $5kN/m^2$ for N>10)

Using the jacking force data from the 49 tunnels, Osumi performed a statistical analysis to determine the Jacking Force Reduction Factor, β. This factor was developed for four (4) types of soil: cohesive, sandy, gravel, and solid. Osumi does not provide any description of the soil type that is used to form the group of soils termed "solid." Table 2.7 provides recommended values for the Jacking Force Reduction Factor as provided by Osumi.

Table 2.7 Jacking Force Reduction Factors from Osumi (2000).

Soil Category	Jacking Force Reduction Factor, β [-]
Cohesive Soil	0.35
Sandy Soil	0.45
Gravel	0.60
Solid Soil	0.35

2.6 Summary

This chapter reviewed models that exist for predicting the normal stresses and frictional components of jacking forces associated with microtunneling and pipe jacking operations. The field of interface friction and the effects of surface roughness on

interface friction characteristics have also been reviewed. However, there has been very little cross-over between these two topics. This provides a tremendous opportunity to improve the state of jacking force prediction models by using the advances in the field of interface friction technology.

CHAPTER 3

CHARACTERIZATION OF PIPE SURFACE ROUGHNESS AND INTERFACE SHEAR TESTING

3.1 Introduction

Pipe surface roughness was characterized for a number of jacking pipe materials to determine its effect on interface friction. These materials included Centrifugally Cast Fiberglass Reinforced Polymer Mortar Pipe (CCFRPM), also referred to as Hobas; Polymer Concrete pipe, commonly known as Polycrete pipe; Vitrified Clay pipe; rolled steel pipe with a painted outer surface and a machined, press-fit joint, commonly known as Permalok Steel; concrete pipe manufactured with the Wet Casting method; and concrete pipe that is manufactured with the Packerhead method. The pipe surfaces were characterized by using a Stylus Profilometer to determine the average roughness of each pipe material. Once the average pipe roughness of each material was established, the pipes were sheared against two characteristically different types of sand to determine the interface friction behavior of each pipe material and to determine if surface roughness impacted interface shear strength.

3.2 Pipe Materials Included in the Study

The pipe materials included in the study are jacking pipes that are most commonly used for microtunneling and pipe jacking applications in North America. Although technology is producing new jacking pipe materials, the pipes included in the study make up the vast majority of the microtunneling installations in the United States to date.

3.2.1 Centrifugally Cast Fiberglass Reinforced Polymer Mortar (CCFRPM) – Hobas

Hobas pipe is made from glass fibers, polymer, resin, mortar, and sand, and is manufactured using a centrifugal casting process. The pipe wall structure is built from the exterior to the interior surface within an external rotating mold. While the mold is rotating at a relatively slow speed, the thermosetting resin, reinforcing glass fibers and aggregates are precisely distributed in specific layers at computer-controlled rates. The resin is specifically formulated to not polymerize during the filling process. When all the material has been positioned, the mold rotational speed is increased to produce centrifugal forces of up to 75-g while the polymerization of the resin begins. These forces compress the composition against the mold causing total de-aeration and full compaction. The cured pipe is then removed from the mold. (Hobas, 2005).

This centrifugal casting process is different from any other jacking pipe and allows for the manufacture of very straight pipe sections, which is extremely beneficial in the pipe jacking process. Hobas pipe can be manufactured to specific jacking capacities by adding extra layers of material during the casting process, producing a thicker-walled pipe that can withstand a higher jacking load.

As with all jacking pipes, the jacking joint has a flush outer wall. The Hobas joint contains a milled end that has a recessed portion containing a gasket. The end is then fitted with a fiberglass sleeve that is flush with the outer diameter of the pipe wall. This creates the bell end of the pipe. Hobas pipe is the only jacking pipe that has a fiberglass bell. Other jacking pipes have a steel (stainless or carbon) or concrete bell section. For added strength, a layer of fiberglass reinforcing is placed on the outer surface of the sleeve and over the outer surface of the first six (6) inches of the pipe. This protects the

joint during jacking and prevents material from embedding under the fiberglass sleeve, causing the sleeve to break in tension.

The male or spigot end is also milled with a recess for the gasket. A gasket is applied and the joint is connected in the field during microtunneling. Figure 3.1 shows a detail of the Hobas joint and a photograph of the joint prior to connection on a microtunneling project.

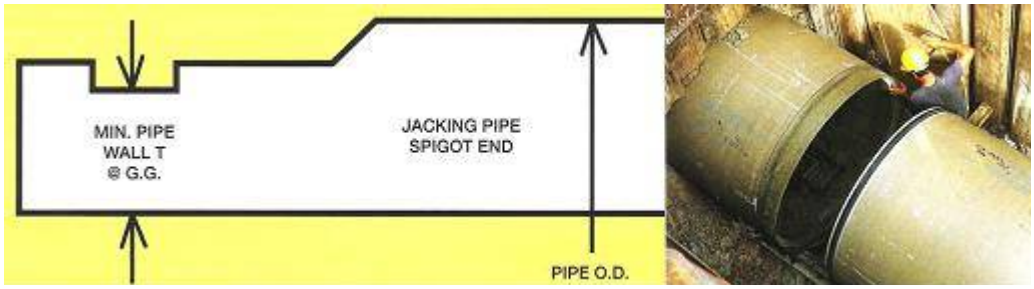

(a) (b)

Figure 3.1. (a) Hobas joint. (b) Hobas Jacking Joint During Connection (Hobas Pipe USA, 2005).

3.2.2 Polymer Concrete Pipe – Polycrete

Polymer Concrete pipe is a composite material containing polyester resin, quartz sand, silicate aggregate, and quartz filler. The pipe is manufactured in a vertical casting process using sets of vertical forms. Precise amounts of materials, controlled by computers, are mixed and loaded into the vertical molds. Vibratory compaction is used to densify the material within the mold, as shown in Figure 3.2.

Figure 3.2. Vertical Molds Casting Polycrete Pipe (Amitech USA, 2005).

The standard Polycrete joint for microtunneling and pipe jacking includes a stainless steel collar that is recessed into the pipe wall. The stainless steel collar mates with a rubber gasket that is beneath the collar, on pipes in the diameter range of eight (8) to 45 inches, or is glued on the pipe with epoxy on pipes in the diameter range of 39 to 78 inches. Three different joint designs are manufactured, depending on pipe diameter.

On all of the jacking joints a plywood compression ring is glued on the load-bearing end of the pipe and shipped with the product. These plywood rings are commonly used with all microtunneling pipes with the exception of steel. They are commonly referred to as “compression rings” and act to evenly transfer the jacking load across the joint, compensating for any gapping, misalignment, or imperfection in the joint that might result from steering corrections or imperfections in the pipe manufacturing process. A tremendous amount of research has been performed on compression rings to show their value in evenly distributing load at jacking pipe joints (Stein, 2005). Their purpose is to minimize any point loading that might occur at the joint.

Polycrete manufacturers in the United States supply these plywood compression rings with the pipe. Other manufacturers, such as Hobas or concrete pipe manufacturers, rely on the contractor to fabricate the plywood rings and apply them in the field. Figure

3.3 shows the three types of Polycrete jacking joints that are available, according to the diameter range manufactured. In all cases the outer-diameter of the pipe is flush-wall.

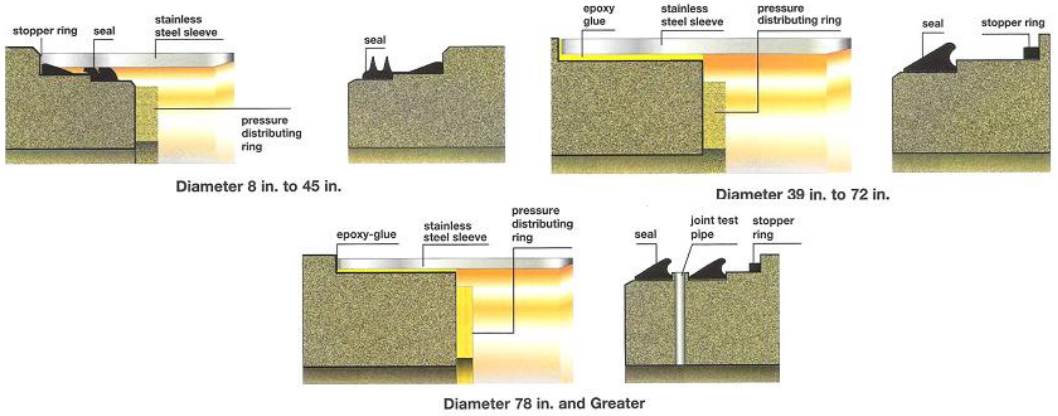

Figure 3.3. Polycrete Jacking Joint Configurations by Pipe Diameter (Amitech USA, 2005).

3.2.3 Vitrified Clay Pipe

Vitrified Clay pipe is comprised of raw clay materials, found in hydrous alumina silicates such as fire clay, shale, and surface clay. Manufacture is a six-step process that includes mining, blending, grinding, and pugging the clay; followed by forming and finishing the pipe. (NCPI, 1998). Once the clays are prepared, the raw blended material is extruded into a mold at a high pressure. The molds are then transferred into a high temperature kiln where the pipe is vitrified at temperatures of over 2000°F. The vitrification process results in a material with compressive strength of approximately 7,000 psi.

The jacking joint is manufactured by grinding a recessed area on each end of the pipe: one for the bell and the other for the spigot. The pipe is fitted with rubber gaskets on both ends and a stainless steel sleeve on the bell end. A plywood compression ring is fitted on the load bearing surface of the bell end of the joint to distribute the jacking

forces. Figure 3.4 shows a joint detail and an 8-foot section of vitrified clay jacking pipe when received at a microtunneling job site.

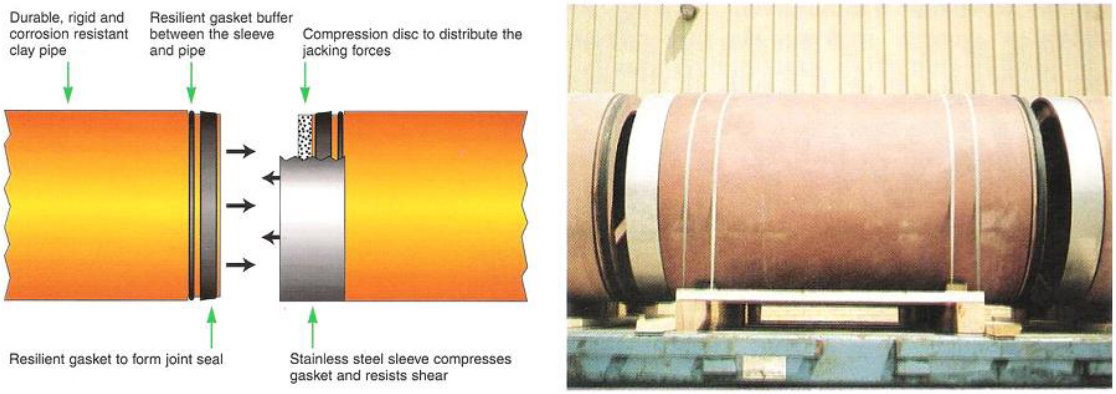

Figure 3.4. Vitrified Clay Pipe Joint Detail and Jacking Pipe after Shipping (Mission Clay Pipe, 2005).

3.2.4 Rolled Steel with Painted Outer Surface and Press-Fit Joint – Permalok

Permalok pipe is rolled steel pipe that is fitted with a machined integral press-fit connection that eliminates the need for welding the pipe in the field. The rolled steel pipe is shipped to the Permalok manufacturer who either mills the ends of the pipe with the Permalok connection or, more commonly, welds the Permalok fitting to the end of the pipe. The pipe is then coated with standard paint to prevent the steel from rusting. It is possible to apply specialized coatings and linings to Permalok pipe; however, jacking bare steel as a casing pipe is the most common application. Figure 3.5 shows the Permalok joint detail. During field installation, epoxy is applied in the joint prior to connecting the Permalok joints to ensure a water-tight connection.

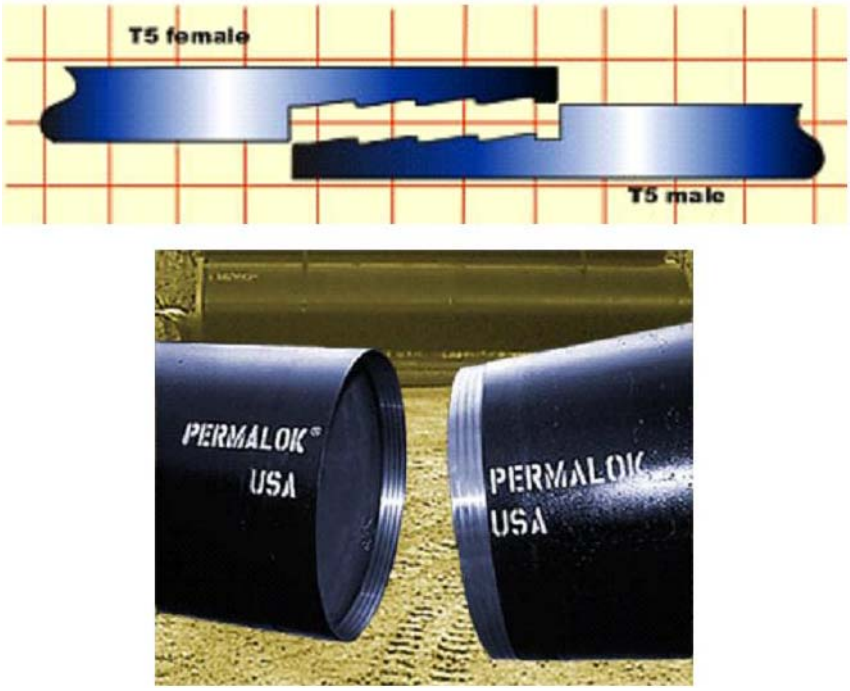

Figure 3.5. Machined Press-Fit Permalok Joint (Permalok USA, 2005).

3.2.5 Concrete Jacking Pipe

Concrete jacking pipe is typically reinforced and can be constructed with or without a reinforcing cylinder. The materials contained in concrete jacking pipe include fine aggregate, coarse aggregate, Portland Cement, reinforcing steel, and water. Concrete pipe is manufactured with five (5) different processes: wet casting, dry casting, vibratory, packerhead, and centrifugal.

Concrete jacking joints are manufactured in a wide variety of styles depending on the pipe manufacturer. Figure 3.6 shows some typical concrete pipe jacking joints.

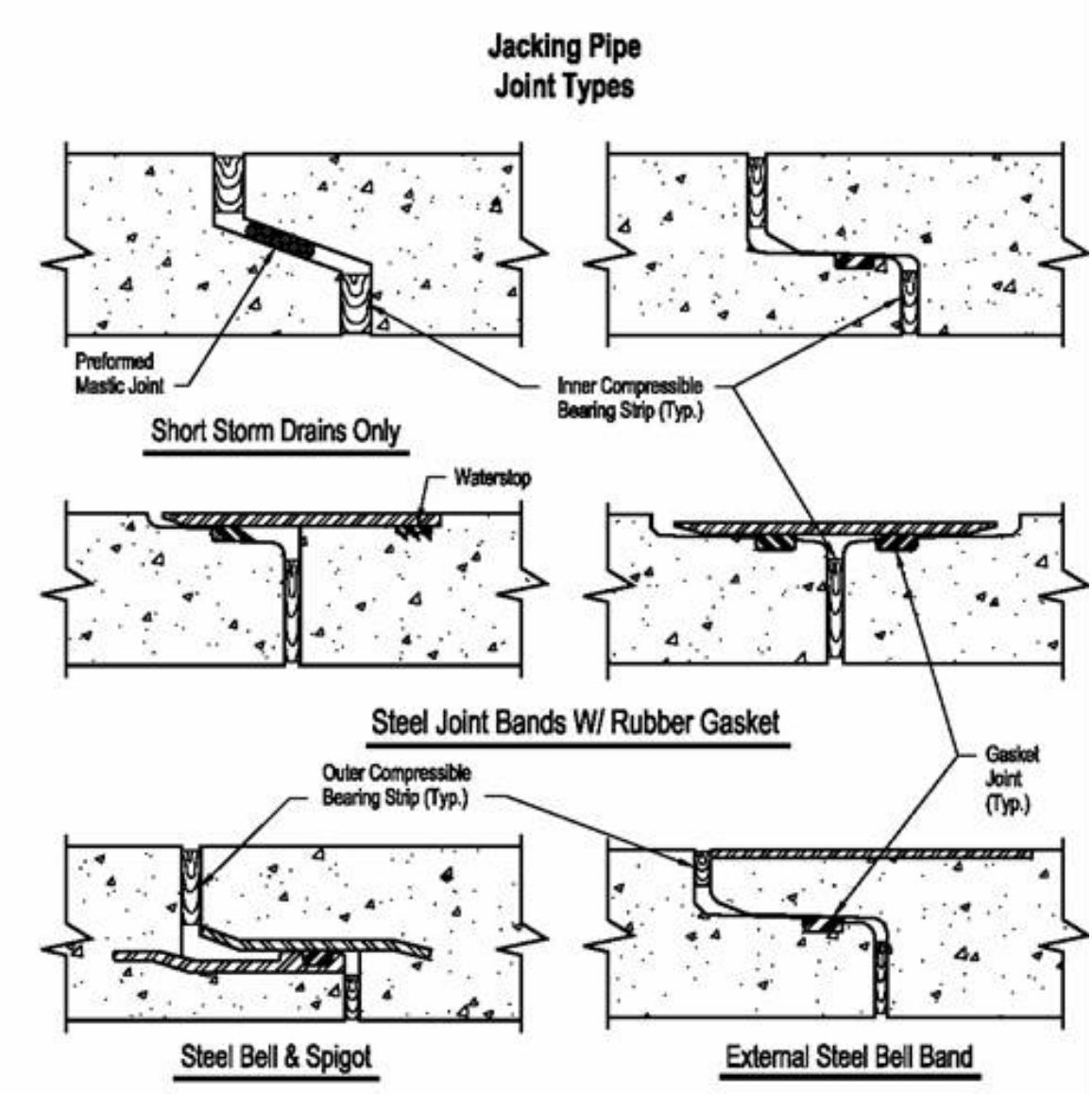

Figure 3.6. Typical Concrete Jacking Pipe Joint Details (www.rinker.com/Hydro Conduit, 2006).

3.2.5.1 Wet Cast Concrete Pipe

Wet Cast Concrete pipe is manufactured by pouring a wet concrete mix into a form that is most commonly mounted in the vertical position. A cone attached to the inner form is used to direct the concrete mix. As the mix is placed in the form it is vibrated using both internal and external vibrators. After the form has been filled, the

cone is removed and the pipe is allowed to cure, typically overnight. The form is then removed and the pipe is moved to a storage area. (OCPA, 2004).

3.2.5.2 Packerhead Concrete

Concrete jacking pipe manufactured with the packerhead process uses a vertical shaft with a circular packing head on the bottom. The shaft and packing head rotate at a high speed as the interior surface of the pipe forms. The form is drawn up through the inside as mix is fed from above. The head has rollers or deflectors mounted on the top which compact the concrete mix. When compaction is complete, the form and pipe are moved to a curing area where the exterior form is removed. (OCPA, 2004)

Some packerhead processes include a vibrating core that follows the packerhead through the pipe-making sequence. The vibrating core is mounted in a pit below the pipe machine and is retracted before the pipe is moved. In other processes, a counter-rotating rollerhead is used. The counter-rotating head is essentially two heads rotating in opposite directions to neutralize any torque transferred to the pipe during the casting process (OCPA, 2004). Figure 3.7 depicts a packerhead producing a concrete pipe and a jacking frame which is jacking Packerhead Concrete on a microtunneling project.

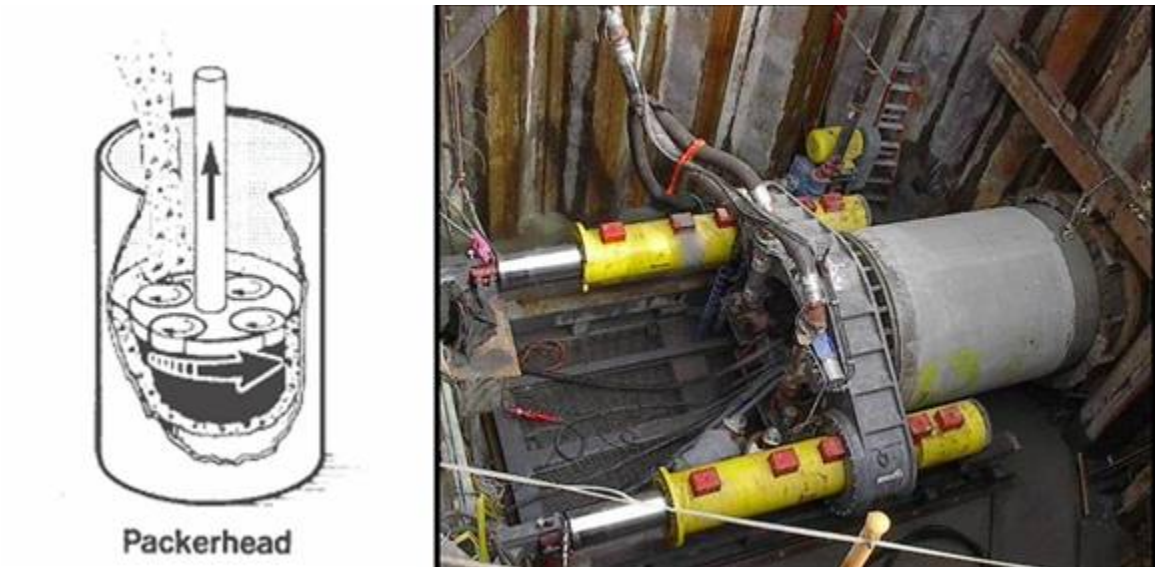

(a) (b)

Figure 3.7. (a) Packerhead Assembly. (OCPA, 2004) (b) Jacking Packerhead Concrete.

3.3 Pipe Surface Roughness Characterization

Material surface roughness has been shown to play a role in interface shear mechanisms and shearing behavior (Dove, 1998). Methods for measuring and quantifying surface roughness have been developed with the advent of automated profiling devices that enable quantitative characterization of the material.

3.3.1 Surface Roughness Parameters

A wide range of measurement parameters have been developed, which has resulted in the emergence of a large number of international standards which address measurement techniques and parameters being proposed (Ward, 1999). However, most of the parameters were developed for specific applications, and therefore are not universally

applicable (DeJong, 2001). DeJong and Frost (2002) have summarized the most common parameters used to characterize surface roughness in Table 3.1.

Table 3.1. Summary of Conventional Surface Roughness Parameters (DeJong and Frost, 2002).

Symbol	Name	Definition	Horizontal Distribution	Vertical Distribution	Relative Aspect
R_a	Average Roughness[1]	$R_a = \frac{1}{L}\int_0^L \lvert z(x)\rvert dx$ where z(x) is a profile height function and L is the evaluation Length		X	
R_q	Root Mean Square (RMS) Roughness[1]	$R_q = \left(\frac{1}{L}\int_0^L Z(x)^2 dx\right)^{\frac{1}{2}}$		X	
R_{sk}	Skewness[1]	$R_{sk} = \frac{1}{R_q^3}\cdot\frac{1}{L}\cdot\int_0^L \left(Z(x)\right)^3 dx$		X	
R_{ku}	Kurtosis[1]	$R_{ku} = \frac{1}{R_q^4}\cdot\frac{1}{L}\cdot\int_0^L \left(Z(x)\right)^4 dx$		X	
Δ_a	Average Slope[1]	$\Delta_a = \frac{1}{L}\int_0^L \left\lvert\frac{dZ}{dx}\right\rvert dx$	X	X	
Δ_q	Root Mean Square (RMS) Slope[1]	$\Delta_q = \left[\frac{1}{L}\int_0^L \left(\frac{dZ}{dx}\right)^2 dx\right]^{\frac{1}{2}}$	X	X	
λ_a	Average Wavelength[1]	$\lambda_a = 2\cdot x\cdot\frac{R_a}{\tan(\Delta_a)}$	X	X	
λ_q	Root Mean Square (RMS) Wavelength[1]	$\lambda_q = 2\cdot x\cdot\frac{R_q}{\tan(\Delta_q)}$	X	X	
$R_{\max}$	Maximum Peak to Valley Roughness[1]	Largest Single Peak to Valley Height		X	
R_p	Maximum Peak to Mean Line Roughness[1]	Largest Single Peak to Mean Line Height		X	
R_t	Mean Line to Lowest Valley Roughness[1]	Largest Mean Line to Valley Roughness		X	
R_n	Normalized Roughness Parameter[3]	$R_n = \frac{R_{\max}(L = D_{50})}{D_{50}}$		X	X
R_L	Profile Roughness Parameter[4]	$R_L = \frac{L_o}{L}$	X	X	

Symbol	Name	Definition	Horizontal Distribution	Vertical Distribution	Relative Aspect
		Where L_o is actual Profile Length and L is Projected Profile Length			
R_S	3-D Surface Roughness Parameter[4]	Actual Surface Area Divided by Projected Surface Area	X	X	
S_m	Average Feature Spacing[1]	$S_m = \frac{1}{n}\sum_{i=1}^{n} S_{mi}$ where S_{mi} is the mean spacing between profile irregularities	X		

[1]ASME B46.1, 1995
[2]Thomas, 1999
[3]Uesugi and Kishida, 1986b
[4]Gokhale and Underwood, 1990

The most universally accepted parameter for quantifying surface roughness is the average roughness, R_a, defined as:

$$R_a = \frac{1}{L}\int_0^L |z(x)|dx \tag{3.1}$$

where: L is the sample length and z is the absolute height of the profile from the mean line (Ward 1999). The average roughness parameter only considers the vertical distribution of the surface features and does not consider the horizontal distribution. This is common to many of the surface roughness parameters, as can be seen in Table 3.1.

3.3.2 Surface Measurement Device

To characterize the surface roughness of each pipe material, a Taylor-Hobson Form Talysurf Series-2 Stylus Profilometer was used. This device uses a contacting needle-like stylus that traverse across the surface of the pipe at a constant rate while taking measurements of the vertical position of the tip of the stylus. A 2 micrometer, 60° diamond tip was fitted to the end of the 120 mm-RS-3120 stylus arm. During each traverse, the tip of the stylus traversed 50 mm across the surface of the pipe, creating a

representative surface profile. The vertical position of the stylus was recorded by an automated data acquisition system with a horizontal increment distance of 0.001 mm between readings. 32 nanometer resolution was achieved with a vertical gauge range of 2.1 mm. The minimum traverse speed was 0.5 mm/sec. Figure 3.8 shows the Stylus Profilometer.

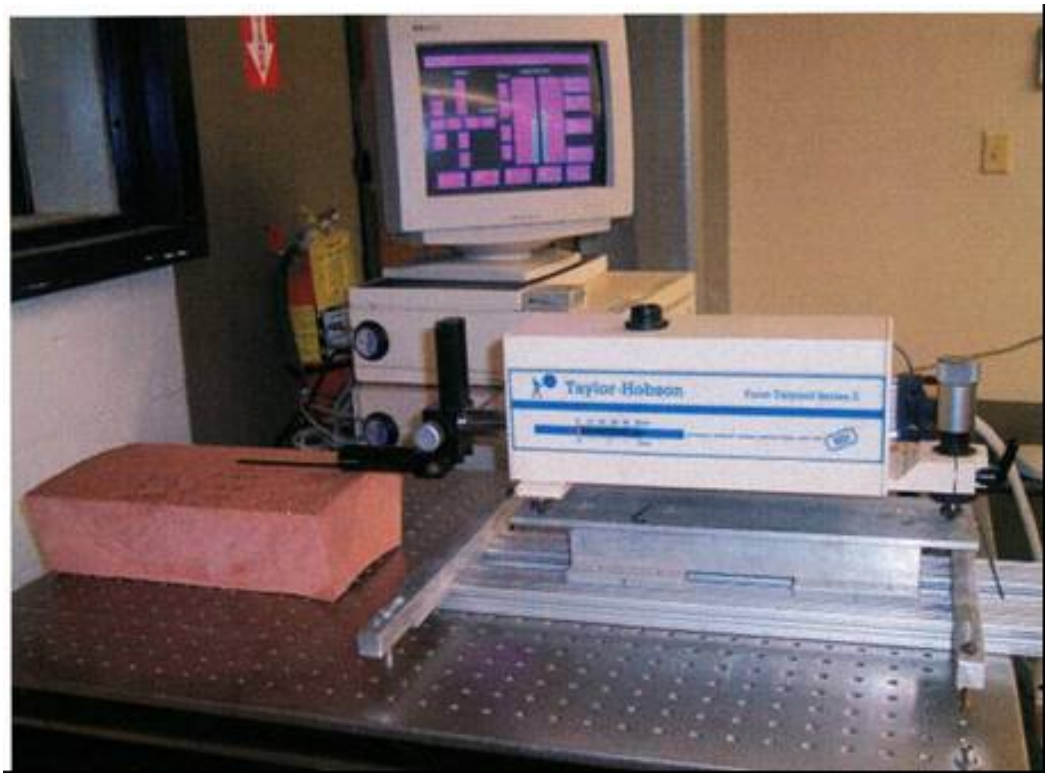

Figure 3.8. Taylor-Hobson Talysurf Series-2 Stylus Profilometer (Iscimen, 2004).

3.3.3 Characterization Testing Program

Profiles were measured at six locations for each pipe material, marked (A) through (F). At each of these locations, five surface profiles were completed for each pipe material. In addition, the surface profile marked (A) was repeated five times. This was performed to determine the repeatability of the measurement and to ensure that the trace

of the profilometer was not altering the surface of the pipe. A total of 54 surface profiles were generated for each pipe material. Figure 3.9 shows a diagram with the typical arrangement for the profilometer tests.

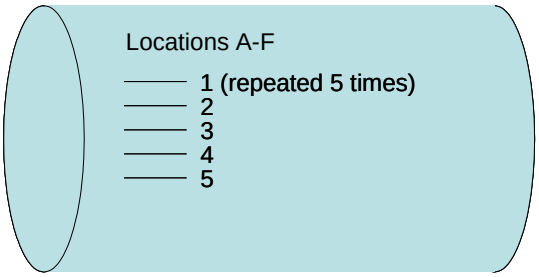

Figure 3.9. Diagram Showing Typical Arrangement of Surface Trace Measurements.

From the stylus profilometer surface profile, the average roughness, R_a, was determined for each trace. Figures 3.10 shows the pipe samples from which measurements were made with the Stylus Profilometer. Approximately one year after the tests were completed, additional testing was performed by Iscimen (2004), who conducted shear tests between the pipe samples and soils. Iscimen began his studies by attempting to repeat some of the surface profile measurements that had been completed as part of this study. However, inconsistencies in the data were observed. This led Iscimen to investigate the calibration and condition of the stylus profilometer equipment.

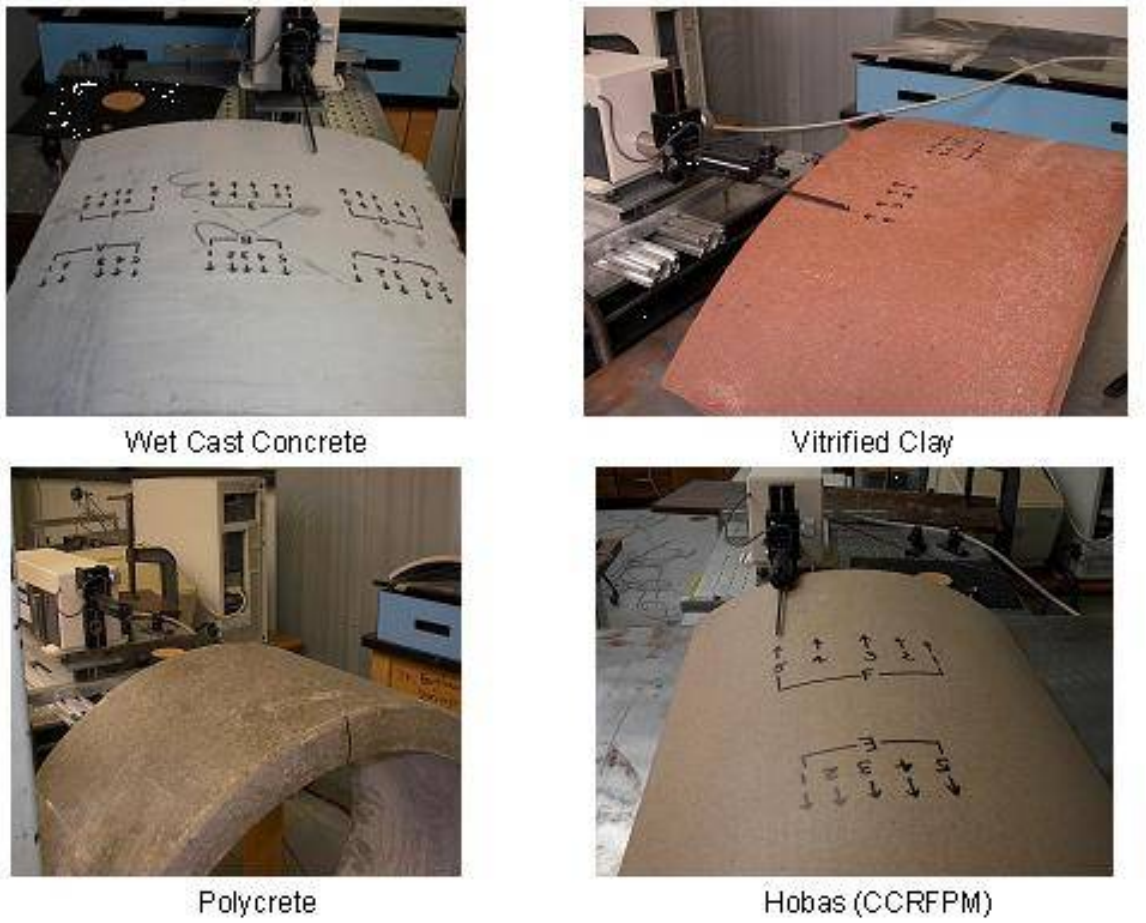

Figure 3.10. Pipe Materials for Surface Characterization.

Iscimen examined the stylus under a microscope and found that the tip of the stylus was significantly worn as shown in Figure 3.11. Since the tip is designed to be a 60°, 2-micrometer conical diamond tip in order to measure the asperities on the continuum, it was clear that the stylus required repair. Once the stylus was repaired, as seen in Figure 3.11b, Iscimen re-calibrated the stylus profilometer and performed new measurements on all pipe samples.

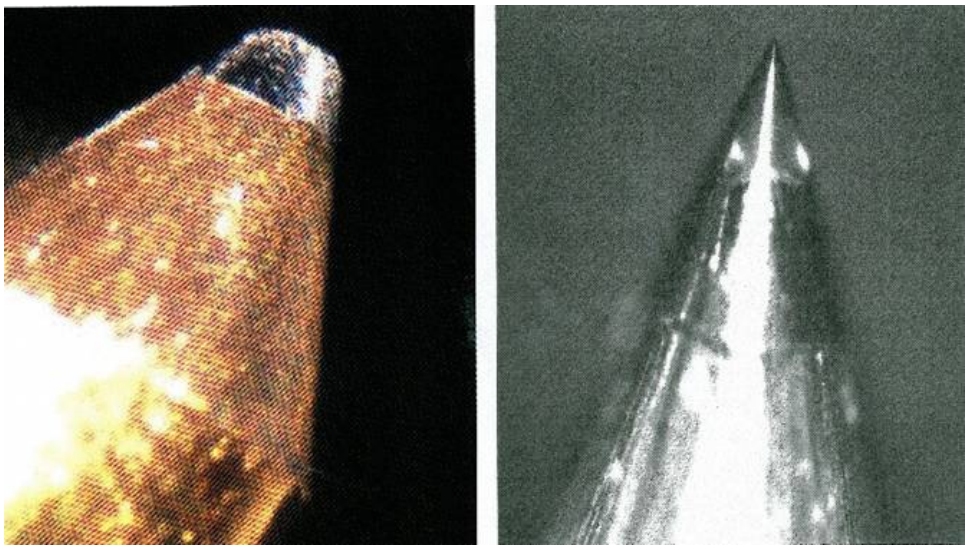

(a) (b)

Figure 3.11. Tip of the Stylus (a) Before Repair and (b) After Repair (Iscimen, 2004).

In addition, Iscimen created two artificially rough surfaces by gluing sandpaper No. 60 and sandpaper No.36 to a piece of Hobas pipe. These artificially rough surfaces helped to broaden the range of surface roughness for analysis. Figure 3.12 shows the artificially created rough surfaces.

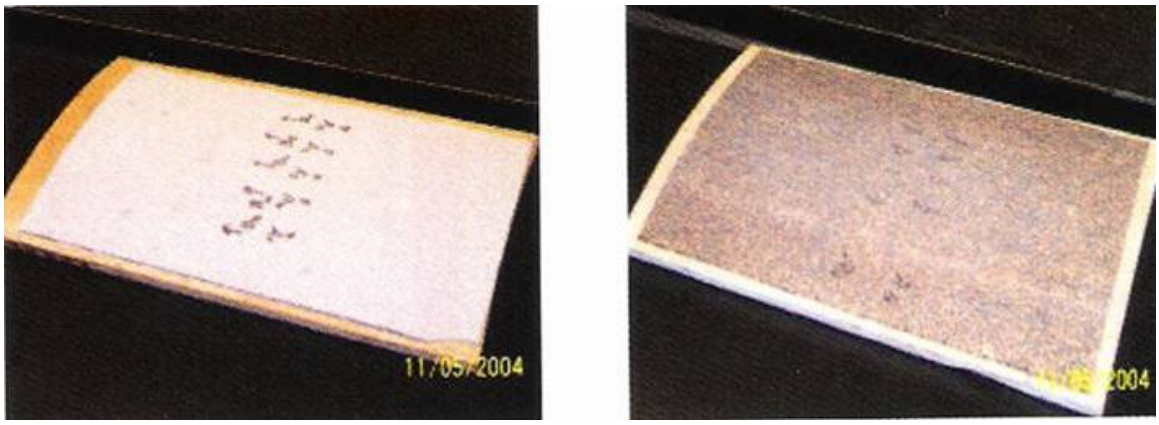

(a) (b)

Figure 3.12. Artificially Rough Surfaces (a) Sandpaper No. 60 and (b) Sandpaper No. 36 (Iscimen, 2004).

3.3.4 Results of Pipe Surface Roughness Characterization

The surface profiles for the pipe material tested revealed a range of average roughness values, as well as a range of variations in the average roughness value. Table 3.2 summarizes the average roughness, standard deviation, coefficient of variation, and repeatability. Details of each test measurement can be found in Iscimen, 2004.

Table 3.2. Results of the Average Roughness Tests on Pipe Materials (Iscimen, 2004).

Parameter	**Hobas**	**Poly-crete**	**Perma-lok**	**Wet Cast Concrete**	**Packer-head Concrete**	**Vitrified Clay**	**No. 60 Sand-paper**	**No. 36 Sand-paper**
Average R_a	6.5	16.9	18.7	24.8	55.1	93.8	60.8	143.2
STDEV	1.2	9.4	8.8	19.5	10.6	12.2	4.1	15.7
% Stdev/ Average	18.3	55.3	47.2	78.5	19.2	13.0	6.7	11.0
Repeat-ability	2.7%	1.5%	4.4%	3.7%	2.5%	1.9%	5.7%	1.3%

The surface profiles for each pipe are shown in Figure 3.13. All of the profiles are shown on the same scale to allow the relative roughness of each material to be appreciated.

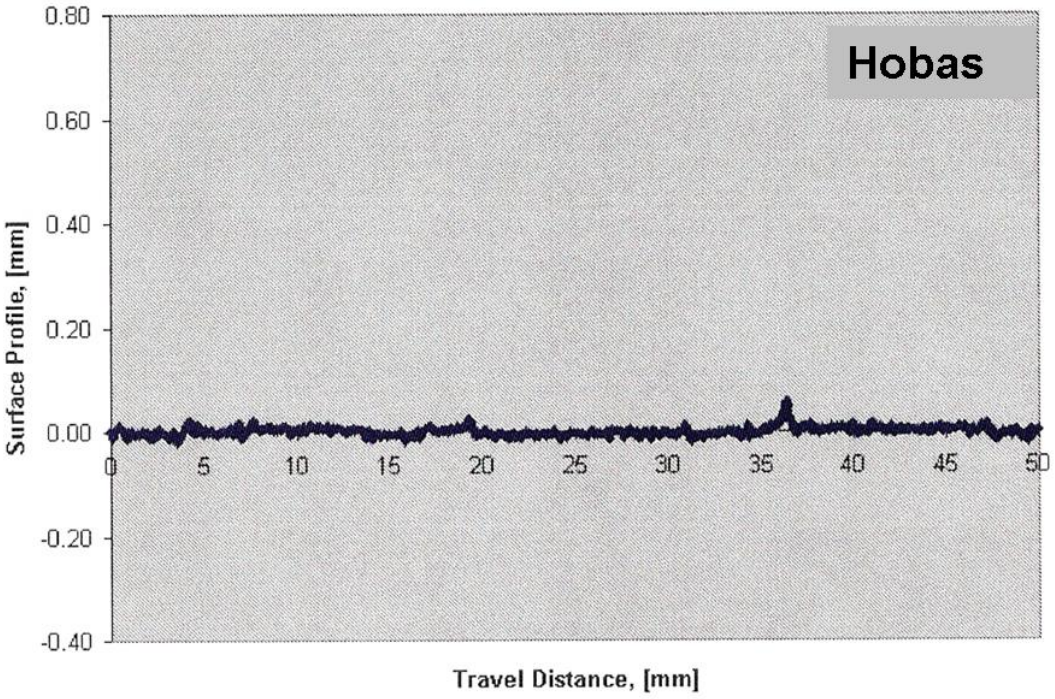

(a) Hobas Surface Profile

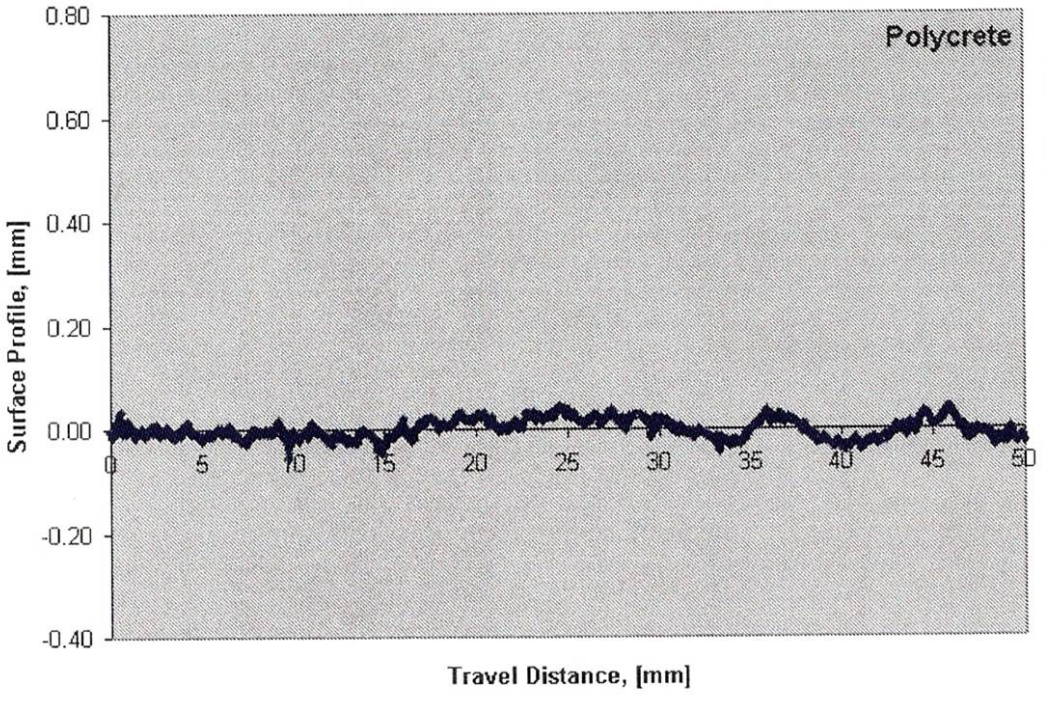

(b) Polycrete Surface Profile

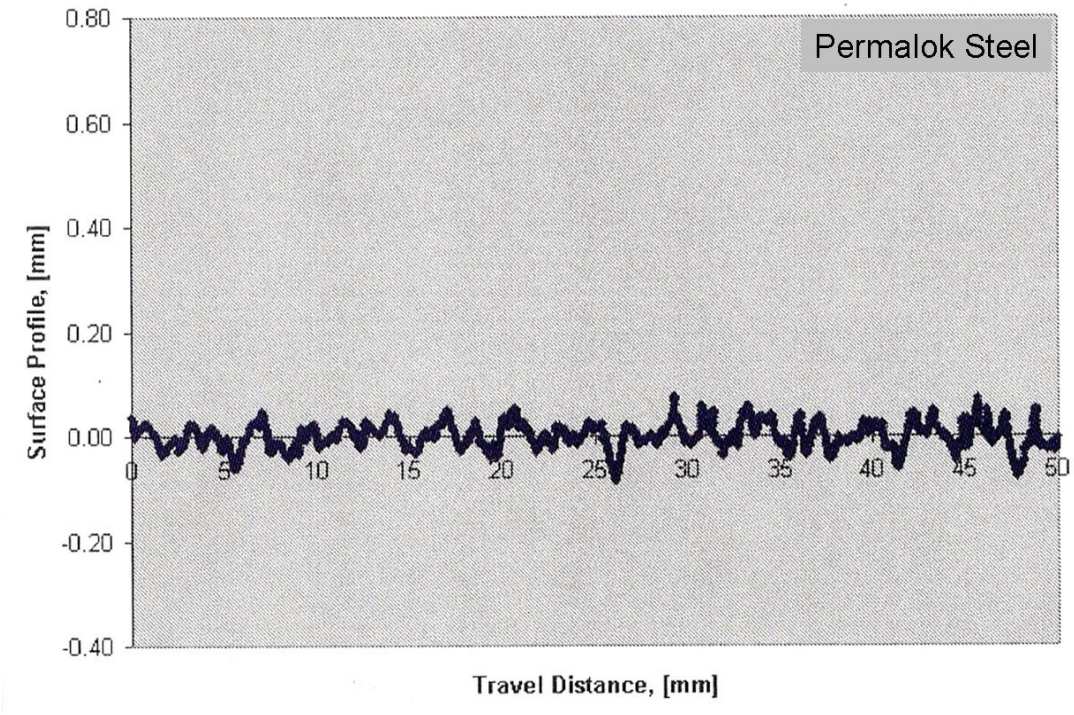

(c) Permalok Steel Surface Profile

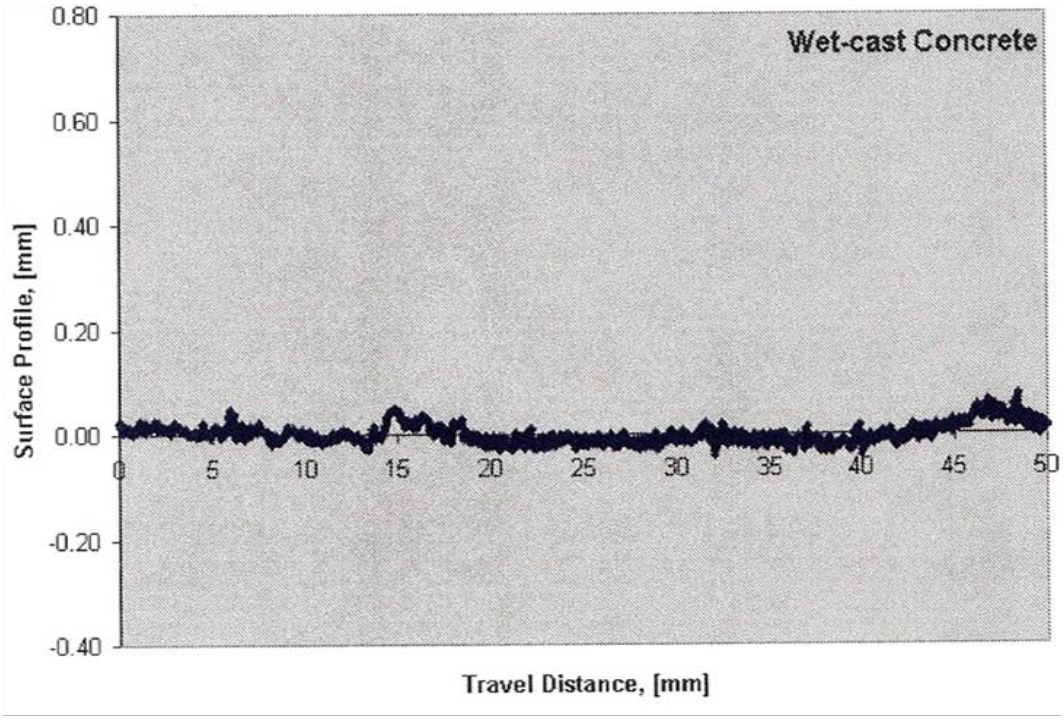

(d) Wet Cast Concrete Surface Profile

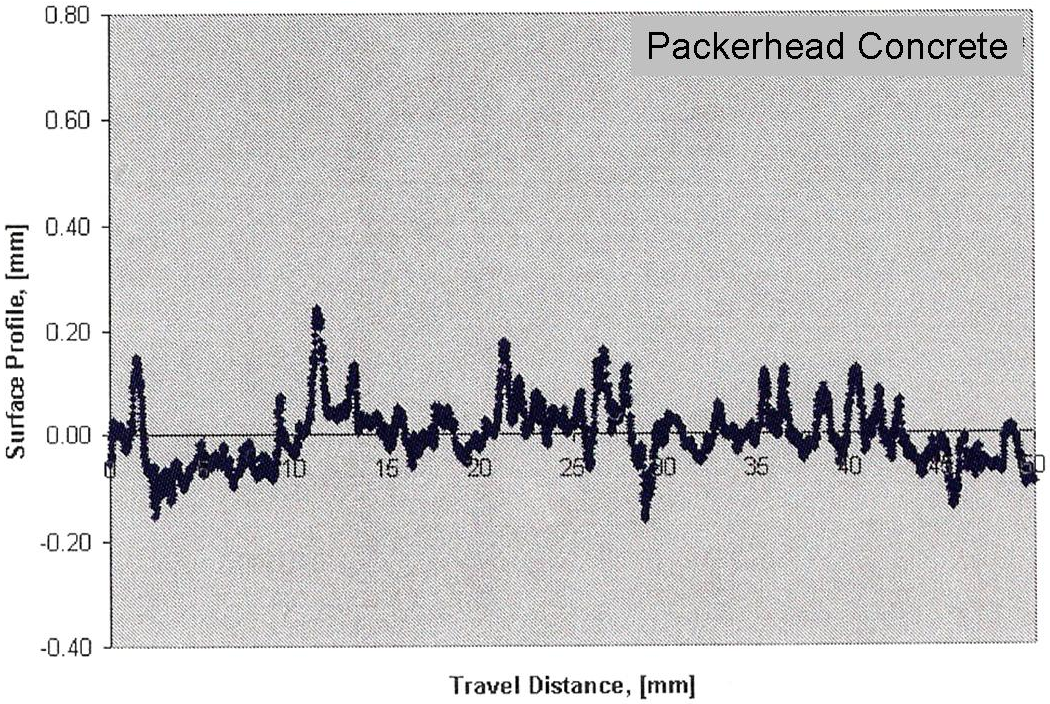

(e) Packerhead Concrete Surface Profile

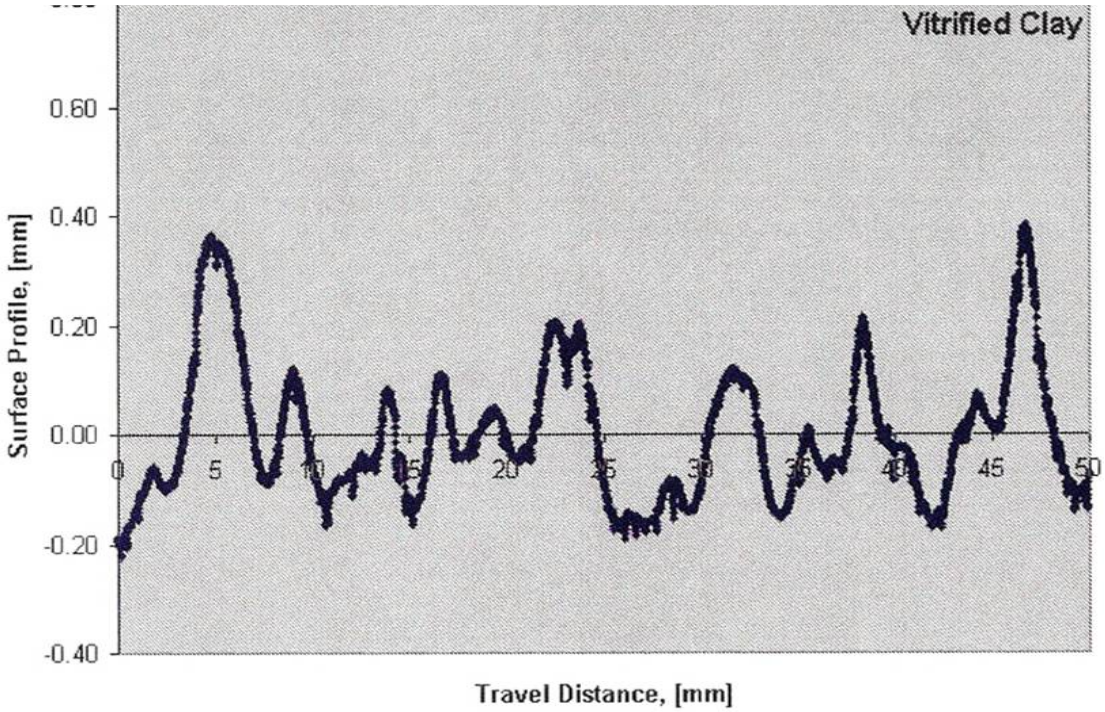

(f) Vitrified Clay Surface Profile

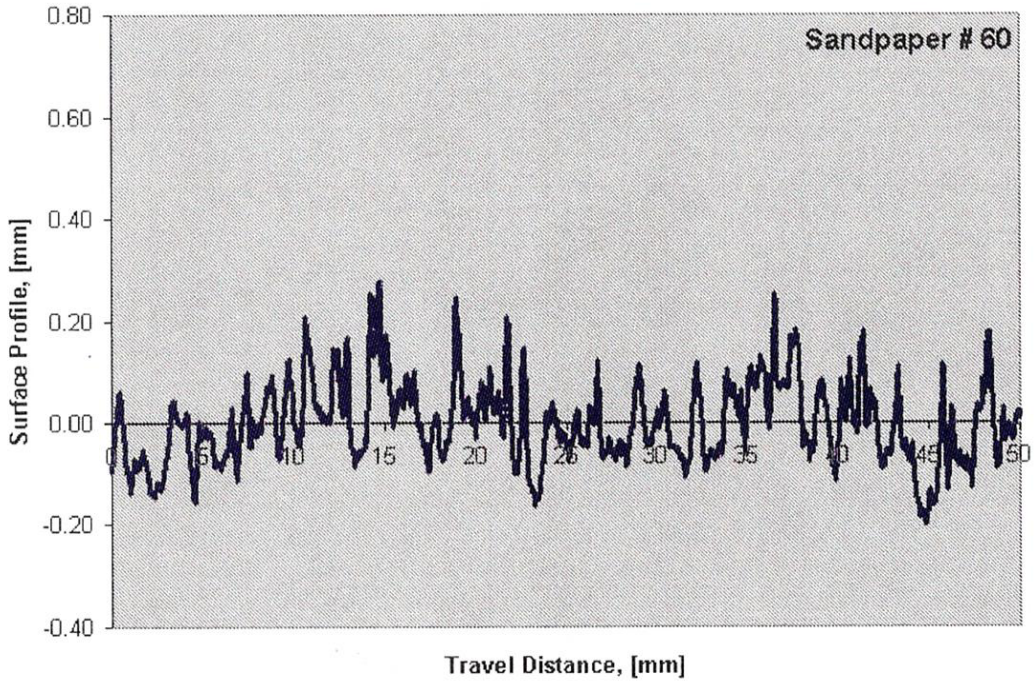

(g) Sandpaper #60 Surface Profile

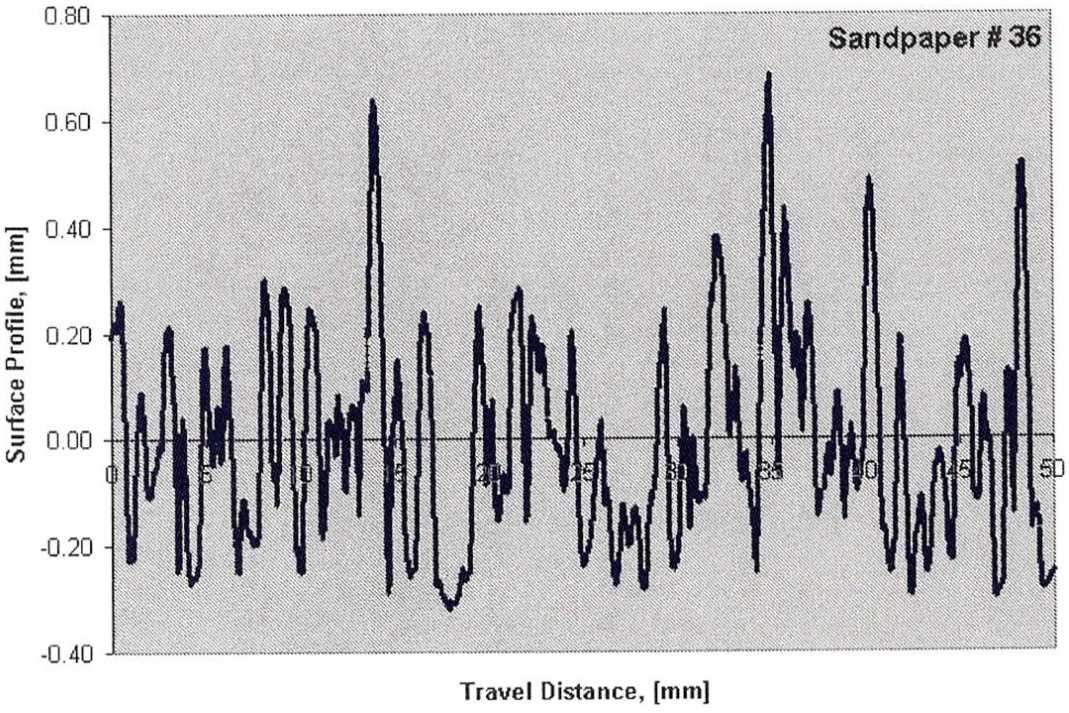

(h) Sandpaper #36 Profile

Figure 3.13. (a) through (h) Surface Profiles for all Materials Tested (Iscimen, 2004).

Some of the pipes had a high variation over the surface area, such as Polycrete, Wet Cast Concrete, and Permalok, whereas others had low variation over the surface, such as Hobas Packerhead Concrete and Vitrified Clay. The average roughness for each of the materials is shown on a single plot in Figure 3.14.

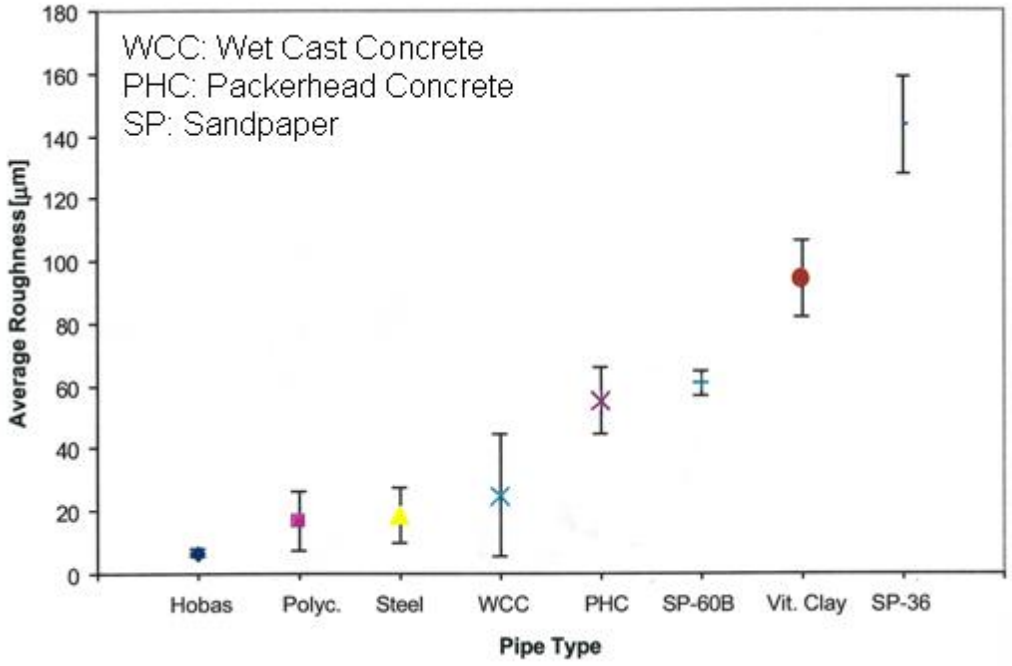

Figure 3.14. Average Roughness for Each Pipe Material and Standard Deviation of Roughness Measurement [μm] (Iscimen, 2004).

3.4 Interface Shear Testing

A series of interface shear tests were conducted to investigate the effects of surface roughness, normal stress, relative density, and particle angularity on shear behavior, and to identify the mechanism of shearing at the interface. All of the pipe materials previously characterized (Hobas, Polycrete, Permalok Steel, Vitrified Clay, Wet Cast Concrete, Packerhead Concrete) and the two artificial surfaces (No.60 and No.36 sandpaper) were included in the shear testing. Two types of sand were used in the test:

Ottawa 20/30, a sub-rounded quartz sand, and Atlanta blasting sand, an angular blasting quartz sand. Shear tests were conducted at five (5) normal stress levels on the Ottawa 20/30 sand: 40, 80, 120, 160, and 200 kPa. Tests on the Atlanta Blasting sand were conducted at 80 kPa. All of the tests were conducted at a target relative density of 80%; however, additional tests were performed at relative densities ranging from 48% to 96% to determine the effect of relative density on the shear behavior of the soil. Although the results are summarized herein, specific details of the testing program can be found in Iscimen, 2004.

3.4.1 Material Properties of the Sands

Two different granular materials were used to determine the effects of angularity on interface shear behavior. These materials were Ottawa 20/30 quartz sand and Atlanta Blasting quartz sand. The index properties of the materials are summarized in Table 3.3.

Table 3.3. Index Properties of Sands used in Shear Testing (Iscimen, 2004).

Material	**D_{50} [mm]**	**C_u [1]**	**C_c [2]**	**G_s [3]**	**e_{max} [4]**	**e_{min} [5]**
Ottawa 20/30	0.64	1.46	0.96	2.65	0.747	0.501
Atlanta Blasting	0.82	1.38	0.77	2.65	1.092	0.734

Note: **1**. $C_u = \frac{D_{60}}{D_{10}}$;

2. $C_c = \frac{D_{30}^2}{D_{10} \cdot D_{60}}$;

3. AASHTO T133;
4. ASTM D4254-91 Method B;
5. ASTM D54253-93 Method 2A

Grain size distribution curves for the Ottawa 20/30 and Atlanta Blasting sands are shown in Figure 3.15.

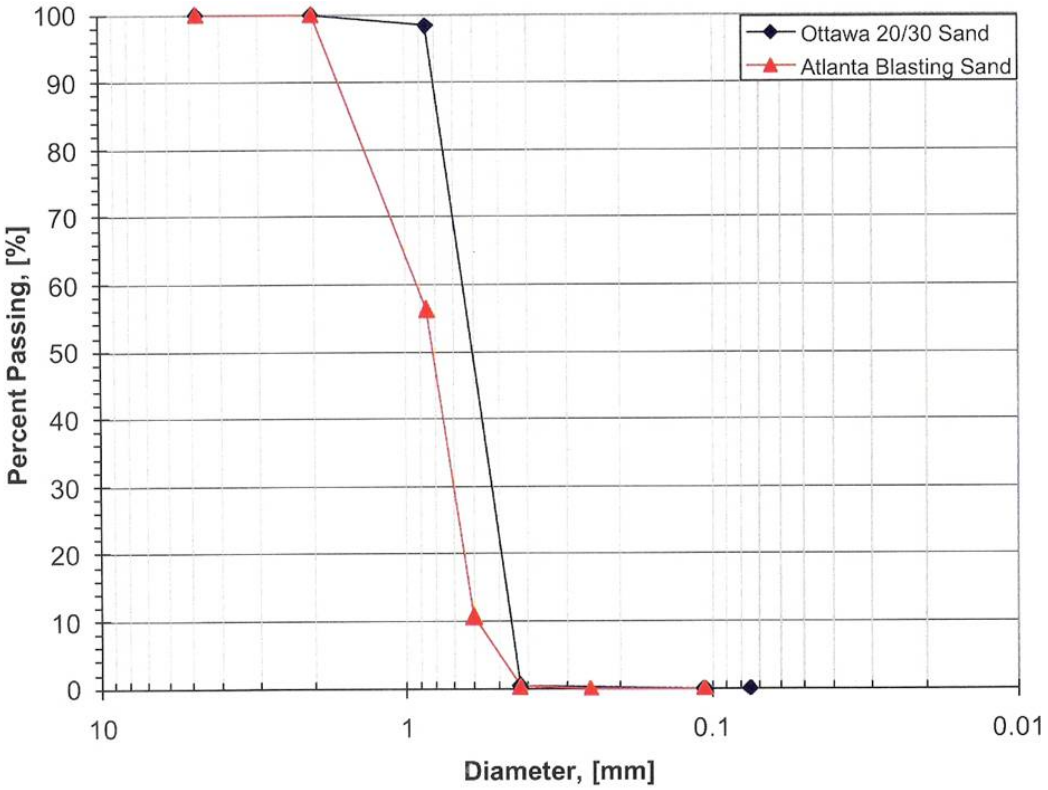

Figure 3.15. Gradation Curve for Ottawa 20/30 and Atlanta Blasting Sands (Iscimen, 2004).

Figure 3.16 shows an image of the particles for each of the sands used in the shear testing.

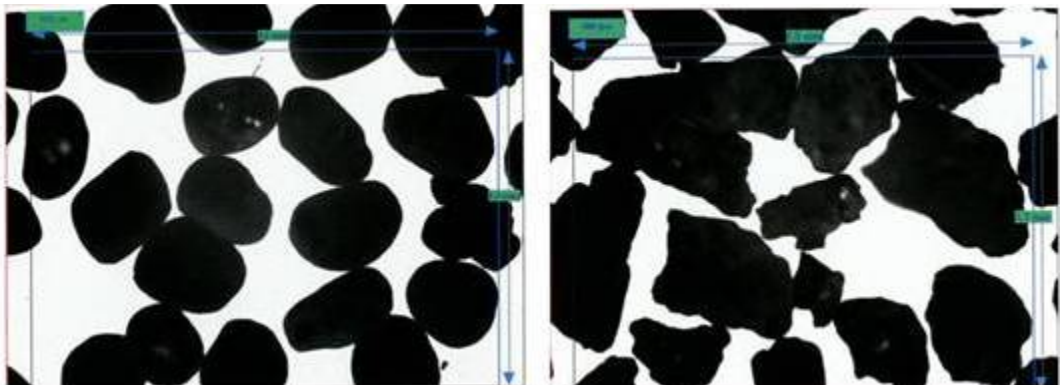

(a) (b)

Figure 3.16. Particle Image for (a) Ottawa 20/30 quartz sand and (b) Atlanta Blasting quartz sand (Iscimen, 2004).

Direct shear tests were performed on both Ottawa 20/30 and Atlanta Blasting sands at 80, 120, and 160 kPa so that the interface shearing characteristics could be compared to the internal shearing characteristics of the soils. The specimens were prepared using air pluviation technique (Frost and Park, 2003) with a targeted relative density of approximately 80%. Results of the direct shear tests are shown in Table 3.4. Details of the tests, including shear force versus horizontal displacement curves, can be found in Iscimen, 2004.

Table 3.4. Peak and Residual Friction Angles Obtained from Direct Shear Tests.

	Ottawa 20/30 Sand	**Atlanta Blasting Sand**
Peak Friction Angle, ϕ_p	38.9°	43.1°
Residual Friction Angle, ϕ_r	27.9°	34.6°

3.4.2 Interface Shear Testing Apparatus

The interface shear tests were performed on a large-displacement constant-stress shear testing apparatus that was developed at Georgia Institute of Technology (Zettler, 1999). A plan view of the shear device is shown in Figure 3.17. The shear box is driven by a DC motor. Gear reducers allow the user to achieve relatively low speeds. The system is controlled electronically by an encoder and speed control system. End switches limit the travel of the shear box and stop the motor automatically when the desired shear displacement is achieved. The normal load is applied by an air-pressurized piston mounted under the shear table. The piston is able to move horizontally on rails when the shear box moves. The pressure is set manually through a control panel and kept constant with a pressure regulator. The magnitude of the pressure is determined and monitored

by a load cell that is mounted between the load crosshead and the loading plate. (Iscimen, 2004).

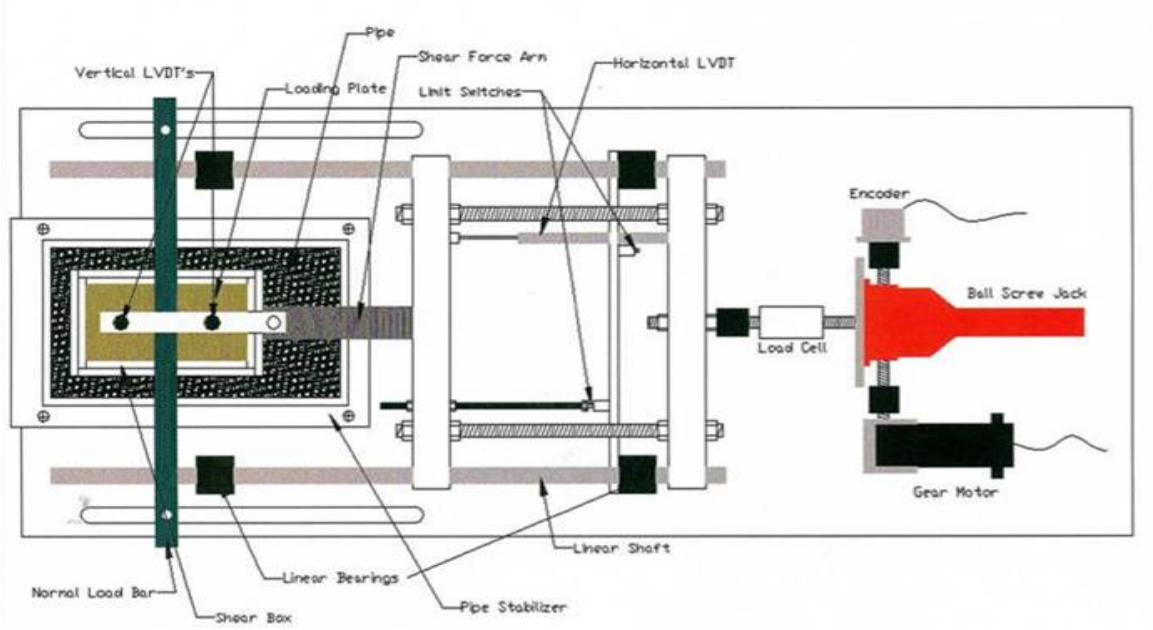

Figure 3.17. Plan view of Large-Displacement Constant-Stress Shear Testing Device (Zettler,1999).

Specific details of the testing apparatus can be found in Zettler, 1999 and Iscimen, 2004. The apparatus was modified to allow interface testing of the pipe coupons within an aluminum container/stabilizer which will be used for future testing as a lubricant pool. Figure 3.18 shows a shear box on top of a pipe coupon.

Figure 3.18. Shear Box on Wet Cast Concrete Pipe Sample (Iscimen, 2004).

A plan view and end view of the interface shear device with the modifications to accommodate the pipe samples is shown in Figure 3.19 and 3.20.

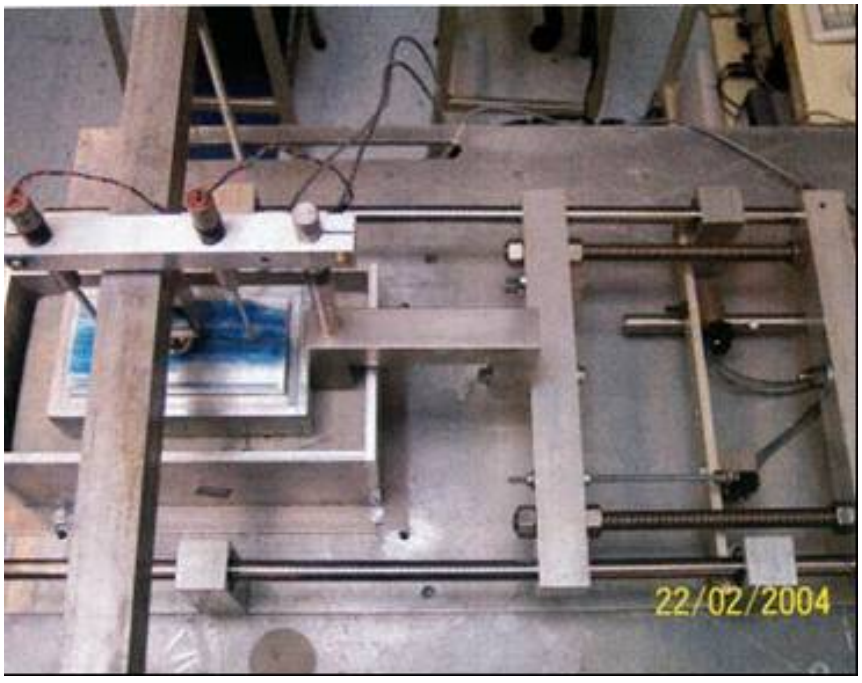

Figure 3.19. Plan View of Interface Shear Device (Iscimen, 2004).

Figure 3.20. End View of Interface Shear Device (Iscimen, 2004).

3.4.3 Interface Shear Test Results and Discussions

Initial interface shear tests were performed with each pipe material and Ottawa 20/30 sand at normal stresses of 40, 80, and 120 kPa. The average relative density of the soil samples was 79.7% ± 3.8%. At each of the normal load testing condition, as the surface roughness of the pipe increased, the interface friction coefficient increased. The difference between the peak coefficient of friction was more pronounced than the residual coefficient of friction at every normal stress level.

Figures 3.21 through 3.26 show the horizontal displacement versus the interface coefficient of friction for the various pipe materials as they are sheared against Ottawa 20/30 sand at a normal loading condition of 80 kPa. For curves at all other normal loading conditions, refer to Iscimen (2004).

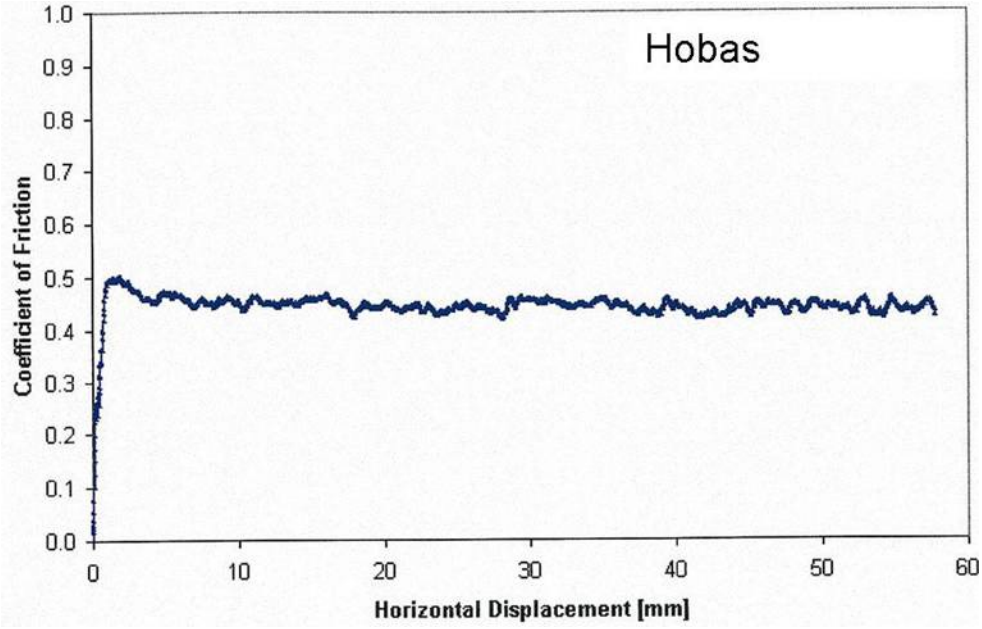

Figure 3.21. Horizontal Displacement vs. Coefficient of Friction for Hobas Pipe Sheared against Ottawa 20/30 Sand at 80 kPa. D_R=79% (Iscimen, 2004).

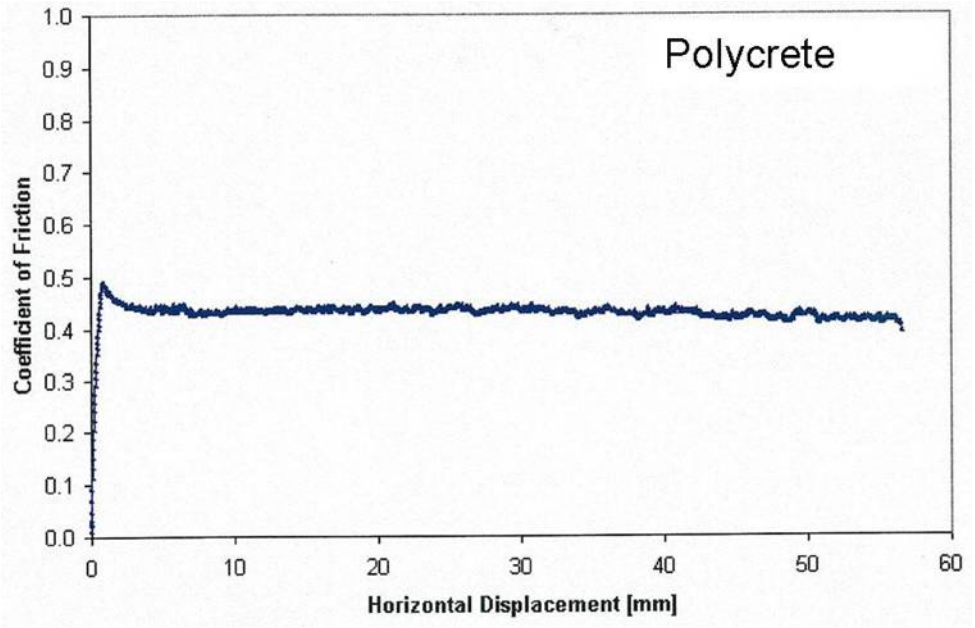

Figure 3.22. Horizontal Displacement vs. Coefficient of Friction for Polycrete Pipe Sheared Against Ottawa 20/30 Sand at 80 kPa. D_R=79% (Iscimen, 2004).

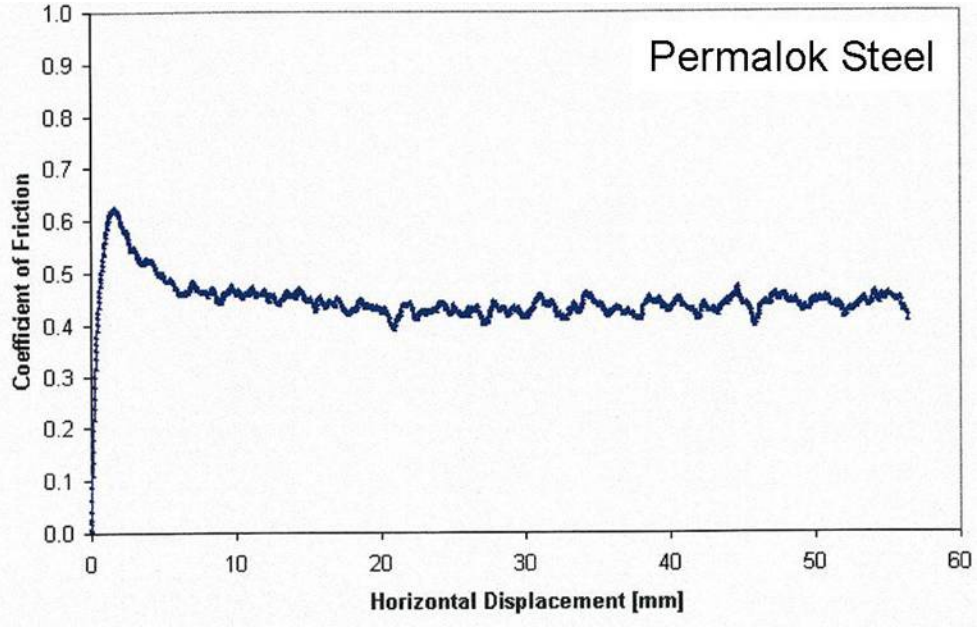

Figure 3.23. Horizontal Displacement vs. Coefficient of Friction for Permalok Steel Pipe Sheared Against Ottawa 20/30 Sand at 80 kPa. D_R=80% (Iscimen, 2004).

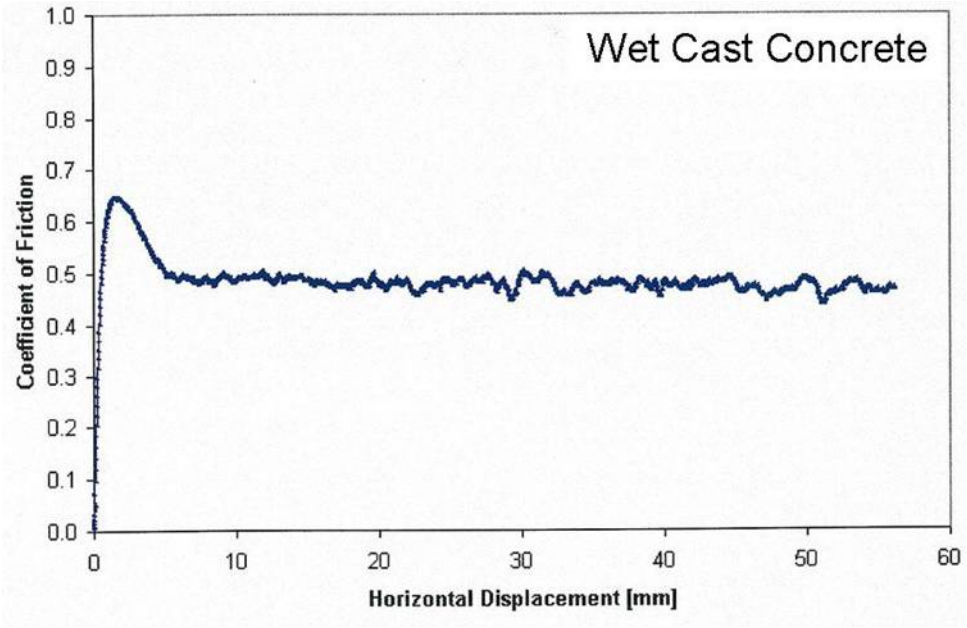

Figure 3.24. Horizontal Displacement vs. Coefficient of Friction for Wet Cast Concrete Pipe Sheared Against Ottawa 20/30 Sand at 80 kPa. D_R=77% (Iscimen, 2004).

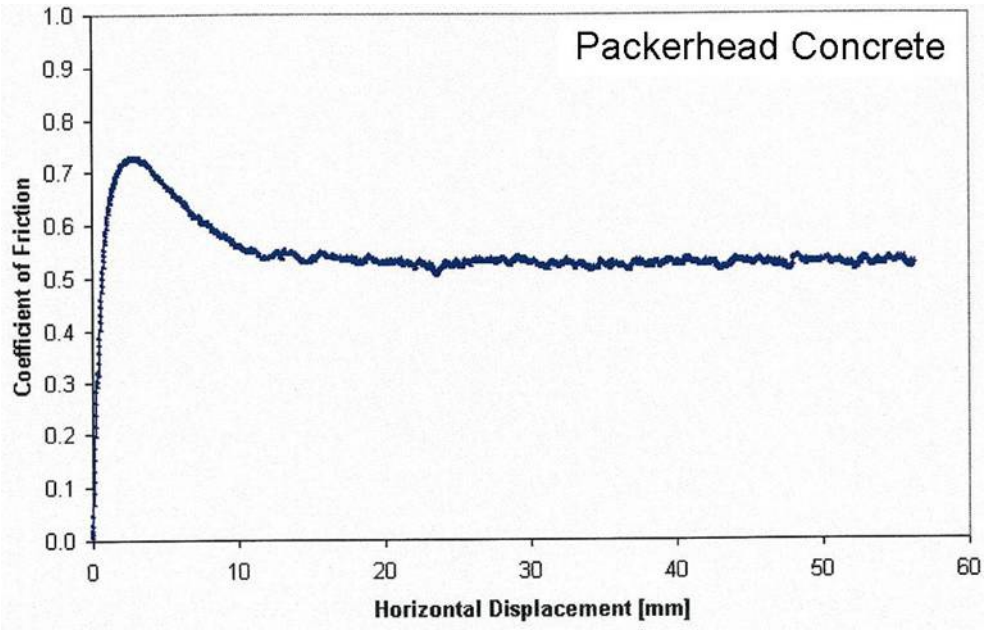

Figure 3.25. Horizontal Displacement vs. Coefficient of Friction for Packerhead Concrete Pipe Sheared Against Ottawa 20/30 Sand at 80 kPa. D_R=80% (Iscimen, 2004).

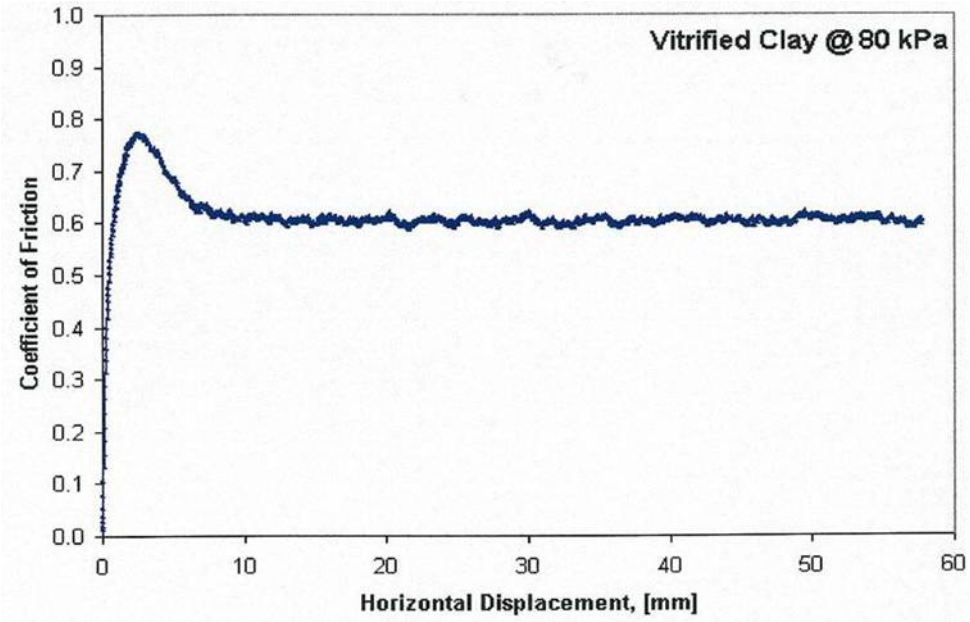

Figure 3.26. Horizontal Displacement vs. Coefficient of Friction for Vitrified Clay Pipe Sheared Against Ottawa 20/30 Sand at 80 kPa. D_R=66% (Iscimen, 2004).

Peak friction values occurred within a relatively small horizontal displacement, with smoother pipes reaching the peak coefficient of friction within a shorter distance than the rougher pipes.

There was a clear post-peak softening for pipes with intermediate and high roughness values, including Permalok Steel, Wet Cast Concrete, Packerhead Concrete, and Vitrified Clay. However, the post-peak softening was not obvious in the smoother pipes including Hobas and Polycrete. This can be attributed to particle sliding on the smoother pipes versus particle rearrangement at the interface of the rougher pipes. This rearrangement occurs until a stable steady state lower bound friction value is reached, representing the residual interface friction value. Results of the shear testing on Ottawa 20/30 sand at 40, 80, and 120 kPa are shown in Table 3.5.

Table 3.5. Peak and Residual Friction Coefficients for Pipe Materials Sheared Against Ottawa 20/30 Sand at Varying Normal Stresses (from Iscimen, 2004).

Pipe Material		**Hobas**	**Polycrete**	**Permalok Steel**	**Wet Cast Concrete**	**Packerhead Concrete**	**Vitrified Clay Pipe**
Average Roughness, R_a [μm]		**6.5**	**16.9**	**18.7**	**24.8**	**55.1**	**93.8**
Coefficient of Friction							
N = 40 kPa	Peak, ϕ_p	0.51	0.50	0.68	0.68	0.81	0.71
	Residual, ϕ_r	0.43	0.42	0.49	0.49	0.54	0.50
N= 80 kPa	Peak, ϕ_p	0.50	0.49	0.62	0.65	0.73	0.63
	Residual, ϕ_r	0.44	0.43	0.44	0.48	0.53	0.48
N= 120 kPa	Peak, ϕ_p	0.48	0.47	0.62	0.63	0.73	0.65
	Residual, ϕ_r	0.42	0.43	0.47	0.45	0.52	0.49

Figures 3.27 and 3.28 show the average roughness vs. the peak and residual coefficient of friction for each pipe material sheared against Ottawa 20/30 sand. The plots show a clear bi-linear relationship and a critical roughness that approximates the internal friction coefficient of the Ottawa 20/30 sand.

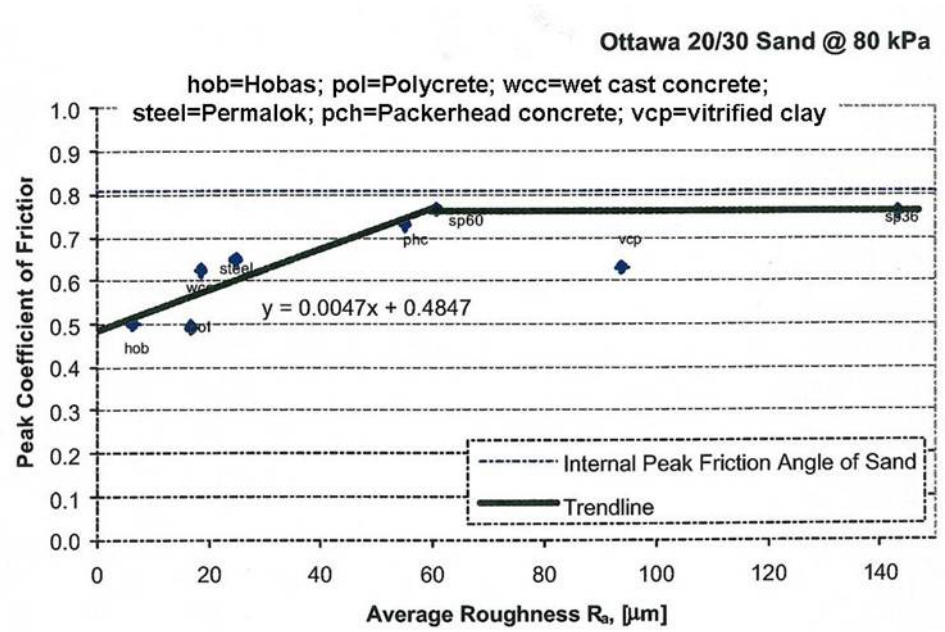

Figure 3.27. Average Roughness vs. Peak Coefficient of Friction for Ottawa 20/30 Sand at 80 kPa (Iscimen, 2004).

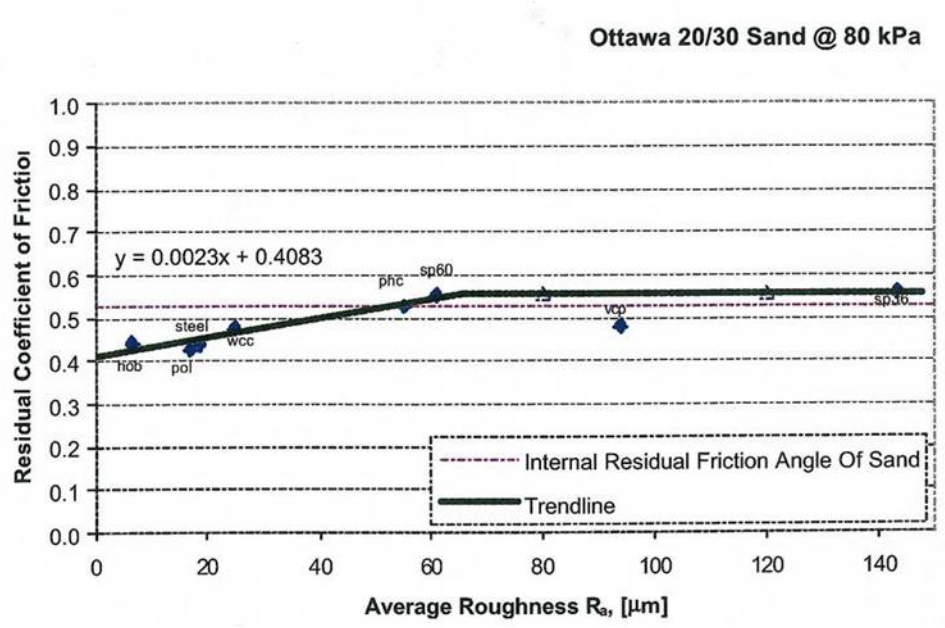

Figure 3.28. Average Roughness vs. Residual Coefficient of Friction for Ottawa 20/30 Sand at 80 kPa (Iscimen, 2004).

Analysis of the shear test results brings forward two interesting phenomena. First, although Polycrete pipe has a higher average roughness than Hobas, the interface friction coefficient at both peak and residual values is slightly less than those values measure for Hobas, with the exception of the residual coefficient of friction at 120 kPa, where Hobas measures 0.42 and Polycrete measures 0.43. This may be attributed to plowing by the soil particles into the Hobas pipe as the hardness of the Hobas, (which is a glass-fiber reinforced material) is lower than the polymer resin concrete, where the plowing effect did not occur.

Second, although Vitrified Clay has the highest value of average roughness, the interface friction coefficient at both the peak and residual states is lower than that of Packerhead Concrete at all normal loads tested and is similar to values measured for Permalok steel and Wet Cast Concrete at normal loads of 120 kPa. This could be attributed to a number of factors: 1) the surface of the Vitrified Clay pipe is much more brittle than the other pipe materials and is susceptible to plowing during shear; therefore, it is possible that the pipe surface is being altered during shearing, or actually becoming smoother during the shearing process. 2) In addition, the surface of the Vitrified Clay is much different than the other pipes in that the asperities are much more spatially distributed, as can be seen in Figure 3.29 with wide horizontal gaps between the peaks and valleys. As such, the average roughness parameter, (which is being used to compare the vitrified clay to the other pipe materials) only takes into account vertical characteristics, and may not provide a good comparison of the vitrified clay to the other pipe materials due to the fact that the surfaces are so characteristically different. The shearing behavior of the Vitrified Clay pipe may be a combination of sliding behavior

that is seen with the smoother pipes in paths or regions between the higher peaks, and particle rearrangement around the peaks prior to reaching the steady state residual shearing behavior. The combination of the shearing mechanisms may result in a lower overall interface coefficient of friction than would be predicted with the average roughness parameter for a pipe that does not display comparatively large horizontal distances between the vertical peaks and valleys on the surface.

Figure 3.29. Close-up of Vitrified Clay Pipe Surface.

3.4.3.1 Effects of Normal Stress

The effects of varying the normal stress can also be seen in Table 3.5 that shows the pipe materials, their average roughness, and their peak and residual coefficient of friction at 40, 80, and 120 kPa.

The trends in the interface shearing behavior were the same for all values of normal stress; however, the post-peak softening on the rougher pipes was more pronounced at the lower normal stress levels indicating that the particles were under less loading, allowing them to move more freely into the steady state residual friction arrangement.

To evaluate the effects of normal stress on the coefficient of interface friction, additional shear tests were conducted on Hobas, Packerhead Concrete, and Vitrified Clay at two additional normal stresses: 160 and 200 kPa. These tests were performed with Ottawa 20/30 sand at a relative density of 80%. Results of these tests are shown in Figures 3.30 and 3.31, plotted on a log-log scale to clearly show the trends.

Figures 3.30 through 3.31 show that the interface coefficient of friction tends to decrease with increasing normal stress until the normal stress reaches approximately 80 kPa where the interface friction coefficient becomes constant. The magnitude of decrease is higher in the peak friction curve than in the residual friction curve. For normal stresses less than 60 kPa, the friction coefficient increases linearly with a decrease in normal load. This can be attributed to a non-linear decrease in contact area with the normal stress. Because the contact area is not decreasing at the same rate as the normal stress, the friction coefficient tends to increase (Archard, 1957).

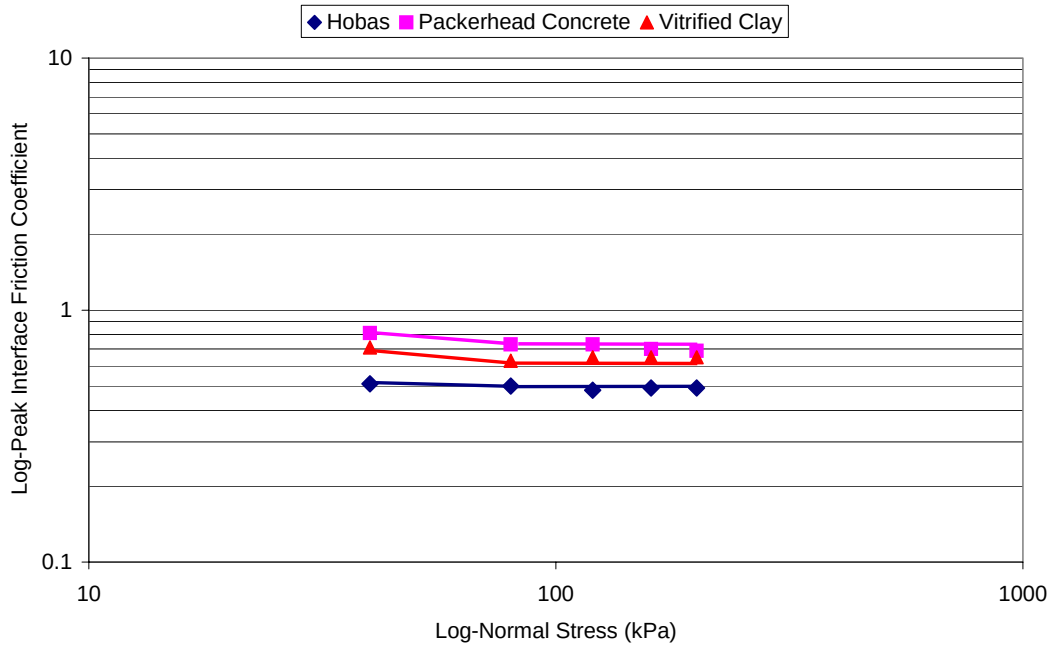

Figure 3.30. Log-Normal Stress vs. Log Peak Interface Friction Coefficient of Ottawa 20/30 Sand with Hobas, Packerhead Concrete, and Vitrified Clay Pipes Tested at a Relative Density of 80% (modified from Iscimen, 2004).

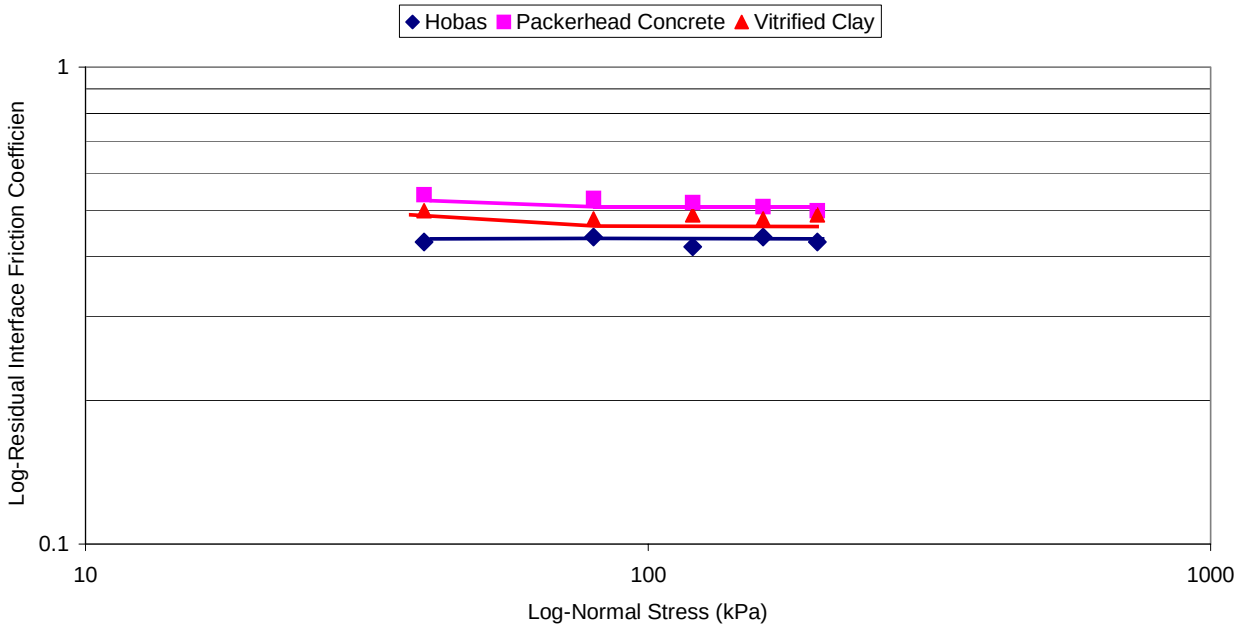

Figure 3.31. Log-Normal Stress vs. Log-Interface Friction Coefficient of Ottawa 20/30 Sand with Hobas, Packerhead Concrete, and Vitrified Clay Pipes Tested at a Relative Density of 80% (modified from Iscimen, 2004).

These findings are consistent with those of Dove and Frost (1999). At normal stresses higher than 60 kPa, the normal stress is high enough to ensure maximum contact of all particles at the surface and the effects of plowing are more pronounced. The coefficient of friction tends to stabilize at the interface, which agrees with the findings of Dove and Frost (1999) for interface frictional behavior between smooth geomembranes and Ottawa 20/30 sand. The effects of plowing were more pronounced on the softer Vitrified Clay and Hobas than on the harder Packerhead concrete.

3.4.3.2 Effects of Angularity

The effects of particle angularity were shown by shearing each pipe material against Atlanta Blasting quartz sand at a normal load of 80 kPa. These results were compared to the previous results of the shearing tests of the pipes against Ottawa 20/30 sand. Figure 3.32 and 3.33 shows the peak and residual coefficient of friction for each pipe material as a function of average roughness.

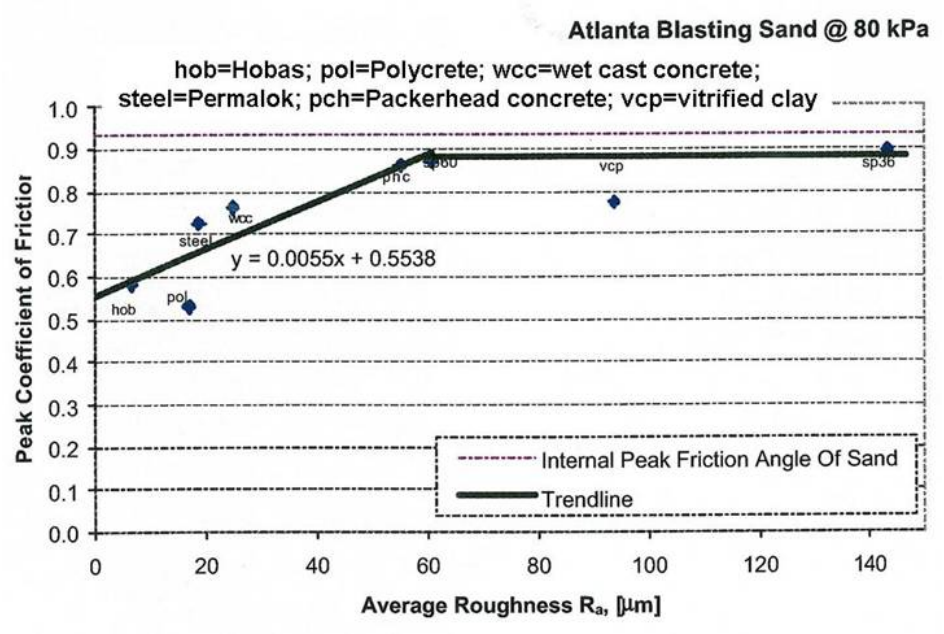

Figure 3.32. Average Roughness vs. Peak Coefficient of Friction for Atlanta Blasting Sand at 80 kPa (Iscimen, 2004).

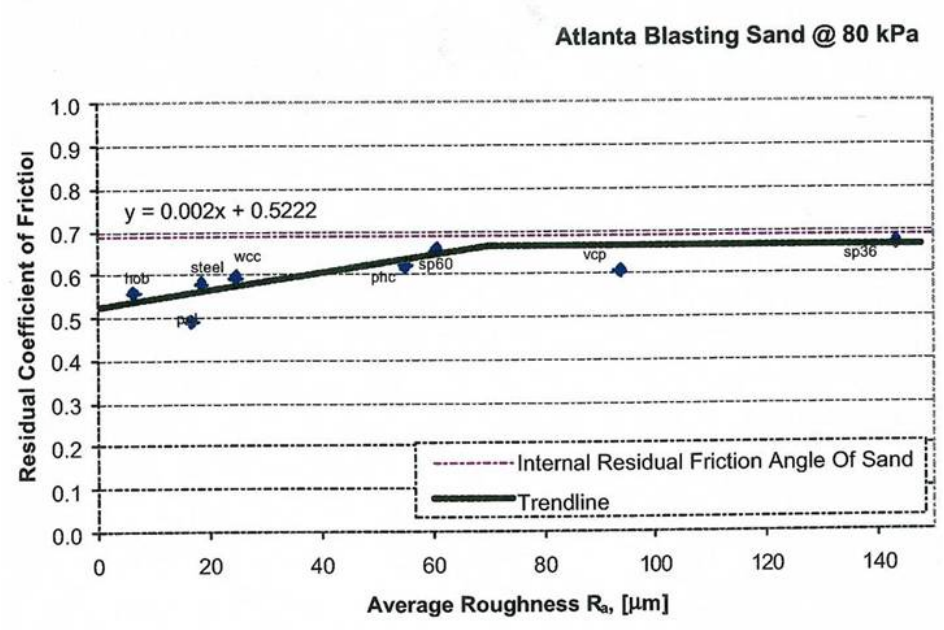

Figure 3.33. Average Roughness vs. Residual Coefficient of Friction for Atlanta Blasting Sand at 80 kPa (Iscimen, 2004).

Peak and residual friction coefficients were higher for each pipe material with the angular Atlanta Blasting sand than with the sub-rounded Ottawa 20/30 sand. This is attributed to the particle interlocking with the pipe as well as the particle interlocking within the soil mass. The interface shear behavior exhibited by the Atlanta Blasting sand was similar to that exhibited by the Ottawa 20/30 sand. Sliding friction was observed on the smoother pipes with very little post-peak softening, while the rougher pipes showed distinct post-peak softening. Table 3.6 shows the results of the shear tests on the pipe materials with Atlanta Blasting sand and compares them to the results of the Ottawa 20/30 sand at 80 kPa.

Table 3.6. Comparison of Coefficient of Friction for Ottawa 20/30 and Atlanta Blasting Sand at 80 kPa (from Iscimen, 2004).

		Coefficient of Friction at 80 kPa			
		Ottawa 20/30		Atlanta Blasting	
Pipe Material	Average Roughness $R_{a\ [\mu m]}$	Peak, ϕ_p	Residual, ϕ_r	Peak, ϕ_p	Residual, ϕ_r
Hobas	6.5	0.50	0.44	0.58	0.56
Polycrete	16.9	0.49	0.43	0.53	0.49
Permalok Steel	18.7	0.62	0.44	0.73	0.58
Wet Cast Concrete	24.8	0.65	0.48	0.76	0.59
Packerhead Concrete	55.1	0.73	0.53	0.86	0.62
Vitrified Clay	93.8	0.63	0.48	0.77	0.61

When comparing the results of the Hobas and Polycrete pipe when sheared against the Atlanta Blasting sand, the effects of plowing are much more pronounced with the Atlanta Blasting sand than for the Ottawa 20/30 sand, with plowing playing a large roll in the interface friction coefficient for the Hobas pipe, especially when comparing the peak and residual coefficient of friction for the Hobas when sheared against the Atlanta Blasting sand. As with the Ottawa 20/30 sand, the plowing effects play a much larger roll with the Hobas than with the Polycrete and although Polycrete has a higher average

roughness value, the coefficient of friction at both the peak and residual state is lower than that measured for the Hobas. This is due to the angularity of the soil particles.

The same trends existed with the vitrified clay pipe with the Atlanta Blasting sand as seen with the Ottawa 20/30 with coefficients of friction for the Vitrified Clay lower than those for the Packerhead Concrete.

3.4.3.3 Effects of Relative Density

A series of five (5) shear tests were performed on Hobas, Packerhead Concrete and Vitrified clay pipe with Ottawa 20/30 sand prepared at relative densities ranging from 47% to 98% to determine the effect of initial relative density on the interface shear behavior. For this series of tests, the normal stress was held constant at 80 kPa. The results of these tests are shown in Figures 3.34 through 3.35.

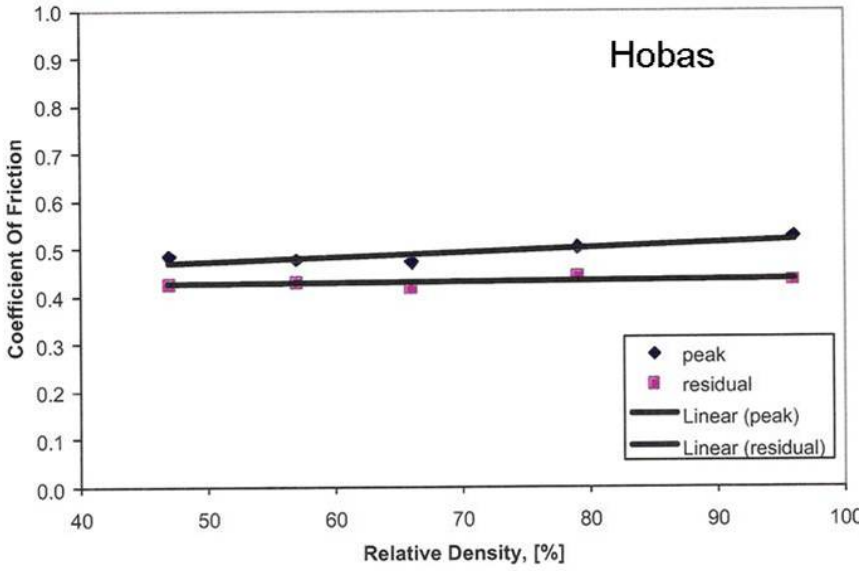

Figure 3.34. Relative Density of Ottawa 20/30 Sand vs. Coefficient of Friction for Hobas Pipe at 80 kPa (Iscimen, 2004).

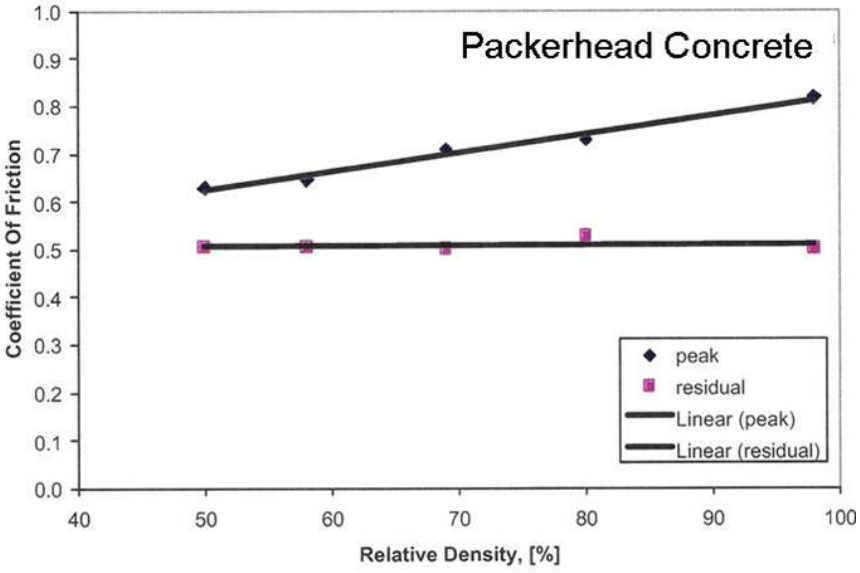

Figure 3.35. Relative Density of Ottawa 20/30 vs. Coefficient of Friction for Packerhead Concrete Pipe at 80 kPa (Iscimen, 2004).

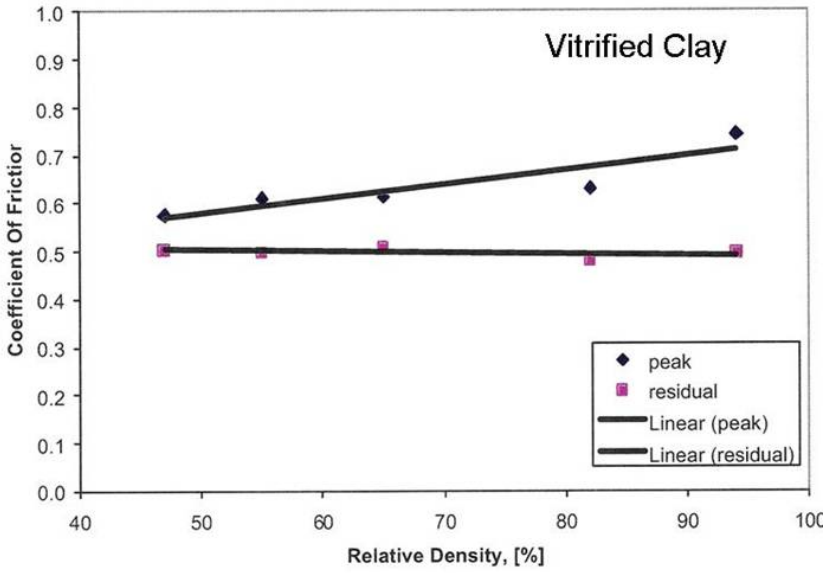

Figure 3.36. Relative Density of Ottawa 20/30 Sand vs. Coefficient of Friction for Vitrified Clay Pipe at 80 kPa (Iscimen, 2004).

Figures 3.34 through 3.36 show that as the relative density increases, the peak coefficient of friction increases. This is due to the higher friction and interlocking within the soil mass and at the interface at the higher relative densities. This effect is much more

pronounced for the rougher pipes, Packerhead Concrete and Vitrified Clay, than for the Hobas, due to the particle rearrangement on the rougher pipes as opposed to the sliding friction on the Hobas surface. One would expect to see even less of an increase with relative density on the Polycrete pipe than was seen with the Hobas sample, as plowing is much less a factor with the Polycrete pipe than with the Hobas sample based on previous tests.

The residual coefficient of friction remained relatively constant at all relative densities tested. This shows that regardless of the initial relative density, the soil stabilizes to a steady-state minimum shearing coefficient of friction within a very short horizontal displacement. The absolute difference between the peak and residual coefficient of friction at high relative densities is noteworthy. Table 3.7 shows these values.

Table 3.7. Absolute Difference between Peak and Residual Coefficient of Friction with Relative Density for Different Pipe Materials.

Relative Density [%]	Hobas	Packerhead Concrete (PHC)	Vitrified Clay (VCP)
Hobas/PHC/VCP	$\phi_p - \phi_r$	$\phi_p - \phi_r$	$\phi_p - \phi_r$
46.8 / 50 / 46.7	0.05	0.07	0.08
56.5 / 58 / 55.5	0.05	0.14	0.11
65.9 / 68.7 / 64.8	0.05	0.21	0.10
95.6 / 98.3 / 94.4	0.10	0.32	0.24

These values become significant when mobilizing the peak friction in order to get to the residual friction state.

3.5 Summary

The surface characteristics for Hobas (Centrifugally Cast Fiberglass Reinforced Mortar Pipe), Polycrete (Polymer Concrete), Permalok Steel, Wet Cast Concrete, Packerhead

Concrete, and Vitrified Clay pipe were determined and their average roughness compared. It was shown that the surface roughness of the pipe had an effect on the interface friction coefficient when the pipe was sheared against two different granular soils. Interface friction coefficients were measured for each pipe material for Ottawa 20/30 sand and Atlanta Blasting sand. This will allow a side-by-side comparison on how the pipe material roughness effects jacking forces on actual projects. This information can be now be used to evaluate jacking forces on a variety of projects where these pipe materials were jacked in granular soils to gain insight into the performance of these pipes in the field.

CHAPTER 4

FIELD CASE HISTORIES

Field research was conducted on eleven microtunneling and one open shield pipe jacking projects. During microtunneling and/or pipe jacking operations, extensive data were collected to monitor a broad range of tunneling operations, attempting to capture all activities that impact jacking forces and tunneling behavior. Tunneling parameters collected during the research included jacking force measurements, advance rates, excavation rates, slurry flow rates, slurry pressures, cutter wheel torque measurements, face pressure, steering corrections, machine attitude/pitch, steering cylinder pressures, slurry chamber pressures, lubrication injection, laser position, machine location, and by-pass valve position. These measurements were taken on 5-foot intervals during tunneling. In addition, soil samples were collected during tunneling, typically on 20-foot intervals. All of these projects are described in this chapter and listed in Table 4.1.

To supplement the field research, three additional tunnels on which the author was able to acquire the information pertaining to the construction of the tunnels but did not participate in field activities were included in the analysis of field case histories. Those are tunnels 9, 10, and 11 from the Alvarado Boulevard project, as listed in Table 4.1. The detailed field information from the Alvarado Boulevard Project provided jacking force data for Polycrete pipe, which was not available from the author's field projects.

4.1 Sacramento Intake Duel Microtunnels Beneath Interstate - 5

The Sacramento River Water Treatment Plant Replacement Intake Project included the construction of two microtunnels beneath Interstate-5 in Sacramento, CA.

Table 4.1 Details of Project Case Histories Included in Study

#	Project/ Tunnel	Pipe Material	Dia-meter [inches]	Tunnel Length [feet]	Crossing Type	Soils	Water above Crown [feet]	Soil above Crown [feet]	Chap-ter Sectio n
1	Sacramento Intake North Microtunnel	Permalok Steel	72	350	Highway I-5	Sand & Silty Sand	None	8 to 25.5	4.1
2	Sacramento Intake South Microtunnel	Permalok Steel	72	350	Highway I-5	Sand and Silty Sand	None	8 to 25.5	4.1
3	Lowell Snohomish BNRR	Permalok Steel	60	210	Highway And Railroad	Loose Silty Sand	5	7 to 22	4.2
4	Clearview 2001	Permalok Steel	60	580	River	Sand with Gravel	60	65	4.3
5	Clearview 2002	Permalok Steel	60	1058	River	Sand with Gravel	80	85	4.4
6	South Tahoe Hwy 50	Wet Cast Concrete	59.5	260	Highway	Sand	None	13	4.5
7	Eastside Interceptor Morris Ave	Packer-head Concrete	87.5	1115	Roadway	Loose Sand	16	17 to 20	4.6
8	Eastside Interceptor Houser Way	Packer-head Concrete	87.5	715	Roadway	Loose Sand	18 to 22	22 to 30	4.7
9	Alvarado JP3 to RP4	Polycrete	46.6	710	Roadway	Silty Sand	15	19	4.8
10	Alvarado JP4 to RP4	Polycrete	46.6	775	Roadway	Silty Sand	9	21	4.9
11	Alvarado Drive 17	Polycrete	25.9	385	Highway	Silty Clayey Sand	3	26	4.10
12	Newark Drive 3	Hobas	38.3	720	Roadway	Silty Sand	8	13	4.11
13	Newark Drive 6	Hobas	38.6	760	Roadway	Silty Sand	4	17 to 19	4.11
14	Newark Drive 12	Hobas	38.3	310	Roadway	Silty Sand	3	16	4.11
15	Newark Subbasin Drive 1-24	Hobas	25.8	340	Roadway	Silty Sand	5	14	4.11

The tunnels were heavily instrumented to collect an extensive amount of information from the tunneling operations. During tunneling, a number of operational parameters were recorded. These parameters included the tunneled length, the approximate station at the heading of the tunneling machine, the cumulative jacking force measured at the main jacking frame, the torque on the cutter wheel of the machine, the slurry flow rates and pressures, the slurry valve positions, the line and grade of the machine, the machines inclination and roll, and the pressure on the steering cylinders. Along with tunneling parameters, extensive field notes were collected to document all field activities.

4.1.1 Description of the Project

A portion of the Sacramento River Intake project included two parallel, 72-inch outer diameter (OD) microtunnels constructed with steel Permalok casing pipes beneath Interstate-5 near the confluence of the American and Sacramento Rivers. The tunnels were each 350 feet in length. After construction of the tunnels, the steel pipelines were subsequently lined with 54-inch water pipelines. The casing pipes were required beneath the Highway by the California Department of Transportation as a means of additional protection for the highway should a breach occur in the 54-inch water pipeline. A plan and profile view of the tunnels are shown in Figure 4.1.

Launch and reception shafts were constructed on the east and west sides of the Interstate respectively. Both shafts were approximately 16 feet deep and constructed to accommodate the construction of parallel tunnels from a single set of shafts. The shafts were constructed by installing auger-drilled H-piles around the perimeter. The piles were

encased in concrete to provide shaft stability. The walls of the shaft were supported with steel plates and wood lagging.

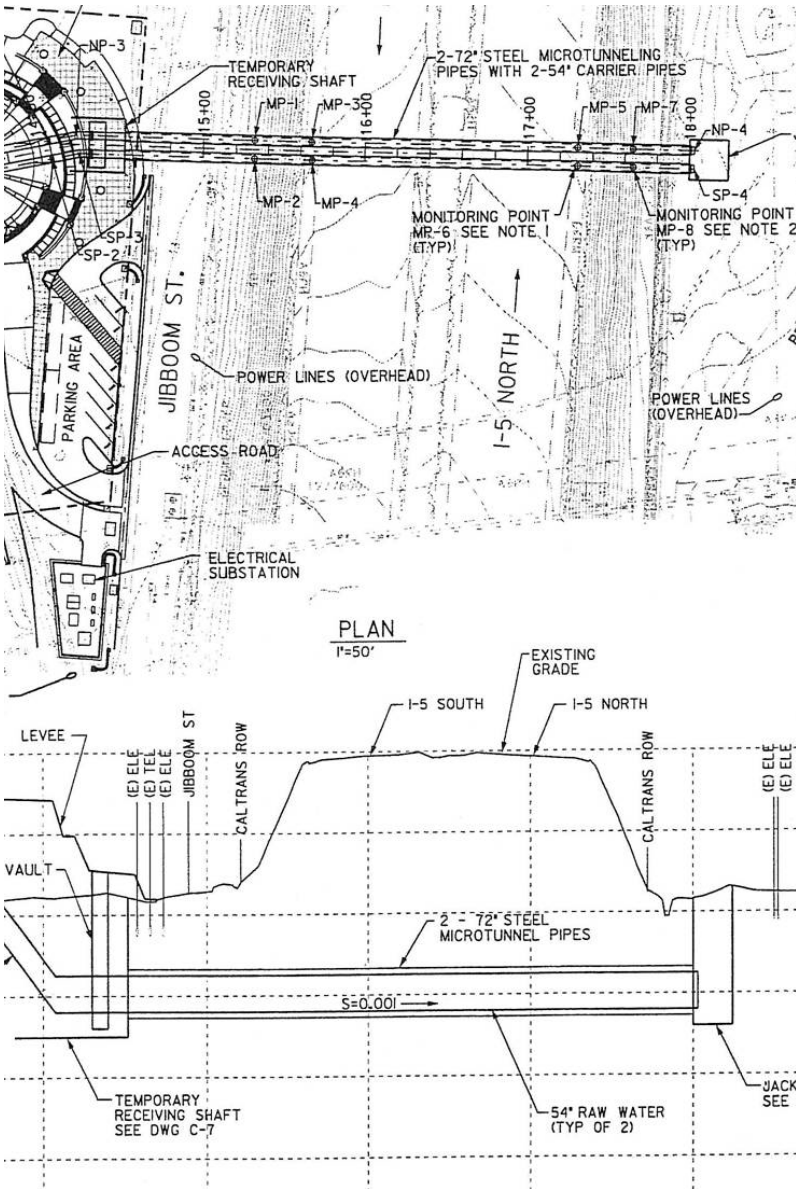

Figure 4.1. Plan and Profile of the Sacramento Intake Project Microtunnels Beneath Interstate-5 (CH2M Hill, 2000)

For both drives, the microtunneling machine was launched from the east launch shaft with approximately 8 feet of overburden above the crown of the pipeline. The

depth of cover over the pipeline quickly increased as the machine progressed beneath the embankment of the interstate. A maximum depth of cover of 25.5 feet existed beneath the Interstate.

The pipe material that was jacked as the casing pipe was Permalok Steel, a rolled steel pipe with a machined integral press-fit joint that eliminates the need to weld the pipe sections during tunneling. The pipe sections are joined together by pushing consecutive joint sections together until they lock at the machined connection. Each pipe joint was 20 feet in length, with the exception of the first pipe section, which was 10 feet in length. The short section of pipe was used to facilitate enhanced steering response near the head of the machine. The pipe outer diameter was 72-inches and the pipe wall thickness was 0.75 inches. The pipe wall thickness was designed to accommodate a jacking load of 1,484 tons with a safety factor of 2.0.

The microtunnels were constructed with an Akkerman soft-ground microtunneling machine as shown in Figure 4.2, with an outer diameter measuring 71.875 inches. The machine was fitted with a soft ground tunneling cutter wheel with a maximum outer diameter of 73.75 inches. The radial overcut on the pipeline was 0.875 inches. The total length of the machine was 21.33 feet with the cutter wheel attached. The machine and pipeline were propelled by a 1,200-ton hydraulic jacking frame located in a launch shaft constructed on the east side of the highway. The contractor launched the machine from the shaft through an “exit can” or exit pipe on which they mounted their launch seal. This launch technique is practiced by some contractors but is not common to all contractors, as most mount the launch seal directly to the shaft wall. Either launch practice is acceptable.

(a) Jacking Shaft Site

(b) Jacking Shaft Under Construction

(c) Setting the Microtunneling Machine

(d) Launch of the Machine

(e) Jacking Frame in the Shaft

(f) Cutter Wheel on Machine

Figure 4.2. Microtunneling Machine and Site Photos.

4.1.2 Geotechnical Conditions Along the Tunnel Alignment

Two vertical borings were drilled along the tunnel alignment for the design, one at the approximate location of the jacking shaft (B-6) and one at the approximate location of the reception shaft. Figure 4.3 shows the location of the borings. No borings were conducted through the Interstate due to limited access and permit restrictions.

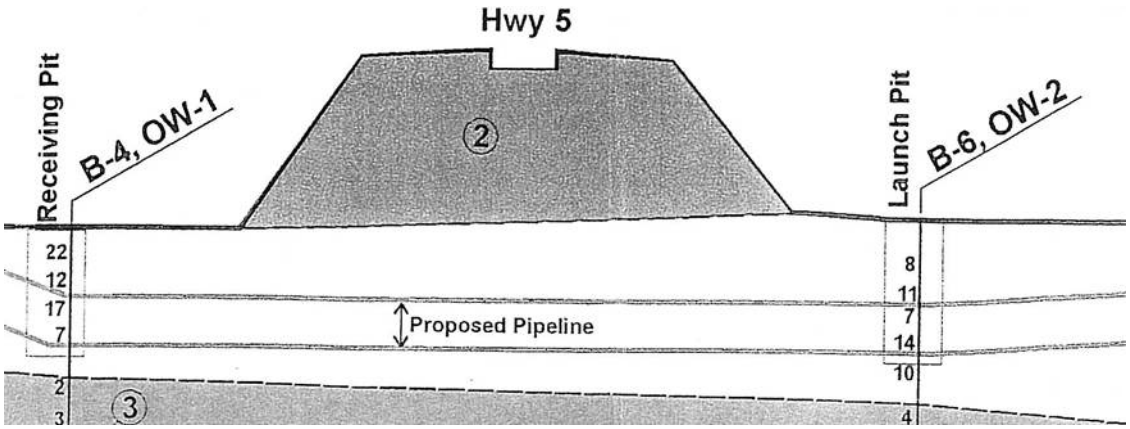

Figure 4.3. Boring Locations for the Sacramento Intake Interstate-5 Microtunnels (AGS, 2000).

The soil conditions at the jacking shaft were a medium dense poorly-graded fine- to medium-grained sand (SP) to a depth of 20 feet, with the tunnel elevation only eight (8) feet below the ground surface. The soil was dry to damp. Groundwater was encountered at a depth of 17 feet below the ground surface. Soil samples were taken with a modified California Split Spoon Sampler and blow counts were modified to give SPT blow counts ranging from 11 to 15 blows per foot. The boring log for B-6 is shown in Figure 4.4. The soil conditions at the elevation of the tunnel at the reception shaft were also a medium dense poorly-graded sand (SP) with corrected blow counts ranging from 12 to 21 blows per foot. Unlike the boring at the jacking shaft, B-4 contained an upper layer of poorly graded sand with silt above the tunnel horizon, a material that is typically considered ideal for microtunneling applications. Figure 4.5 shows the boring log for Boring B-4 at the reception shaft location.

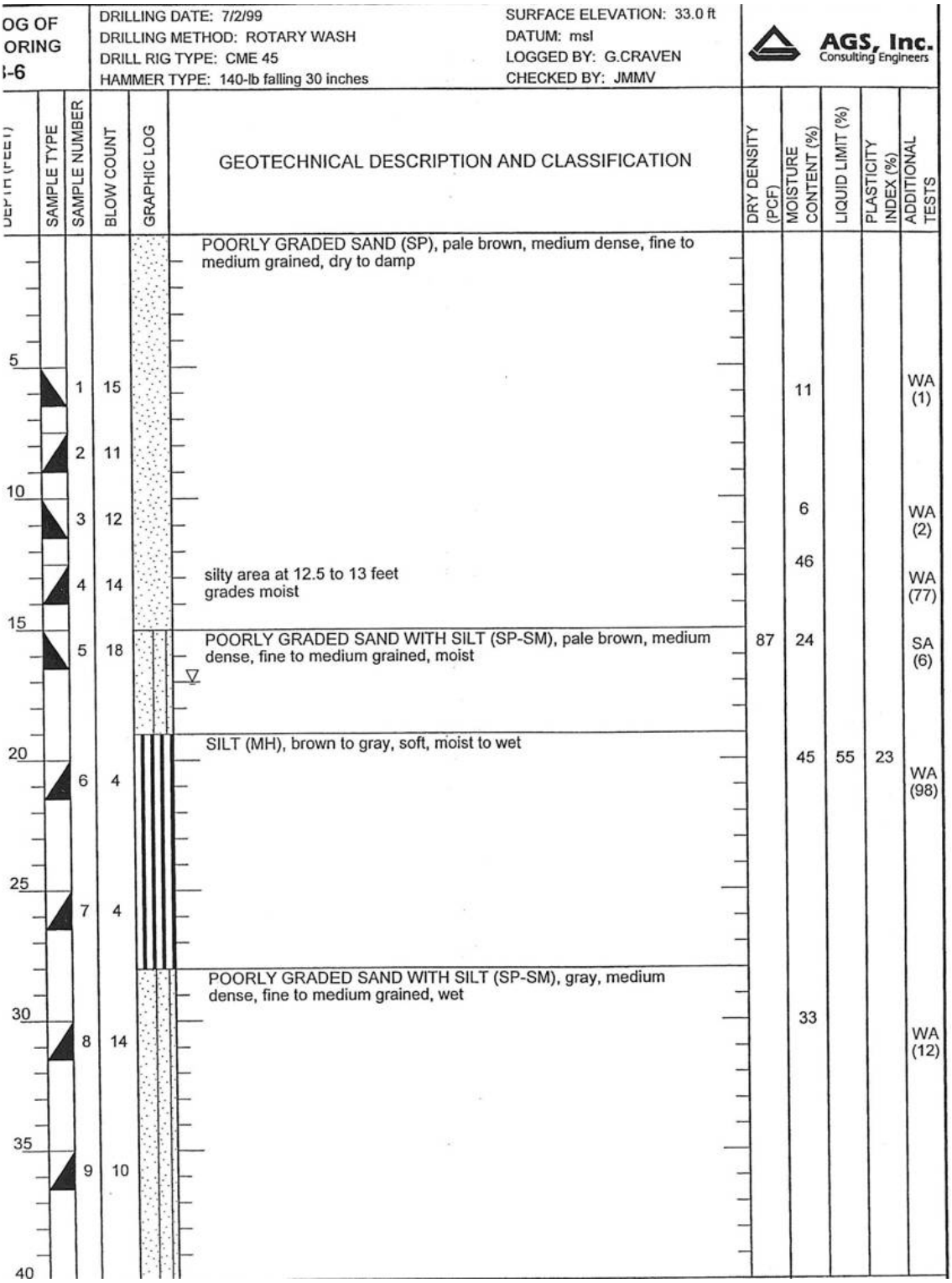

Figure 4.4. Boring B-6 Located at the Jacking Shaft for the Sacramento Intake Project (AGS, 2000).

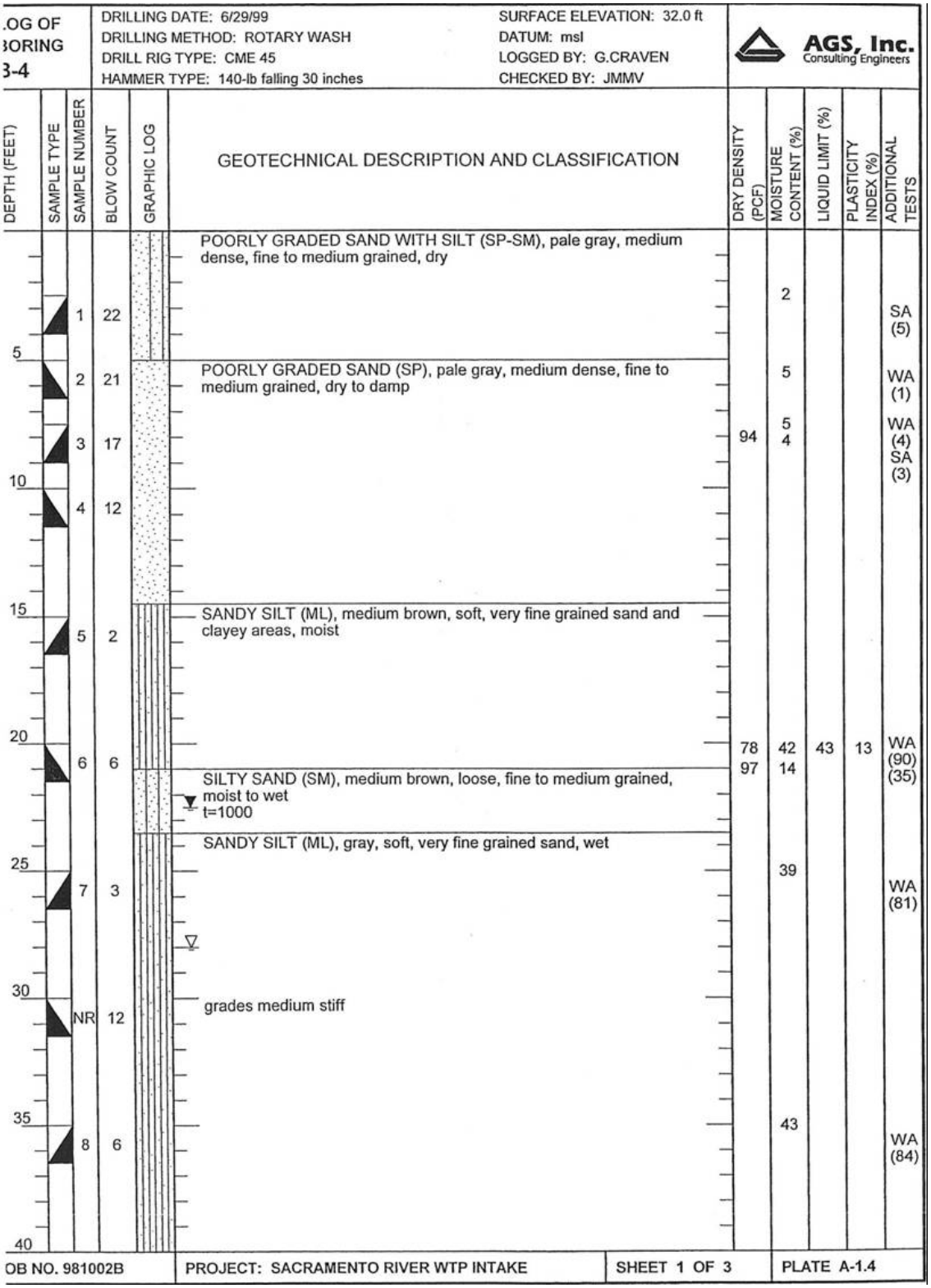

Figure 4.5. Boring B-4 Located at the Reception Shaft (AGS, 2000).

4.1.3 Construction of the North Microtunnel

The construction of the North microtunnel drive began on December 12, 2001 with the launch of the microtunnel machine. In preparation for the launch, the contractor cut a hole in the shaft wall and jacked an oversized 86-inch starter-casing three feet in length through the opening in the shaft wall. A gasketed rubber seal with adjustable side plates was welded to the starter casing. The machine was launched through the seal and the starter-casing. During the placement of the starter casing, 6 to 8 cubic yards of soil sloughed into the shaft, creating a sinkhole on the outside of the shaft wall. This soil was removed from the shaft and used to backfill the sink-hole after the machine was launched.

Upon advancing the machine approximately 2 feet from the shaft wall, the machine encountered some concrete rubble that was waste material from the installation of the auger-bored H-piles. This caused a rapid increase in the torque on the face and cutter wheel of the machine. Because the machine was not completely buried, it did not provide a stabilizing resistance against the torque. As a result, the machine rolled in the shaft during the launch. However, the machine was able to excavate through the concrete. Once the machine progressed 5 feet, roll of the machine was no longer a problem.

For the first 70 feet of tunneling, the operator was periodically using high-pressure water jets located at the face of the machine to aid in the excavation process. As a result, the torque on the machine cutter wheel often approached the baseline torque of 36 percent, indicating that the operator was over-excavating the soil at the face. At 69 feet into the drive, the machine passed beneath a sub-surface settlement monitoring point.

The resulting settlement was 55 inches and a sink-hole developed above the machine. Tunneling was stopped to assess the settlement problems prior to excavating beneath the Interstate. The contractor was instructed to stop using the high-pressure water nozzles for excavation and to maintain a minimum torque of 50-60 percent. This resulted in a higher face pressure, allowing the machine to stabilize the excavation, minimizing the possibility of further settlement.

As the drive progressed, there were substantial increases in jacking forces. These increases caused excessive movement in the shaft. The thrust block behind the jacking frame was poured in direct contact with the H-piles. As a result, the shaft walls and floor moved as a unit. When the jacking forces reached 250 tons, at approximately 100 feet into the drive, the shaft movement caused the laser to move off of the steering target located in the head of the machine when the jacking forces were applied. Tunneling was stopped while the contractor built a new laser stand that isolated the laser from the thrust block. At 143 feet into the drive, the jacking forces had reached approximately 630 tons. The contractor stopped tunneling due to concerns that the entire shaft might fail under the high jacking loads. The contractor then began lubricating along the pipe string. As a result of the lubrication, the jacking forces decreased to approximately 350 tons. Although the shaft continued to move, creating guidance control problems, the contractor continued to tunnel, believing the shaft would not fail under the lower jacking loads.

Microtunneling continued until approximately 293 feet into the drive when the contractor hit some buried rubble on the west side of the Interstate. Due to the increase in torque readings at this location, the contractor believed that the machine had reached the reception shaft. However, after measurement, it was discovered that the machine was 55

feet away from the reception shaft. The contractor continued to excavate in the debris and reactivated the high-pressure water jets in the heading. This caused soil to flow into the head of the machine as they were attempting to excavate the debris. Although they were able to excavate through the debris, a sink-hole developed on the west side of the Interstate embankment, under the sidewalk on Jibboom Street, due to the over-excavation. The contractor continued to tunnel and the tunneling machine reached the reception shaft 348 feet into the drive.

The north tunnel drive was constructed between December 12 and December 19, 2001. The average tunneling rate was 43.5 feet per day. Table 4.1 summarizes the microtunneling of the north drive of the project.

Table 4.2. Overview of Microtunneling on the North Drive.

Date	Tunneled Length [feet]	Cumulative Length [feet]	Notes
12/12/01	5	5	Launch of the microtunneling machine. Hit concrete rubble at 2 feet into drive.
12/13/01	46	51	Tunneled 16 feet of machine, Pipe #1 (10 feet) and Pipe #2 (20 feet)
12/14/01	40	91	Tunneled Pipes #3 and #4. Settlement detected at 69 feet into drive. Sink-hole developed on east embankment.
12/15/01	52	143	Tunneled Pipes #5, #6, and 12 feet of #7.
12/16/01	8	151	Tunneled 8 feet of Pipe #7. Contractor concerned about high jacking forces and shaft movement.
12/17/01	80	231	Tunneled Pipes #8, #9, #10, and #11.
12/18/01	62	293	Tunneled Pipes #12, #13, #14, and 2 feet of #15. Hit buried debris at 293 feet. Sink-hole developed under sidewalk.
12/19/01	55	348	Tunneled 18 feet of Pipe #15, Pipe #16, and 17 feet of pipe #17 when tunneling machine reached reception shaft.

4.1.3.1 Jacking Forces on the North Microtunnel Drive

The frictional component of the jacking forces for the North Tunnel Drive ranged from 7 to 597 tons. Figure 4.6 shows the frictional component of the jacking force

measured in tons. The measurement shown on the graph is the jacking force measured at the main jacking frame in the jacking shaft minus the combined load measured on the three steering jacks located in the machine behind the steering joint, approximately 10 feet behind the cutter wheel of the machine. Therefore, the measurement represents the frictional load on the outer surface of the machine from the articulation joint to the tail section of the machine, plus the frictional load on all trailing pipes behind the machine at the time the reading was recorded.

When analyzing a jacking force record, it is important to note the number of complex operations that occur during the launch, and how that affects the data measurements. For the Sacramento River Intake Project, a steel cylinder was jacked from the jacking shaft on which they mounted the launch seal. In addition, there was a tremendous amount of disturbed soil around the launch shaft. Since the machine is 20 feet in length, with the steering cylinders located at approximately 8 feet from the face, the measured readings over the first 8 feet are actually drag measurements due to drag forces against the machine in the shaft (likely due to the type of machine cradles used by the contractor to level the machine). These forces will not be on the pipe once the machine is launched. The machine will not be fully buried in native soil until it has fully exited the shaft and completely cleared the launch can as well as the disturbed soil. In the case of the Sacramento project, this was a minimum of 30 feet.

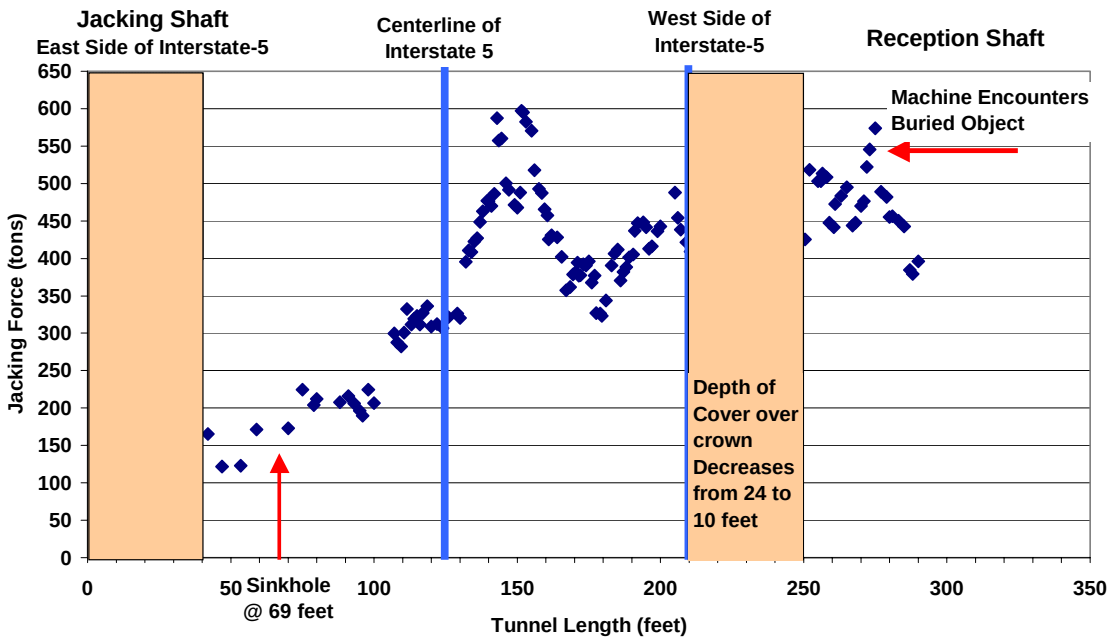

Figure 4.6. Frictional Component of Jacking Force for the North Microtunnel Drive of the Sacramento Interstate-5 Microtunnel Crossing.

4.1.3.2 Lubrication during Microtunneling

During the tunneling operations, bentonite lubrication was injected into the annular space through lubrication ports in the pipeline. The lubrication ports were located at five contractor-selected positions along the pipeline. One lubrication port was located at the tail of the microtunneling machine, approximately 21 feet from the face of the machine at the 12-o'clock position. This was the only lubrication port utilized throughout the first 143 feet of tunneling.

The following four sets of lubrication ports were located in Pipes #4, #7, #9, and #11 located approximately 81, 141, 181, and 221 feet behind the head of the machine respectively. The ports were positioned at the 10- and 2-o'clock positions on the

pipeline. These ports were periodically activated throughout the drive. Table 4.3 shows the lubrication pattern used by the contractor.

Because the operator continued to switch injection locations and did not continuously lubricate the pipe string, the vast majority of the lubrication was applied between station 55 and 116. These stations were lubricated multiple times from different lubrication ports. A cumulative total of only 119 feet of the 348-foot drive received lubrication. No lubrication was applied to the pipeline beyond station 264.

4.1.3.3 Isolation of Jacking Force Segments on the North Drive

Through the first 40 feet of the drive, the depth over the crown was increasing from 8 to 24 feet and no lubrication was applied to the pipe string. From 50 to 100 feet, the depth of cover over the crown was relatively constant and remained at 24 feet throughout this interval. Throughout this interval, lubrication was not applied to the pipeline and the jacking stress was 0.07 tons per square foot of surface area of pipe. The frictional component of the jacking forces for the segment between 50 and 100 feet is shown in Figure 4.7.

At 100 feet into the drive the soil conditions markedly changed and the tunneling machine entered a sandy formation with a much higher in situ density. This was evident by the face pressure forces on the microtunneling machine. Through this segment, the jacking forces markedly increased to a value of approximately 640 tons. The jacking stress in this segment increased to 0.33 tons/ft^2. Figure 4.8 shows the frictional component of the jacking forces from 100 to 150 feet.

Table 4.3. Lubrication on the North Drive.

Tunneling Interval [feet]	Lubrication Location	Station Receiving Lubrication [feet]	Total Lubricated Length [feet]	Percent of Tunnel Lubricated
0 – 100	None	None	Zero	0
100 – 134	Tail of Machine; 21 feet behind head	79-113	34	25
135 – 140	None	None	34	24
141 – 149	Pipe #4;81 feet behind head	60 – 68	43	29
150 – 151	Pipe #7; 141 feet behind head	9 – 10	45	30
152 – 160	Pipe #4	71 – 79	53	33
161 – 165	Tail of Machine	140 – 144	57	35
166 – 167	Pipe #7	26 – 27	59	35
168 – 169	Tail of Machine	147 – 148	61	36
169 – 170	Pipe #4	88 – 89	61	36
171 – 175	Pipe #7	30 – 34	65	37
175 – 176	Tail of Machine	154 – 155	67	38
177 – 190	None	None	67	35
191 – 192	Pipe #9; 181 feet behind head	10 – 11	68	35
192 – 193	Pipe #7	51 – 52	70	36
193 – 196	Pipe #4	112 – 115	72	37
196 – 197	Pipe #7	55 – 56	72	37
199 – 210	Pipe #4	118 – 129	83	40
211 – 215	Pipe #9	30 – 34	83	39
216 – 221	Pipe #7	75 – 80	83	38
223 – 231	Pipe #4	141 – 150	91	39
231-232	Pipe #9	50 – 52	91	39
233-234	Pipe #7	92 – 93	91	39
235-239	Pipe #4	154 – 158	94	39
240-241	Tail of Machine	219 – 220	96	40
242-245	Pipe #9	61 – 64	96	39
247-251	Pipe #7	106 – 110	96	38
252-255	Tail of Machine	231 – 234	100	39
256-257	Pipe #7	115 – 116	100	39
258-259	Pipe #4	217 – 218	102	39
259-265	None	None	102	38
265-266	Tail of Machine	244	103	39
266-268	Pipe #4	185 – 187	105	39
269-270	Pipe #7	88 – 89	105	39
271-272	Pipe #11; 221-feet behind head	50 – 52	106	39
272-273	Pipe #9	91 – 92	106	39
273-275	Pipe #7	132 – 134	108	39
277-280	Pipe #4	196 – 199	112	40
281-285	Tail of Machine	260 – 264	117	41
286-287	Pipe #4	205 – 206	118	41
288-290	Pipe #11	67 – 69	118	41
290-348	None	None	118	34

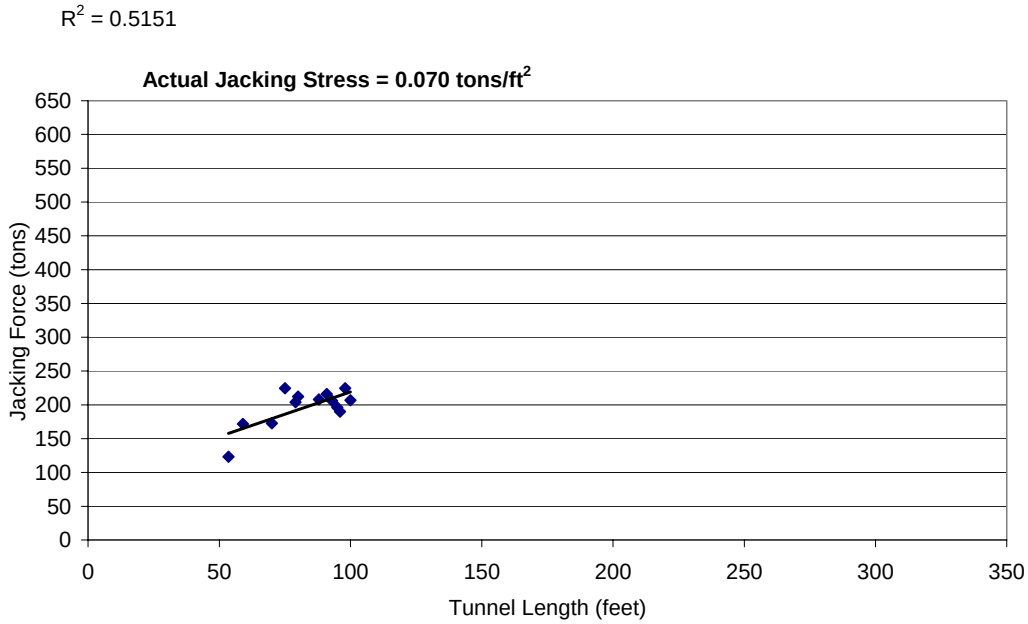

Figure 4.7. Frictional Component of the Jacking Force for the North Microtunnel of the Sacramento Intake Project from 20 to 75 feet.

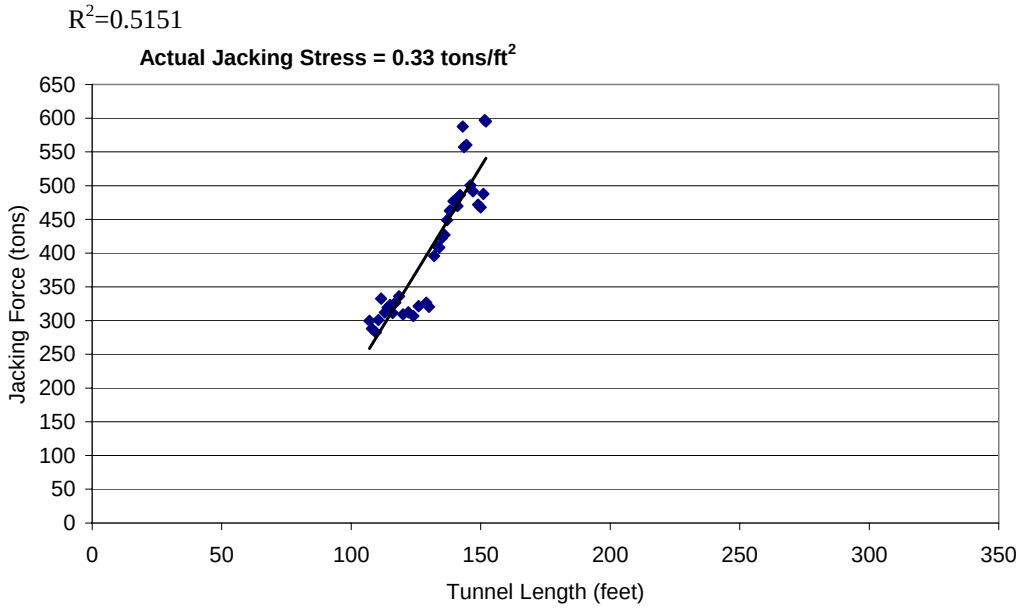

Figure 4.8. Length vs. Jacking Force for the North Microtunnel Bore of the Sacramento River Intake Project from 100 to 150 feet.

At 150 feet into the drive, the operator began to use high pressure water jets at the face of the machine to aid in the excavation. The lubrication records indicate that the operator began to pump lubrication at the tail section of the machine, 21 feet behind the face, and the frictional component of the jacking forces dropped. At 141 feet into the drive the contractor began lubricating once again and jacking forces began markedly decreasing. This decrease continued from 150 to 180 feet into the tunnel drive. At that point, although the contractor continued to lubricate, the section over which the lubrication was applied had previously been lubricated; therefore, the lubrication was no longer effective in decreasing the overall jacking loads. At 180 feet into the tunnel drive the jacking forces again began to increase and continued to increase through 205 feet into the drive at a rate of 0.25 tons per square foot of surface area as can be seen in Figure 4.9.

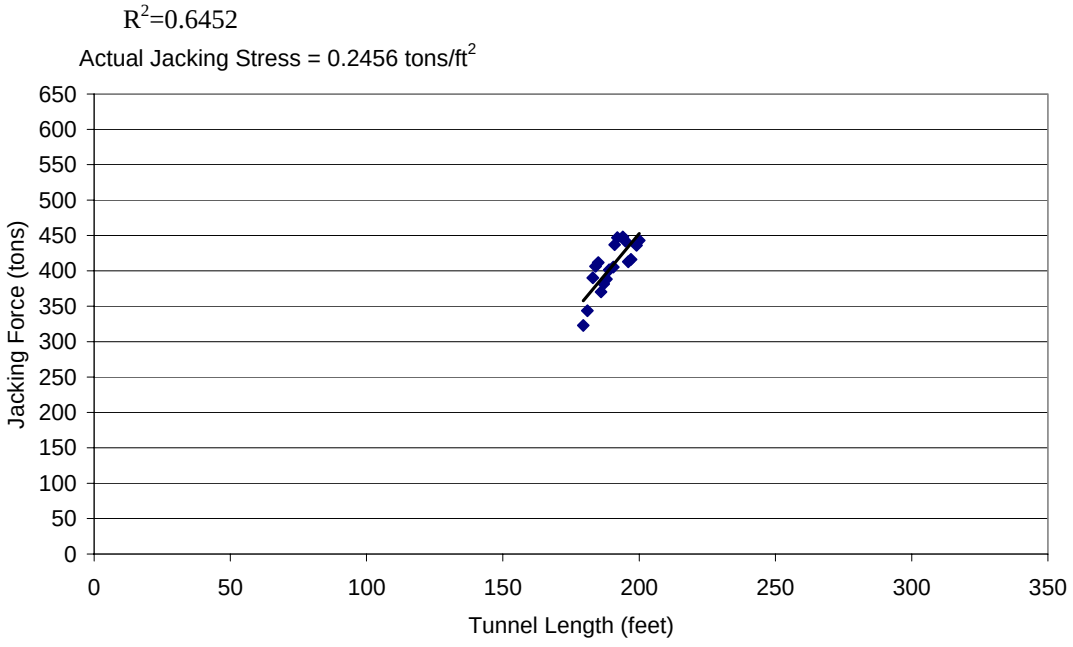

Figure 4.9. Length vs. Jacking Force for the North Microtunnel of the Sacramento River Intake Project from 180 to 205 feet.

4.1.3.4 Overview of Normalized Friction Coefficients

Table 4.4 provides an overview of the normalized friction coefficients along the North Tunnel alignment.

Table 4.4. Jacking Stress on Isolated Segments of North Microtunnel Drive for the Sacramento River Intake Project.

Segment Along Tunnel alignment [feet]	Jacking Stress [tons/ft^2]	Notes	[R^2 Value]
50-100	0.07	No Lubrication	0.5151
100-150	0.33	Change in Soils	0.8231
180-205	0.25	Ineffective Lubrication	0.6452

4.1.4 Construction of the South Microtunnel

Prior to the launch on the South microtunnel, new cutting bits were installed on the machine. The new cutter wheel outer diameter was 74 inches. Like the first drive, the contractor elected to install an over-sized 86-inch starter casing through the wall of the shaft. Again, soil sloughed into the shaft. Approximately 8 to 10 cubic yards of sand was removed from the shaft and used to fill the sink-hole created on the outside of the shaft after the launch was complete.

Because of the problems with shaft stability, the contractor grouted behind the back wall of the shaft in an attempt to stabilize the soil and minimize the shaft movement during the South drive. The contractor chose compaction grouting behind the eastern wall of the launch shaft.

The South microtunnel drive began on January 9, 2002. During the first day of tunneling, the contractor was able to install the machine and the first 10-foot Permalok pipe section, for a total of 31 feet of tunneling.

On the second day of tunneling, January 10, 2002, the contractor installed 120 feet of pipe, for a total of 151 feet of tunneling. Unlike the first drive, the operator did

not activate the high-pressure water nozzles for excavation and no surface settlement was detected.

As the jacking forces increased along the drive, the thrust block began to crack, indicating the launch shaft was moving considerably under the applied jacking load. The contractor had concerns about the integrity of the shaft and tunneling progress was slowed. The contractor was able to complete the tunnel without catastrophic failure of the shaft. The South Drive was constructed between January 9 and January 13, 2002. The average tunneling rate of 70 feet per day was achieved. Table 4.5 shows the progress of the tunneling on the South Drive.

Table 4.5. Overview of Microtunneling on the South Drive.

Date	Tunneled Length [feet]	Cumulative Length [feet]	Notes
1/9/02	31	31	Launch of the microtunneling machine. Tunneled 21-foot machine and Pipe #1 (10 ft)
1/10/02	120	151	Tunneled Pipes #2, #3, #4, #5, #6, and #7.
1/11/02	60	211	Tunneled Pipes #8. #9 and #10. Thrust block begins to crack due to high jacking forces.
1/12/02	80	291	Tunneled Pipes #11, #12, #13, and #14.
1/13/02	57	348	Tunneled Pipes #15, #16. and 17 feet of pipe #17 when tunneling machine reached the reception shaft.

4.1.4.1 Jacking Forces on the South Microtunnel Drive

The frictional component of the jacking forces on the South tunnel drive ranged from 5 to 500 tons as shown on Figure 4.10. As with the North tunnel drive, the frictional component of the jacking force was measured by subtracting the force at the steering cylinders from the force at the main jacking frame.

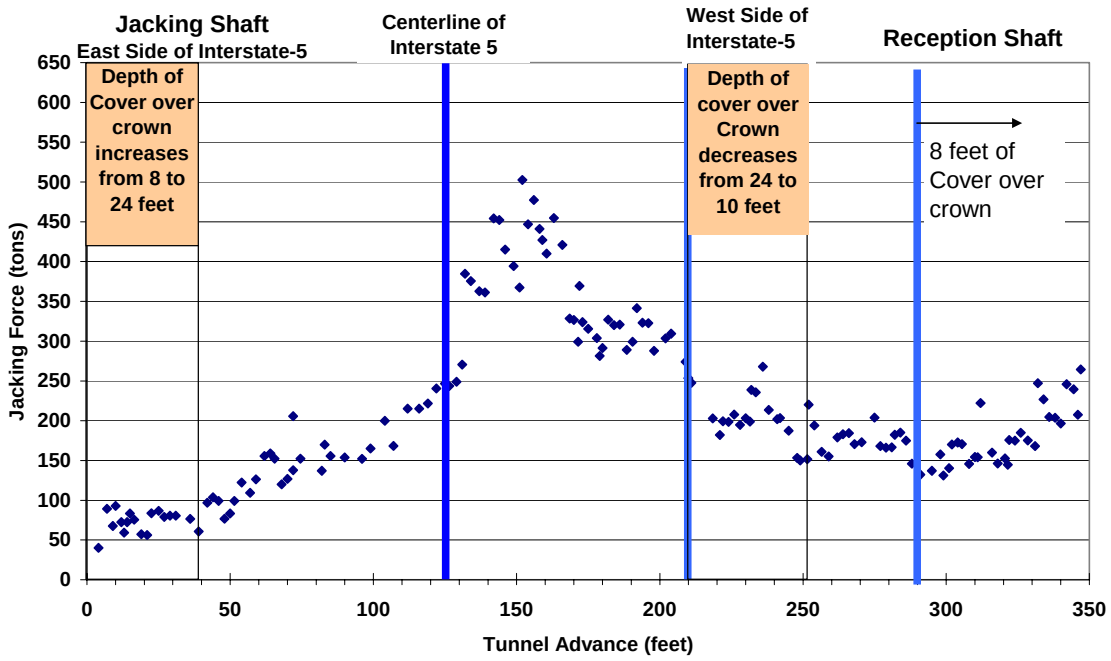

Figure 4.10. Length vs. Jacking Force for the South Microtunnel of the Sacramento River Intake Project.

4.1.4.2. Lubrication during Tunneling

Due to the magnitude of the jacking forces and the movement of the jacking shaft experienced on the North microtunnel, the contractor elected to install bentonite ports in every other pipe behind the microtunneling machine, providing more flexibility on the lubrication injection. However, like the North microtunnel, the lubrication was not evenly dispersed along the tunnel alignment, and only 57% of the tunnel alignment received bentonite lubrication. Table 4.6 shows the lubrication along the South microtunnel drive.

Table 4.6. Lubrication on the South Drive.

Tunneling Interval [feet]	Lubrication Location	Station Receiving Lubrication [feet]	Total Lubricated Length [feet]	Percent of Tunnel Lubricated
0-75	None	None	0	0
76-81	Pipe 2	34-40	7	9%
59-139	Tail	38-118	66	47%
140-148	Pipe 2	99-107	66	44%
149-151	Pipe 2	108-110	69	44%
149-151	Pipe 6	28-30	78	46%
152-159	Tail	131-138	78	49%
160-162	Pipe 6	39-41	78	48%
163-167	Pipe 4	82-86	78	47%
168-187	Tail	147-166	88	47%
188-191	Pipe 6	67-70	88	46%
192-193	Tail	171-172	90	47%
194-201	Pipe 6	73-80	90	45%
202-203	Tail	181-182	92	45%
204-208	Pipe 6	83-87	92	44%
209-215	Tail	188-194	99	46%
216-220	Pipe 8	55-59	99	45%
221-251	Tail	200-230	130	52%
252-257	Pipe 10	51-56	130	51%
258-293	Tail	237-272	166	57%
294-297	Pipe 2	253-256	166	56%
298-309	Pipe 4	217-228	166	54%
310-311	Pipe 6	189-190	166	53%
312-315	Pipe 8	151-154	166	53%
316-348	Tail	295-327	199	57%

Lubrication injection occurred primarily at the tail section of the machine. Over 66 feet of the drive, lubrication occurred at other locations along the pipeline; however, the tail section had previously lubricated these locations when the tunneling machine passed through.

4.1.4.3 Isolation of Jacking Force Segments on the South Drive

The frictional component of the jacking force plot was isolated into several segments for analysis. Over the first 40 feet of the drive the depth of cover over the crown of the pipeline was increasing rapidly from 8 feet to 24 feet. Lubrication was not applied to the pipeline until approximately 75 feet into the drive. Figure 4.11 shows the

unlubricated segment of the drive from 20 to 75 feet. Over this interval the jacking stress was 0.084 tons/ft^2.

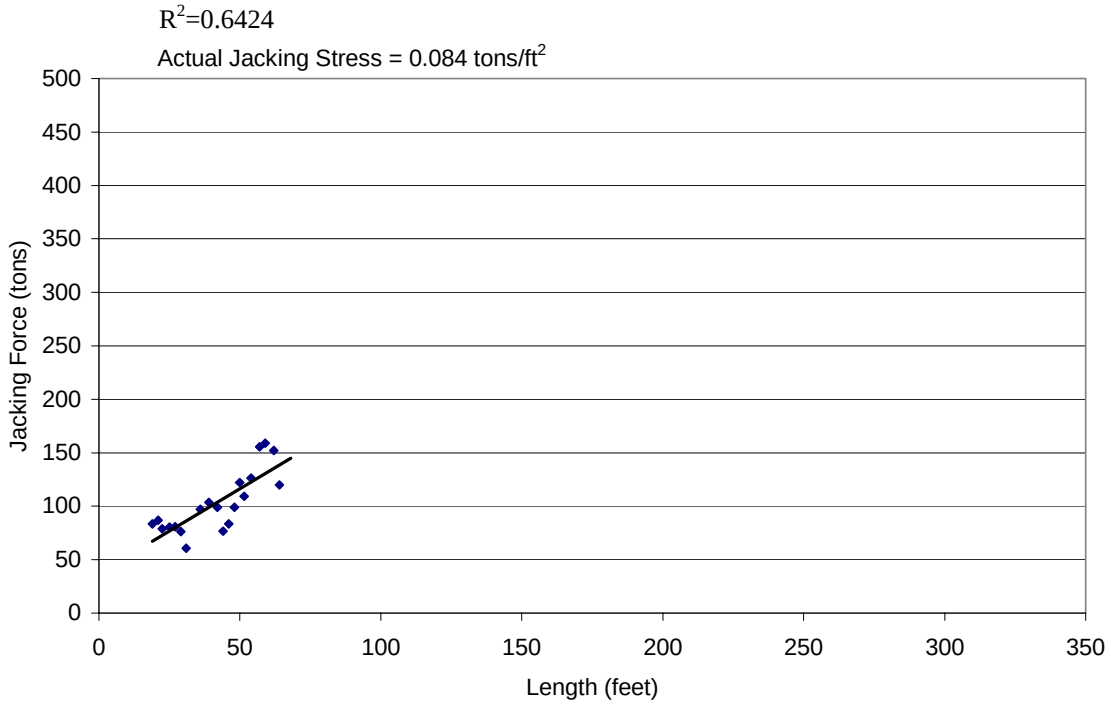

Figure 4.11. Length vs. Jacking Force for the South Microtunnel of the Sacramento River Intake Project from 20 to 75 feet.

Like the North microtunnel, there was a notable change in the soil conditions beneath Interstate-5 and the jacking forces increased. In the zone from 75 to 130 feet, there was a gradual increase in jacking forces, with the jacking stresses increasing to 0.11 tons/ft^2, as shown in Figure 4.12. Lubrication throughout this zone was not pumped at sufficient volumes to decrease the jacking forces and was therefore ineffective. At 130 feet into the drive the jacking forces dramatically increased to approximately 500 tons, similar to the increase seen on the North microtunnel. In the interval between 130 and 150 feet the jacking stress was 0.27 tons/ft^2. As with the North microtunnel, the high

pressure water jets were used at the face for excavation and lubrication was used to decrease the jacking forces. The use of the high-pressure water jets caused significant disturbance of the natural ground conditions resulting in localized surface settlement.

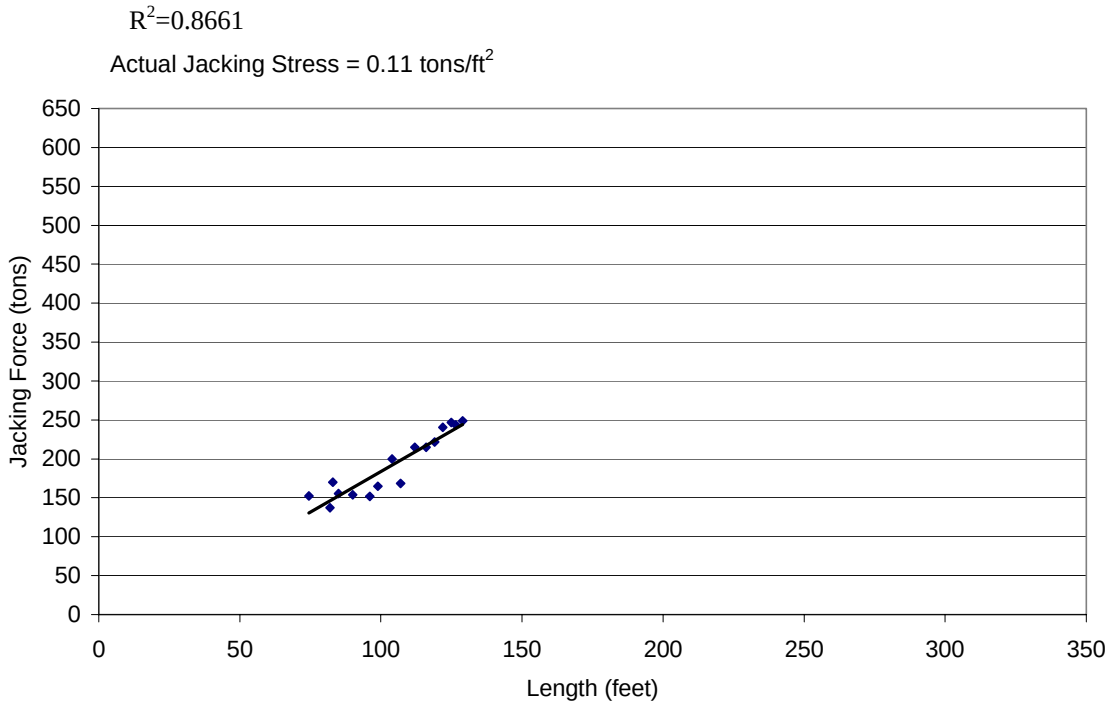

Figure 4.12. Length vs. Jacking Forces for the South Microtunnel of the Sacramento River Intake Project from 75 to 130 feet.

Once the tunneling had progressed to 210 feet into the drive, the tunneling machine was beyond Interstate-5 and the ground surface elevation decreased while tunneling from 210 to 250 feet into the drive. The ground surface elevation stabilized at a depth of 10 feet. From 290 feet into the tunnel drive until the termination of the tunnel at approximately 350 feet, the ground surface elevation remained relatively constant at 8 feet above the crown of the pipe with a jacking stress of 0.09 tons/ft^2. Figure 4.13 shows the frictional component of the jacking force throughout this interval.

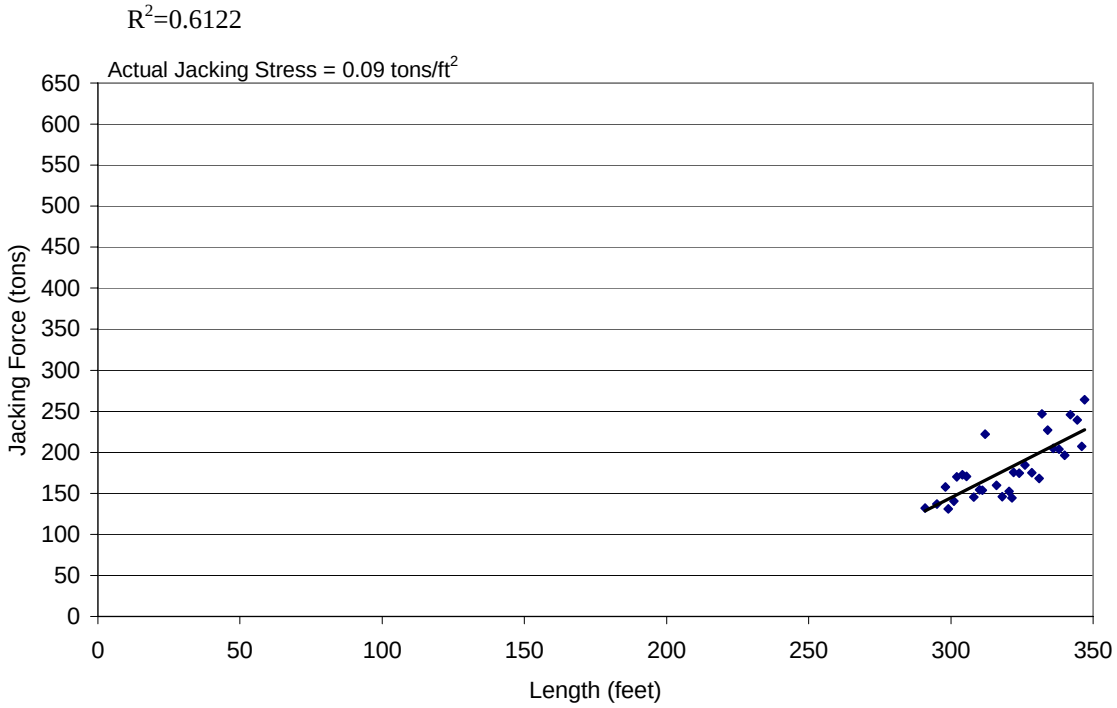

Figure 4.13. Length vs. Jacking Forces for the South Microtunnel of the Sacramento River Intake Project from 290 to 345 feet.

4.1.4.4 Overview of Normalized Friction Coefficients

Table 4.7 provides an overview of the jacking stress on the selected segments of the South Microtunnel on the Sacramento River Intake Project.

Table 4.7. Jacking Stress on Isolated Segments of the South Microtunnel Drive for the Sacramento River Intake Project.

Segments of Tunnel Alignment [feet]	Jacking Stress [tons/ft^2]	Notes	[R^2 Value]
20-75	0.084	No Lubrication	0.6424
75-130	0.11	Change in Soils	0.8661
290-350	0.09	No Lubrication	0.6122

4.2 Lowell Snohomish River Road-- Burlington Northern Railroad Crossing

The Clearview Water Supply Project included the construction of a 42-inch diameter force main that traversed part of Snohomish County just north of Seattle, Washington. Several microtunnels were included in the project to cross critical structures such as rivers, wetlands, railroads, and highways. In all cases, an oversized casing was microtunneled beneath the critical structure and the 42-inch product pipe was placed within the completed microtunnel. One of the microtunnels on the project was the crossing of the Lowell Snohomish River Road and the Burlington Northern Railroad.

4.2.1 Description of the Project

The project included microtunneling a 60-inch Permalok Steel casing beneath the Lowell Snohomish River Road, a two-lane road with light traffic traveling at high speeds, and then proceeding beneath a section of the Burlington Northern-Santa Fe Railroad that carried high-speed rail traffic. The total length of the tunnel was 210 feet. After construction of the tunnel, the pipeline would be subsequently lined with a 42-inch pressure water line for a water distribution system. A profile view of the crossing is shown in Figure 4.14

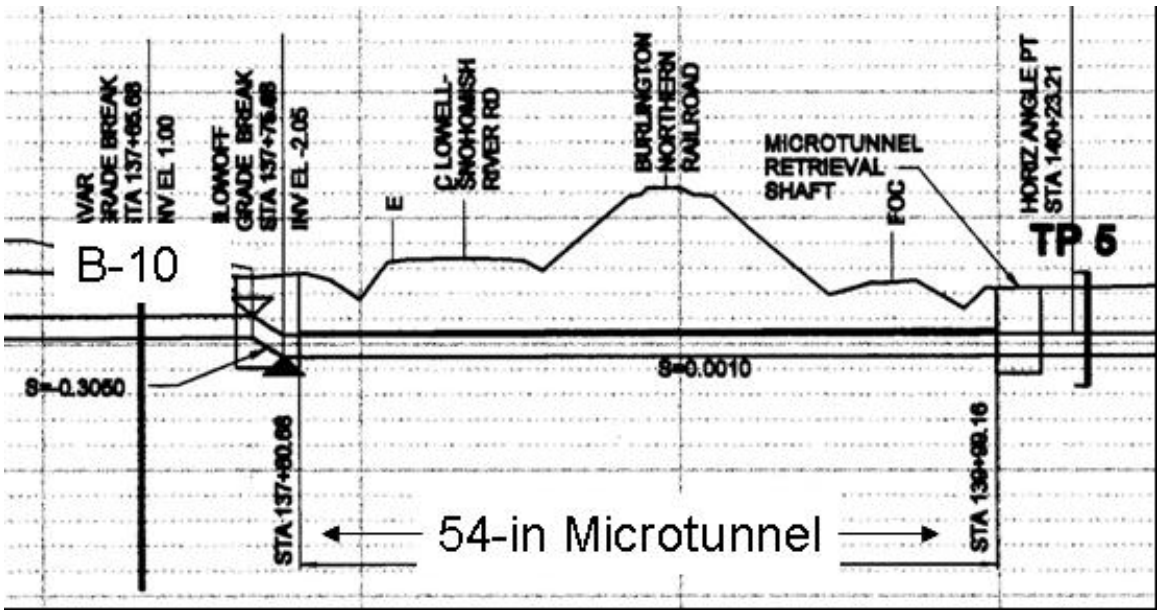

Figure 4.14. Design Profile for the Lowell Snohomish River Road – Burlington Northern Railroad Crossing (Montgomery Watson, 2000).

The launch shaft was constructed on the north side of the Lowell-Snohomish River Road and was approximately 18 feet deep. The shaft was constructed by driving interlocking sheet piles in a rectangular cell and excavating the soil from within the cell. Dewatering wells were placed around the shaft to aid in the construction of the launch shaft but their use was terminated once a tremie seal was established in the bottom of the shaft and a sump was established to pump out any small amounts of water that infiltrated the shaft. The launch shaft is shown in Figure 4.15.

Figure 4.15. Launch Shaft Constructed from Interlocking Sheet Piles.

The reception shaft was atypical of microtunneling operations due to the shallow depth of cover over the pipeline at the exit location. Since there was less than eight (8) feet of cover over the crown of the pipeline at the exit location on the south side of the Burlington Northern Santa Fe Railroad tracks, the contractor elected to set a trench box in line with the tunnel machine and place a steel plate over the typically open end. They then planned to lift the steel plate when the machine arrived at the box and push the machine into the trench box for removal from within the trench box.

Figure 4.16. Trench Box Reception Shaft. Steel Plate (in background of photo) Pulled Up to Allow Microtunneling Machine to Enter into the Area Protected by Trench Box.

The machine was launched with approximately 10 feet of cover, traversed beneath a ditch on the side of the road, and progressed beneath the Lowell Snohomish River Road with approximately 12 feet of cover. Beneath the Railroad, the maximum depth of cover was approximately 22 feet. Upon exit the machine traversed a ditch where the machine depth was as low as 4 feet and exited with approximately 7 feet of cover.

The pipe material was Permalok Steel, a rolled steel pipe with machined integral press-fit joints, eliminating the need to weld individual sections of steel. Pipe joints were 20 feet in length with the exception of the first joint which was 10 feet in length. The outer diameter of the pipe was 60-inches and the wall thickness was ¾-inches. The microtunnel was constructed with an Iseki Unclemole soft ground microtunneling machine with an outer diameter of 62-inches with a one inch overcut on the diameter. The machine does not have a cutter wheel like all other brands of microtunneling machines; instead, it has cutter bars or arms that rotate in an elliptical orbit about a central cone to crush the material that comes into the face of the machine. The face of the Iseki microtunneling machine is shown in Figure 4.17. The first section of the

machine was 10-feet, 9-inches. The trailing section, which was fabricated from a section of Permalok pipe and attached to the back of the Iseki machine with an adapter kit, measured 10-feet, 3-inches. Therefore, the full length of the machine and trailing apparatus was 21 feet prior to the first section of Permalok pipe.

Figure 4.17. Face of the 62-inch OD Iseki Machine with Oscillating Cutter Arms.

The machine was launched through a launch seal that was mounted directly to the shaft wall on the sheet piles. The sheet piles were then cut away prior to tunneling. In order to prevent the ground from caving into the shaft during the launch process, the contractor pre-grouted behind the launch wall of the shaft to stabilize the soil.

4.2.2 Geotechnical Conditions Along the Tunnel Alignment

For the project design, one vertical boring and one test pit were constructed to determine the soil conditions for the crossing. Figure 4.19 is a plan view of the site showing the locations of these geotechnical features.

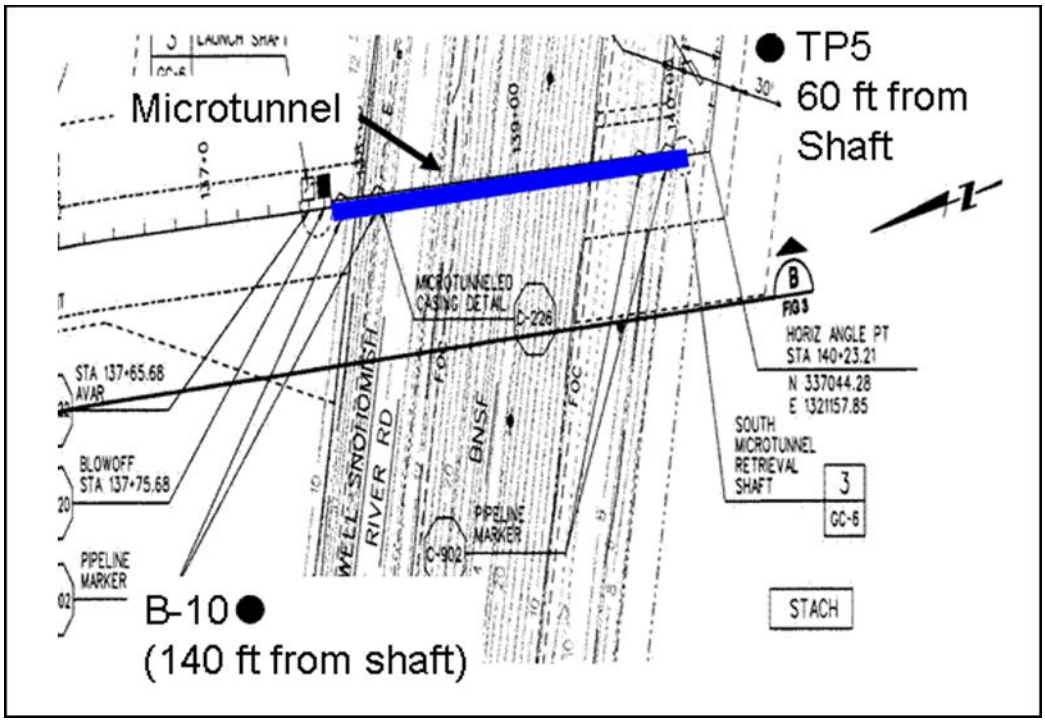

Figure 4.18. Plan View of Site showing Boring and
Test Pit Locations (modified from Montgomery Watson, 2000).

Boring, B-10 was drilled to determine conditions at the jacking shaft, although it was drilled 140 from the shaft location. In addition, test pit TP-5, was constructed 60 feet from the reception shaft location. No borings were constructed along the alignment, through the roadway, or in the Railroad Right of Way as the designer elected not to procure permits for the geotechnical work in these areas considering the short length of the tunnel.

Boring B-10 indicated that the upper 10 feet of soil would be a silty sand with a blow count of 5 blows per foot. However, it was difficult to extrapolate this information to the tunnel due to the fact that the ground surface elevation at the boring location was not measured. Therefore, extrapolation of the boring information to the ground surface elevation at the tunnel site was not possible. Of particular alarm was the information at an elevation of 10 feet where the boring indicated a Blow Count of zero, and a note that

the split spoon sampler sank under its own weight. This would be extremely problematic for tunneling operations as there was concern over whether the soil had sufficient bearing capacity to support the weight of the tunneling machine. Boring B-10 is shown in Figure 4.19. The test pit that was excavated to determine soil conditions at the reception shaft indicated sandy silt (ML) to a depth of 7 feet. From 7 feet to the termination of the test pit at 18 feet, they encountered silt (ML) and silty sand (SM). The test pit log noted loose to medium dense consistency and very fine sands. The test pit caved badly at a depth of 10 feet and had to be terminated at 18 feet due to the excessive caving. Organics were not noted on the reception shaft side of the tunnel alignment. The log of the test pit is shown in Figure 4.20.

4.2.3 Construction of the Microtunnel

The launch of the microtunneling machine took place on November 15, 2001. The first day of tunneling was spent launching the machine (measuring 10-feet, 9-inches), the trailing can or steering section (measuring 10-feet, 3-inches), and the first 20-foot Permalok pipe. The tunneled material was primarily silty sand. On November 16, 2001 tunneling progressed at a very fast pace and 120 feet of pipe was installed in 15 hours. The material through which the machine was tunneling was primarily sand with approximately 20 percent silt. On November 17, 2001 the tunnel was completed with the final 51 feet of tunneling taking only 8.5 hours to complete, including two hours of downtime when the contractor elected to clean the silt from the slurry tank due to the thickening of the slurry. No significant events occurred during tunneling that would notably impact the jacking forces.

CH2M HILL

PROJECT NUMBER	BORING NUMBER	
139866.A0.07	B-10	SHEET 1 OF 3

SOIL BORING LOG

PROJECT CLEARVIEW WATER SUPPLY PIPELINE LOCATION NORTH OF LOWELL-SNOHOMISH RIVER ROAD

ELEVATION NOT MEASURED DRILLING CONTRACTOR GREGORY DRILLING, INC., REDMOND, WA

DRILLING METHOD AND EQUIPMENT MUD ROTARY/CME 850 TRACK RIG WITH AUTOMATIC HAMMER

WATER LEVELS NOT MEASURED START 11/24/97 FINISH 11/25/97 LOGGER P. DAVIS

DEPTH BELOW SURFACE (FT)	SAMPLE INTERVAL	SAMPLE TYPE AND NUMBER	SAMPLE RECOVERY	STANDARD PENETRATION TEST RESULTS 6"-6"-6" (N)	SOIL DESCRIPTION: SOIL NAME, USCS GROUP SYMBOL, COLOR, MOISTURE CONTENT, RELATIVE DENSITY OR CONSISTENCY, SOIL STRUCTURE, MINERALOGY	COMMENTS: DEPTH OF CASING, DRILLING RATE, DRILLING FLUID LOSS, TESTS AND INSTRUMENTATION
5.0	5.0					
	6.5	1-SS	1.5	2-3-2 (5)	SILTY SAND, (SM), gray, wet, loose, fine-grained sand, with some organics.	Natural Water Content = 29 %
10.0	10.0					
	11.5	2-SS	1.5	0-0-0 (WOH)	ORGANIC SILT, OH, gray, wet, very soft, approximately 10 percent organics and wood debris.	Natural Water Content = 73 % Liquid Limit = 89 % Plasticity Index = 23 %
						Encountered water at 10.5 feet.
15.0	15.0					
	16.5	3-SS	1.2	2-3-3 (6)	SANDY SILT, ML, dark gray to gray, wet, firm, fine grained sand.	Laboratory Visual Classification
20.0	20.0					
	21.5	4-SS	1.5	0-0-1 (1)	ORGANIC SILT, (OH), brown, wet, very soft, with visible organics.	Natural Water Content = 143 %
	23.5	5-ST	2.0	PUSH	Top 1.5 inches: ORGANIC SILT, OH, gray, wet, very soft (slough?). Middle 9.5 inches: ORGANIC SILT, OH, gray, wet, soft, with visible organics. Bottom 15.5 inches: ORGANIC SILT, OH, gray, wet, soft, interbedded with stiffer peat layers.	HYDROMETER ANALYSIS: Silt = 100% Natural Water Content = 70 % Liquid Limit = 70 % Plasticity Index = 23 % UNCONFINED COMPRESSION TEST: Shear Strength, Su = 6.5 psi LAB VANE SHEAR TEST: Average Su = 13.5 psi
	25.0					

Figure 4.19. Boring Log B-10 Drilled to Determine Soil Properties at the Launch Shaft for the Lowell Snohomish River Road- Burlington Northern Railroad Crossing (CH2M Hill, 2001).

Project No.: 139866.A0.07

TEST PIT LOG

Project: Clearview Water Supply Pipeline
Contractor: Sonrise Excavating Inc.
Excavation Equipment: Komatsu- PC 120
Logger: K Green

Depth Below Surface (FT)	Sample: Interval	Sample: Type and Number	Soil Description: Soil name, color, moisture content, relative density or consistency, soil structure, mineralogy, uscs group symbol	Symbolic Log	Comments: Difficulty in excavation, running gravel condition, collapse of walls, sand heave, debris encountered, water seepage gradational contacts, tests, instrumentation
			Location: North Side of Valley by Railroad		**Test Pit No. TP-5**
			Elevation:		
			Date Excavated: 10 Nov 1997		Water Level: ~3.5 feet
					Sheet 1 of 1
1.0	0.0 10"		SANDY SILT (ML), dark brown, moist, with some organics.		Topsoil
2.0	10" 3ft		SANDY SILT (ML), moist to wet, soft, mottled.		
3.0	3ft 7ft		SANDY SILT (ML), wet, mottled, with thin sandy zones.		Seepage at 3.5 feet
4.0					
5.0					
6.0					
7.0	7ft 18ft		SILT (ML) and SILTY SAND (SM), blue-gray, non-plastic, soft / loose to medium dense, very fine sand.		
8.0					
9.0					
10.0					Started caving badly when depth is at 10 feet.
11.0					
12.0					Finer grained below about 12 feet (lesser sand).
13.0					
14.0					Several thin sandy zones from 12 to 18 feet.
15.0					
16.0					Test pit caved to 10 feet wide by 14 feet long.
17.0					Soft, loose to medium dense alluvial sediments.
18.0			BOTTOM OF TEST PIT @ 18 feet.		Terminated test pit due to caving.
19.0					
20.0					

Figure 4.20. Test Pit Log for Soil Conditions at the Reception Shaft Location (CH2M Hill, 2001).

4.2.4 Jacking Forces on the Microtunnel

The frictional component of the jacking forces was measured by subtracting the face pressure acting over the area of the face of the microtunneling machine from the total jacking load measured at the main jacking frame in the jacking shaft. The frictional component of the jacking forces on the microtunnel crossing ranged from 24 tons to a maximum of 95 tons. Figure 4.21 shows the frictional component of the jacking force along the entire microtunnel drive.

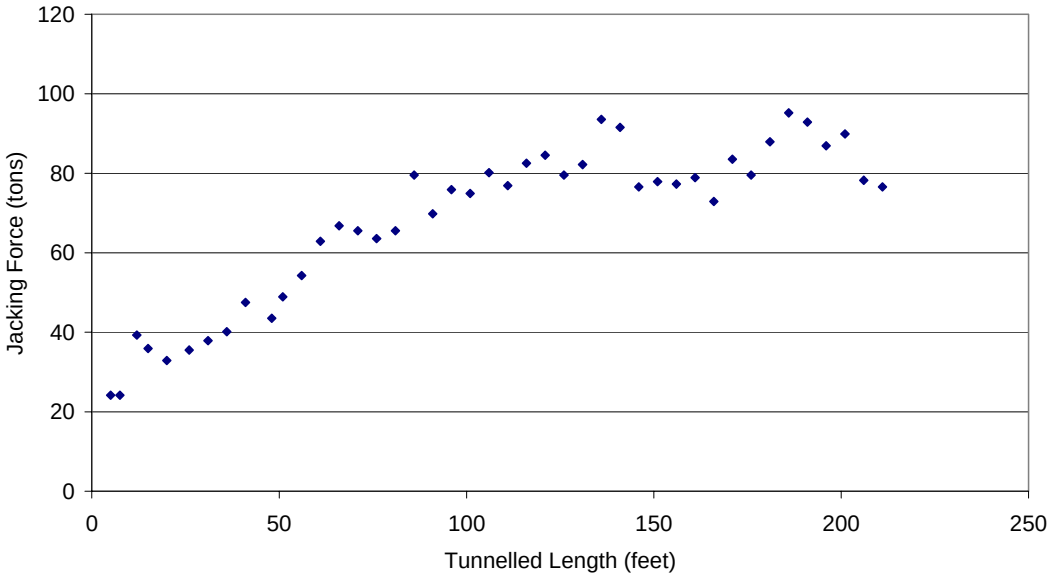

Figure 4.21. Length vs. Jacking Force for the Lowell Snohomish River Road BNRR Crossing

4.2.5 Lubrication During Tunneling

A bentonite lubrication system was used during the entire microtunneling drive. However, the bentonite lubrication system was not automated and was not capable of any automated pumping between ports located within the pipeline. A small bentonite

batching plant, as shown in Figure 4.22, was located at the surface and a laborer manually mixed 50-pound bentonite bags with water in the batch plant prior to pumping the bentonite to ports that were manually connected and opened along the pipeline by an operator in the shaft. The tunneling crew or the microtunneling machine operator did not record pumping volumes. Bentonite was injected at only one location throughout the first 120 feet of tunneling: through the port located in the tail section of the trailing can of the machine. At 120 feet into the drive, an additional bentonite port was connected approximately 60 feet behind the cutting edge of the machine. Bentonite was pumped through this port and the port in the tail shield for the remainder of the drive. Bentonite lubrication was pumped continuously throughout all tunneling operations.

4.2.6 Isolation of Tunneling Segments for Specific Analysis

The machine was launched through the sheet pile wall into a grout bulb that was placed by the contractor to stabilize the ground outside the shaft. The machine was 21 feet in length and the first pipe section was attached to the tail end of the machine. Figure 4.23 is a graph of the frictional component of the jacking forces from 20 to 120 feet of tunneled length. Over this interval, the jacking stress is 0.03 tons per square foot of pipe surface area.

Figure 4.22. Bentonite Batch Plant located on Ground Surface.

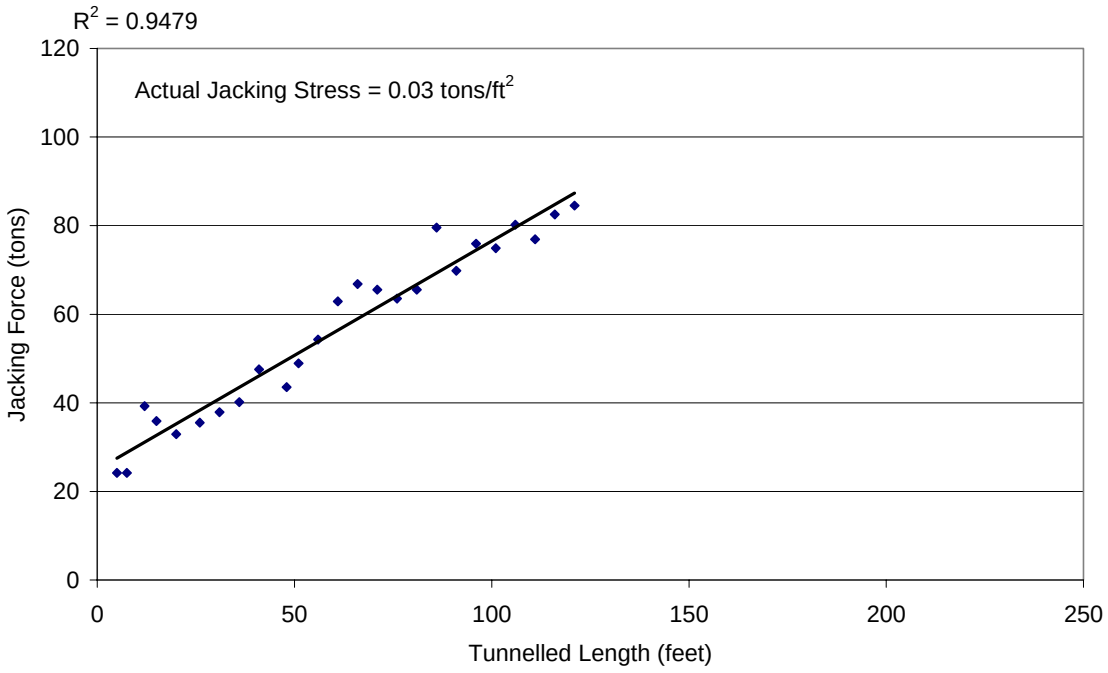

Figure 4.23. Length vs. Jacking Force for the Lowell Snohomish River Road – Burlington Northern Railroad Crossing from 20 to 120 feet.

At 120 feet into the drive, the lubrication on the pipeline changes, as does the slope of the jacking force curve. Figure 4.24 shows another isolated segment between 146 and 186 feet into the tunnel drive. Throughout this segment the jacking stress is 0.02 tons per square foot of pipe surface area.

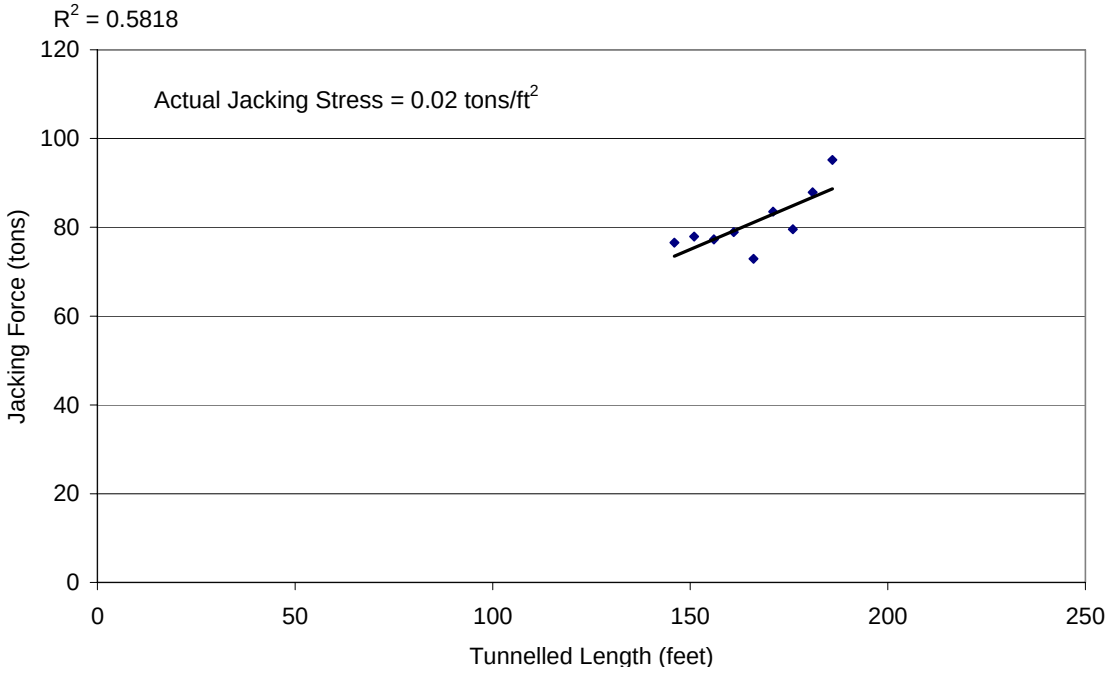

Figure 4.24. Length vs. Jacking Force for the Lowell Snohomish River Road – Burlington Northern Railroad Crossing from 146 to 186 feet.

4.2.7 Summary of the Jacking Stresses on Isolated Tunneling Segments

Table 4.8 provides a summary of the normalized frictional coefficients for the isolated sections of the drive analyzed above.

Table 4.8. Jacking Stress on Isolated Segments of the Lowell Snohomish River Road – Burlington Northern Railroad Crossing.

Segments Along Tunnel Alignment [ft]	Jacking Stress [tons/ft^2]	Notes	[R^2 Value]
20-120	0.03	Moderate Lubrication	0.9479
146-186	0.02	Increased Lubrication	0.5818

4.3 Clearview Snohomish River Crossing 2001

The Clearview Water Supply Project included the construction of a 42-inch diameter force main that traversed beneath the Snohomish River in Snohomish, Washington. The force main was installed within a 60-inch casing pipe that was designed as a 1,150 foot microtunnel beneath the Snohomish River.

4.3.1 Description of the Project

The 60-inch microtunnel was constructed with Permalok steel casing beneath the Snohomish River in very challenging geotechnical conditions. Due to the depth of the Snohomish River, and the estimated 100-year scour depth, the pipeline design elevation was 85 feet below the ground surface elevation at the jacking shaft and over 100 feet below the ground surface at the reception shaft. Due to the extreme depths of the pipeline, the high groundwater table, and the challenging geotechnical conditions, limited shaft construction options were available to the contractor. The engineer specified a sunk-in-place concrete caisson for the jacking shaft and allowed the contractor to choose the construction method for the reception shaft. Due to permitting restrictions along the south bank of the Snohomish River, the jacking shaft was forced away from the river bank approximately 550 feet, forcing the design length of the microtunnel to increase significantly and consequently markedly increasing the overall risk of the microtunnel operations. A profile view of the designed microtunnel crossing is shown in Figure 4.25. The 28-foot inner diameter launch shaft was constructed by pouring the three (3)-foot concrete shaft walls in a 10-foot circular concrete lift. The soil from within the concrete ring was then excavated, allowing the 10-foot ring to sink on it’s own weight.

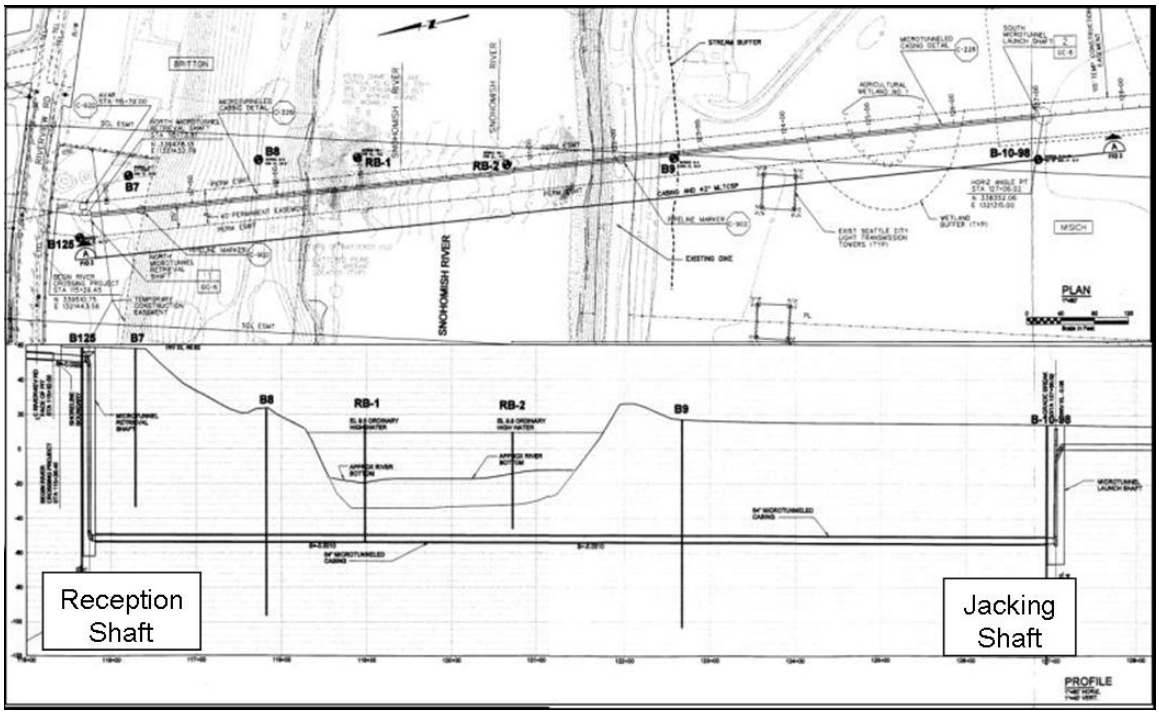

Figure 4.25. Plan and Profile of Snohomish River Crossing (Montgomery Watson, 2000).

Once the lift had sunk to near the ground surface, the next concrete lift was formed and poured and the cycle was repeated until the desired depth of approximately 90-feet was reached. The entire shaft was excavated "in-the-wet" to prevent caving at the shaft bottom. A 12-foot concrete tremie plug was placed at the bottom of the shaft to prevent uplift and the shaft floor was structurally tied to the shaft walls for added protection against uplift. Figure 4.26 show the concrete caisson jacking shaft during construction.

The reception shaft that was constructed on the bluff along the north side of the river was constructed using an auger drilling method to a depth of approximately 110 feet. The top 20-feet of the shaft was cased with a 20-foot diameter "over-sized casing." A large auger drill rig drilled a pilot hole in the center of the over-sized casing to the full shaft depth. The pilot hole was approximately 4-feet in diameter.

Figure 4.26. Poured Concrete Caisson Lift Prior to Sinking.

The entire pilot hole was filled with a thick polymer to support the ground and prevent caving of the open bore. The pilot hole was then enlarged with a reamer to a 20-foot finished diameter with a set of reaming tools that was fitted to the auger drilling rig. As with the pilot hole, the walls of the shaft were stabilized using polymer. Once the shaft was fully excavated to the 20-foot diameter, an inner-casing, measuring 16-feet diameter, was set into the excavated shaft to full depth and the annulus between the inner casing and the excavated soil was grouted using tremie methods. A grout plug was placed in the bottom of the shaft to prevent uplift of the shaft. Once the concrete shaft walls and floor were poured, the polymer was pumped from within the inner-casing and the shaft was complete. Figure 4.27 shows the reception shaft and the drill rig.

(a) (b)

(c) (d)

Figure 4.27. Auger Drilled Shaft on North Side of Snohomish River a) Auger with Reaming Wings b) Auger with Reaming Wings Connected to Drill c) Crane Lifting Full Section of Inner Casing d) Setting Inner Casing in Polymer-Filled Drilled Shaft.

The pipe material used for microtunneling was Permalok Steel, a rolled steel pipe with machined integral press-fit joints, eliminating the need to weld individual sections of steel. The pipe joints were 20 feet in length with the exception of the first joint which was 10 feet in length. The outer diameter of the pipe was 60-inches and the wall thickness was ¾-inches. The microtunnel was constructed with an Iseki Unclemole soft ground microtunneling machine with an outer diameter of 62-inches with a one inch overcut on the diameter. As with the Lowell Snohomish River Road-Burlington Northern Railroad Crossing Project, the Iseki machine did not have a cutter wheel. Rather, it had cutter bars or arms that rotated with an elliptical orbit about a central cone

to crush the material that comes into the face of the machine. The face of the Iseki microtunneling machine is shown in Figure 4.28. The first section of the machine was 10-feet 9-inches. The trailing section which was fabricated from a section of Permalok pipe and attached to the back of the Iseki machine with an adapter kit measured 10-feet, 3-inches. Therefore, the full length of the machine and trailing apparatus was 21 feet prior to the first section of Permalok pipe.

Figure 4.28. Face of Iseki Machine with Oscillating Cutter Arms.

The machine was launched through the caisson wall and the launch seal was mounted directly to the concrete on the caisson wall, forcing the microtunneling machine to tunnel through the concrete prior to entering into the native soil. This launch procedure allowed the contractor to launch the machine without having to employ ground stabilization measures.

4.3.2 Geotechnical Conditions Along the Tunnel Alignment

For the project design, seven vertical boring were completed, including two in-river borings. The geotechnical conditions along the tunnel alignment were grouped into two primary groups by the geotechnical engineer on the project: “older alluvium” and “transitional beds.” The older alluvium was granular in nature and contained high percentages of gravel. The boring logs showed repeated zones of poorly graded sands with gravel as well as well graded sands and gravels. The geotechnical report also noted the presence of cobbles and the possibility of encountering boulders within the formations.

The transition beds, however, contained a much higher fines content and the boring logs indicate poorly graded sands with silt along the tunnel alignment. Of major concern for the designers was the presence of wood that was found in the borings that were attempted in the Snohomish River. Many logs or trees were encountered by the vertical borings in the Snohomish River and the borings hit refusal when trying to drill through the logs. These logs were thought to have been buried during landslide or volcanic events and were known to be buried in the Snohomish River Valley at depths exceeding the design elevation of the pipeline. These logs concerned the designers, as microtunneling machines historically have difficulty tunneling through wood.

Boring B-10-98 at the elevation of the tunnel is shown in Figure 4.29. This boring shows the older alluvium material in which the tunnel would start at a depth of approximately 65 feet to the crown of the pipeline. The soil along the north bluff that was characterized as transition bed soils by the geotechnical engineer on the project were shown on vertical boring B125. The section of the boring showing the tunnel horizon is shown in Figure 4.30.

4.3.3 Construction of the Microtunnel

Microtunneling for the Snohomish River crossing began on December 10, 2001. The contractor elected to conduct operations 24 hours per day, using two 12-hours shifts. Table 4.9 shows the tunneling progress for the first 582 feet of microtunneling operations.

Table 4.9. Progression Rates for the Snohomish River Crossing 2001.

Date	Day Shift Production [feet]	Night Shift Production [feet]	Cumulative Production [feet]
December 10, 2001	21	20	41
December 11, 2001	40	40	121
December 12, 2001	70	70	261
December 13, 2001	24	60	345
December 14, 2001	60	60	465
December 15, 2001	60	30	555
December 16, 2001	25	2	582

Tunnel progression rates were considered very good between December 11 and December 15, averaging 51.4 feet per 12 hour shift. This is especially good since the contractor was working from a deep launch shaft which typically slows pipe connection times. However, at 580 feet into the microtunnel drive, the tunnel production came to an abrupt halt as the machine was having difficulty excavating the native material which contained gravel and cobbles. Many pieces of crushed granite were collected from the coarse shaker screen of the separation plant. The jacking forces markedly increased in this zone to 560 tons and sounds transmitted from the crushing chamber of the machine when the cutter head was rotating indicated rocks were being crushed

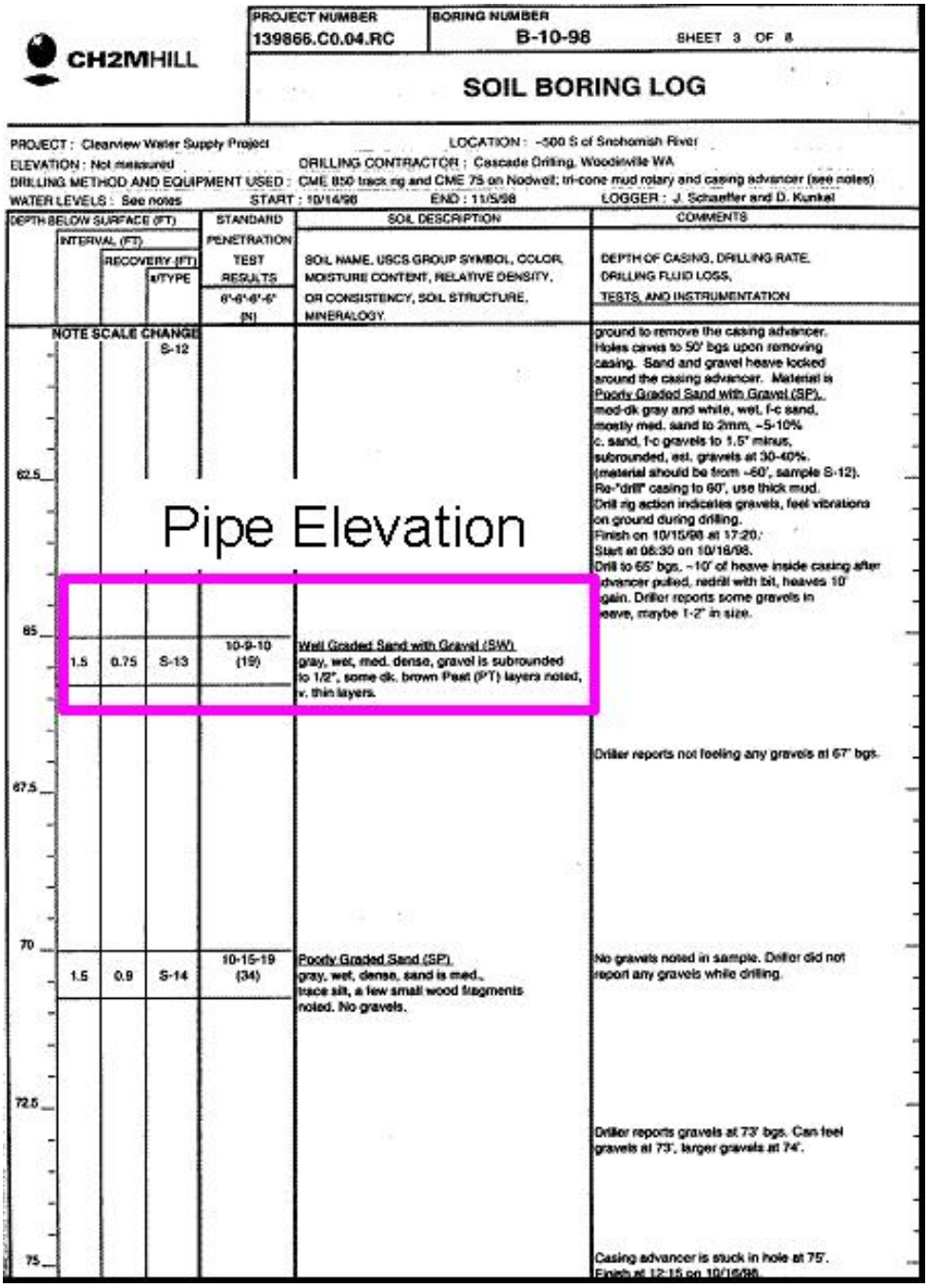

CH2MHILL

PROJECT NUMBER 139866.C0.04.RC | BORING NUMBER B-10-98 | SHEET 3 OF 8

SOIL BORING LOG

PROJECT : Clearview Water Supply Project — LOCATION : ~500 S of Snohomish River
ELEVATION : Not measured — DRILLING CONTRACTOR : Cascade Drilling, Woodinville WA
DRILLING METHOD AND EQUIPMENT USED : CME 850 track rig and CME 75 on Nodwell; tri-cone mud rotary and casing advancer (see notes)
WATER LEVELS : See notes — START : 10/14/98 — END : 11/5/98 — LOGGER : J. Schaeffer and D. Kunkel

DEPTH BELOW SURFACE (FT)	INTERVAL (FT)	RECOVERY (FT)	#/TYPE	STANDARD PENETRATION TEST RESULTS 6"-6"-6"-6" (N)	SOIL DESCRIPTION: SOIL NAME, USCS GROUP SYMBOL, COLOR, MOISTURE CONTENT, RELATIVE DENSITY, OR CONSISTENCY, SOIL STRUCTURE, MINERALOGY	COMMENTS: DEPTH OF CASING, DRILLING RATE, DRILLING FLUID LOSS, TESTS, AND INSTRUMENTATION
	NOTE SCALE CHANGE		S-12			ground to remove the casing advancer. Holes caves to 50' bgs upon removing casing. Sand and gravel heave locked around the casing advancer. Material is Poorly Graded Sand with Gravel (SP), med-dk gray and white, wet, f-c sand, mostly med. sand to 2mm, ~5-10% c. sand, f-c gravels to 1.5" minus, subrounded, est. gravels at 30-40%. (material should be from ~60', sample S-12). Re-"drill" casing to 60', use thick mud. Drill rig action indicates gravels, feel vibrations on ground during drilling. Finish on 10/15/98 at 17:20. Start at 08:30 on 10/16/98. Drill to 65' bgs. ~10' of heave inside casing after advancer pulled, redrill with bit, heaves 10' again. Driller reports some gravels in heave, maybe 1-2" in size.
62.5						
	Pipe Elevation					
65	1.5	0.75	S-13	10-9-10 (19)	Well Graded Sand with Gravel (SW) gray, wet, med. dense, gravel is subrounded to 1/2", some dk. brown Peat (PT) layers noted, v. thin layers.	
67.5						Driller reports not feeling any gravels at 67' bgs.
70	1.5	0.9	S-14	10-15-19 (34)	Poorly Graded Sand (SP) gray, wet, dense, sand is med., trace silt, a few small wood fragments noted. No gravels.	No gravels noted in sample. Driller did not report any gravels while drilling.
72.5						Driller reports gravels at 73' bgs. Can feel gravels at 73', larger gravels at 74'.
75						Casing advancer is stuck in hole at 75'. Finish at 12:15 on 10/15/98.

Figure 4.29. Vertical Boring at the Jacking Shaft showing Soil at the Tunnel Horizon (CH2M Hill, 2000).

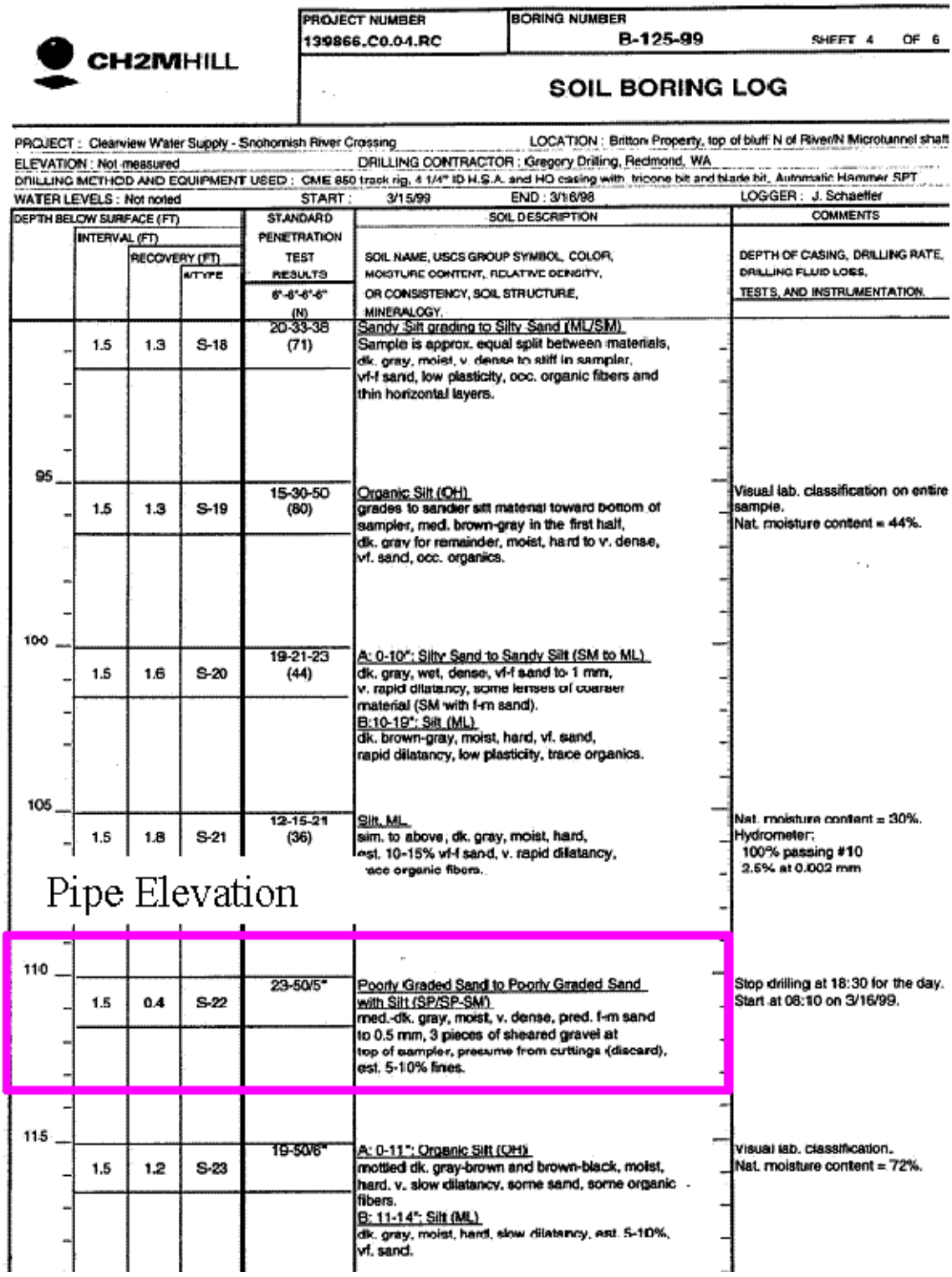

CH2MHILL

PROJECT NUMBER	BORING NUMBER	
139866.C0.04.RC	B-125-99	SHEET 4 OF 6

SOIL BORING LOG

PROJECT : Clearview Water Supply - Snohomish River Crossing — LOCATION : Britton Property, top of bluff N of River/N Microtunnel shaft
ELEVATION : Not measured — DRILLING CONTRACTOR : Gregory Drilling, Redmond, WA
DRILLING METHOD AND EQUIPMENT USED : CME 850 track rig, 4 1/4" ID H.S.A. and HO casing with tricone bit and blade bit, Automatic Hammer SPT
WATER LEVELS : Not noted — START : 3/15/99 — END : 3/16/98 — LOGGER : J. Schaefler

DEPTH BELOW SURFACE (FT)	INTERVAL (FT)	RECOVERY (FT)	TYPE	STANDARD PENETRATION TEST RESULTS 6"-6"-6" (N)	SOIL DESCRIPTION: SOIL NAME, USCS GROUP SYMBOL, COLOR, MOISTURE CONTENT, RELATIVE DENSITY, OR CONSISTENCY, SOIL STRUCTURE, MINERALOGY.	COMMENTS: DEPTH OF CASING, DRILLING RATE, DRILLING FLUID LOSS, TESTS, AND INSTRUMENTATION.
	1.5	1.3	S-18	20-33-38 (71)	Sandy Silt grading to Silty Sand (ML/SM) Sample is approx. equal split between materials, dk. gray, moist, v. dense to stiff in sampler, vf-f sand, low plasticity, occ. organic fibers and thin horizontal layers.	
95	1.5	1.3	S-19	15-30-50 (80)	Organic Silt (OH) grades to sandier silt material toward bottom of sampler, med. brown-gray in the first half, dk. gray for remainder, moist, hard to v. dense, vf. sand, occ. organics.	Visual lab. classification on entire sample. Nat. moisture content = 44%.
100	1.5	1.6	S-20	19-21-23 (44)	A: 0-10": Silty Sand to Sandy Silt (SM to ML) dk. gray, wet, dense, vf-f sand to 1 mm, v. rapid dilatancy, some lenses of coarser material (SM with f-m sand). B:10-19": Silt (ML) dk. brown-gray, moist, hard, vf. sand, rapid dilatancy, low plasticity, trace organics.	
105	1.5	1.8	S-21	12-15-21 (36)	Silt, ML sim. to above, dk. gray, moist, hard, est. 10-15% vf-f sand, v. rapid dilatancy, occ organic fibers.	Nat. moisture content = 30%. Hydrometer: 100% passing #10 2.5% at 0.002 mm
					Pipe Elevation	
110	1.5	0.4	S-22	23-50/5"	Poorly Graded Sand to Poorly Graded Sand with Silt (SP/SP-SM) med.-dk. gray, moist, v. dense, pred. f-m sand to 0.5 mm, 3 pieces of sheared gravel at top of sampler, presume from cuttings (discard), est. 5-10% fines.	Stop drilling at 18:30 for the day. Start at 08:10 on 3/16/99.
115	1.5	1.2	S-23	19-50/6"	A: 0-11": Organic Silt (OH) mottled dk. gray-brown and brown-black, moist, hard, v. slow dilatancy, some sand, some organic fibers. B: 11-14": Silt (ML) dk. gray, moist, hard, slow dilatancy, est. 5-10%, vf. sand.	Visual lab. classification. Nat. moisture content = 72%.

Figure 4.30. Vertical Boring at the Reception Shaft Showing Soil at the Tunnel Horizon (CH2M Hill, 2000).

The automated guidance system indicated that the machine was tilting or riding upwards. The contractor surveyed the machine and confirmed the upward tilt. All attempts to correct the attitude of the machine by adjusting the steering cylinders of the machine failed. Further advancement caused a gap to open between the machine and the steering joint (located at the invert in the rear of the machine). Steel bracing was welded across the joint to prevent further opening of the gap. Spikes in jacking forces and MTBM torque and a drastic increase in vertical alignment suggested the MTBM was against a large object and was being forced upwards.

At 580 feet into the drive, crushing noises in the crushing chamber subsided, indicating that all material that had previously been in the crushing chamber had been passed through the machine. The force on the top steering cylinder reached 550 tons indicating that the encountered object was at the crown of the machine, outside of the crushing chamber. Loud noises that appeared to originate from impact of the overcut cutters with the rock could be heard as the cutting arms of the machine rotated. Machine torque increased sharply as the cutting arms impacted the object, occasionally causing the machine to stall. By the end of the push (from 580 to 582 feet), the loud impact noises were no longer heard on the machine's microphone and small pieces of carbide steel were recovered in the slurry material at the separation plant. It was assumed that the periphery carbide cutting bits had been severely damaged, resulting in a loss of overcut. The obstruction was inferred to be a boulder located in the upper portion of the alignment. Repeated attempts to steer the machine downward with the hydraulic steering rams failed. Attempts to dislodge or move the machine past the obstruction with the 600 ton intermediate jacking station also failed. Tunneling was stopped and the drive was

terminated. The location of the machine placed it beneath the Snohomish River, approximately 60 feet from the south bank.

4.3.4 Jacking Forces on the Microtunnel

The frictional component of the jacking force was measured by subtracting the face pressure acting over the area of the face of the microtunneling machine from the total jacking load measured at the main jacking frame in the jacking shaft. The frictional component of the jacking force ranged from 38 tons to 145 tons. The high jacking loads recorded at the end of the drive were due to operations attempting to dislodge the machine from the boulder and are not indicative of normal jacking operations. A graph of the frictional component of the jacking forces is shown in Figure 4.31.

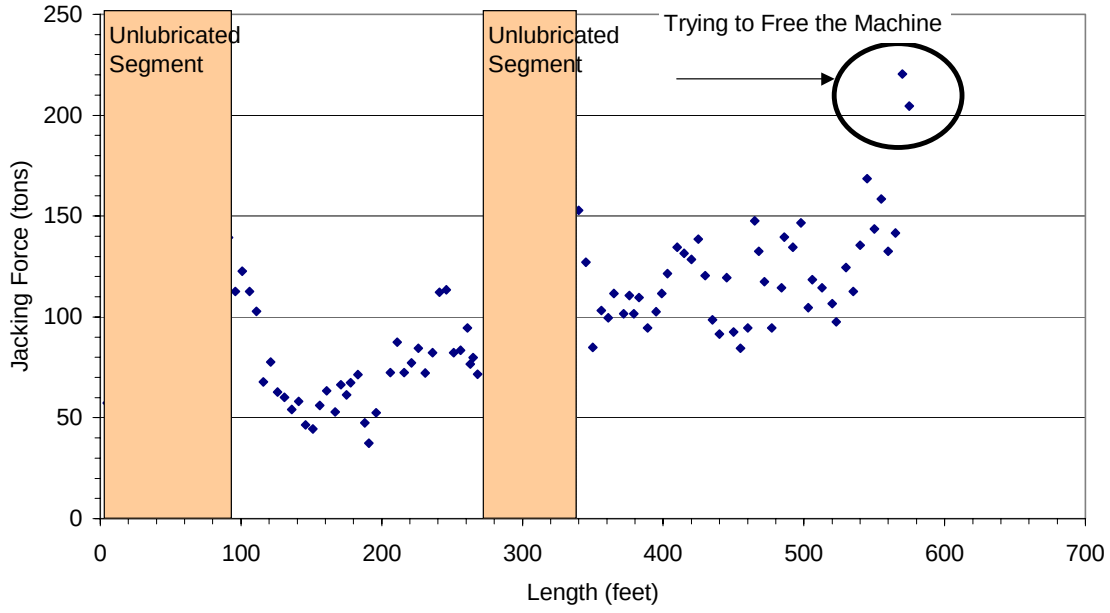

Figure 4.31. Length vs. Jacking Forces for the Clearview Snohomish River Crossing 2001 Project.

4.3.5 Lubrication During Tunneling

A bentonite lubrication system was used during tunneling. However, the lubrication system was not connected to any of the ports in the pipeline until the tunnel had progressed 100 feet. At 100 feet into the tunnel alignment, the contractor connected a manifold bentonite system to bentonite ports that were located at the crown of the pipeline. The bentonite ports were placed at the 10-, 12-, and 2- o'clock positions in the pipeline and were located on 20-foot centers along the tunnel length. The contractor selectively pumped through these bentonite ports, pumping through no more than three individual ports at one time. For example, at 100 feet into the pipeline, the contractor began pumping bentonite through pipe #2, located 50 feet from the leading edge of the microtunneling machine. Lubrication stopped at 150 feet during tunneling because the bentonite lubrication system was empty. This was not discovered until 240 feet into tunneling when the system was replenished and lubrication was resumed.

At 275 feet into the drive, lubrication stopped. This was due to the fact that the contractor had run out of bentonite on the site and was waiting for delivery of additional bentonite. Tunneling from 275 to 340 feet occurred without bentonite, until the contractor received the shipment of bentonite, and lubrication of the tunnel resumed.

4.3.6 Isolation of Tunneling Segments for Specific Analysis

The microtunneling machine was launched through the shaft wall and tunneled through 3 feet of the concrete in the caisson wall. The machine then tunneled through an area that was disturbed by the construction of the caisson and into the native soil. The machine was 21 feet in length and therefore would be fully in native ground once the jacking record reflected a tunneled length of 21 feet.

Figure 4.32 shows the frictional component of the jacking forces from 20 to 90 feet into the drive. Over this length the contractor was not applying any lubrication to the drive. The jacking stress was increasing at a rate of 0.074 tons per square foot of surface area. Once the contractor began lubricating, the jacking forces decreased to approximately 50 tons at 150 feet into the microtunnel drive. The jacking forces then began to increase over the length span of 150 to 240 feet of the tunnel drive when lubrication was stopped. Figure 4.33 shows the jacking force from 150 to 240 feet in the drive. The jacking stress over this span was 0.03 tons/ft^2, approximately 40 percent of the jacking stress prior to the lubrication procedure.

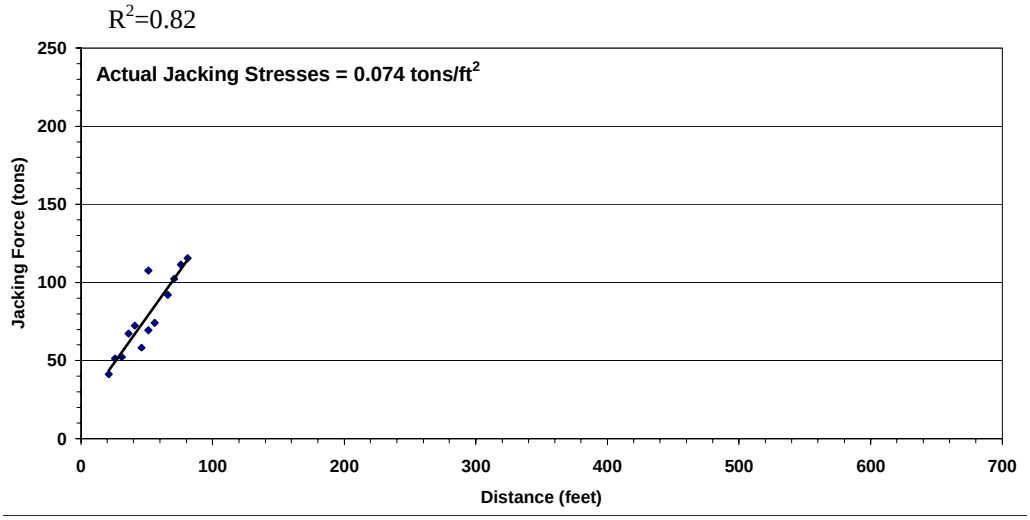

Figure 4.32. Length vs. Jacking Force for the Clearview Snohomish River Crossing 2001 from 20 to 90 feet.

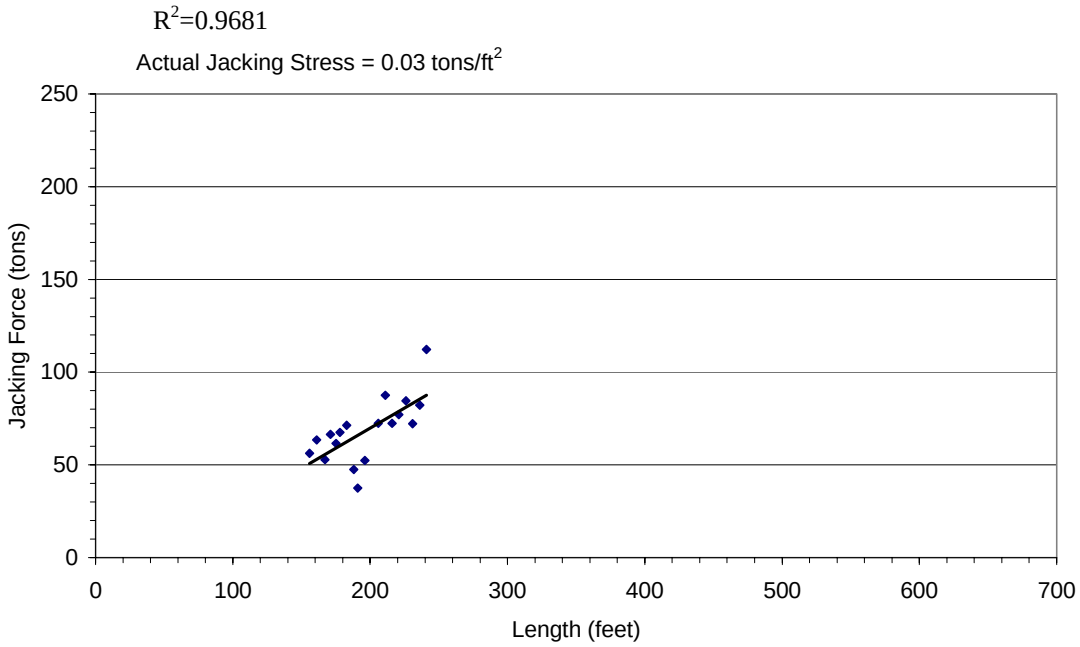

Figure 4.33. Length vs. Jacking Force for the Clearview Snohomish River Crossing 2001 from 150 to 240 feet.

At 275 feet into the drive there was a steep increase in jacking force where the lubrication of the tunnel was stopped. This increase in jacking force continued through 340 feet when the jacking forces markedly spiked and the contractor resumed lubrication procedures. Figure 4.34 shows the jacking stress throughout this segment at 0.06 tons per square foot of surface area.

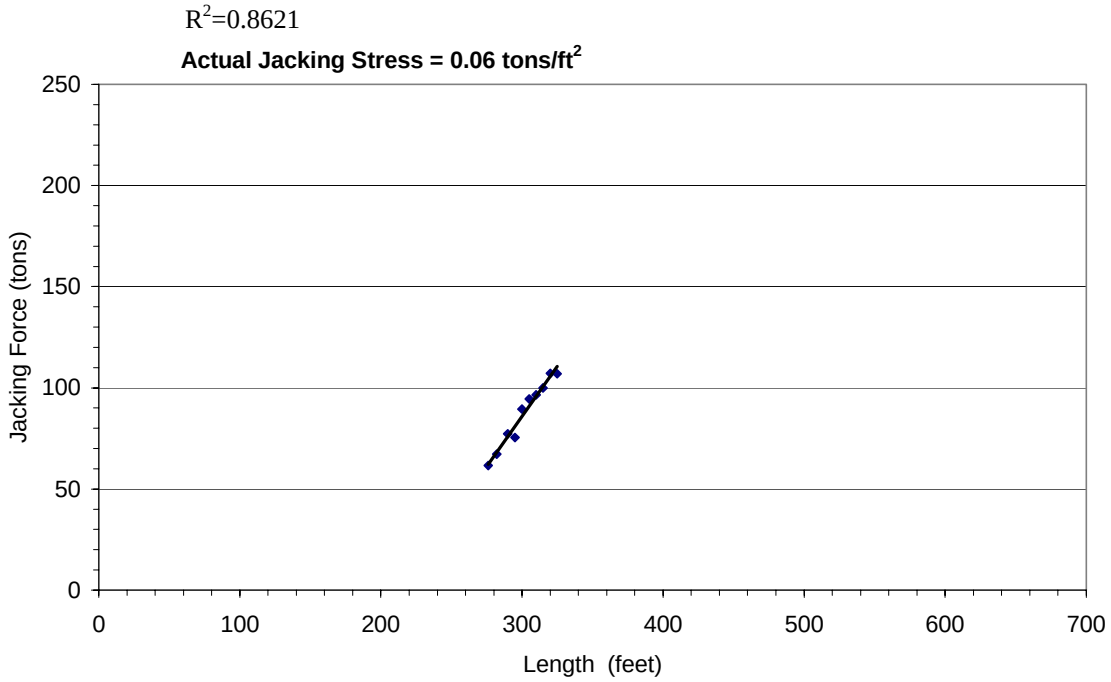

Figure 4.34. Length vs. Jacking Force for the Clearview Snohomish River Crossing 2001 from 275 to 340 feet.

The last isolated segment is at the end of the drive between 389 and 425 feet, through this segment, lubrication was stopped once again. The jacking stresses in this segment are 0.074 tons/ft2, equal to the jacking stresses in the first 90 feet of the tunnel drive where no lubrication was applied to the tunnel. Figure 4.35 shows the jacking forces throughout this segment.

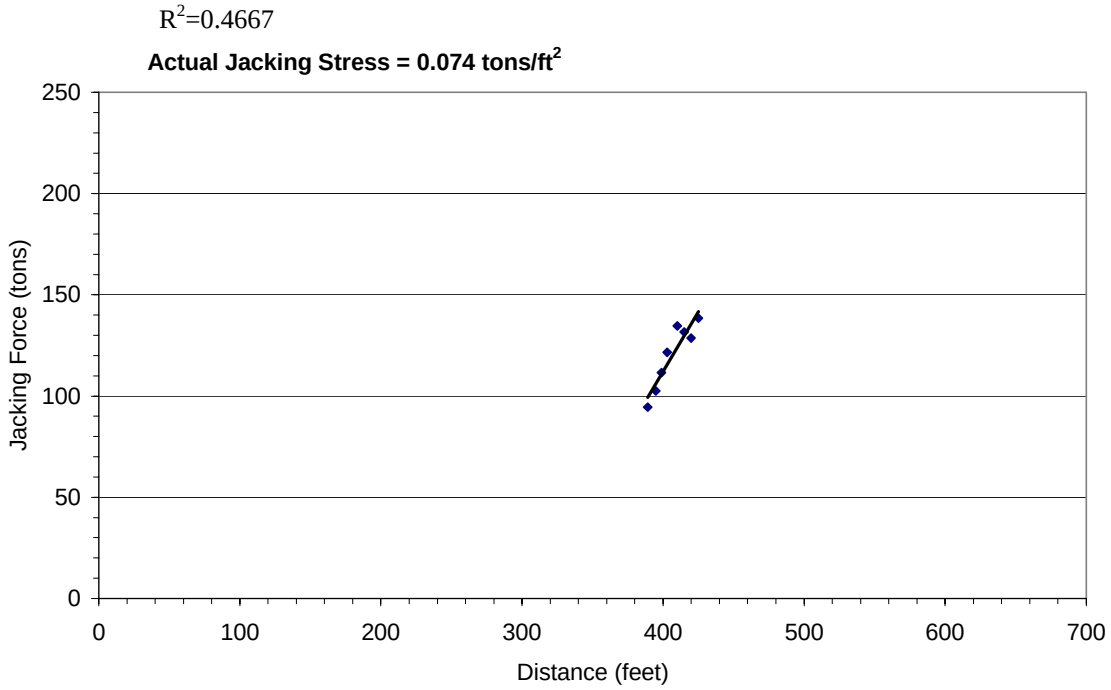

Figure 4.35. Length vs. Jacking Force for the Clearview Snohomish River Crossing 2001 Project from 390 to 425 feet.

4.3.7 Summary of Jacking Stresses on Isolated Tunneling Segments

Table 4.10 provides a summary of jacking stresses on the isolated segments of the Clearview Snohomish River Crossing 2001 project.

Table 4.10. Jacking Stresses on Isolated Segments of the Clearview Snohomish River Crossing 2001 Project.

Segments of Tunnel Alignment [feet]	Jacking Stress [tons/ft^2]	Notes	R^2 Value
20-90	0.074	No Lubrication	0.82
150-240	0.03	Increase after start of lubrication	0.4667
275-340	0.06	No Lubrication	0.968
390-425	0.074	No Lubrication	0.862

4.4 Clearview Snohomish River Crossing 2002

The first attempt to install the 42-inch diameter force main beneath the Snohomish River in Snohomish, Washington with microtunneling methods in 2001 failed due to the microtunneling machine encountering a boulder that was impassable. However, the pipeline beneath the Snohomish River was still required to complete the pipeline project. Therefore a new microtunnel was designed adjacent to the failed microtunnel and constructed in 2002.

4.4.1 Description of the Project

Like the original crossing design, the second river crossing design was a 60-inch microtunnel, constructed with Permalok Steel casing. To limit the number of new permits that the design team had to secure, it was decided to locate the new tunnel within the same right-of-way as the old tunnel. The design team tried to use the existing shafts for tunnel construction to limit the additional cost of construction for the river crossing. However, tunneling at a higher elevation was deemed too risky due to the possibility of encountering the wood that was known to exist in the bottom of the river. Tunneling at a lower elevation required deepening the jacking shaft, which, in turn, required removing the 12-foot thick concrete plug in the base of the shaft, which had required jet grouting through the tremie plug since the concrete base slab was used for stability of the shaft. This shaft deepening procedure was very costly and risky. Therefore it was decided to abandon the existing shaft and construct a new jacking shaft approximately 80 feet north and 40 feet east of the existing jacking shaft. The new tunnel alignment began approximately 20 feet deeper than the original alignment and terminated at the original

design termination location. This allowed the contractor to use the existing reception shaft.

Figure 4.36. Photograph of the Original and New Concrete Caisson Jacking Shaft.

By starting the Snohomish River Crossing 20 feet deeper than the original design and ending the crossing at the original design location at the auger drilled shaft, the new tunnel alignment passed the abandoned tunnel machine and the large boulder within six feet on the tangential distance, as shown in the schematic in Figure 4.37

The pipe material used for microtunneling was Permalok Steel, a rolled steel pipe with machined integral press-fit joints, eliminating the need to weld individual sections of steel. The pipe joints were 20 feet in length with the exception of the first joint which

was 10 feet in length. The outer diameter of the pipe was 60-inches and the wall thickness was ¾-inches.

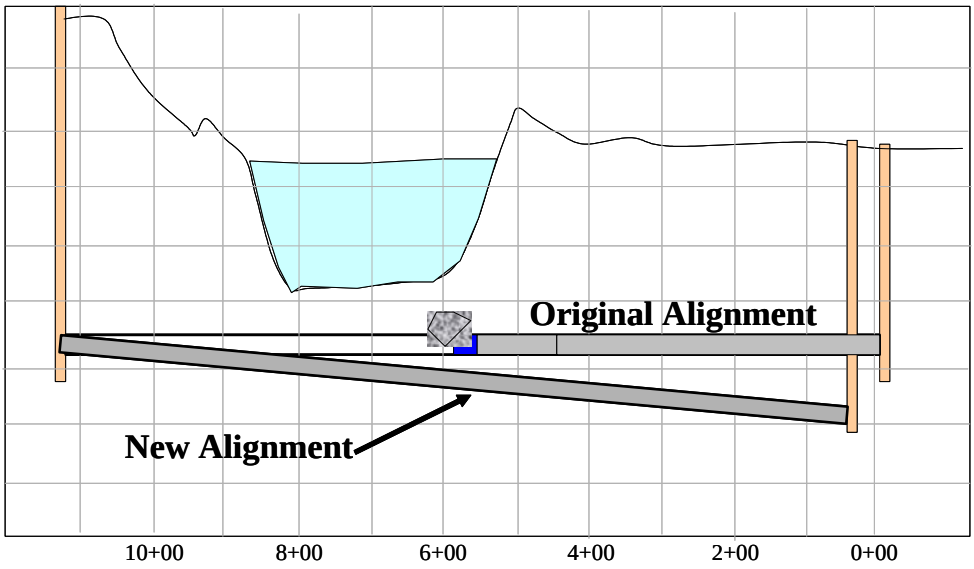

Figure 4.37. Profile of Original and New Alignment for the Clearview Snohomish River Crossing 2002.

For the second attempt of the Snohomish River Crossing the contractor used a different type of microtunneling machine than on the first attempt. A 62-inch Lovat MTS microtunneling machine was used with a combination rock cutter head. The rock head was chosen to excavate through large boulders should any be encountered on the second drive beneath the river. The head of the Lovat machine is shown in Figure 4.38.

As with the first attempted Snohomish River crossing, the machine was launched through the caisson wall and the launch seal was mounted directly to the concrete on the caisson wall, forcing the microtunneling machine to tunnel through the concrete prior to entering into the native soil. This launch procedure allowed the contractor to launch the machine without having to employ ground stabilization measures.

Figure 4.38. LovatMTS Microtunneling Machine with Mixed Face Rock Cutting Head used for the Second Attempt of Crossing the Snohomish River.

4.4.2. Geotechnical Conditions Along the Tunnel Alignment

The geotechnical conditions for the second attempted crossing were expected to be very similar to the first crossing. Although the crossing began 20 feet deeper, the soil boring at the jacking shaft indicated similar soils 20 feet below the original design elevation of the tunnel. Details of the geotechnical conditions can be found in Section 4.3.2.

4.4.3 Construction of the Microtunnel

Microtunneling for the Snohomish River 2002 crossing began on November 26, 2002. The contractor elected to conduct operations 24 hours per day, using two 12-hours shifts. Table 4.11 shows the tunneling progress for the 1058.5 foot microtunnel drive.

Table 4.11. Progression Rates for the Snohomish River Crossing 2002.

Date	Day Shift [feet]	Night Shift [feet]	Cumulative [feet]
November 26, 2002	11.5	11.5	23
November 27, 2002	20	20	63
November 28, 2002	35	9	107
November 29, 2002	40	40	187
November 30, 2002	45	35	267
December 01, 2002	20	60	347
December 02, 2002	60	25	432
December 03, 2002	37	13	482
December 04, 2002	45	40	567
December 05, 2002	52.5	42.5	662
December 06, 2002	65	60	787
December 07, 2002	40	44	871
December 08, 2002	60	50	981
December 09, 2002	10	67.5	1058.5

Tunnel progression rates were markedly slower with the Lovat machine than with the Iseki machine because the face of the Lovat machine was much more closed than the Iseki, which allowed more material to enter into the machine. With the smaller face openings on the Lovat machine, the torque on the face of the machine was relatively high, forcing the operator to run the machine at slower speeds, allowing the material to come into the crushing chamber of the machine for excavation and removal by the slurry system.

4.4.4 Jacking Forces on the Microtunnel

The frictional component of the jacking force was measured by subtracting the combined force on the steering cylinders at the face of the machine from the total jacking load measured at the main jacking frame in the jacking shaft. The frictional component of the jacking force ranged from 25 tons to 375 tons. A graph of the frictional component of the jacking forces is shown in Figure 4.39.

4.4.5 Lubrication During Tunneling

Unlike the original drive beneath the Snohomish River, an automated bentonite lubrication system was used to lubricate the pipeline. This bentonite system was capable of distributing bentonite in a much more sophisticated manner than on the original drive resulting in a much more efficient pipe lubrication system. Unfortunately a detailed lubrication record of the exact lubrication ports through which lubrication was applied was not available from the contractor. The contractor did start applying lubrication to the drive once the tunnel had progressed approximately 50 feet into the drive and continued to lubricate continuously throughout the drive; however, the lubrication volumes are unknown.

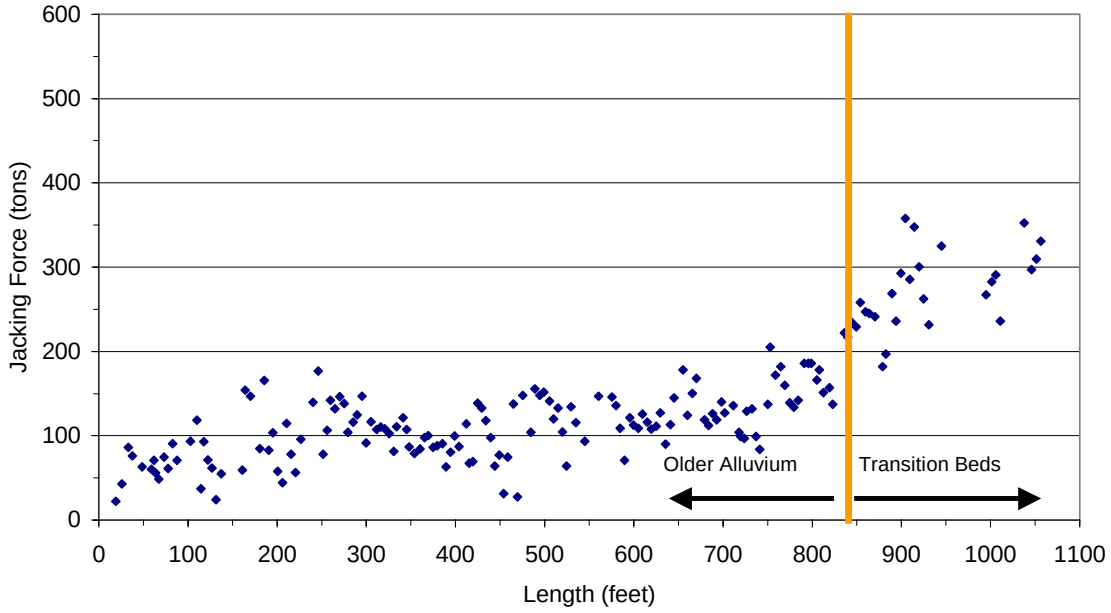

Figure 4.39. Length vs. Frictional Component of Jacking Force on the Clearview Snohomish River Crossing 2002.

4.4.6 Isolation of Tunneling Segments for Specific Analysis

The microtunneling machine was launched through the shaft wall and tunneled through three (3) feet of the concrete in the caisson wall. The machine then tunneled through an area that was disturbed by the construction of the caisson and into the native soil. The machine was 21 feet in length and therefore the pipe material was in the native ground when the jacking record reflected a length of approximately 25 feet.

The segment between 50 and 110 feet of the tunnel drive was lubricated; however, a very nominal amount of lubrication was pumped to the annular space of the tunnel. Figure 4.40 shows the jacking forces between 50 and 110 feet into the drive. In this section, the jacking stress was 0.056 tons per square foot of pipe surface area.

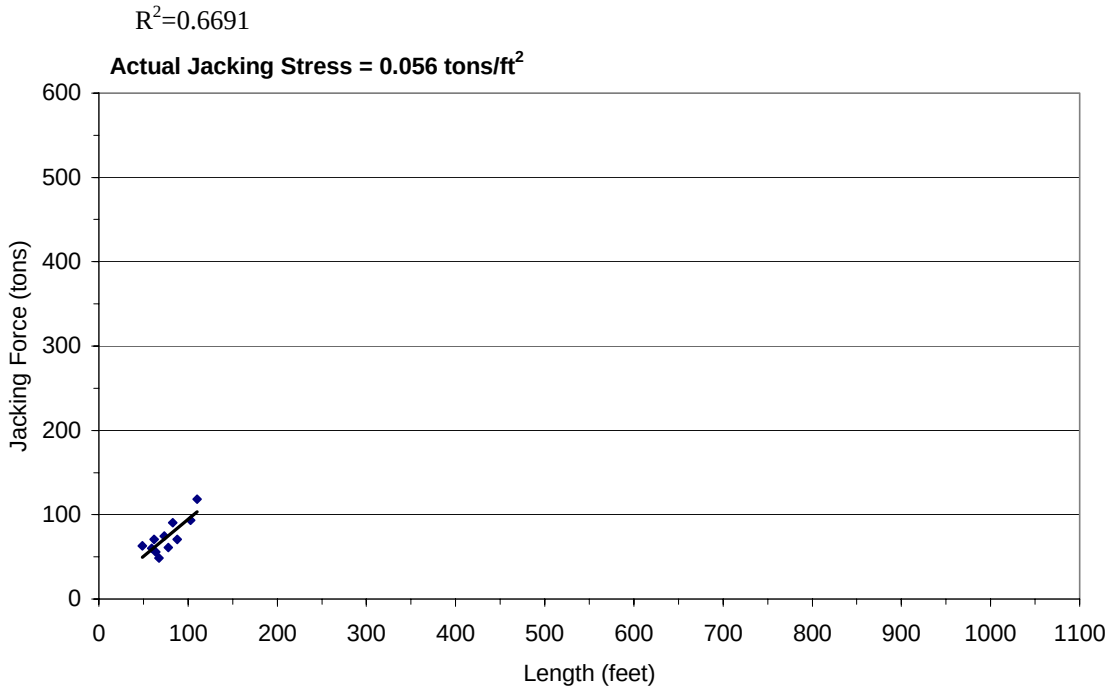

Figure 4.40. Length vs. Jacking Forces for the Clearview Snohomish River Crossing 2002 from 50 to 110 feet.

Between 110 and 810 feet, lubrication along the drive was markedly increased. Figure 4.41 shows the frictional component of the jacking forces from 110 to 810 feet. This length represents the entire length over which the tunnel was within older alluvium soils which contained primarily poorly graded gravel with sand, and poorly graded gravel with silt. The jacking stress through this segment is 0.005 tons/ft^2.

Over this portion of the tunnel lubrication was applied through the automated lubrication system; therefore, lubrication could be applied through several ports along the pipeline. This system was much more advanced than the lubrication system used on the 2001 drive beneath the Snohomish River where the lubrication ports had to be individually plumbed and the lubrication could only pump to a single port location at any given time.

The third isolated segment is between 810 feet and 945 feet. Lubrication was no longer pumped to the pipeline after 810 feet and jacking forces began to increase. Figure 4.42 shows the jacking forces through this segment. Jacking stresses throughout this segment were 0.05 tons/ft^2, equal to the segment between 50 and 110 feet where minimal lubrication was applied.

4.4.7 Summary of Jacking Stresses on Isolated Tunneling Segments

Table 4.12 provides a summary of jacking stresses for the isolated segments of the drive selected for analysis above.

Table 4.12. Jacking Stress on Isolated Segments of Snohomish River Crossing 2002.

Segments Along Alignment [feet]	Jacking Stress [tons/ft^2]	Notes	R^2 Value
50-110	0.05	Minimal Lubrication	0.6691
110-810	0.005	Older Alluvium	0.2329
810-945	0.05	No Lubrication	0.3194

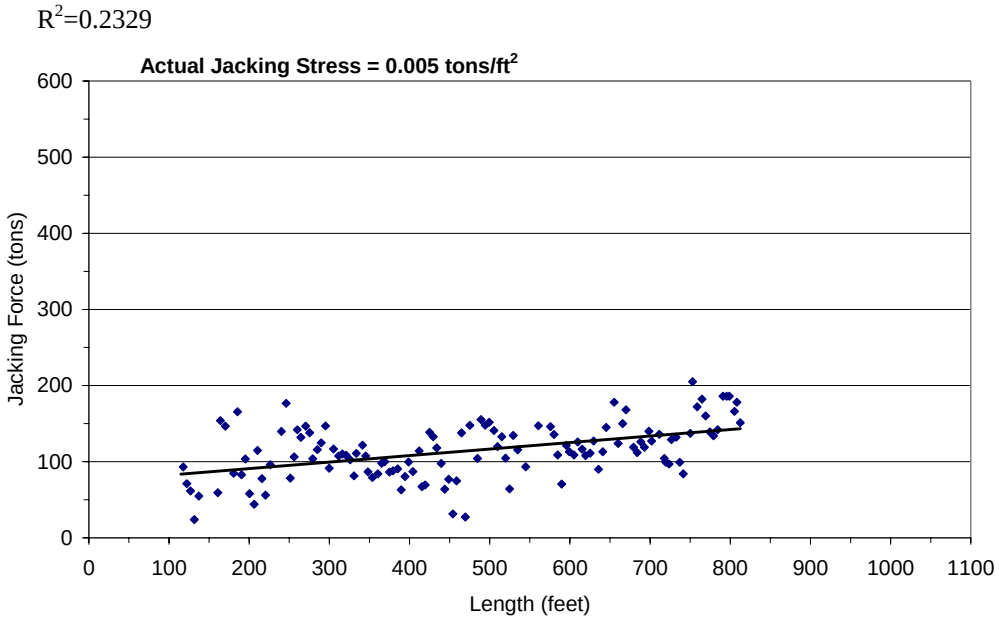

Figure 4.41. Length vs. Jacking Force for the Clearview Snohomish River Crossing 2002 from 110 to 810 feet.

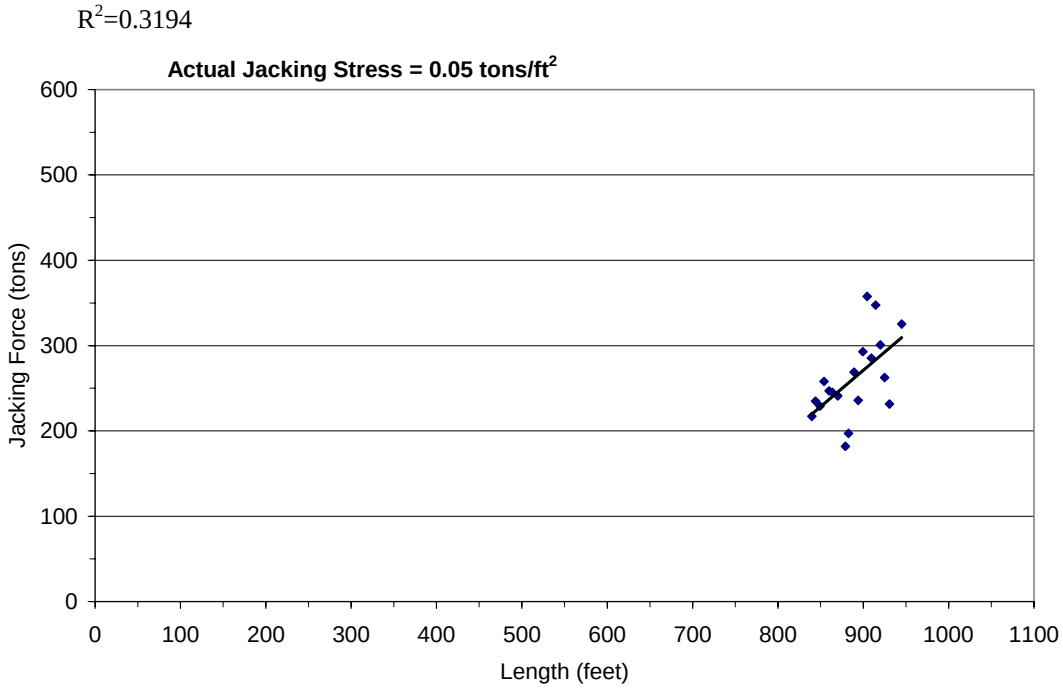

Figure 4.42. Length vs. Jacking Force for the Clearview Snohomish River Crossing 2002 from 810 to 945 feet.

4.5 South Tahoe Highway 50 Crossing

The City of South Lake Tahoe commissioned the design of a pipeline that would control storm flows and prevent unwanted erosion into Lake Tahoe. As part of the project, a portion of the pipeline traversed beneath Highway 50 in the downtown portion of South Lake Tahoe, near Stateline, Nevada. Due to the high volume of traffic flow on Highway 50 and the limited number of alternate routes through South Lake Tahoe, the City specified trenchless construction methods for the installation of the pipeline beneath Highway 50.

4.5.1. Description of the Project

The trenchless portion of the project included installing a 48-inch ID by 59.5 inch OD concrete pipe by trenchless methods. During the design phase of the project, it was discovered that the groundwater table was below the invert of the pipeline. Therefore, the designers were not overly concerned about the loss of face stability during tunneling operations and allowed the contractor to choose between microtunneling, open shield pipe jacking, and auger boring. The drive length was 260 feet long between two specified manhole locations. Due to limited construction access and lay down areas, the designer specified the locations of the jacking and reception shafts. Figure 4.43 shows a profile of the tunnel beneath Highway 50.

The low bidder on the project chose to use open shield pipe jacking as the preferred construction method. With this trenchless method, the face of the machine is completely open and the operator sits within the tunneling shield, and is able to control excavation and monitor the stability of the tunnel heading. The jacking efforts are

controlled by an operator located in the jacking shaft who coordinates jacking the pipe with another operator in the tunnel shield by voice commands through headsets.

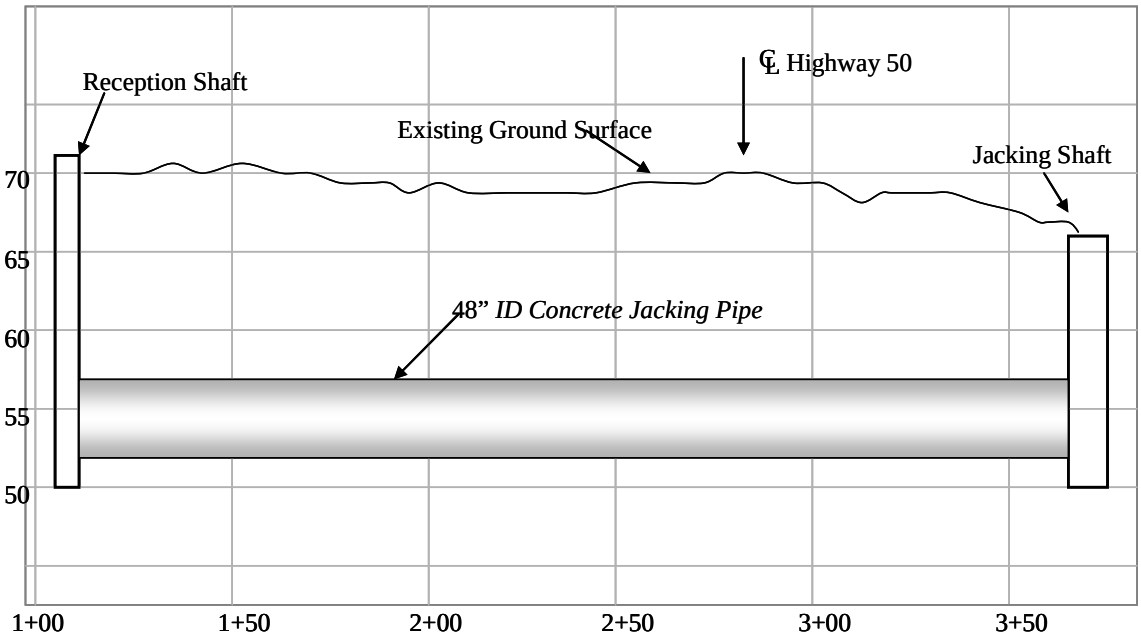

Figure 4.43. Profile of Rocky Point Highway 50 Crossing.

The particular machine used for the Rocky Point project was manufactured by Akkerman and uses a wheel to excavate the soil. Soil comes into the shield on a conveyor and is conveyed to a muck bucket that is transported out of the tunnel via locomotive. The main difference between the open shield pipe jacking method and microtunneling is that the open shield method does not provide positive face pressure at the heading and, as a result, is not appropriate for tunneling in unstable soils. Figure 4.44 shows the Akkerman shield that was used on the Rocky Point Project and Figure 4.45 shows a view from within the shield.

Figure 4.44. Akkerman Open Shield Machine Showing the Cutter Wheel and Gauge Cutters.

Figure 4.45. Photo taken within Concrete Pipe looking toward Tunnel Shield with Operator on Left Side and Conveyor in Center of Photo.

Because there was no groundwater at the elevation of the pipeline, the jacking shaft and the reception shaft were constructed with stacked trench boxes to save costs. Trench box shafts are not commonly used for microtunneling operations because typically do not provide adequate stability or thrust resistance to the jacking loads; however, with jacking frames that are used on open shield pipe jacking systems, they can be used successfully.

The pipe material used on the project was Wet Cast Reinforced Concrete pipe. The pipe had a 48-inch inner diameter with a 59.5-inch outer diameter. Individual pipes were manufactured in 10-foot segments. The pipes had a flush-wall double bell and spigot jacking joint with a double-gasket for the pipe jacking application.

4.5.2 . Geotechnical Conditions Along the Alignment

Very little geotechnical work was completed for the project and no vertical borings were conducted for the trenchless crossing of Highway 50. Although highly unusual considering the risk that accompanies trenchless crossings, especially in the Tahoe Basin, there was a large volume of information about the soils in the immediate area indicating that the soil was likely to be very dense well graded sand. As tunneling progressed, the face of the excavation was examined many times and the sand was, in fact, very dense and would stand vertically at the face. The sand was deposited in thin layers, as was clear from the variation in colors and the teeth on the machine left indentations in the formation. A Highway 50 Crossing for a different pipeline project, located approximately 1000 feet from the crossing, had vertical borings that yielded blow counts in the range of 35 to 45 blows per foot at the elevation of the bore.

4.5.3. Construction of the Tunnel

Construction of the tunnel began on June 26, 2003 and was completed on July 2, 2003. Table 4.13 shows the tunneling progress over the entire tunnel drive.

Table 4.13. Tunneled Length per day for Rocky Point Highway 50 Crossing.

Date	Tunneled Length [ft]	Cumulative Length [ft]
June 27, 2003	16 feet (machine) 40 feet (Pipes 1-4)	64 feet
June 28, 2003	80 feet (Pipes 5 – 12)	144
June 29, 2003	0	144
June 30, 2003	40 feet (Pipes 13-16)	184
July 1, 2003	60 feet (Pipes 17-22)	244
July 2, 2003	10 feet and Retrieve (Pipe 23)	254

The machine was launched through a steel plate that blocked the end of the trench box closest to the highway. A hole was cut in the steel plate through which the machine was pushed. Figure 4.46 shows the jacking shaft with the open shield machine set on the jacking rails just prior to pushing the machine out of the trench box to begin tunneling.

Figure 4.46. Open Shield Machine in Jacking Shaft Launching Machine Through Front Wall of Shaft.

4.5.4 Jacking Forces on the Tunnel

The jacking forces on the tunnel was measured at the pressure gauge on the hydraulic cylinders on the main jacking unit in the jacking shaft. Since the shield did not have a closed face and was not pressurized, a face pressure component was not subtracted from the main jacking pressure to determine a frictional component of the jacking force. It is assumed that the overall jacking force is primarily frictional loading on the machine and the pipeline. Figure 4.47 shows the jacking force as a function of length over the entire drive beneath Highway 50.

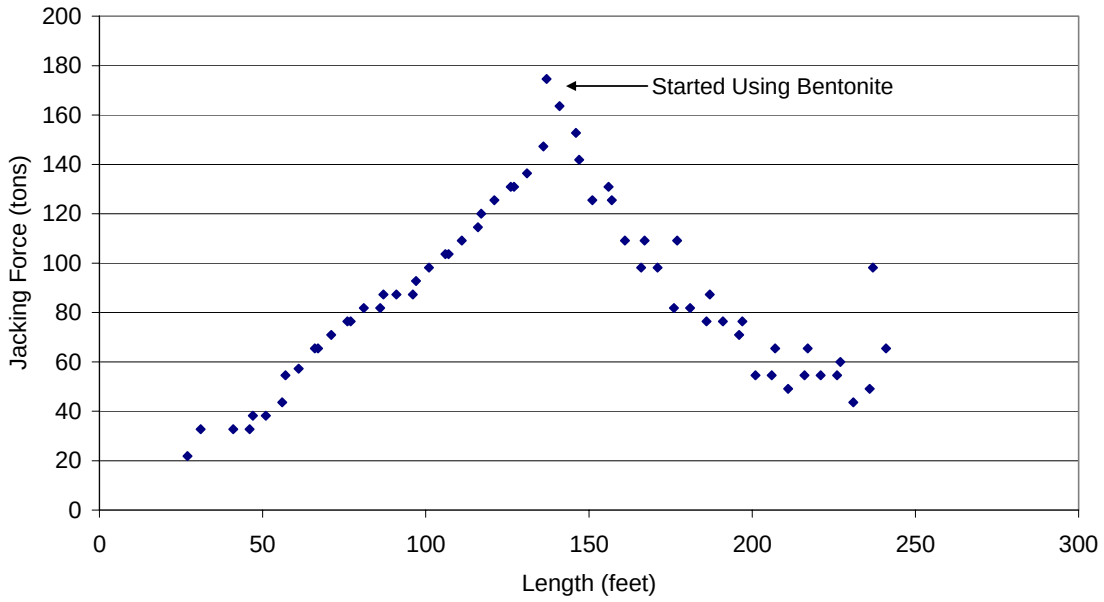

Figure 4.47. Length vs. Jacking Forces on the South Lake Tahoe Highway 50 Crossing.

4.5.5. Lubrication During Tunneling

The contractor elected not to use any lubrication during tunneling until 140 feet into the drive. At 140 feet into the drive it became apparent that if the contractor continued to jack the pipe without any lubrication and the jacking forces continued with the same linear trend, the jacking frame on site was not capable of delivering the necessary load to the pipeline in order to complete the drive. Therefore, the contractor decided to pump bentonite from ports in the pipeline approximately 50 feet behind the heading to the jacking shaft starting at 140 feet into the drive. This practice continued until completion of the drive. The actual volumes of bentonite are unknown.

4.5.6. Isolation of Tunneling Segments for Specific Analysis

The microtunneling machine was launched through the wall and was pushed for 16 feet until the machine was completely buried and jacking of the concrete pipe began. Jacking without lubrication continued from 16 feet into the drive until 140 feet into the drive. Figure 4.48 shows the jacking forces over this segment of the drive. Throughout this interval, the jacking stress was 0.074 tons per square foot of pipe surface area.

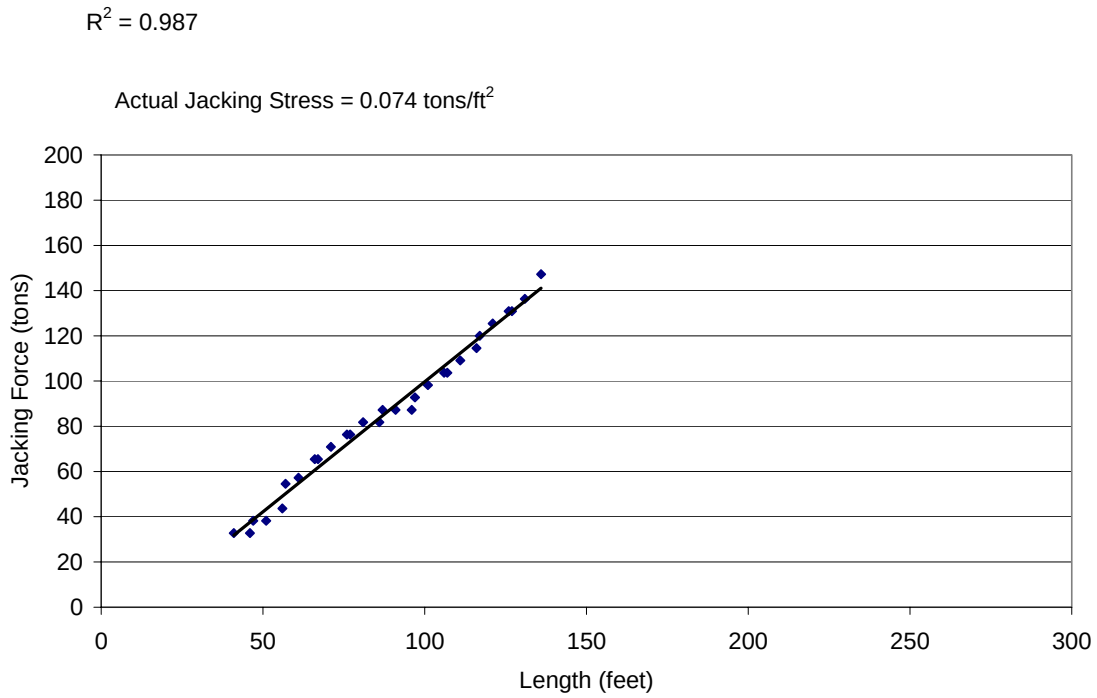

Figure 4.48. Length vs. Jacking Force for the South Lake Tahoe Highway 50 Crossing from 50 to 140 feet.

4.6 Eastside Interceptor – Morris Avenue Tunnel

The Department of Natural Resources Wastewater Treatment Division of King County, Washington, located in Seattle, Washington commissioned a pipeline project that included the installation of a new pipeline along the south shore of Lake Washington in Renton, Washington. The original sewer pipeline had been damaged in the 1954 earthquake due to liquefiable soils in the vicinity of the pipeline. King County commissioned the design of a new sewer to replace the damaged pipeline in 1999 and the pipeline was constructed in 2002.

4.6.1 Description of the Project

A portion of the Eastside Interceptor project included the installation of 1,115 feet of microtunnel in a single drive along Morris Avenue. The 87.5 inch outer diameter tunnel was constructed with the installation of reinforced concrete pipe with a 72-inch flow diameter. Due to the high groundwater heads and the liquefiable sands and silts known to exist at the project site, the specifications were restricted to microtunneling as the only construction alternative available to the contractor. The depth of cover over the crown of the pipeline ranged from 17 to 20 feet over the entire length of the drive.

The project was located in a highly congested neighborhood with construction taking place within 150 feet of residential homes. Settlement of the ground surface was of great concern due to the geotechnical conditions and dictated many of the project design features. For example, the project specification called for jet grouting at all shaft locations to ensure that shafts were "water tight" and restricted any dewatering at the site location. Jet grouting operations to completely cut off groundwater inflows proved to be very difficult in the site soils and the contractor had difficulty isolating the shafts from the groundwater at the site. Figure 4.49 shows a profile of the Morris Avenue drive along with the boring locations and an interpretive geotechnical cross-section. The figure also shows the elevation of the water table recorded at piezometers installed at select boring locations.

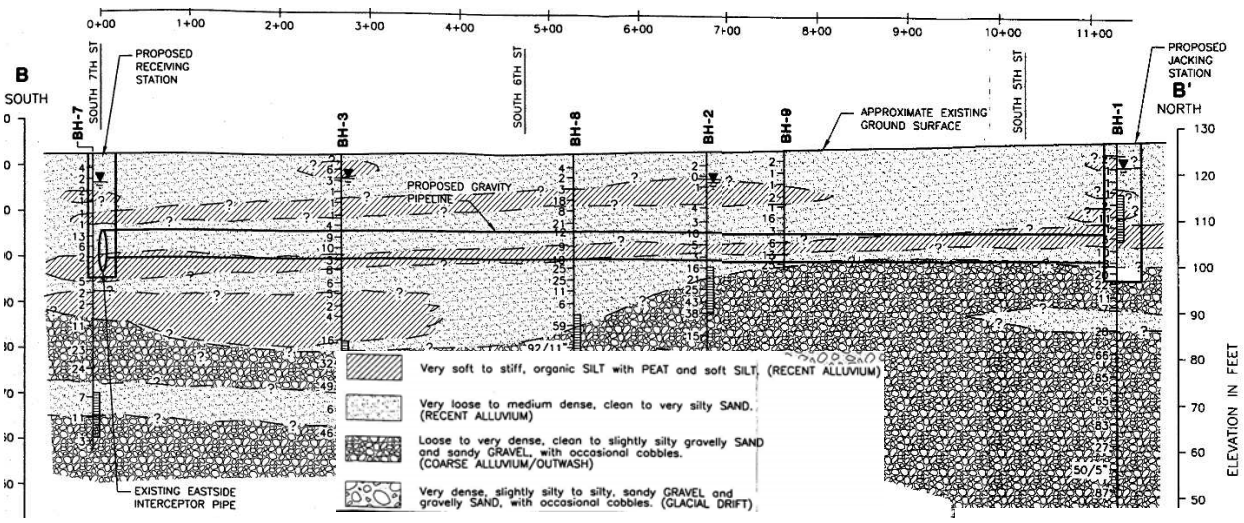

Figure 4.49. Eastside Interceptor – Profile of Morris Avenue Drive.

The contractor installed the jet grouting at the shaft locations and then drove steel sheet piles within the jet grouted area. Soil was then excavated from inside the sheet pile cell within the jet grouted zone to create the jacking and reception shafts. Figure 4.50 shows the jacking shaft during construction and the completed jacking shaft with the jacking frame set in the shaft. In section (b) of Figure 4.50 the contractor is mounting the launch seal through which the microtunneling machine will exit the shaft.

The contractor selected a LovatMTS microtunneling machine for the construction of the microtunnel. The machine was 88.5 inches in diameter, creating a one inch overcut on the diameter and was fitted with drag picks to facilitate movement of the material into the slurry chamber of the shield. Figure 4.51 shows the cutting face of the LovatMTS machine.

(a) (b)

Figure 4.50. (a) Construction of the Sheet Pile Jacking Shaft Within the Jet Grouted Area (b) Completed Jacking Shaft with Jacking Frame (forefront) and mounting launch seal (background).

Figure 4.51. Cutting Wheel of LovatMTS Microtunneling Machine Used on Eastside Interceptor Project – Morris Avenue Drive.

4.6.2 Geotechnical Conditions Along the Alignment

A great deal of geotechnical investigation and associated studies were completed for the Eastside Interceptor project. This included many project borings, a ground penetrating radar survey, production of a geotechnical data report, production of a geotechnical interpretive report, and production of a geotechnical baseline report. For the Morris Avenue drive, six vertical borings were completed and an interpretive geotechnical cross-section was produced for the contractor prior to bid (as shown in Figure 4.49).

In addition, intensive construction management during the construction of the tunnel included the collection of soil samples on 10-foot intervals along the tunnel alignment. These samples were qualitatively described by the on-site construction inspector to provide a relative percentage of the type of material that was excavated by the microtunneling machine at the time that the soil sample was collected. This material was mixed with water at the time of excavation to create a slurry and was then separated from the water by the slurry separation system, which had hydro cyclones for removing fine sands, shaker screens for removing coarse sands, and allowed all materials of the slit and clay sizes to remain in solution. Of note, the percentage of silt in the material was estimated at 10 percent due to the fact that it was necessary for the contractor to vacuum out the slurry water on a regular basis to keep the slurry from thickening and causing excessive slurry face pressures.

Figures 4.52 and 4.53 are boring logs that correspond to vertical borings that were taken at the jacking and reception shaft for the design of the Morris Avenue drive. These logs provide information on the in situ soil density by providing blow counts for selected soil samples.

DRILLING COMPANY: Geo-Tech Exploration
DRILLING METHOD: CME 75, Mud Rotary
SAMPLING METHOD: 300-lb Safety Hammer, 3-inch Split Spoon Sampler
SURFACE ELEVATION: 127 ± feet

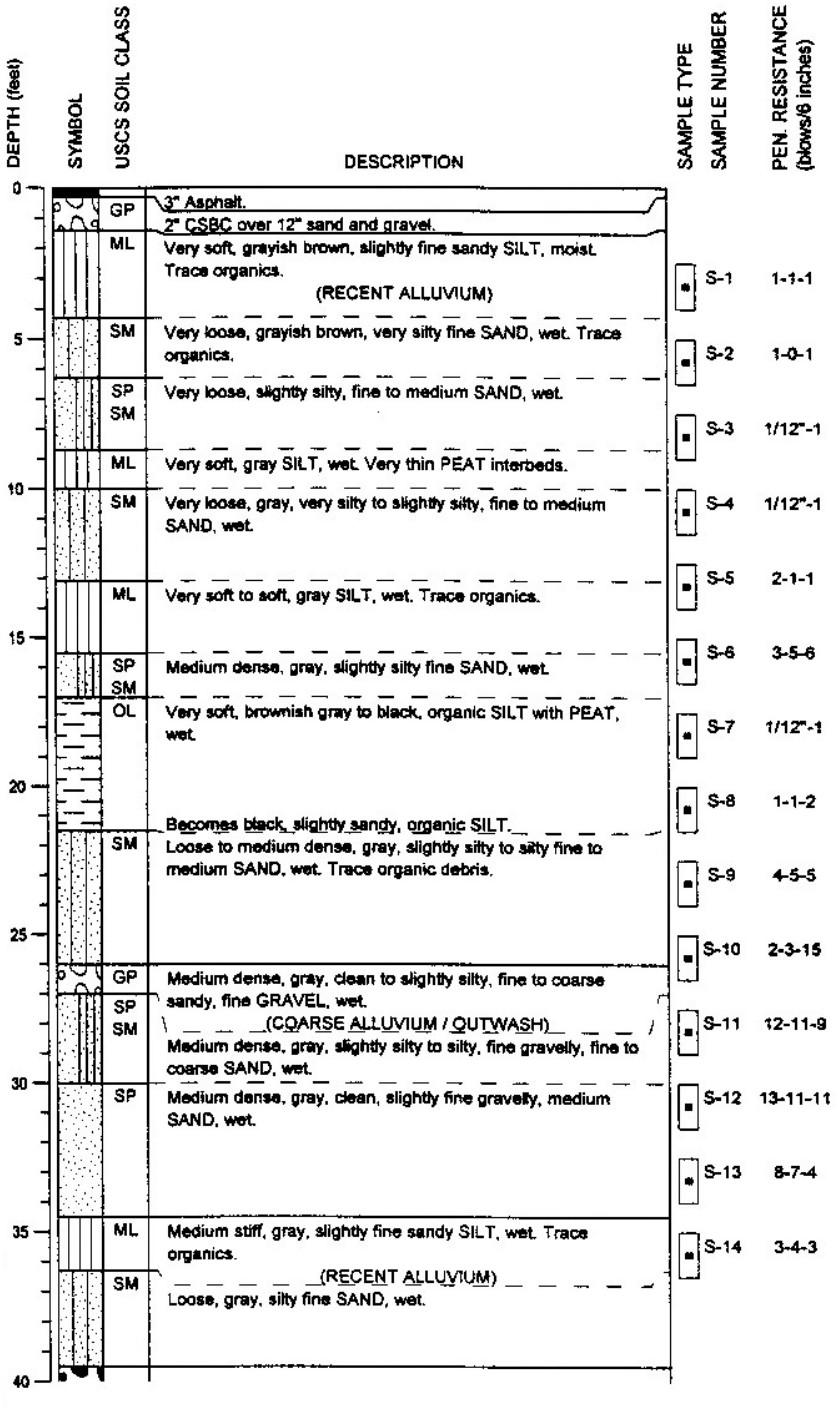

Figure 4.52. Boring Log BH-1 Located at the Jacking Shaft (Hong West, 2000).

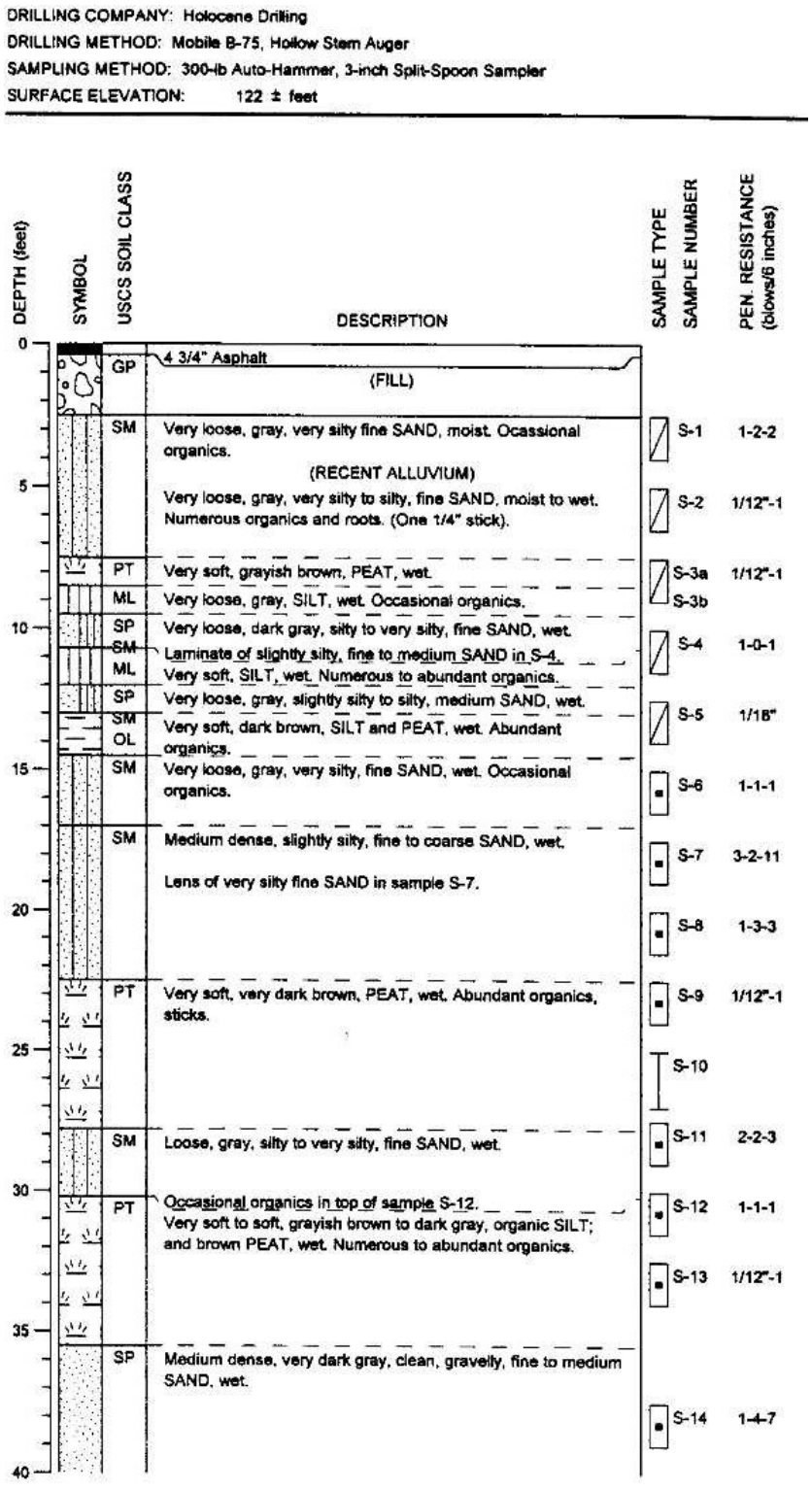

Figure 4.53. Boring Log BH-7 Located at the Reception Shaft (Hong West, 2000).

It should be noted that the blows were imparted to the soil with a non-standard hammer weighing 300 pounds as noted on the borings and the sampler collecting the "undisturbed" soil samples is a 3-inch modified California Split Spoon Sampler. As a result, the penetration resistance as reported on the boring logs must be evaluated carefully and corrected to Standard Penetration Tests.

4.6.3 Construction of the Microtunnel

The microtunnel was launched on May 31, 2002 and was completed on June 28, 2002. Table 4.14 shows the progress of the tunnel on a daily basis and provides some notes of significance.

During the tunneling there were many days of decreased overall progression due to difficulty with soil separation. Much of the silt and clay size particles remained in suspension in the slurry water. As a result, the slurry would become thick and difficult to pump. This would result in high slurry pressures and difficulty in pumping the material from the tunnel to the soil separation plant on the surface. To alleviate this problem, vacuum trucks were brought to the site and the thick slurry was pumped from the slurry tanks and hauled to disposal sites. The slurry water was then replaced with clean water. The removal and replacement of thick slurry with clean slurry took several hours and severely impacted overall progression rates.

4.6.4 Jacking Forces on the Microtunnel

The frictional component of the jacking forces over the microtunnel drive ranged from 108 tons to near 1070 tons. Figure 4.54 shows the frictional component of the jacking forces as a function of the length of the tunnel drive.

Table 4.14. Daily and Cumulative Progression on the Morris Avenue Microtunnel Drive.

Date [2002]	Pipes Tunneled	Length [ft]	Cumulative Length [ft]	Notes
May 31	Microtunneling Machine	11	11	
June 1	Microtunneling Machine	12	23	
June 3	Pipe #1	12	35	
June 4	Pipe #2	12	47	
June 5	Pipes 3, 4, 5	36	83	
June 6	Pipes 6,7,8	36	119	
June 7	Pipes 9, 10, 11	36	155	
June 8	4 feet of Pipe 12	4	159	Jacking Forces High. Installed Intermediate Jacking Station and Pumped Bentonite
June 9	2 feet of Pipe 12	2	161	Pushed Pipe only 2 feet on Sunday
June 10	6 feet of Pipe 12	6	167	Problem with Soil Separation System
June 11	Pipes 13, 14, 15	36	203	
June 12	Pipes 16, 17, 18	36	239	
June 13	Pipes 19, 20, 21, 22, 23	60	299	
June 14	Pipe 24	12	311	
June 15	Pipes 25, 26, 27, 28	48	359	
June 17	Pipes 29, 30, 31, 32	48	407	Some clay and Gravel
June 18	Pipes 33, 34, 35, 36, 37	60	467	
June 19	Pipes 38, 39, 40, 41	48	535	
June 19	Pipes 42, 43, 44	36	571	Night Shift
June 20	Pipes 45, 46, 47	36	607	
June 20	Pipes 48	12	619	Night Shift Removal of suspended solids in slurry tanks
June 21	Pipes 49, 50	24	643	
June 21	Pipes 51, 52, 53, 54, 55, 56. 57	84	727	Night Shift and Weekend
June 24	Pipes 58, 59	24	751	
June 24	Pipes 60, 61, 62	36	787	Night Shift
June 25	Pipes 63, 64, 65, 66	48	835	
June 25	Pipes 67, 68	24	859	Night Shift
June 26	Pipes 69, 70, 71, 72	48	907	
June 26	Pipes 73, 74, 75, 76	48	955	Night Shift
June 27	Pipes 77, 78, 79, 80, 81	60	1015	
June 27	Pipes 82, 83, 84, 85, 86	60	1075	Night Shift
June 28	Pipes 87, 88, 89, 90	39	1114	End of Tunnel

4.6.5 Lubrication During Microtunneling

An automated lubrication system was used to apply lubrication along the pipeline during tunneling. However, this system was new to the contractor, who experienced

many difficulties with the system during tunneling operations. The contractor did apply lubrication to the tunnel during the first 171 feet of tunneling; however the lubrication system was working sporadically and the jacking forces were climbing at an alarming rate.

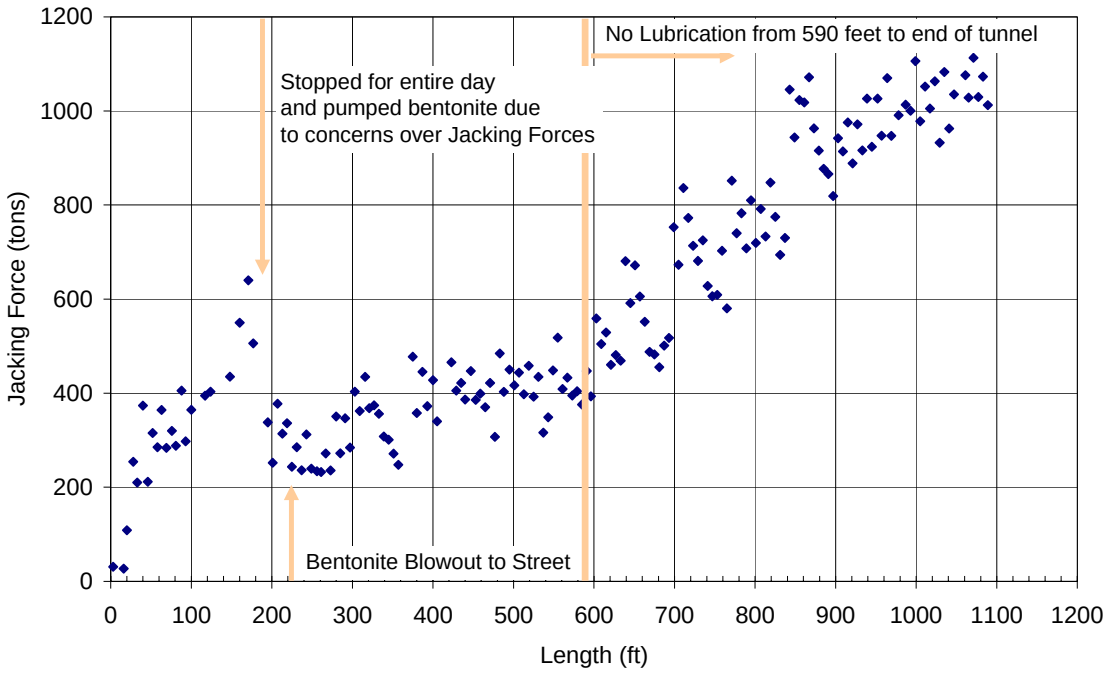

Figure 4.54. Length vs. Jacking Force for the Eastside Interceptor Morris Avenue Drive

At 193 feet into the drive the contractor suspended tunneling operations for a day and pumped bentonite through ports in the tunnel on 10-foot spacing for a period of 12 hours. The tunnel was pushed only 4 feet on that day. On the following day, bentonite was pumped at the tunnel heading again and the tunnel heading was pushed only 2 feet (this was on a Sunday and the contractor was concerned that if the tunnel was not kept moving that it might seize).

When normal tunneling operations resumed on the following Monday, the contractor was lubricating at high enough volumes and pressures that the bentonite fractured the natural ground and began running out on the ground surface.

The application of bentonite along the pipeline continued until 590 feet when the automated bentonite system completely malfunctioned. Although the automated system was indicating that bentonite was pumping, the bentonite tanks were remaining full as the tunnel progressed. The system could not sustain sufficient pressure to overcome the earth pressures at the discharge locations at a distance over 590 feet from the bentonite plant. Therefore, beyond 590 feet into the drive, bentonite lubrication was not applied to the pipeline.

4.6.6 Isolation of Tunneling Segments for Specific Analysis

The first segment for analysis is the section from 30 to 175 feet where the contractor was applying sporadic lubrication to the tunnel drive. In this zone of the tunnel, the soil was approximately 80 percent sand with 20 percent fines. Figure 4.55 shows the jacking forces from 30 to 175 feet. The jacking stress along this segment is 0.09 tons per square foot of pipe surface area.

From 285 to 590 feet, the contractor was applying a large amount of lubrication to the soil surrounding the pipeline. In this zone there is a marked decrease in the jacking forces. Figure 4.56 shows the jacking forces as a function of length throughout this length. The normalized friction coefficient throughout this zone with massive lubrication is 0.01 tons per square foot of surface area.

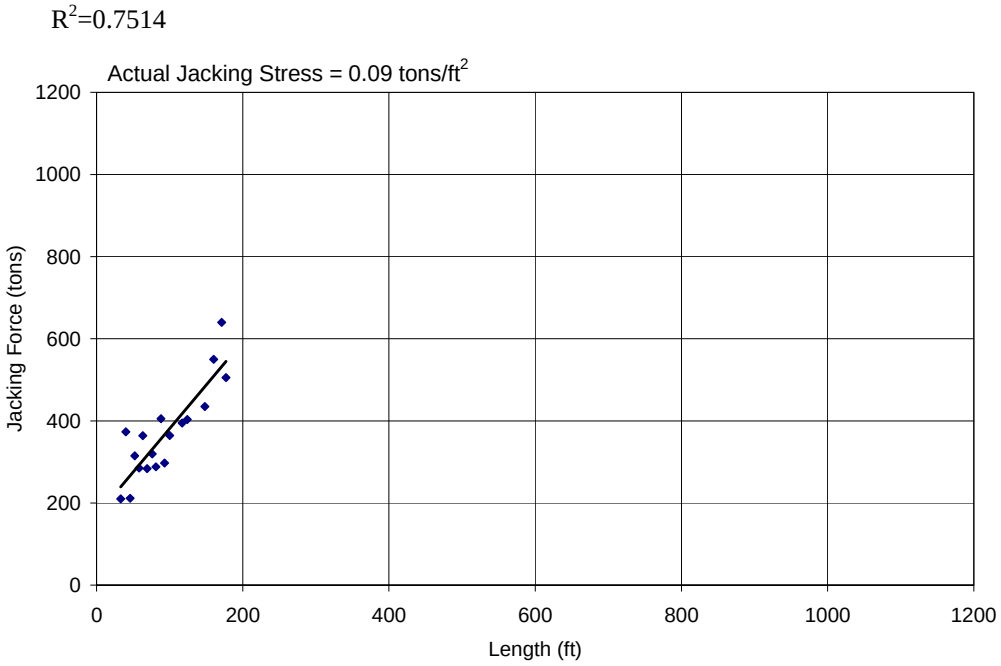

Figure 4.55. Length vs. Jacking Force for the Eastside Interceptor Morris Avenue Drive from 30 to 175 feet.

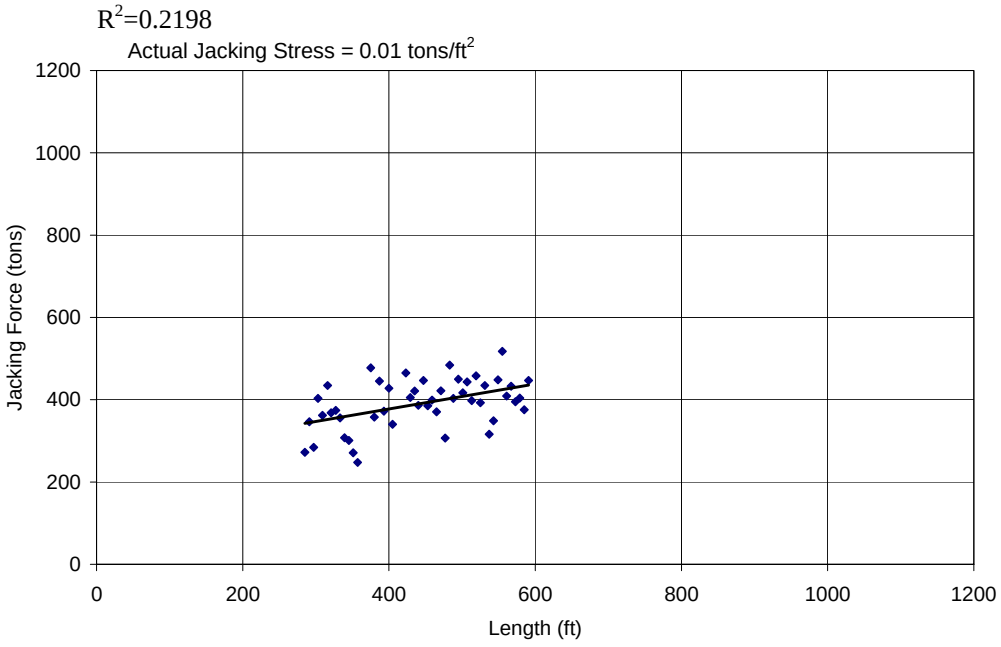

Figure 4.56. Length vs. Jacking Force for the Eastside Interceptor Morris Avenue Drive from 285 to 590 feet.

After 590 feet into the drive, the contractor was no longer able to lubricate the pipeline due to problems with the lubrication system. The jacking forces begin to increase at a much higher rate. From 590 feet into the drive until the end of the drive at 1,114 feet the jacking forces increase at a rate of 0.06 tons per square foot of pipe surface area. Figure 4.57 shows the jacking force as a function of length for this section of the drive.

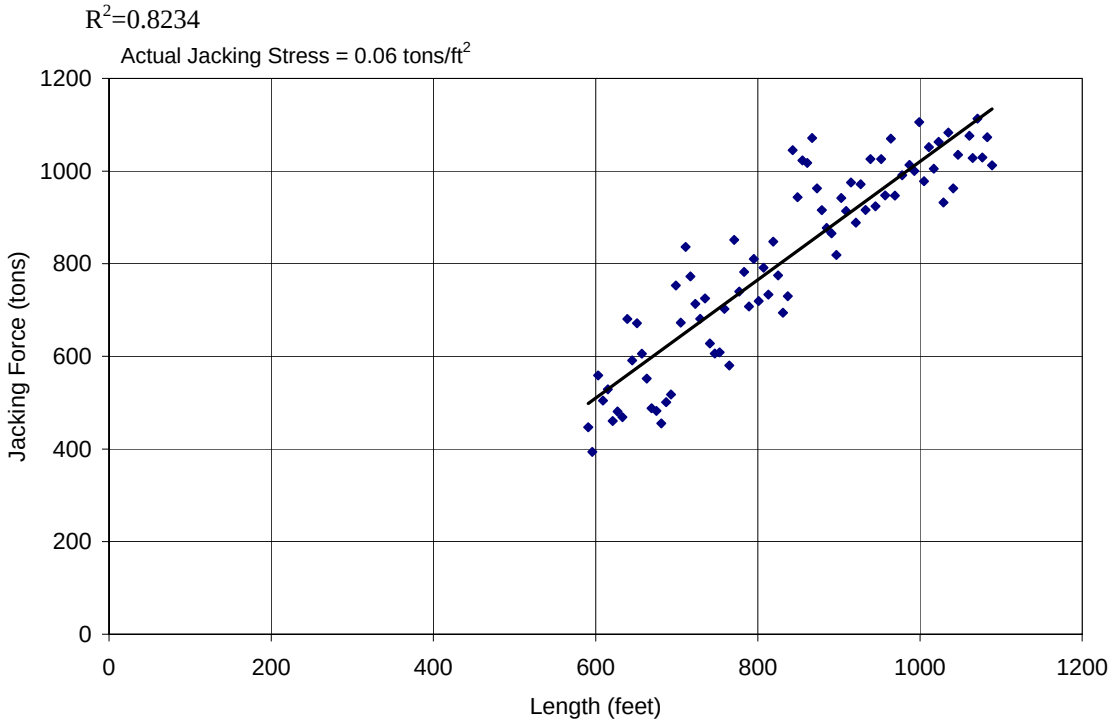

Figure 4.57. Length vs. Jacking Force for the Eastside Interceptor Morris Avenue Drive from 590 to 1085 feet.

4.6.7 Summary of Jacking Stresses on Isolated Tunneling Segments

Table 4.15 provides a summary of jacking stresses on isolated segments of the Morris Avenue Drive of the Eastside Interceptor project.

Table 4.15. Jacking Stresses on Isolated Segments of the Morris Avenue Drive.

Segments Along Tunnel Alignment [feet]	Jacking Stress [tons/ft^2]	Notes	R^2 Value
30-175	0.09		0.7514
285-590	0.01	Saw-tooth Behavior – Possible pore pressure dissipation	0.2198
590-1140	0.06	No Lubrication	0.8234

4.7 Eastside Interceptor – Houser Way Tunnel

In addition to the Morris Avenue tunnel as described in section 4.6, an additional tunnel was constructed for the Department of Natural Resources Wastewater Treatment Division of King County as a portion of the Eastside Interceptor Project. Like the Morris Avenue tunnel, the original sewer pipeline had been damaged in the 1954 earthquake due to liquefaction of the soils in the vicinity of the pipeline. King County commissioned the design of a new sewer to replace the damaged pipeline in 1999 and the pipeline was constructed in 2002.

4.7.1 Description of the Project

The Houser Way portion of the project included the installation of 675 feet of microtunneling in a single drive along Houser Way. The 87.5-inch outer diameter tunnel was constructed with Packerhead Concrete pipe with a 72-inch flow diameter. The pipe was manufactured with the packerhead concrete method. Due to the high groundwater heads and the liquefiable sands and silts known to exist at the project site, the specifications were restricted to microtunneling as the only construction alternative available to the contractor. The depth of cover over the crown of the pipeline ranged from approximately 22 to 30 feet over the entire length of the drive.

As with the Morris Avenue tunnel, the site was located in a highly congested neighborhood with construction taking place within 150 feet of residential homes. Ground surface settlement was of great concern due to the geotechnical conditions. As a result, jet grouting was required at all shaft locations to ensure that shafts were "water tight" and dewatering was restricted at all site location. Figure 4.58 shows a profile of the Houser Way drive along with the boring locations and an interpretive geotechnical cross-section. The figure also shows the elevation of the water table recorded at piezometers installed at select boring locations.

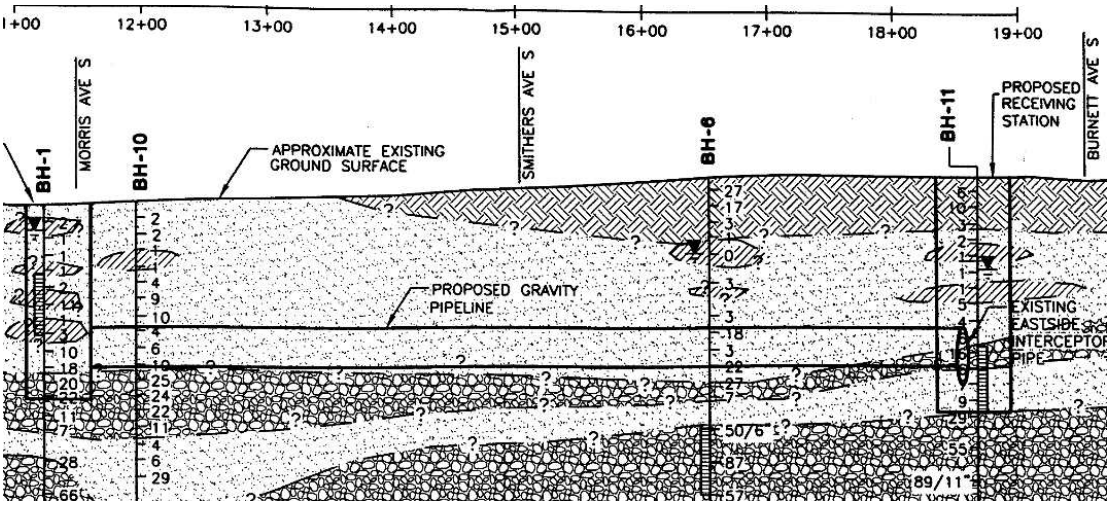

Figure 4.58. Eastside Interceptor – Profile of Houser Way Drive (Hong West, 2000).

As with the Morris Avenue drive, the contractor installed the jet grouting at the shaft locations and then drove steel sheet piles within the jet grouted area. Soil was then excavated from inside the sheet pile cell within the jet grouted zone to create the jacking and reception shafts.

A LovatMTS microtunneling machine was used for the construction of the microtunnel. The machine was 88.5 inches in diameter, creating a one (1)-inch over cut on the diameter and was fitted with drag picks to facilitate movement of the material into the slurry chamber of the shield. Figure 4.59 shows the cutting face of the LovatMTS machine.

Figure 4.59. Cutting Wheel of LovatMTS Microtunneling Machine Used on Eastside Interceptor Project – Houser Way Drive.

4.7.2 Geotechnical Conditions Along the Alignment

A tremendous amount of geotechnical investigation and associated studies were completed for the Eastside Interceptor project. This included many project borings, a ground penetrating radar survey, production of a geotechnical data report, production of a geotechnical interpretive report, the production of a geotechnical baseline report. For the

Houser Way drive, four vertical borings were completed and an interpretive geotechnical cross section was produced for the contractor prior to bid (as shown in Figure 4.58).

Figures 4.60 and 4.61 are boring logs that correspond to vertical borings that were drilled at the jacking and reception shaft for the design of the Houser Way drive. These logs provide information on the in situ soil density by providing blow counts for selected soil samples. However, it should be noted that the blows were imparted to the soil with a non-standard hammer weighing 300 pounds as noted on the borings, and the sampler collecting the "undisturbed" soil samples is a 3-inch modified California Split Spoon Sampler. As a result, the penetration resistance as reported on the boring logs must be evaluated carefully and corrected to Standard Penetration Tests.

4.7.3 Construction of the Microtunnel

The microtunnel was launched on August 1, 2002 and was completed on August 22, 2002. Table 4.16 shows the progress of the tunnel on a daily basis and provides some notes of significance.

4.7.4 Jacking Forces on the Microtunnel Drive

The frictional component of the jacking forces over the microtunnel drive ranged from 200 tons to near 550 tons. Figure 4.62 shows the frictional component of the jacking forces as a function of the length of the tunnel drive.

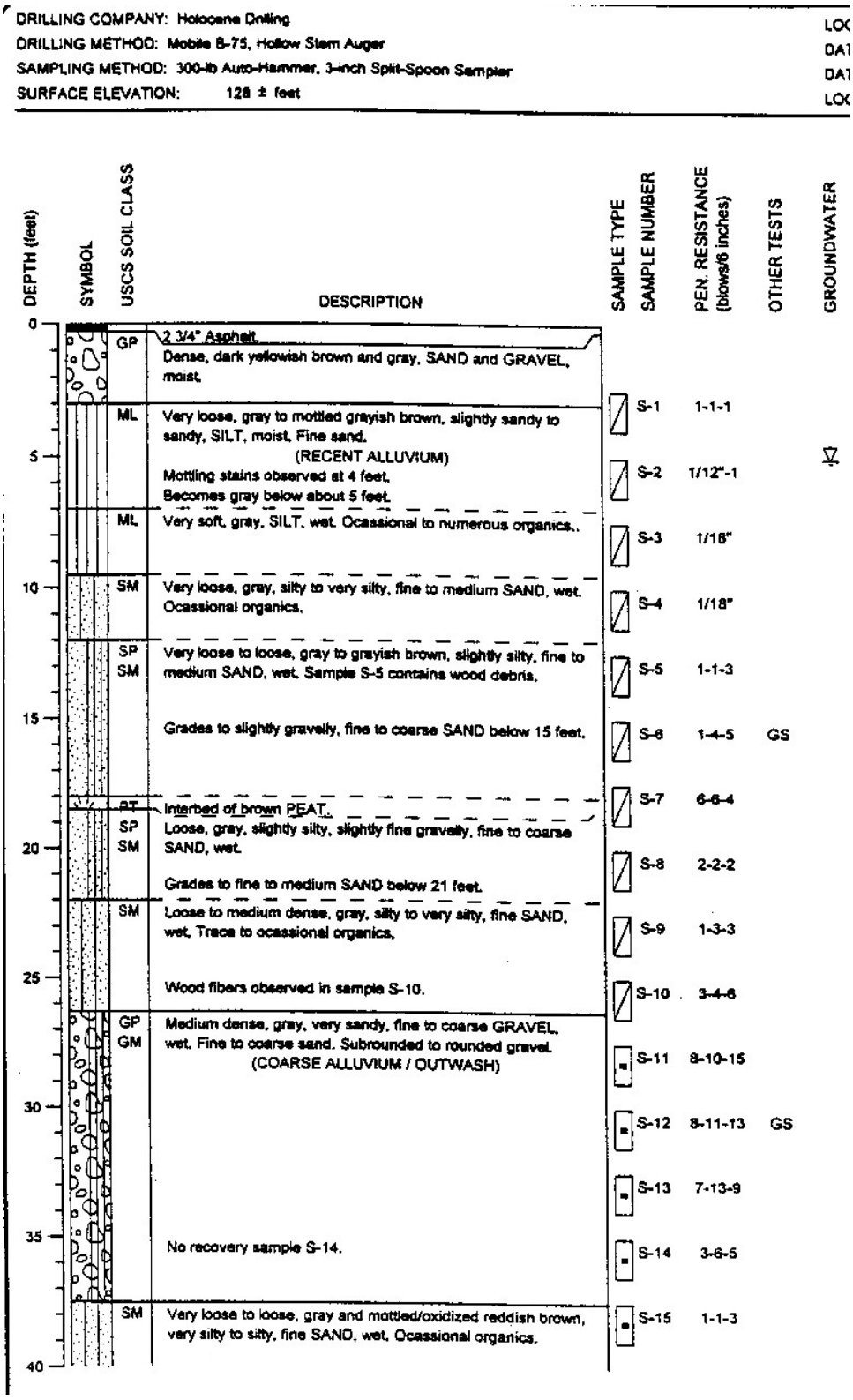

Figure 4.60. Boring Log BH-1 located at the Jacking Shaft (Hong West, 2000).

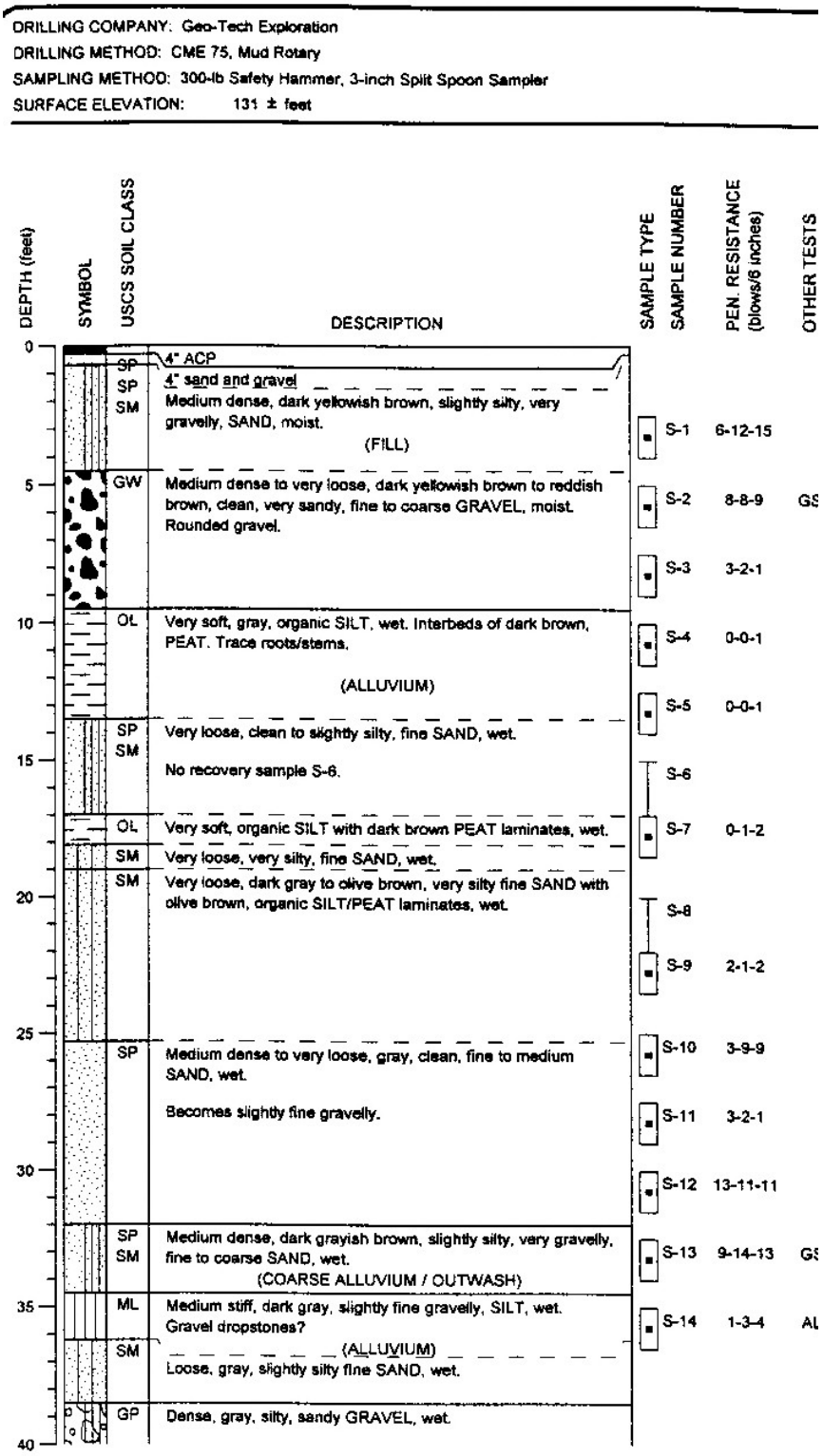

Figure 4.61. Boring Log BH-6 Located at the Reception Shaft (Hong West, 2000).

.

Table 4.16. Daily and Cumulative Progression on the Houser Way Microtunnel Drive.

Date [2002]	Pipes Tunneled	Length [ft]	Cumulative Length [ft]	Notes
Aug 1	Microtunneling Machine	12.5	12.5	
Aug 2	2 feet of Trailing Can	2	14.5	
Aug 3	10.5 ft of Trailing Can, Pipes 1, and 2	31.5	46	
Aug 5	Pipe #3	12	58	
Aug 8	Pipes 4, 5, 6, 7	48	106	
Aug 9	Pipes 8 (IJS 1) 9, 10, 11, 12	54	160	
Aug 10	Pipes 13, 14, 9 ft of 15	35	195	
Aug 12	Pipes 3 ft of 15, 16, 17, 18	39	234	
Aug 13	Pipes 19, 20, 21, 22, 23	60	296	
Aug 14	Pipes 24, 25, 26, 27, 28	60	354	
Aug 15	Pipes 29, 30, 31, 32	48	402	
Aug 16	Pipes 33, 34, 35, 36, 37, 38, 39, 40	96	498	
Aug 17	Pipes 41, 42, 43, 44	48	546	
Aug 18	Pipe 45	12	558	
Aug 19	Pipes 46, 47, 48, 49, 50, 51, 52	84	642	
Aug 20	Pipes 53, 54	48	690	
Aug 21	Pipe 55	12	702	Replacing MTBM
Aug 22	Pipe 56	12	714	Replacing Trailing Can

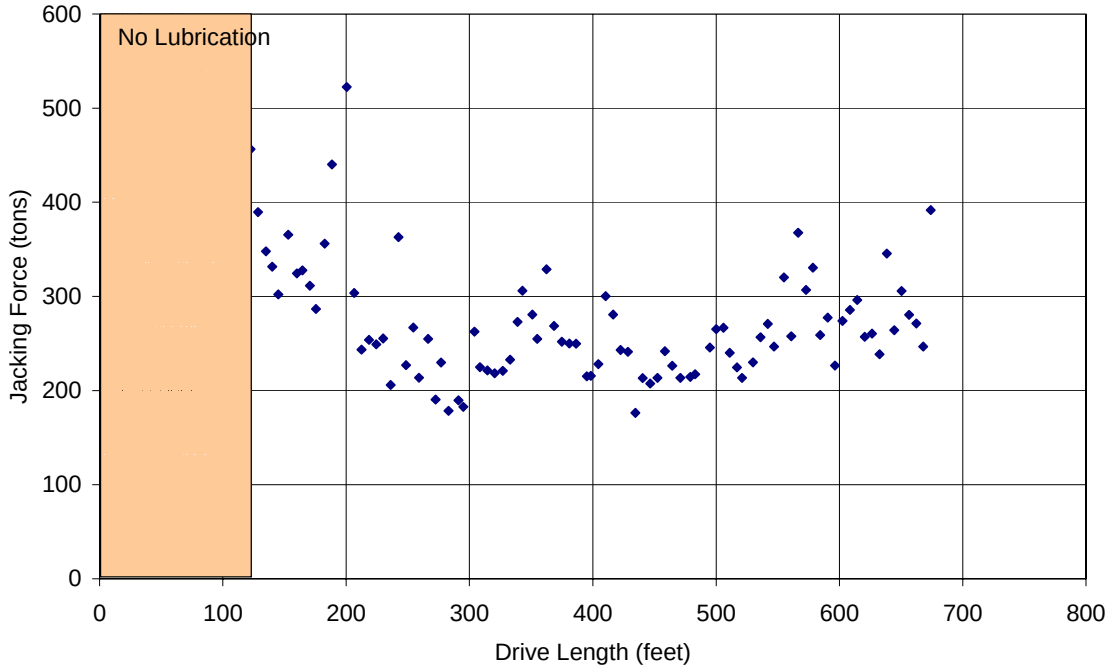

Figure 4.62. Length vs. Jacking Force for the Eastside Interceptor Houser Way Drive.

4.7.5 Lubrication During Tunneling

An automated lubrication system was used to apply lubrication along the pipeline during tunneling. A complex lubrication scheme was used along the pipeline. Lubrication injection boxes were installed in pipe segments in the trailing can, a section located immediately behind the machine, and in subsequent pipe segments. As the pipeline was microtunneled through the ground, the operator chose which of the lubrication boxes to activate. When the lubrication system was activated, the bentonite lubrication would not pump to all activated pipe sections at one time. Rather, bentonite would be pumped to the activated pipe sections sequentially for 20-second intervals. Throughout the pipeline, lubrication boxes were installed in the trailing can and pipe numbers 1, 5, 9, 12, 15, 18, 21, 24, and 27. With the 20-second interval pattern, if all nine stations were activated, bentonite would be pumped through the trailing can for 20

seconds, followed by 3 minutes where no pumping would take place while the system cycled through the other nine bentonite pumping locations. The actual lubrication pumping scheme is depicted in Figure 4.63.

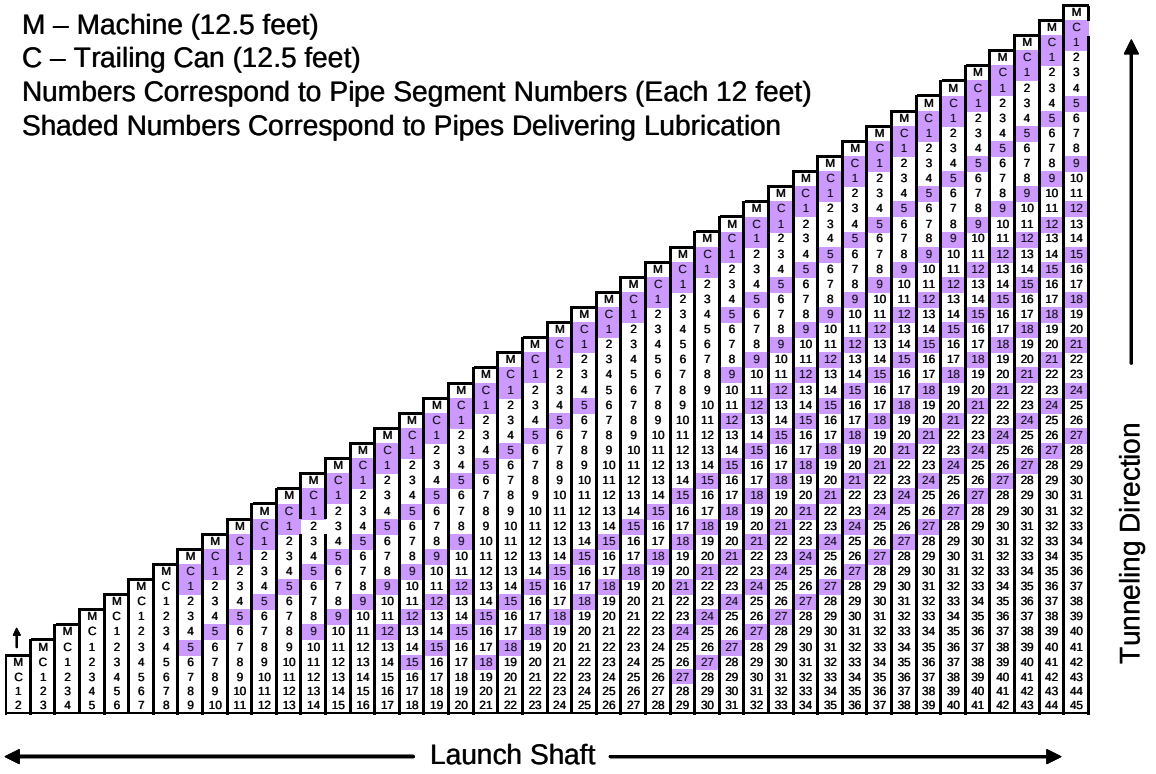

Figure 4.63. Lubrication Scheme used on the Houser Way Microtunnel Project.

Figure 4.63 shows when each of the lubrication ports were active while the tunnel was jacked forward from the jacking to the reception shaft. For example, on the left of the figure, the first column shows the machine, the trailing can, and pipes one (1) and two (2) with no lubrication. The first time lubrication was applied to the pipe was during tunneling of pipe number nine (9) when lubrication was applied at the trailing can and

pipes one (1) and five (5) as indicated by the shaded portion of the column. Similarly, on the far right of Figure 4.63, while the last pipe on the project, pipe 45 was pushed from the jacking shaft, lubrication was pumped on 20-second intervals from the trailing can and pipes 1, 5, 9, 12, 15, 18, 21, 24, and 27.

4.7.6 Isolation of Tunneling Segments for Specific Analysis

The first segment for analysis is the section from launch to 120 feet where the contractor is not applying lubrication to the tunnel. In this zone of the tunnel, the soil was approximately 80 percent sand with 20 percent fines. Figure 4.64 shows the jacking forces from 10 to 120 feet. The jacking stress along this segment is 0.083 tons per square foot of pipe surface area.

After the initial section of 120 feet, lubrication was applied to the pipeline and the jacking forces decreased until approximately 272 feet into the drive, when the forces again began to increase. Figure 4.65 shows the jacking force from 272 to 362 feet. Throughout this section the jacking stress was 0.054 tons per square foot of surface area.

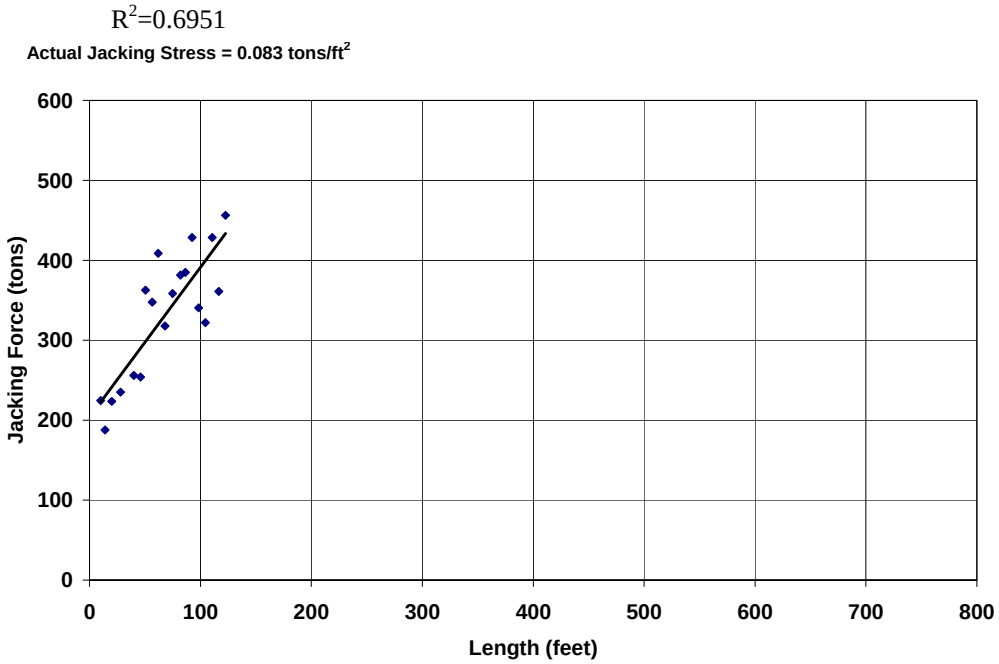

Figure 4.64. Length vs. Jacking Force for the Eastside Interceptor Houser Way Drive from 0 to 120 feet.

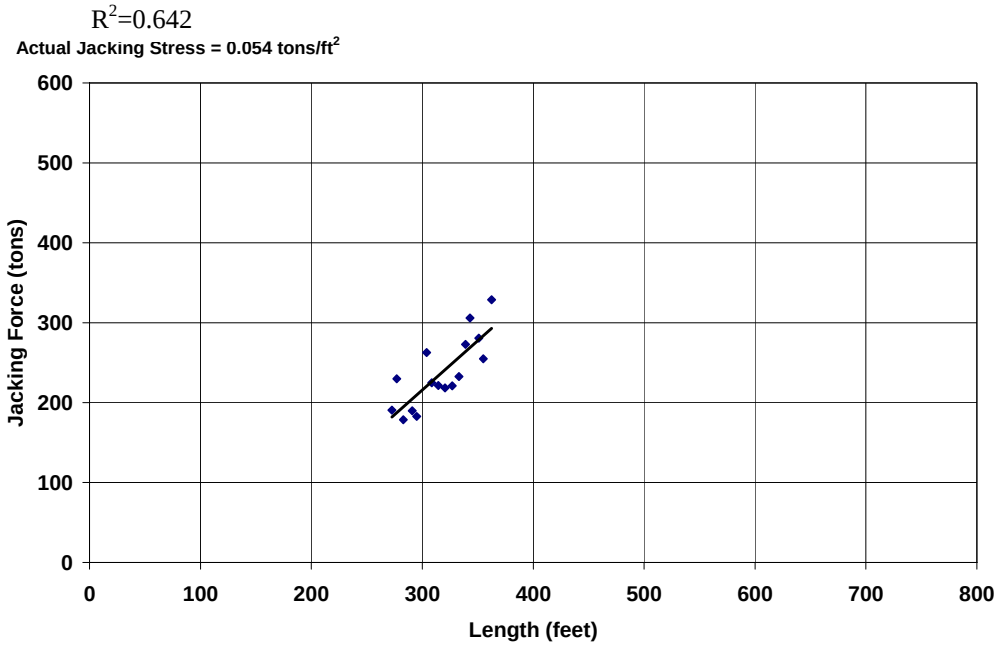

Figure 4.65. Length vs. Jacking Force for the Eastside Interceptor Houser Way Drive from 272 to 362 feet.

After 362 feet the jacking forces again decrease until approximately 440 feet into the drive where an increase is again observed in the section between 440 and 505 feet. The increase in jacking forces through this region, however, is not as pronounced as the jacking stress increases at a rate of 0.033 tons per square foot of surface area as shown in Figure 4.66.

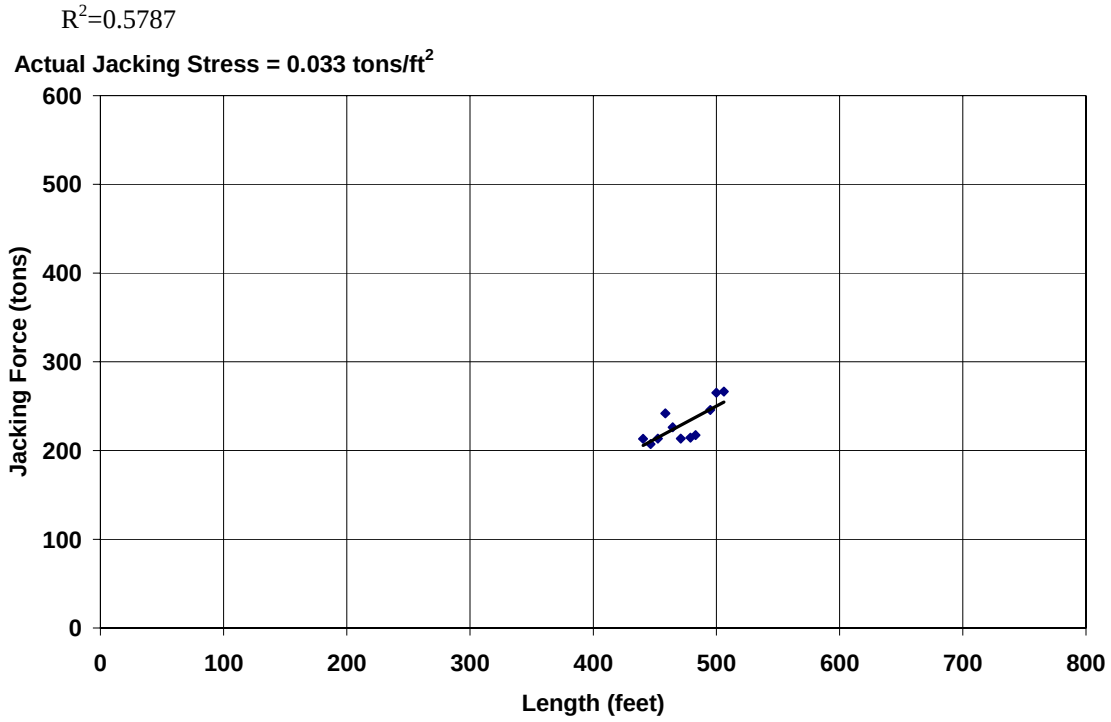

Figure 4.66. Length vs. Jacking Force for the Eastside Interceptor Houser Way dRive from 440 to 505 feet.

The last isolated segment for analysis occurs at the end of the drive where there is a marked increase in jacking forces. Throughout the region between 530 and 580 feet the jacking forces increase at a rate of 0.09 tons per square foot of surface area, a markedly higher jacking stress than in the previous section. The stresses in this zone are

comparable to the unlubricated zone at the beginning of the microtunneling drive. This is shown in Figure 4.67.

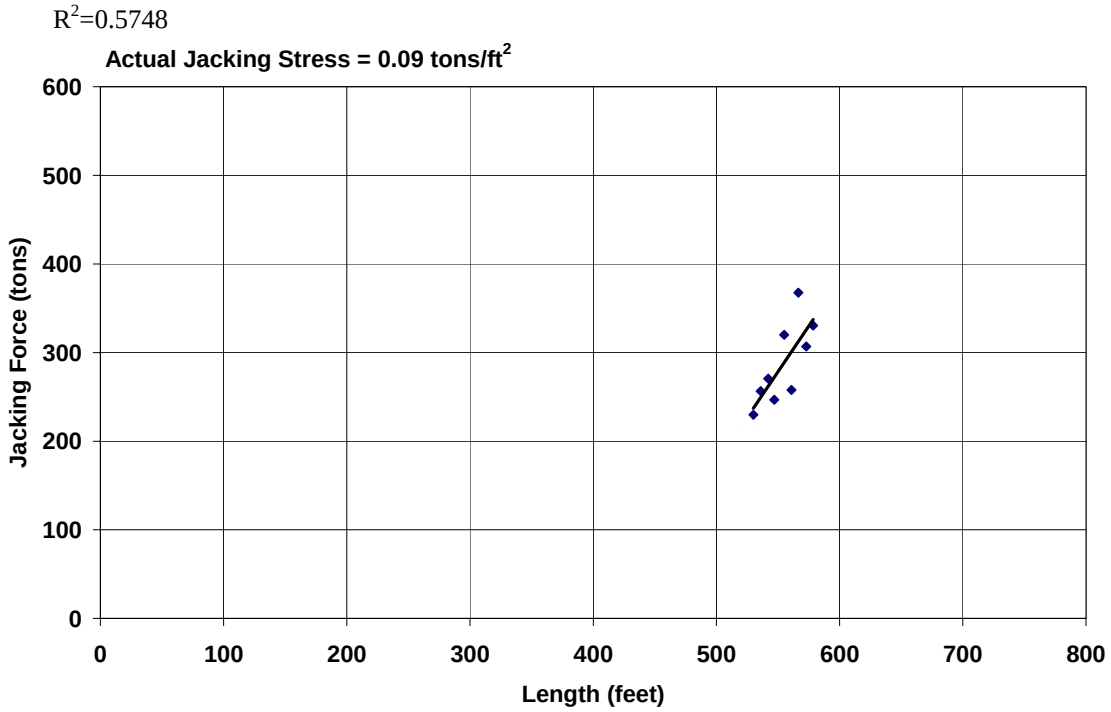

Figure 4.67. Length vs. Jacking Force for the Eastside Interceptor Houser Way Drive from 530 to 580 feet.

4.7.7 Summary of Jacking Stress for Isolated Tunneling Segments

Table 4.17 provides a summary of jacking stresses on isolated segments of the Houser Way Drive.

Table 4.17. Jacking Stresses on Isolated Segments of Houser Way Drive.

Zones of analysis along tunnel alignment [feet]	Normalized Jacking Force [tons/ft^2]	Notes	R^2 Value
10-120	0.083	Non-lubricated	0.6951
272-362	0.054		0.642
440-505	0.033		0.5787
530-580	0.090	Higher than non lubricated zone	0.5787

4.8 Alvarado Trunk Sewer – Jacking Pit 3 to Reception Pit 4

The Alvarado Trunk Sewer, located in Union City and Freemont, CA contained several sections of microtunneling. Union Sanitary District commissioned the design in 2001 and the sewer was constructed in 2004. Microtunneling was the preferred construction alternative due to the depth of the sewer and the high impacts that open cut construction would have had on the surrounding area.

4.8.1 Description of the Project

The microtunnel drive between Jacking Pit 3 (JP3) and Reception Pit 4 (RP4) included the installation of 710 feet of Polycrete pipe with microtunneling in a single drive. The pipe had an outer diameter of 46.6 inches and an inner diameter of 39.4 inches. Polycrete was chosen due to its superior corrosion resistant characteristics and axial jacking strength. This pipe, relatively new to the microtunneling industry, was manufactured in Germany and at a new manufacturing plant in Louisiana.

The shafts on the project were constructed with piles and lagging. These shafts proved to be easier to construct in shapes that were not square to facilitate jacking in multiple directions at pivot points along the alignment.

Depth of cover above the pipeline was relative constant throughout the entire drive length at approximately 19 feet. This is shown in Figure 4.68 which shows the design profile of the pipeline.

An Akkerman microtunneling machine with a soft ground cutting head was used for construction of the microtunnel. The head was configured with drag picks and bullet bits. The machine had an 48-inch outer diameter, creating an overcut of approximately 1.5 inches on the diameter.

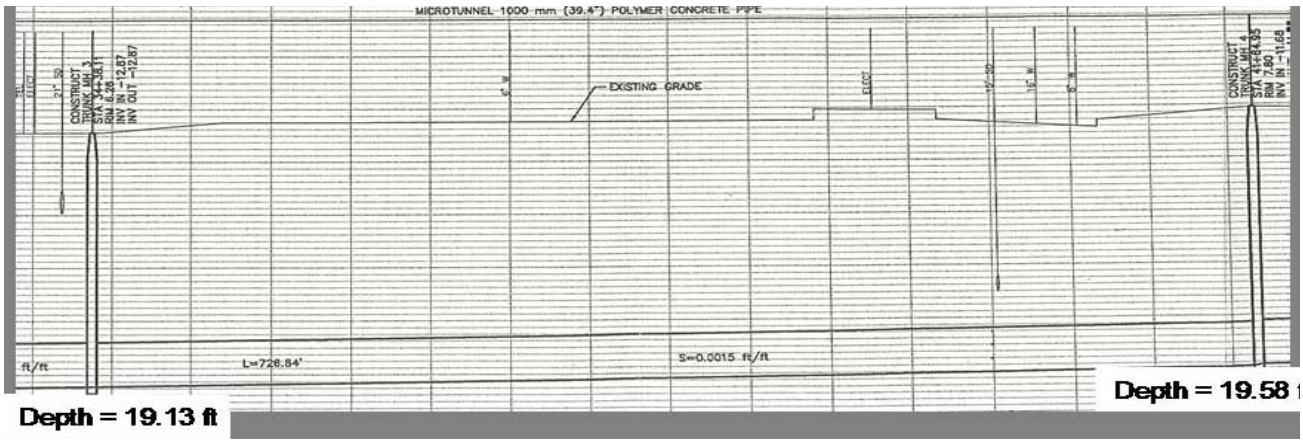

Figure 4.68. Alvarado Boulevard Trunk Sewer – Profile of Drive from Jacking Pit 3 to Reception Pit 4 (Calderwood, 2004).

4.8.2 Geotechnical Conditions Along the Alignment

An extensive geotechnical investigation was completed for the Alvarado Trunk Sewer project. The geotechnical investigation included many project borings, soil sampling, and extensive soil testing. A geotechnical data report, a geotechnical interpretive report, and a geotechnical baseline report were produced for the project. For the drive between Jacking Pit 3 and Reception Pit 4, 3 vertical borings were completed: one at each shaft location and one in the middle of the bore. Figures 4.69 and 4.70 are boring logs that correspond to vertical borings that were drilled at the jacking and reception shaft for the design of the drive. These logs provide information on the in situ soil density by providing blow counts for selected soil samples.

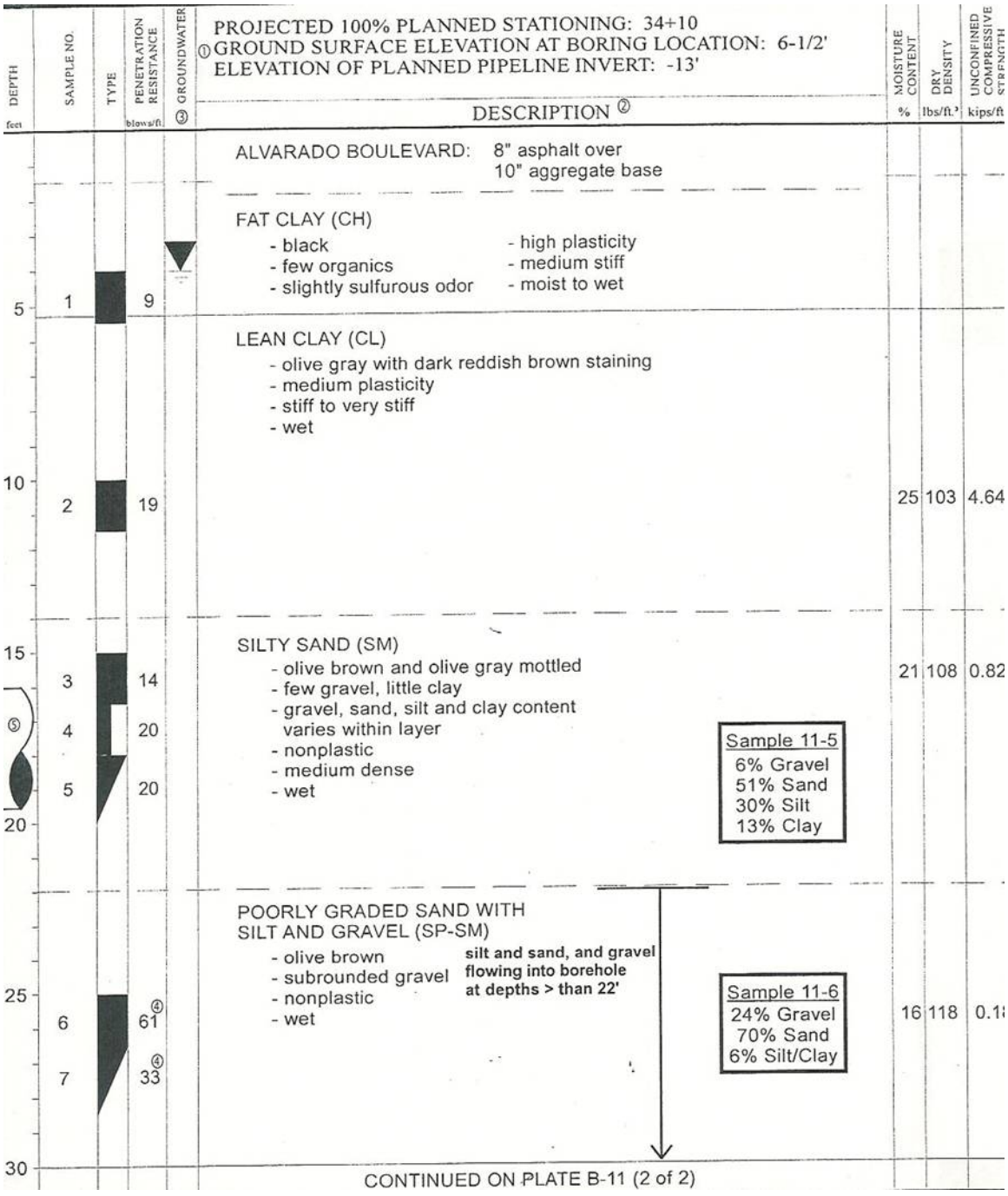

Figure 4.69. Boring Log B-11 Located at the Jacking Shaft – JP3 (Mathy et al, 2004).

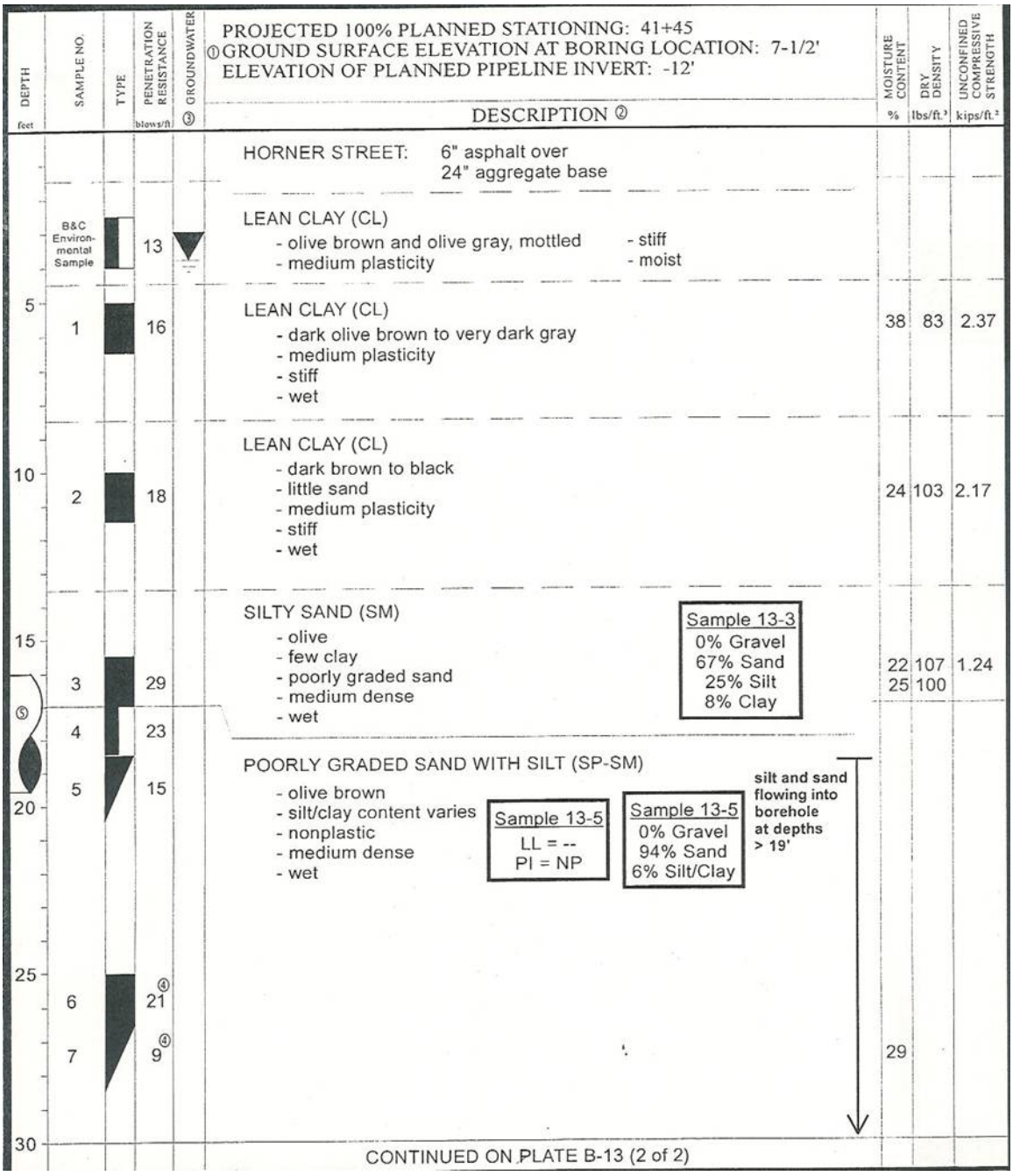

Figure 4.70. Boring Log B-13 Located at the Reception Shaft – RP4
(Mathy, et al., 2004)

4.8.3 Construction of the Microtunnel

The microtunnel was launched on December 17, 2003 and was completed on January 30, 2004. Table 4.18 shows the progress of the tunnel on a daily basis and provides some notes of significance.

Table 4.18. Daily and Cumulative Progression on the Alvarado Trunk Sewer Drive Jacking Pit 3. to Reception Pit 4.

Date	Pipes Tunneled	Length [ft]	Cumulative Length [ft]	Notes
12/17/03	Microtunneling Machine(11), Trailing Can(11), Pipes 1,2,3,4,5	11+11+ 40	62	
12/18/03	Pipes 6, 7, 8, 9, 10, 11, 12, 13, 14, 15, 16, 17, 18	104	166	
12/19/03	Pipes 19, 20, 21, 22, 23,	40	206	
12/22/03	Pipes 24, 25, 26, 27, 28, 29, 30	56	266	
1/5/04	Pipes 31, 32, 33, 34	32	298	Lead IJS Pipe #34
1/6/04	Pipes 35 (IJS), 36, 37, 38, 39,	40	338	Hit something at 337 feet
1/14/04	Pipes 40, 41	16	354	Capped bentonite line at machine due to leak. Used IJS to get moving. Machine diving. Having trouble developing face pressure.
1/16/04	Pipes 42, 43, 44, 45	32	386	Installed bentonite valve at #1 pipe after installation of pipe #43
1/19/04	Pipes 46, 47, 48, 49, 50	40	426	
1/20/04	Pipes 51, 52, 53, 54, 55	40	466	Started pumping bentonite at front again
1/21/04	Pipes 56, 57, 58, 59, 60, 61	48	514	
1/22/04	Pipes 62, 63, 64, 65, 66, 6768, 69, 70, 71	80	594	
1/23/04	Pipes 72, 73, 74, 75, 76, 77, 78, 79, 80	72	676	
1/26/04	Pipe 81, 82, 83, 84, 85, 86	48	724	Hit wall within first few feet of Pipe #86

4.8.4 Jacking Forces on the Microtunnel

The frictional component of the jacking forces over the microtunnel drive ranged from 15 tons to near 325 tons. Figure 4.71 shows the frictional component of the jacking forces as a function of the length of the tunnel drive.

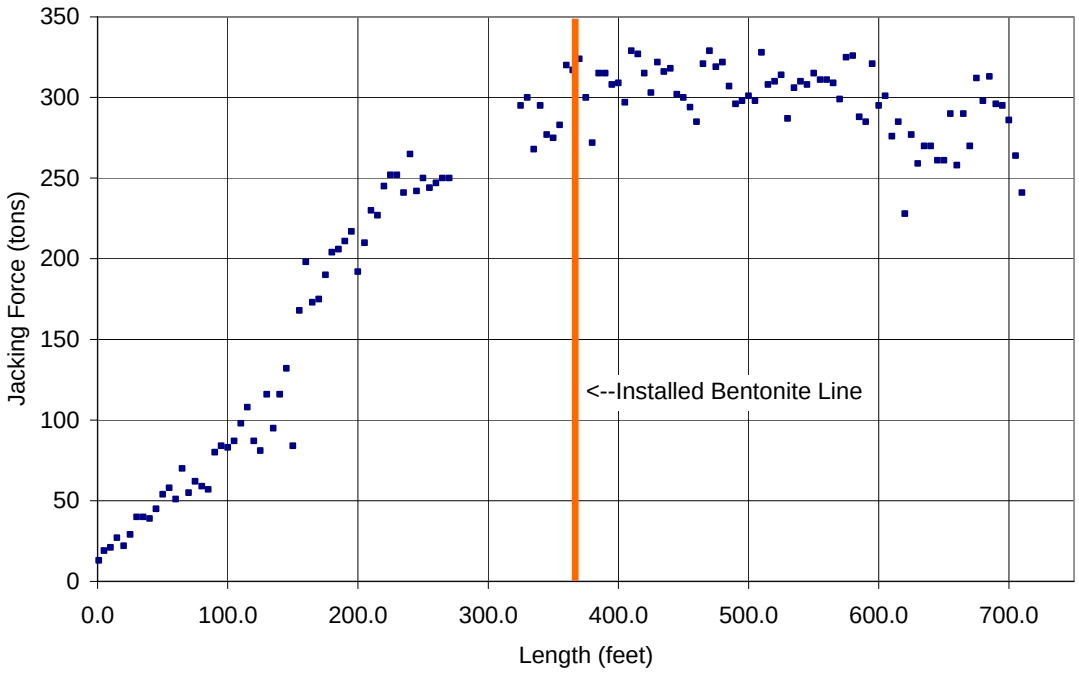

Figure 4.71. Length vs. Jacking Force for the Alvarado Boulevard Project Jacking Pit 3 to Reception Pit 4.

4.8.5 Lubrication During Tunneling

Bentonite lubrication was delivered along the tunnel through a manifold 2-inch pipeline that was plumbed to a port in the machine. The pumping of lubrication was not started until approximately 100 feet into the drive. However, there was a leak in the port at the tunnel machine heading and the lubrication was leaking into the tunnel machine and pipeline instead of pumping to the outside of the pipeline. At 350 feet into the tunnel, the lubrication port in the tail section of the machine was capped off. Then, at 386 feet into the tunnel, a lubrication port was manually installed into the first pipe section and lubrication was applied through this port from 386 feet into the tunnel drive until the end of the tunnel.

4.8.6 Isolation of Tunneling Segments for Specific Analysis

The first segment for analysis is the section from launch to 85 feet. Throughout this segment, no lubrication was pumped, even to the malfunctioning port at the tail section of the shield. Figure 4.72 shows the jacking forces from 20 to 85 feet. The jacking stress along this segment is 0.045 tons per square foot of pipe surface area.

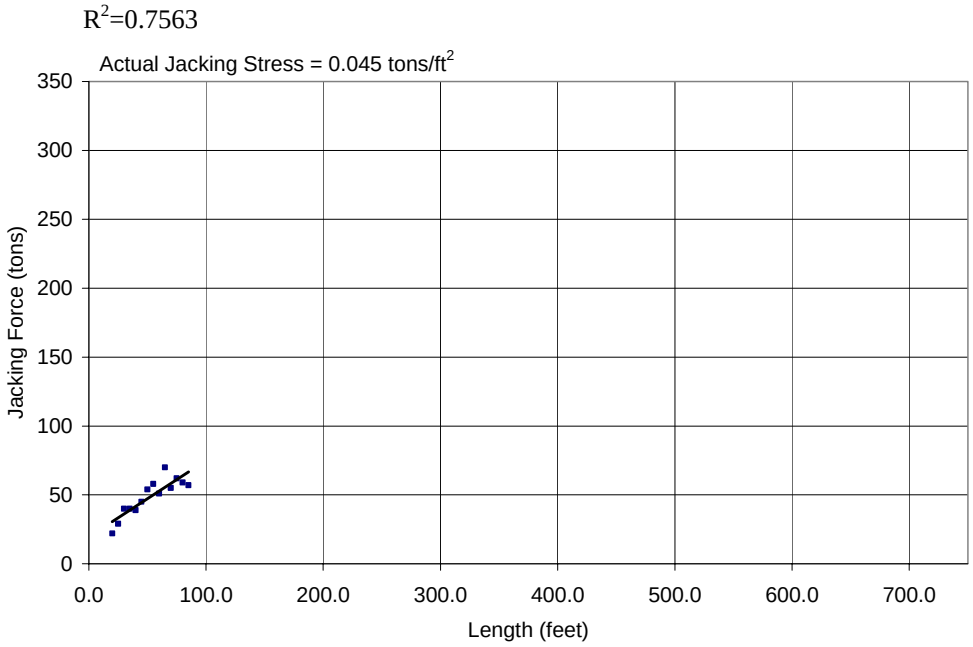

Figure 4.72. Length vs. Jacking Forces for the Alvarado Boulevard Project Jacking Pit 3 to Reception Pit 4 from 20 to 85 feet.

After the initial section of 85 feet, lubrication was applied to the pipeline at the tail section of the machine; however, the lubrication port was malfunctioning. Evaluating the jacking stress from 20 to 386 feet, where lubrication began in pipe one (1) at a functioning port, reveals that the lubrication in the tail section was completely ineffective

as the jacking stress from 20 to 386 feet remained at 0.07 tons per square foot of surface area. This can be seen in Figure 4.73.

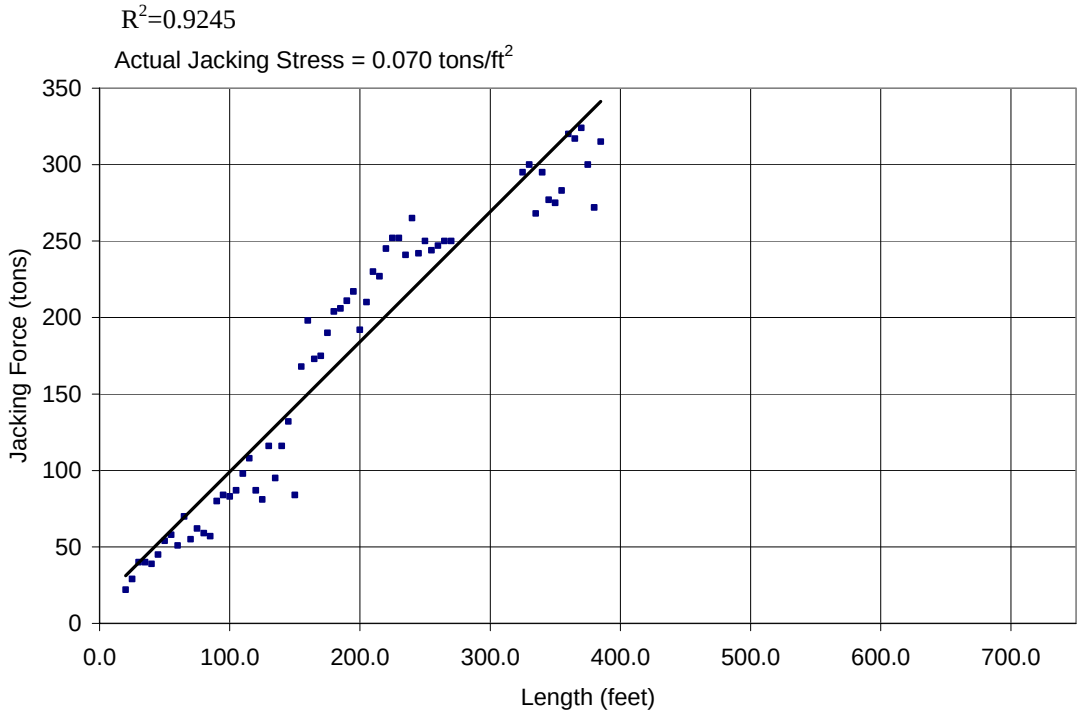

Figure 4.73. Length vs. Jacking Force for the Alvarado Boulevard Project Jacking Pit 3 to Reception Pit 4 from 20 to 385 feet.

Figure 4.73 clearly shows that the lubrication applied in the tail shield had no effect on lowering the jacking forces on the drive throughout the first 386 feet. Once the lubrication was applied, the jacking forces no longer increased on the project and remained in the range between 250 and 350 tons as can be seen in Figure 4.71.

4.8.7 Summary of Jacking Stresses on Isolated Tunneling Segments

Table 4.19 provides a summary of normalized frictional coefficients on the Morris Avenue Drives.

Table 4.19. Jacking Stresses on Isolated Segments of the Microtunnel Drive from Jacking Shaft 3 to Reception Shaft 4 – Alvarado Trunk Sewer Project.

Segments Along Tunnel alignment [feet]	Jacking Stress [tons/ft^2]	Notes	R^2 Value
20-65	0.072	Non-lubricated	0.8916
20-386	0.070	Ineffective Lubrication	0.9245

4.9 Alvarado Trunk Sewer – Jacking Pit 4 to Reception Pit 4

Another of the microtunnel drives on the Alvarado Trunk Sewer, located in Union City and Freemont, CA was between stations 49+58 and 41+64. This drive shared a common reception pit with the drive from Jacking Shaft 3 (JP3), meaning both microtunnel drives terminated in reception pit 4.

4.9.1 Description of the Project

The microtunnel drive between Jacking Pit 4 (JP4) and Reception Pit 4 (RP4) included the installation of 775 feet of Polycrete pipe with microtunneling in a single drive. The pipe had an outer diameter of 46.6 inches and an inner diameter of 39.4 inches. Polycrete was chosen due to its superior corrosion resistant characteristics and axial jacking strength. This pipe, relatively new to the microtunneling industry, was manufactured in Germany and in a new manufacturing plant in Louisiana.

The shafts on the project were constructed with piles and lagging. These shafts proved to be easier to construct in shapes that were not square to facilitate jacking in multiple directions at pivot points along the alignment. Depth of cover above the pipeline on this drive ranges from 19 to 22 feet. A profile of the design alignment is shown in Figure 4.74.

An Akkerman microtunneling machine with a soft ground cutting head was used for construction of the microtunnel. The head was configured with drag picks and bullet bits. The machine had an 48-inch outer diameter, creating an overcut of approximately 1.5 inches on the diameter.

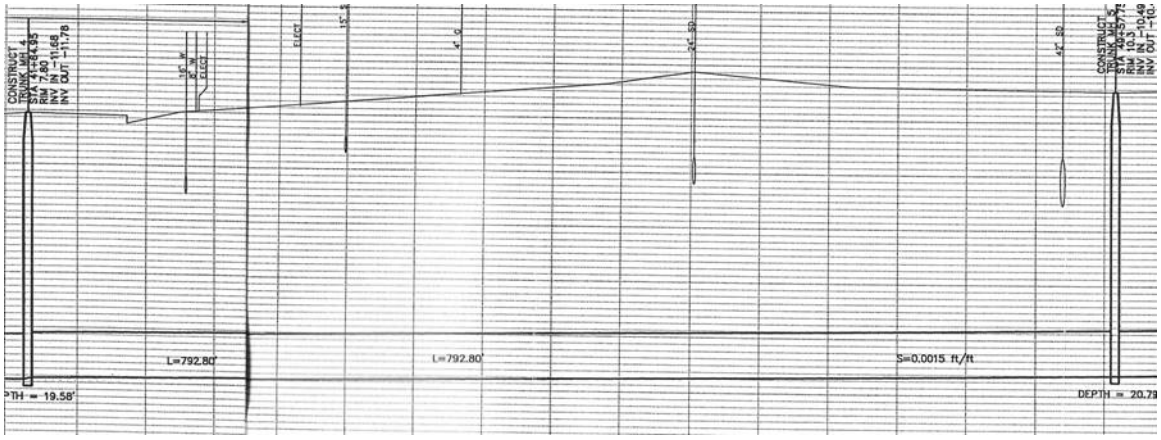

Figure 4.74. Alvarado Boulevard Trunk Sewer – Profile from Jacking Pit 4 to Reception Pit 4 (Calderwood, 2004).

4.9.2 Geotechnical Conditions Along the Alignment

An extensive geotechnical investigation was completed for the Alvarado Trunk Sewer project. The geotechnical investigation included many project borings, soil sampling, extensive and extensive soil testing. A geotechnical data report, a geotechnical interpretive report, and a geotechnical baseline report were produced for the project. For the drive between Jacking Pit 4 and Reception Pit 4, 3 vertical borings were completed: one at each shaft location and one in the middle of the bore.

Figure 4.75 corresponds to a vertical borings at the jacking shaft (JP4) and Figure 4.76 corresponds to a vertical boring mid-way between the jacking and reception shaft. Soil conditions at the reception shaft are depicted in Figure 4.70 in Section 4.8.

4.9.3 Construction of the Microtunnel

The microtunnel was launched on February 9, 2004 and was completed on February 19, 2004. Table 4.20 shows the progress of the tunnel on a daily basis and provides some notes of significance.

Table 4.20. Daily and Cumulative Progression on the Alvarado Trunk Sewer Drive Jacking Pit 4. to Reception Pit 4.

Date	Pipes Tunneled	Length [ft]	Cumulative Length [ft]	Notes
2/9/04	Microtunneling Machine (11), Trailing Can(11), Pipes 1	11+11+8	30	
2/10/04	Pipes 2, 3, 4, 5, 6, 7, 8, 9, 10, 11, 12, 13, 14, 15, 16	120	150	Started pumping bentonite at head at 74 feet into the tunnel drive
2/11/04	Pipes 17, 18, 19, 20, 21, 22, 23, 24, 25, 26, 27, 28, 29, 30, 31, 32, 33	136	286	
2/12/04	Pipes 34, 35, 36, 37, 38, 39, 40, 41, 42, 43, 44(ijs), 45, 46	104	390	
2/13/04	Pipes 47, 48, 49, 50, 51, 52, 53,	56	446	
2/17/04	Pipes 54, 55, 56, 57, 58, 59, 60, 61, 62, 63, 64, 65, 66, 67, 68, 69	128	574	Hit some wood and had trouble sustaining face pressure – machine dropping at 550 feet
2/18/04	Pipes 70, 71, 72, 73, 74, 75, 76, 77, 78, 79, 80, 81, 82	104	678	Hit something at 660 feet and caused the machine to roll significantly
2/19/04	Pipes 83, 84, 85, 86, 87, 88, 89, 90, 91, 92, 93, 94	96	774	Hit reception shaft while tunneling pipe 94

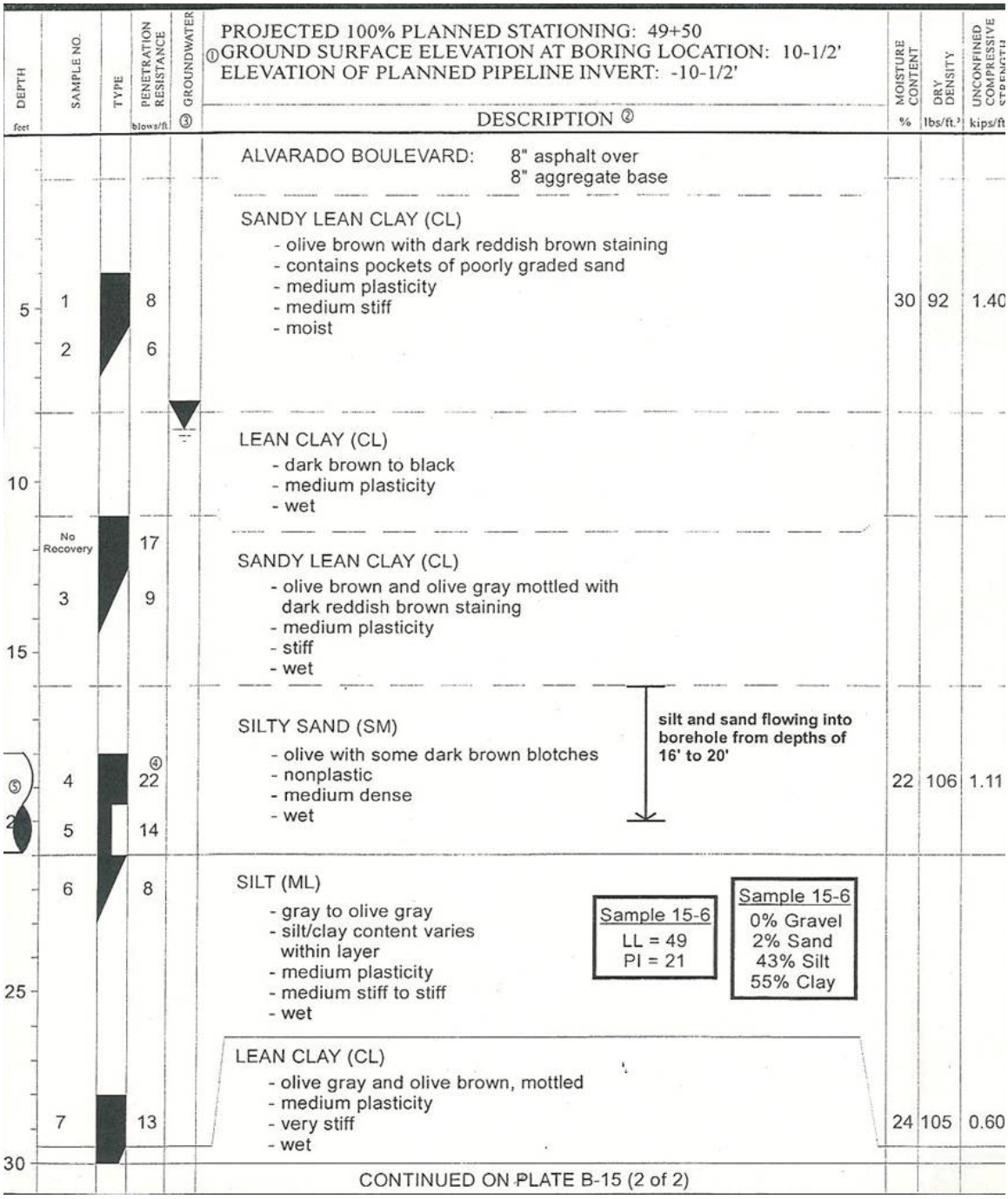

Figure 4.75. Boring Log B-15 Located at the Jacking Shaft – JP4 (Mathy et al., 2004).

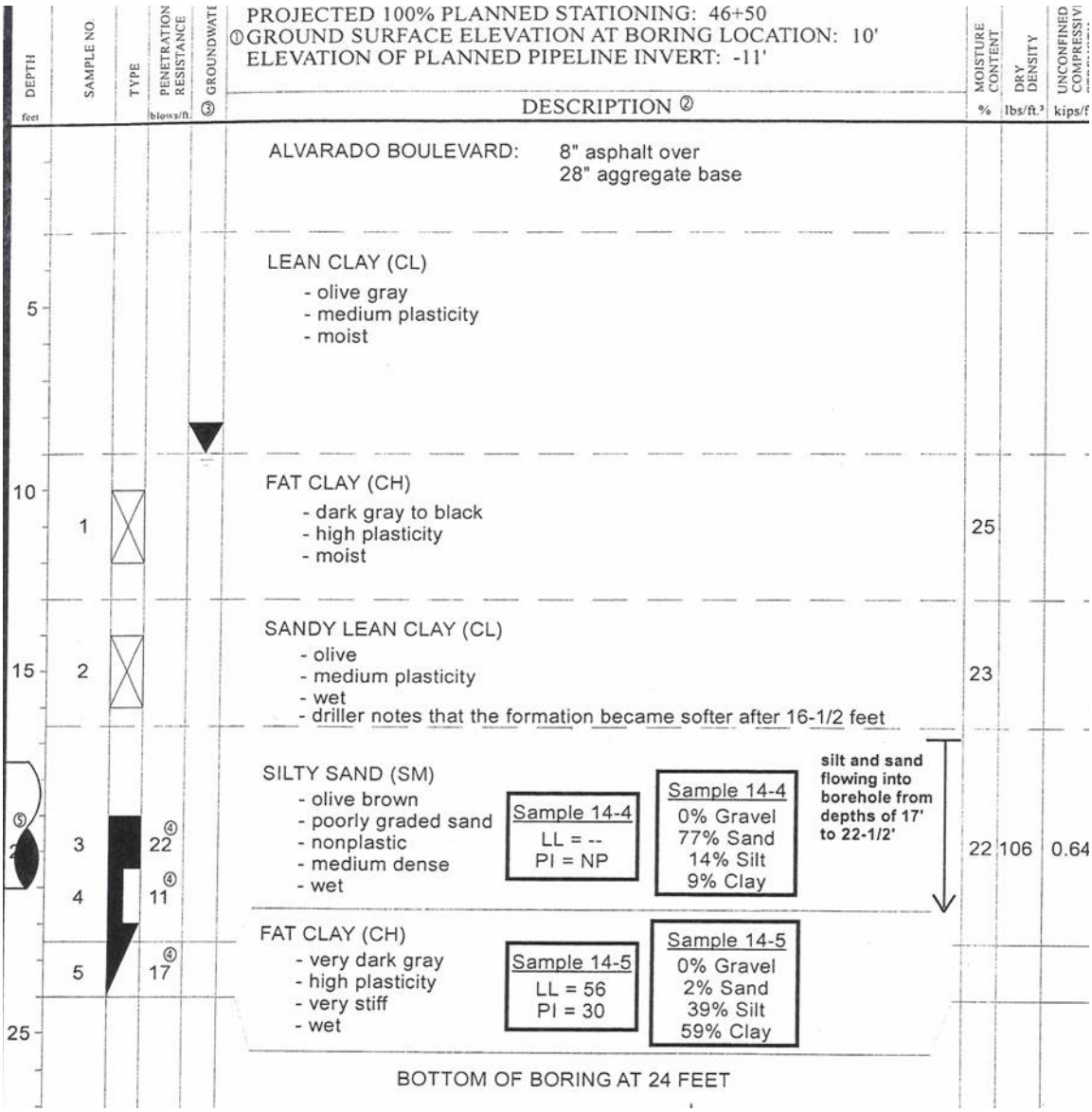

Figure 4.76. Boring Log B-14 Located Mid-Drive between JP4 and RP4 (Mathy, et al., 2004).

4.9.4 Jacking Forces on the Microtunnel

The frictional component of the jacking forces over the microtunnel drive ranged from 10 tons to near 250 tons. Figure 4.77 shows the frictional component of the jacking forces as a function of the length of the tunnel drive.

4.9.5 Lubrication During Tunneling

Bentonite lubrication was delivered along the tunnel through a 2-inch pipeline that was plumbed to a port in the tail section of the machine. The port was located at the 12-o'clock position. The contractor began pumping lubrication at 74 feet into the tunnel drive and continued pumping through that single port throughout the entire drive. No other lubrication ports were activated during tunneling.

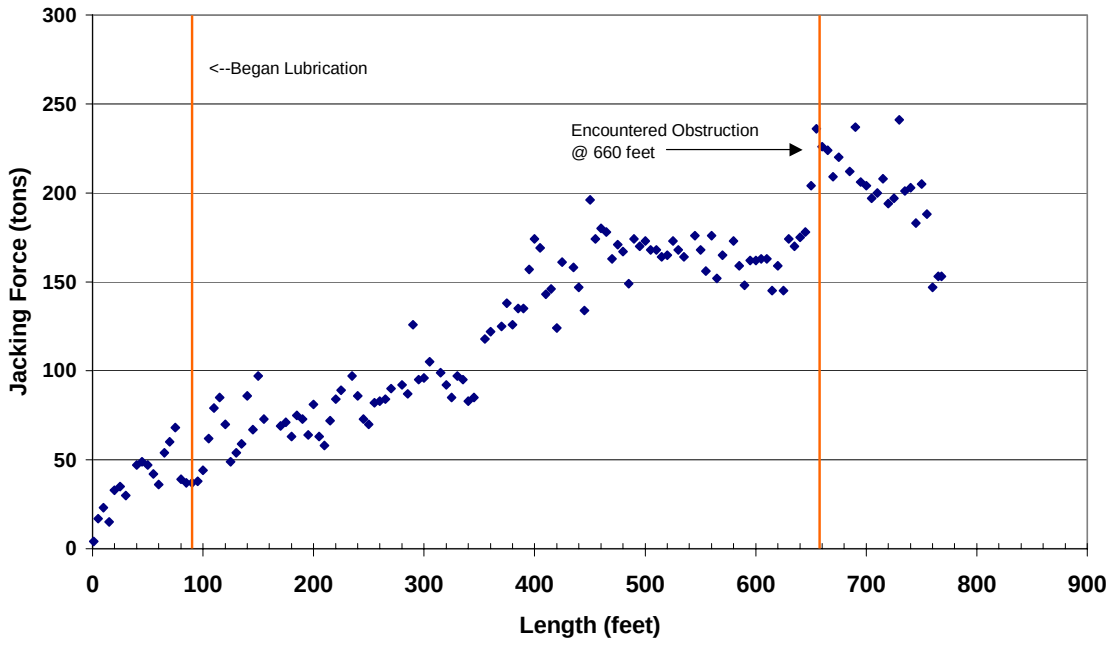

Figure 4.77. Length vs. Jacking Force for the Alvarado Boulevard Project Jacking Pit 4 to Reception Pit 4.

4.9.6 Isolation of Tunneling Segments for Specific Analysis

The first segment for analysis is the section from launch to 50 feet. Throughout this segment, no lubrication was pumped. Figure 4.78 shows the jacking forces from 10 to 50 feet. The jacking stress along this segment is 0.049 tons per square foot of pipe surface area.

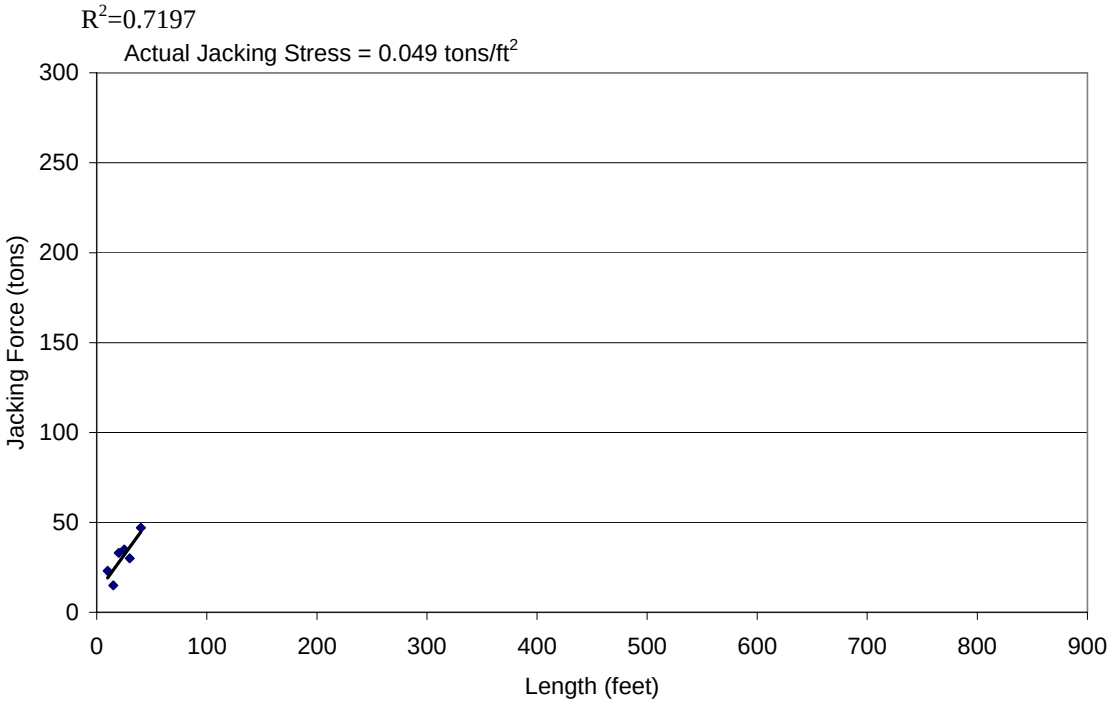

Figure 4.78. Length vs. Jacking Force for the Alvarado Boulevard Project Jacking Pit 4 to Reception Pit 4 from 10 to 50 feet.

After the initial section of 50 feet, lubrication was applied to the pipeline at the tail section of the machine. In evaluating the jacking stress from 200 feet to 495 feet the jacking forces increased at a much lower rate of 0.03 tons per square foot of surface area. This can be seen in Figure 4.79. Figure 4.79 clearly shows that the lubrication applied in the tail shield had a significant effect on lowering the jacking forces on the drive.

At 550 feet in the drive, there is a decrease in the jacking force, this is a point where the operator notes that the material is very soft and that they are having difficulty maintaining any face pressure on the machine. The operator also notes that the machine has encountered wood. The last sudden increase in jacking force is at 660 feet into the drive where the operator notes that an obstruction was encountered. This can be seen on Figure 4.77.

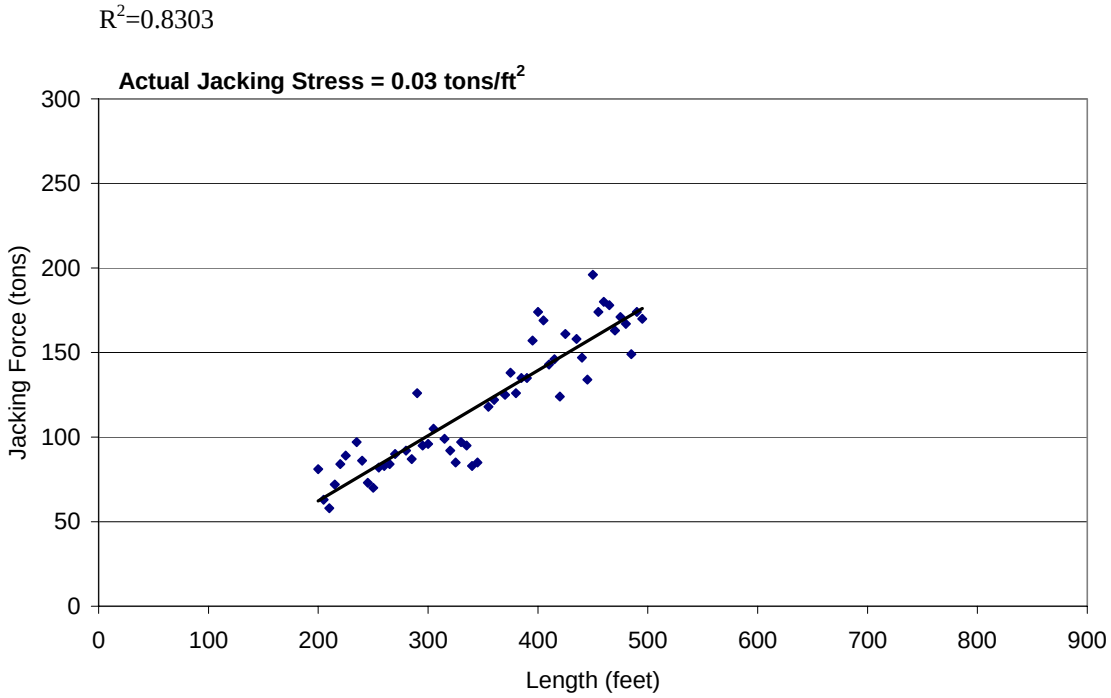

Figure 4.79. Length vs. Jacking Force for the Alvarado Boulevard Jacking Pit 4 to Reception Pit 4 from 200 to 495 feet.

4.9.7 Summary of Jacking Stresses for Isolated Tunneling Segments

Table 4.21 provides a summary of normalized frictional coefficients on the drive from Jacking Pit 4 to Reception Pit 4

Table 4.21. Jacking Stresses on Isolated Segments of the Microtunnel Drive from Jacking Pit 4 to Reception Pit 4.

Segments Along Tunnel alignment [feet]	Normalized Jacking Force [tons/ft^2]	Notes	R^2 Value
10-50	0.049	Non-lubricated	0.7197
200-495	0.030	Lubrication from one port in tail shield	0.8303

4.10 Alvarado Trunk Sewer – Drive 17

The Alvarado Boulevard Trunk Sewer Project included a Phase 2 that contained microtunneling with 24-inch Polycrete pipe.

4.10.1 Description of the Project

Drive 17 on the Alvarado project was constructed from Manhole 17 to Manhole 18 with microtunneling. 24-inch Polycrete pipe was jacked behind an Akkerman soft ground microtunneling machine. The drive began at a depth of 25.9 feet and ended at a depth of 19.3 feet. A profile of the design alignment is shown in Figure 4.80.

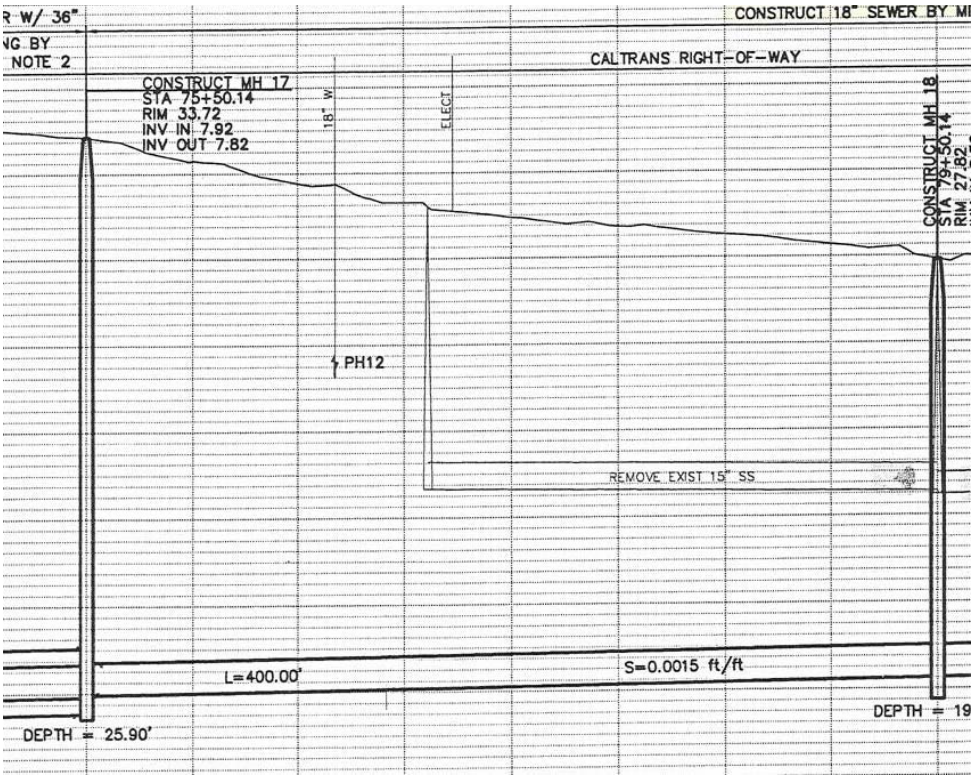

Figure 4.80. Alvarado Boulevard Trunk Sewer – Profile of Drive 17 from Manhole 17 to Manhole 18 (Calderwood, 2002).

4.10.2 Geotechnical Conditions Along the Alignment

Three vertical borings were drilled for the design of the microtunnel and soil samples were collected and tested for the design. Figures 4.81 through 4.83 show the vertical boring logs with the location of the design depth of the pipeline shown on the boring. Boring B-43 was drilled at the at the Jacking Shaft (Manhole 17); Boring B-45 was drilled approximately 200 feet into the alignment, measured from the jacking shaft; and boring B-45 was drilled at the reception shaft.

4.10.3 Construction of the Microtunnel

The microtunnel was launched on April 27, 2005 and was completed on May 5, 2005. Table 4.22 shows the progress of the tunnel on a daily basis and provides some notes of significance.

Table 4.22. Daily and Cumulative Progression on the Alvarado Trunk Sewer Drive 17.

Date	Pipes Tunneled	Length [ft]	Cumulative Length [ft]	Notes
4/27/05	Microtunneling Machine(9), Trailing Can(7)	9+7	16	
4/28/05	Trailing Can (7) Pipes 1, 2, 3, 4, 5	7+40= 47	63	
4/28/05	Pipes 6, 7, 8, 9, 10, 11, 12, 13	64	127	
4/28/05 2nd Shift	Pipes 14, 15, 16, 17, 18, 19	48	175	
4/29/05	Pipes 20, 21, 22, 23, 24	40	215	
5/2/05	Pipes 25, 26, 27, 28, 29, 30, 31, 32, 33	72	287	
5/3/05	Pipes 34, 35, 36, 37, 38, 39, 40, 41, 42, 43, 44	88	375	
5/5/05	Pipes 45	8	383	Bit exposed in shaft on pipe 45

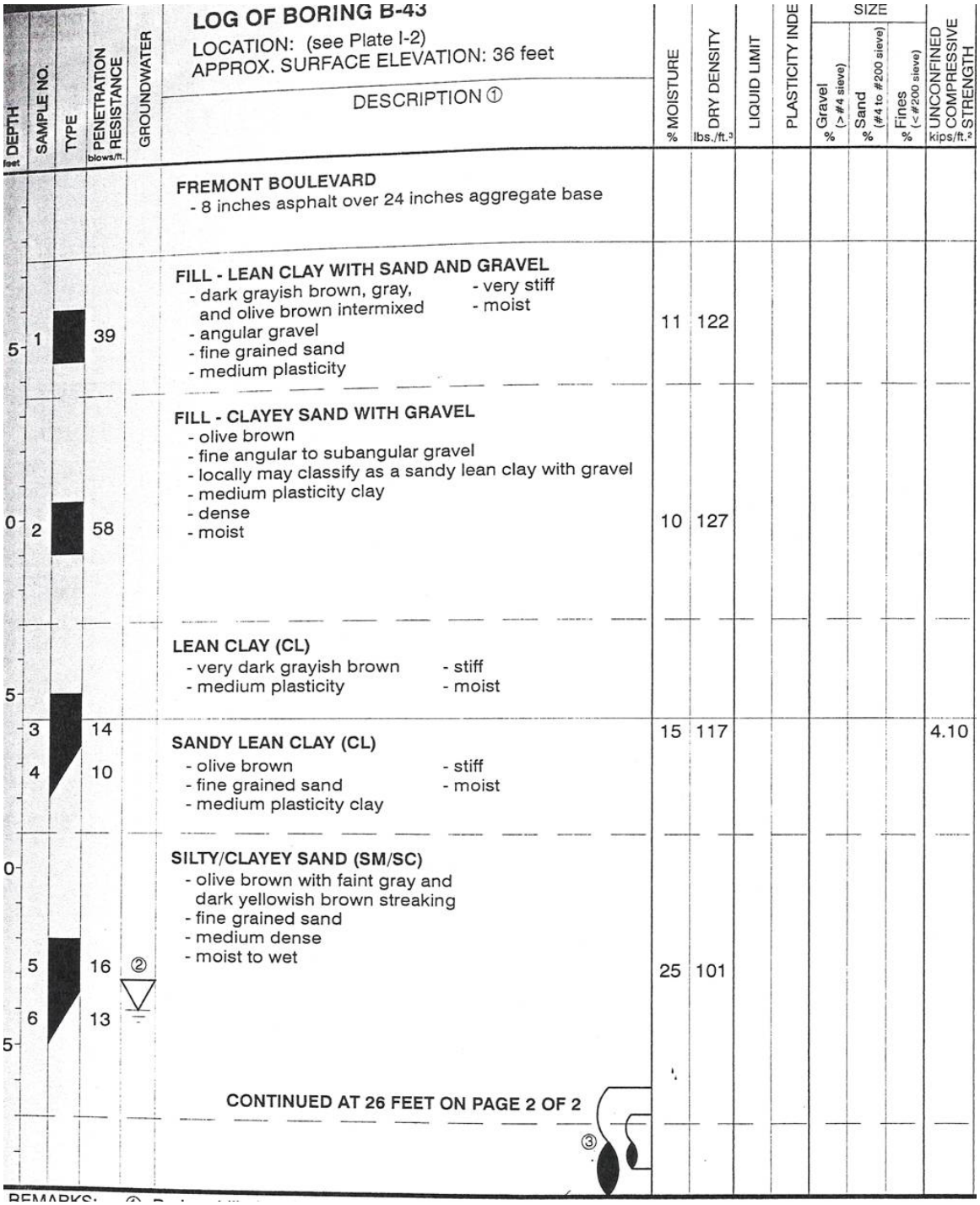

Figure 4.81. Boring B-43 Drilled at the Approximate Location of the Jacking Shaft on Drive 17 (Mathy et al., 2002).

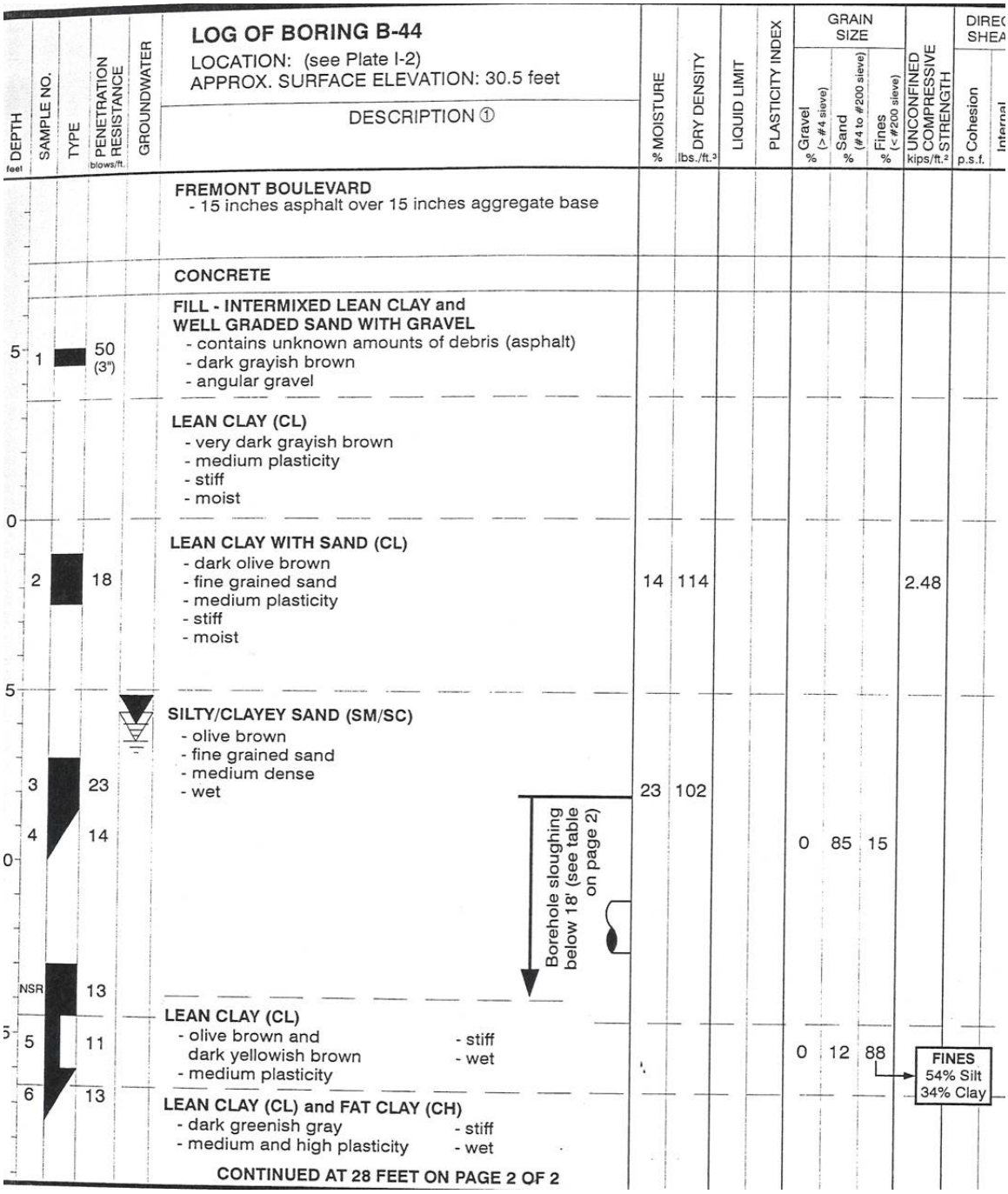

Figure 4.82. Boring B-44 Drilled Mid-Drive on Drive 17 (Mathy et al., 2002).

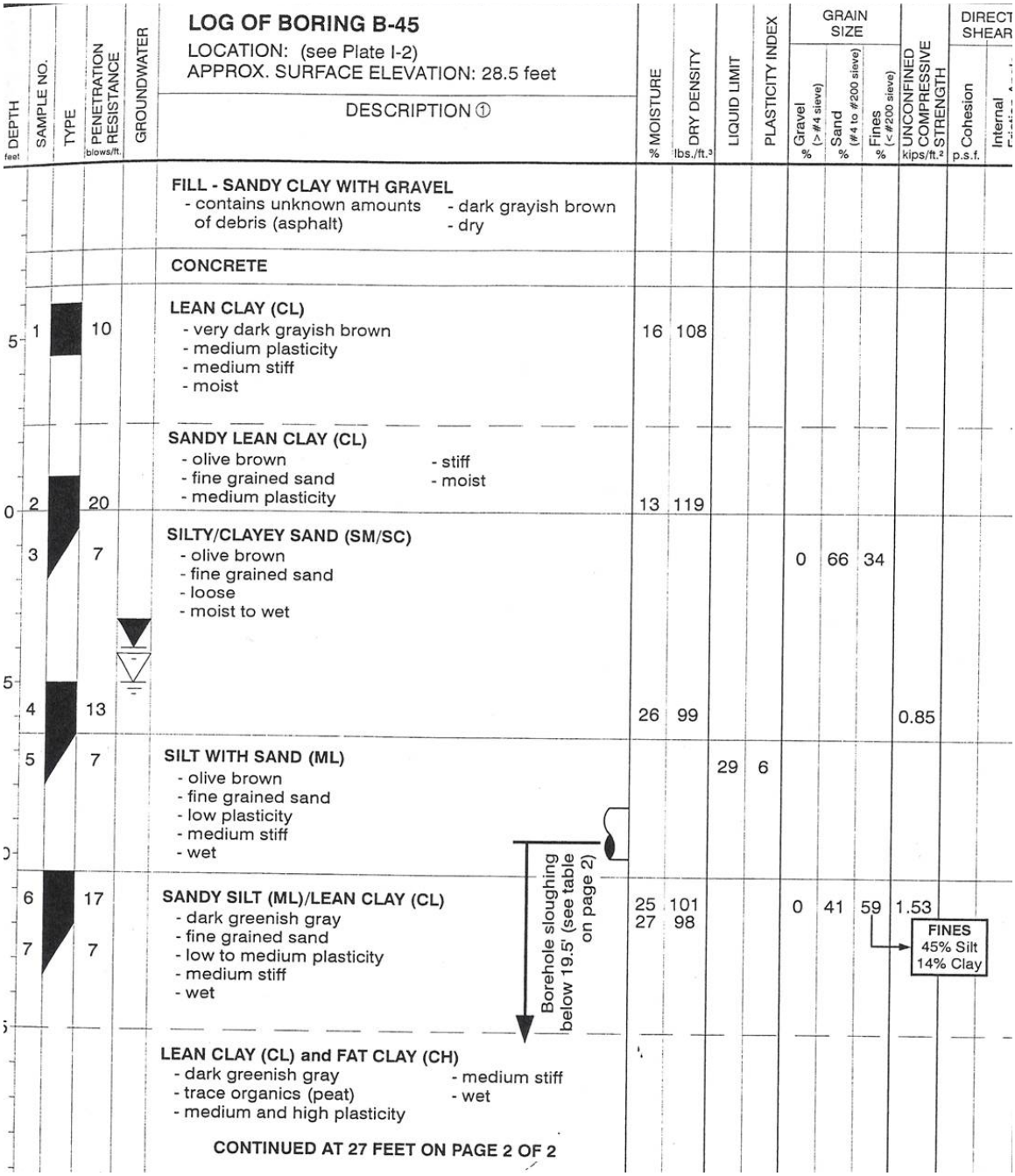

Figure 4.83. B-45 Drilled at Approximate Location of Reception Shaft on Drive 17 (Mathy et al., 2002).

4.10.4 Jacking Forces on the Microtunnel

The frictional component of the jacking forces for Drive 17 ranged from 18 to 124 tons. Figure 4.84 shows the frictional component of the jacking forces as a function of the tunnel length over the entire drive.

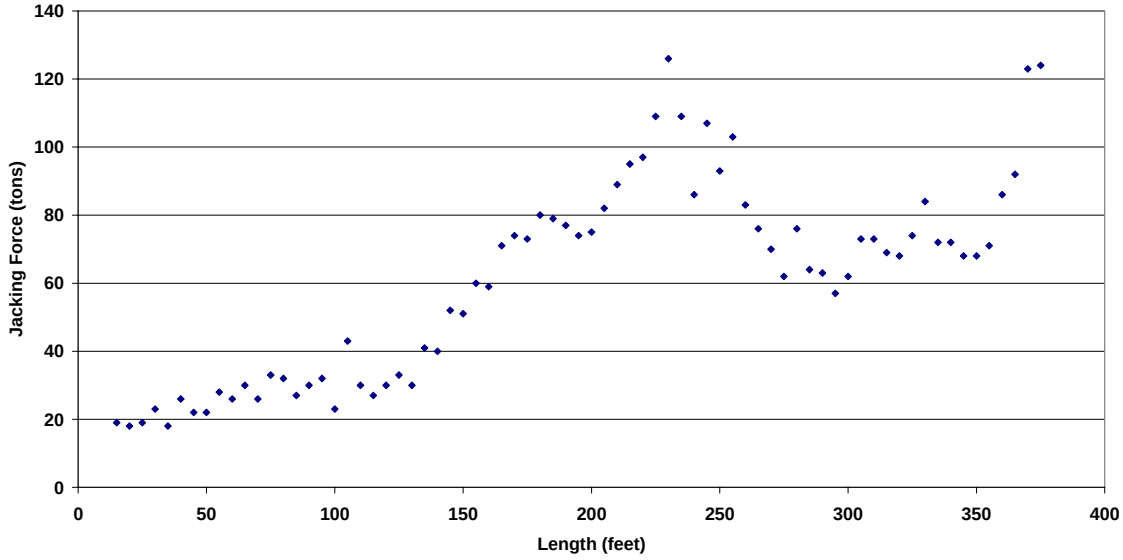

Figure 4.84. Length vs. Jacking Force for the Alvarado Boulevard Project Drive 17.

4.10.5 Lubrication During Tunneling

Due to the small diameter of the pipeline, the only lubrication port that was active during tunneling was located at the end of the tail section of the machine. Lubrication was not applied to the pipeline until 240 feet into the drive. At 240 feet into the drive the operator notes indicate that they began pumping bentonite continuously from the port in the tail section throughout the length of the drive.

4.10.6 Isolation of Tunneling Segments for Specific Analysis

The first segment of the tunnel for specific analysis if from launch of the tunnel through approximately 100 feet. Throughout this zone the jacking stress was 0.026 tons/ft^2. Figure 4.85 shows the frictional component of the jacking force from 15 to 100 feet.

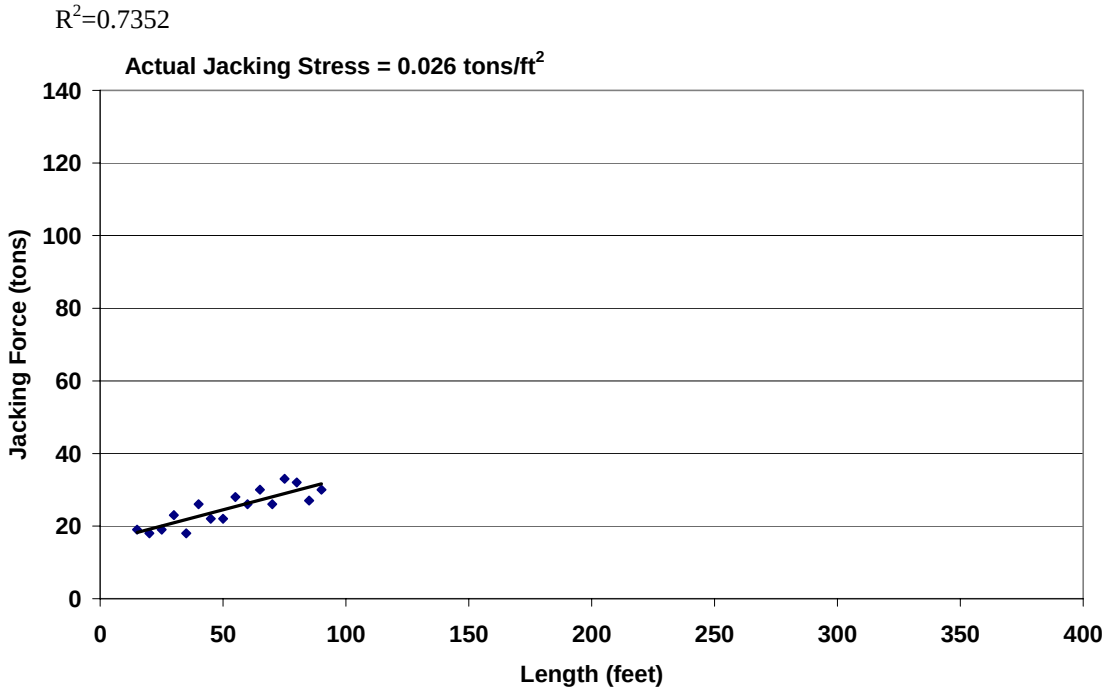

Figure 4.85. Length vs. Jacking Force for the Alvarado Boulevard Project Drive 17 from 20 to 100 feet.

The next segment for analysis is from 100 to 180 feet where there is a distinct change in the jacking stresses. At this location the operator notes that the percentage of silt and clay in the soil has decreased and that the soil is "almost all sand." Figure 4.86 shows the jacking forces from 100 to 180 feet where the jacking stress is 0.12 tons/ft^2.

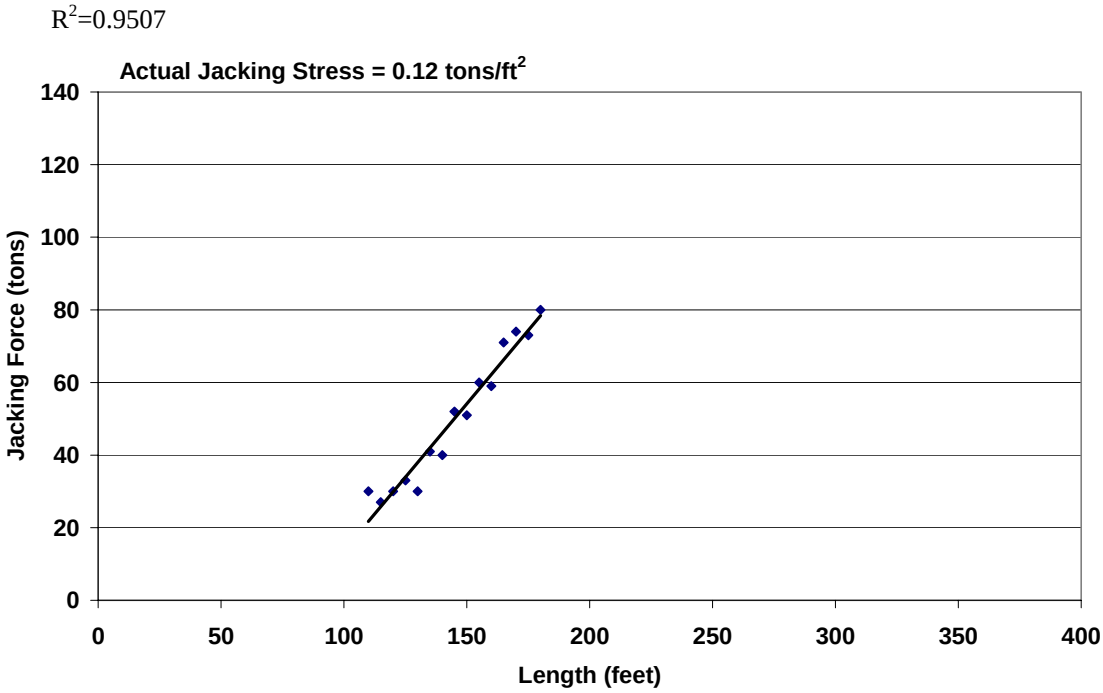

Figure 4.86. Length vs. Jacking Force for the Alvarado Boulevard Project Drive 17 from 100 to 180 feet.

The last segment is from 290 to 360 feet where the jacking forces begin to increase after the initial decrease from the lubrication effects. Throughout this zone, the jacking stress is 0.027 tons/ft^2. Figure 4.87 shows the jacking force from 290 to 360 feet in the drive.

R^2=0.3423

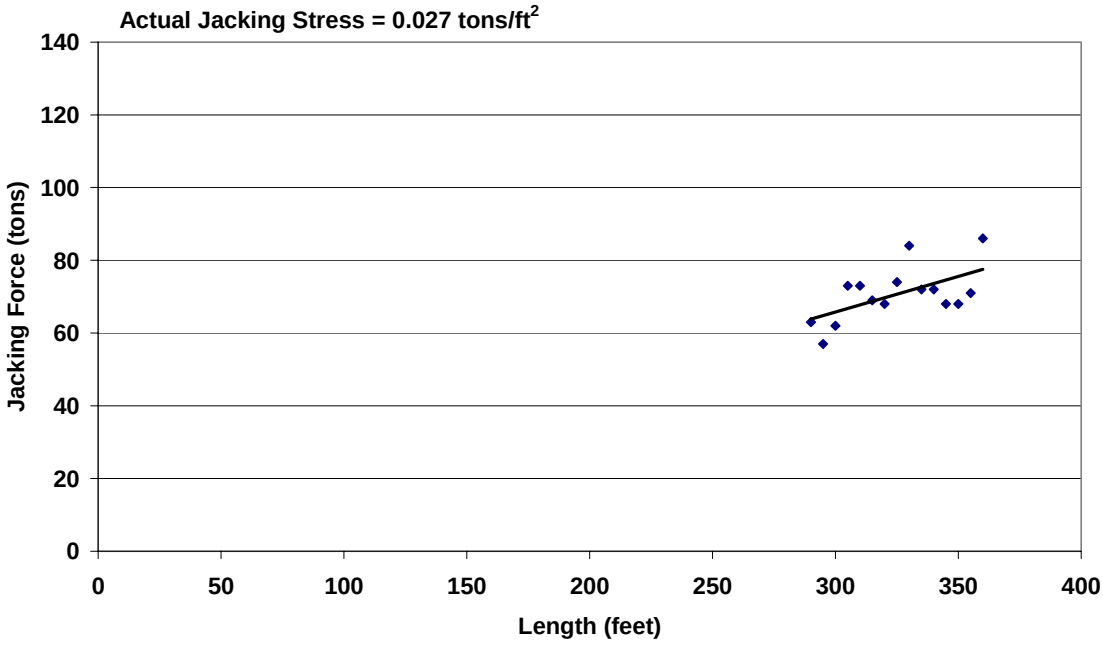

Figure 4.87. Length vs. Jacking Force for the Alvarado Boulevard Project Drive 17 from 290 to 360 feet.

4.10.7 Summary of Jacking Stresses for Isolated Tunneling Segments

Table 4.23. Jacking Stresses on Isolated Segments of the Microtunnel Drive 17 of the Alvarado Boulevard Trunk Project.

Segments Along Ttunnel Alignment [feet]	Jacking Stress [tons/ft^2]	Notes	R^2 Value
15-100	0.026	Non-Lubricated Segment	0.7352
100-180	0.12	Change in Soil Conditions	0.9507
290-360	0.027	Increase after Lubrication	0.3423

4.11 Newark Subbasin Lower Level Relief Sewer

The Newark Subbasin Lower Level Relief Sewer was constructed for the Union Sanitary District in Oakland, California. The project was located at the Central Newark Lift Station, at the base of the Dumbarton Bridge.

4.11.1 Description of the Project

The project included the construction of several microtunneling segments with 24-inch and 36-inch Hobas CCFRPM (Centrifugally Cast Glass-Fiber Reinforced Polymer Mortar) pipe. All microtunneling on the project was performed with an Iseki Unclemole microtunneling system as shown in Figure 4.88.

Figure 4.88. Iseki Microtunneling Machine used to Construct 36-inch Microtunnels on Newark Subbasin Project.

Microtunneling shafts were constructed from interlocking sheet piles. Concrete blocks were poured at the forward and back walls of the shafts. The concrete blocks at the forward walls were used to mount launch seals as shown in Figure 4.89. The concrete blocks poured at the back walls of the shafts were used for thrust walls to distribute the jacking forces into the soil behind the shaft wall as shown in Figure 4.90.

(a) (b)

Figure 4.89. (a) Concrete block at front wall of sheet pile shaft. (b) Launch Seal Mounted on Concrete Wall.

Figure 4.90. Jacking Frame against concrete Thrust Wall on Back Wall of Sheet Pile Jacking Shaft.

4.11.2 Geotechnical Conditions along the Alignment

The geotechnical conditions along the alignment were primarily sands, silts, and clays. Numerous vertical borings were drilled for the project and a geotechnical report was written and distributed for the designers and bidders. Figures 4.91 and 4.92 show borings B-11 and B-12 with the pipe elevations noted on the bore logs. Boring B-13 was drilled in the vicinity of the 24-inch diameter Hobas pipe installation. Figure 4.93 shows B-13 with the pipe elevation noted on the bore log.

4.11.3 Construction of Drive 3

Microtunnel Drive 3 was approximately 720 feet in length. The depth of cover over the crown of the pipeline ranged from 11 to 13 feet. Figure 4.94 shows a profile of the ground cover over the tunnel crown. Three borings were drilled for the drive and the soils in the zone of the pipeline were described as silty sand; silty, clayey sand; and medium dense sand.

Construction of Drive 3 began on February 19, 1995 and was completed on March 4, 1995. Table 4.24 provides the daily and cumulative production rates as well as any notes of significance recorded by the operator.

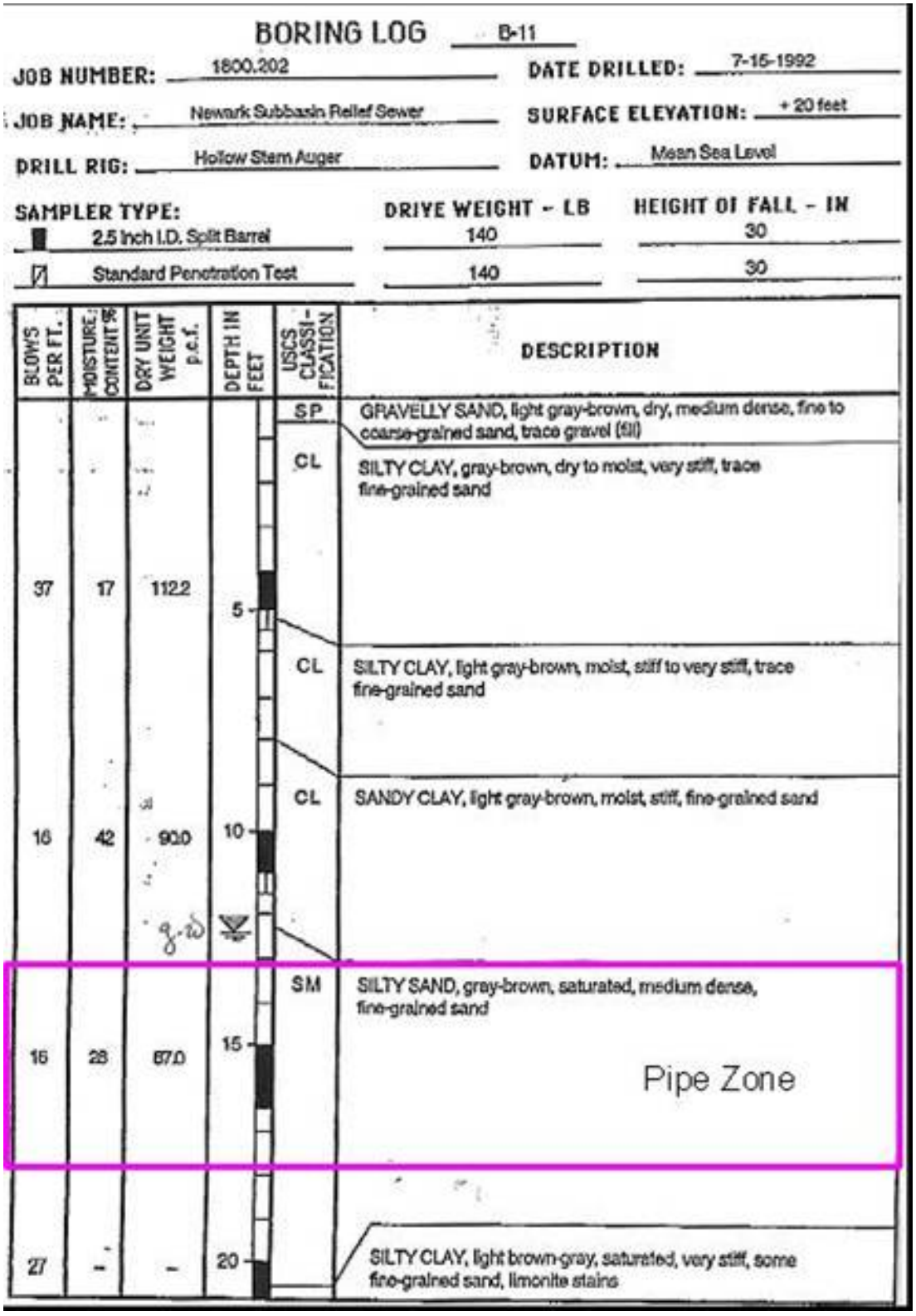

Figure 4.91 Boring B-11 Drilled for the Newark Subbasin Project (Brown and Caldwell, 1993).

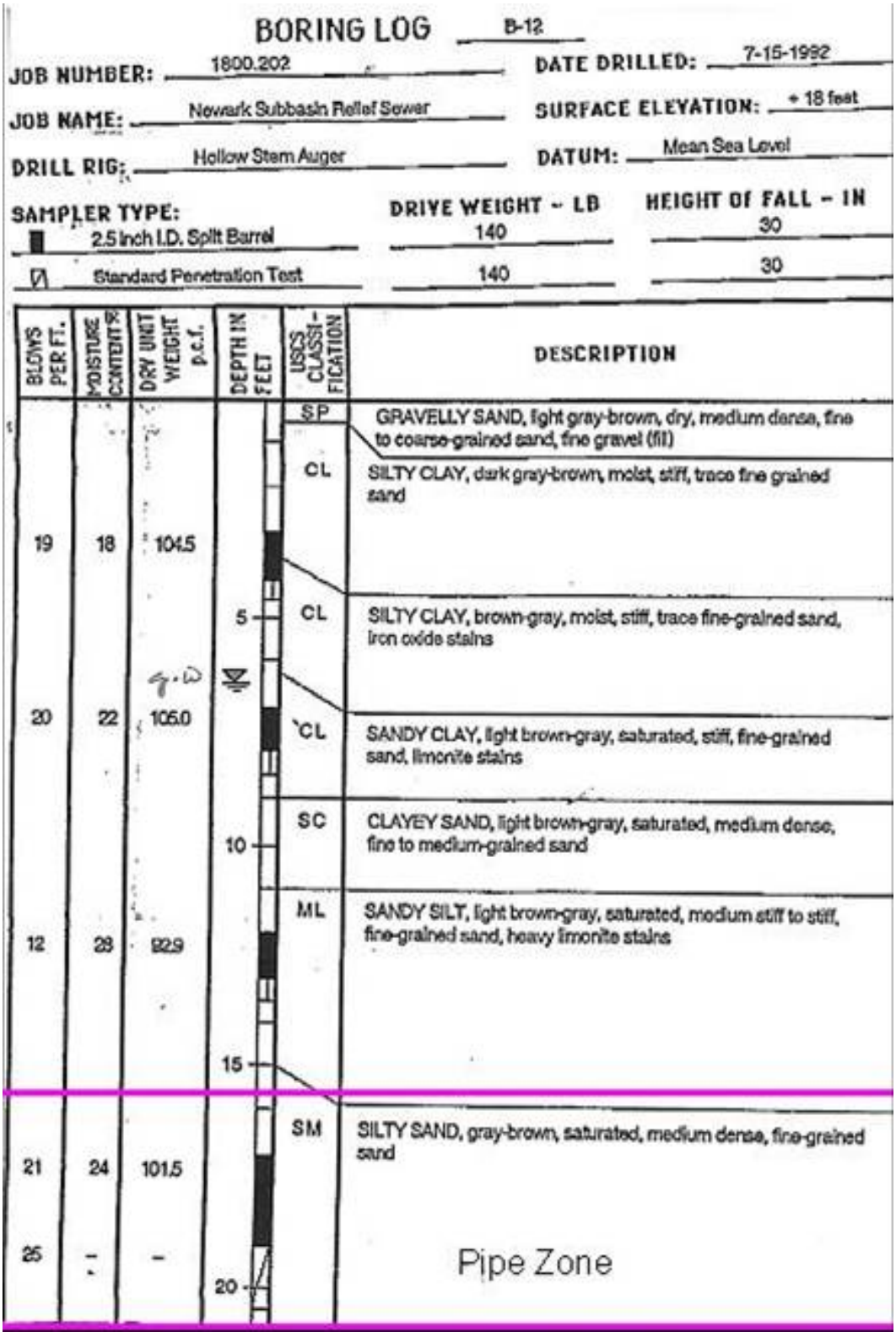

Figure 4.92 Boring B-12 Drilled for the Newark Subbasin Project (Brown and Caldwell, 1993).

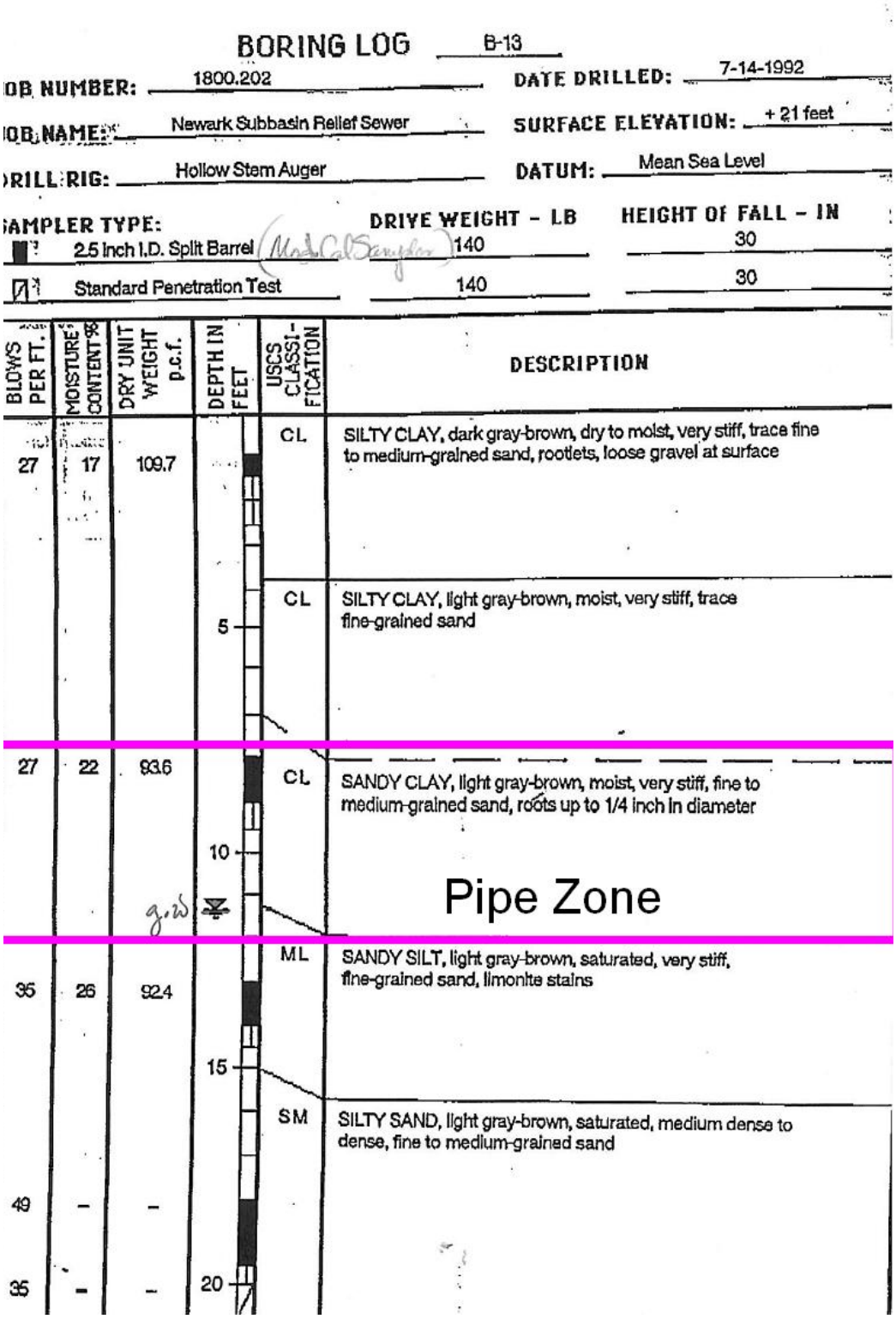

Figure 4.93. Boring B-13 in vicinity of 24-inch Hobas Microtunneling (Brown and Caldwell, 1993).

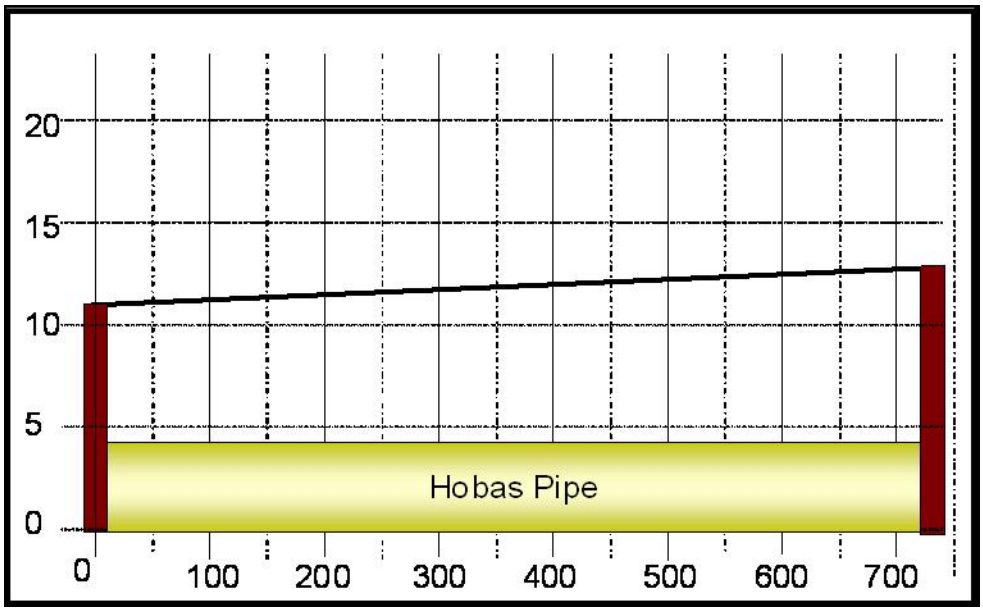

Figure 4.94. Profile of Newark Subbasin Drive 3.

Table 4.24. Daily and Cumulative Production Rates for Drive 3 of the Newark Subbasin 36-inch Diameter Microtunneling.

Date	Pipes Tunneled	Length [ft]	Cumulative Length [ft]	Notes
2/18/95	Machine	20	20	
2/22/95	Pipes 1, 2	20	40	
2/23/95	Pipes 3, 4	20	60	Clogged slurry lines. PVC coming through slurry. Dug out a piece of concrete from in front of machine.
2/24/95	Pipes 5, 6, 7, 8, 9, 10, 11, 12	80	140	Soil contained more sticky clay on pipe 9
2/25/95	Pipes 13, 14, 15, 16, 17, 18, 19, 20	80	220	
2/26/95	Pipes 22, 23, 24, 25, 26, 27, 28, 29, 30	90	310	
2/27/95	Pipes 31, 32, 33, 34, 35, 36, 37IJS	70	380	Installed IJS pipe number 37
2/28/95	Pipes IJS38, 39, 40	30	410	IJS took 4 hours
3/1/95	Pipes 41, 42, 43, 44, 45, 46, 47, 48	80	490	
3/2/95	Pipes 49, 50, 51, 52, 53, 54, 55, 56, 57, 58	100	590	
3/3/95	Pipes 59, 60, 61, 62, 63, 64, 65, 66, 67	90	680	
3/4/95	Pipes 68, 69, 70, 71, 72	50	730	Hit the reception pit on pipe 72

4.11.3.1 Jacking Forces on Drive 3

The frictional component of the Jacking Forces on Drive 3 ranged from 10 to 190 tons. Figure 4.95 shows the frictional component of the jacking forces along the drive. The frictional component was calculated by subtracting the measured earth pressure from the total jacking force, measured at the main jacking frame located in the jacking shaft.

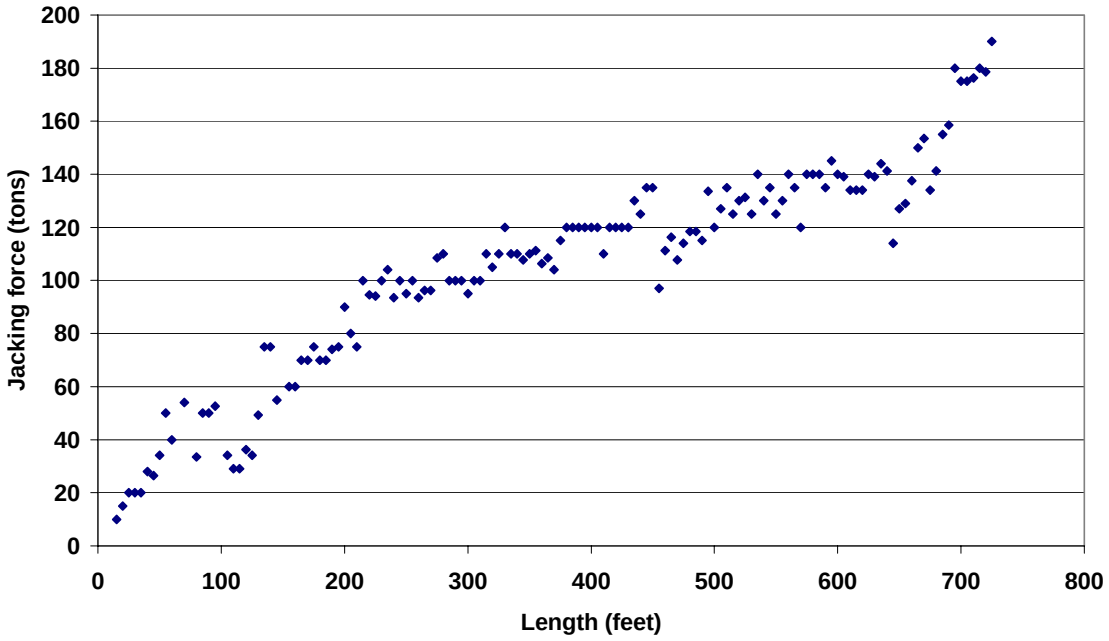

Figure 4.95. Length vs. Jacking Force for the Newark Subbasin Project Drive 3.

4.11.3.2 Lubrication During Tunneling

Small amounts of lubrication were pumped at approximately 100 feet into the alignment for approximately one pipe section of 8 feet. At approximately 275 feet into the tunnel drive, lubrication was pumped at the tail section of the machine until approximately 650 feet into the drive when lubrication was stopped.

4.11.3.3 Isolation of Jacking Force Segments of Drive 3 for Specific Analysis

The first segment of the tunnel drive for specific analysis is from the launch of the tunnel machine until approximately 100 feet into the drive. Along this segment no lubrication was applied to the tunnel and the jacking stress was 0.051 tons/ft^2. Figure 4.96 shows the frictional component of the jacking force from launch to 100 feet.

The next segment for specific analysis is from 110 to 240 feet. Over this section lubrication was not applied to the tunnel. These sections are analyzed separately because at 100 feet there was an event where the machine encountered a block of concrete that had to be excavated from the face. As a result, there is a small anomaly in the jacking record that caused these two sections to form in the jacking force graph. Figure 4.97 shows the jacking forces from 110 to 245 feet where the jacking stress is again 0.048 tons/ft^2.

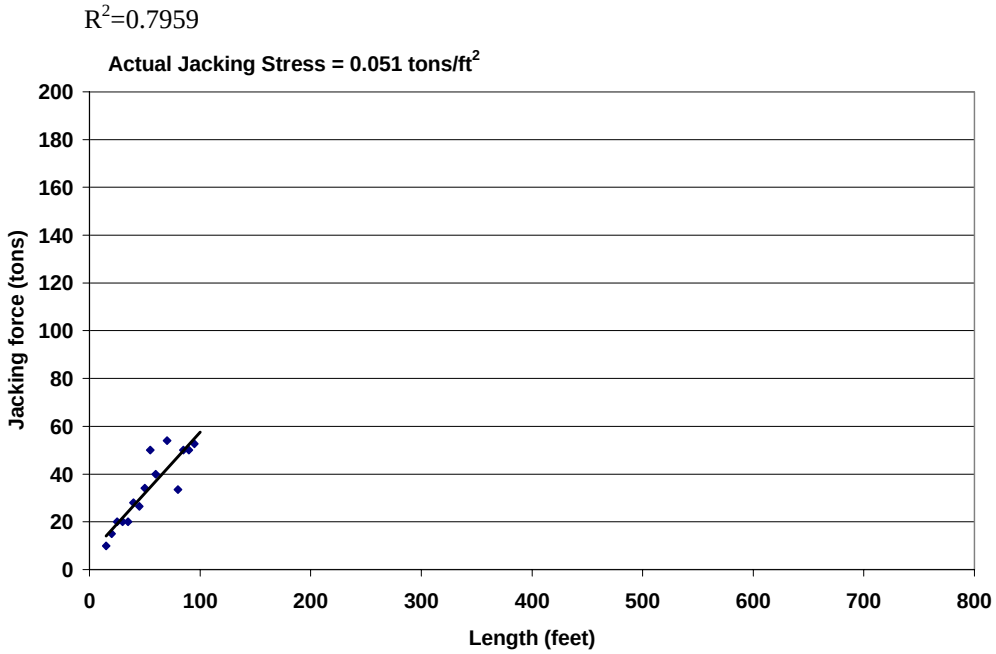

Figure 4.96. Length vs. Jacking Force for the Newark Subbasin Project Drive 3 from 15 to 100 feet.

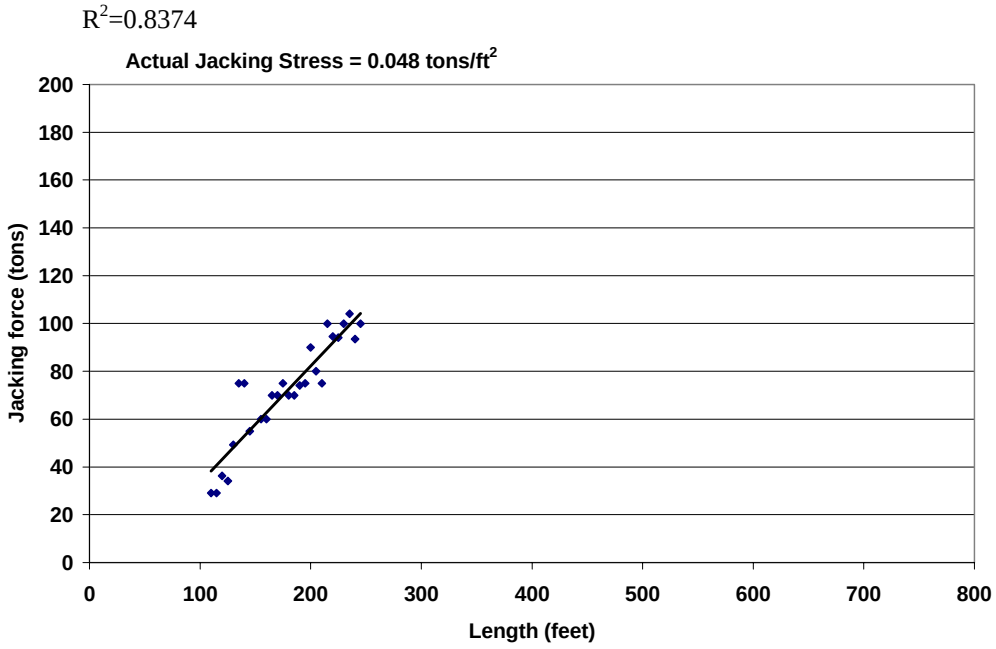

Figure 4.97. Length vs. Jacking Force for the Newark Subbasin Project Drive 3 from 110 to 295 feet.

The third segment for analysis is throughout the lubricated zone. This segment is from 245 feet to 635 feet into the drive. Figure 4.98 shows the frictional component of the jacking force through this section of the drive. The jacking stress through the segment is 0.011 tons/ft^2.

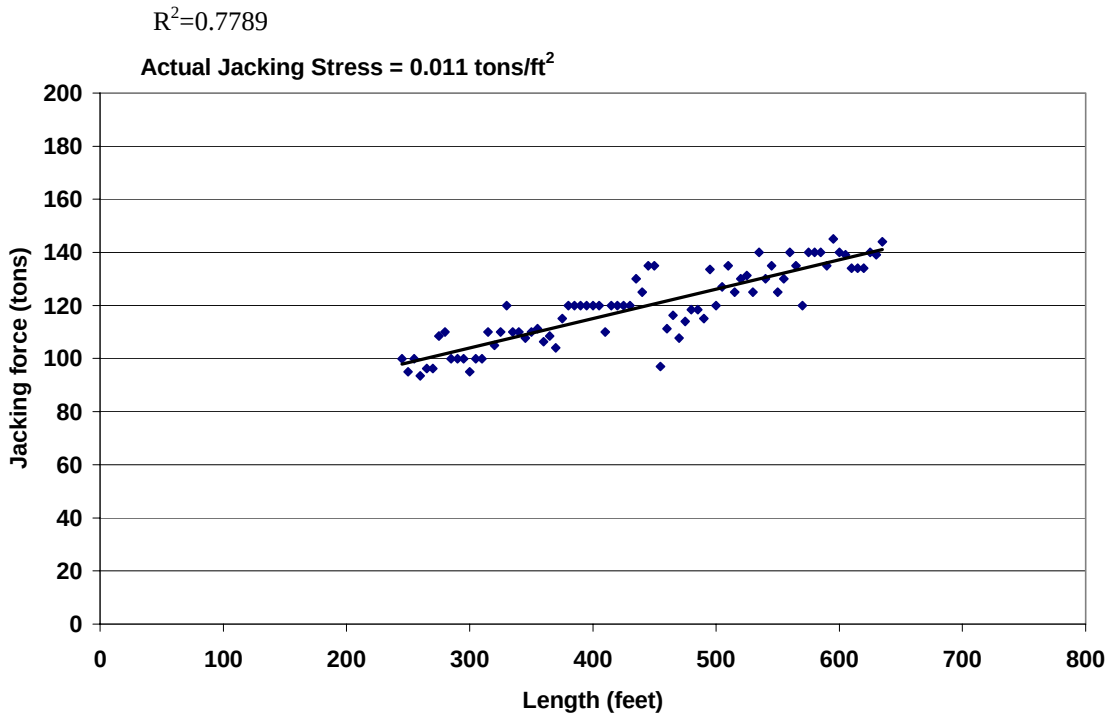

Figure 4.98. Length vs. Jacking Force for the Newark Subbasin Project Drive 3 from 245 to 635 feet.

4.11.4. Construction of Drive 6

Microtunnel Drive 6 was approximately 760 feet in length. Two borings were drilled for the design. Soils in the zone of the pipeline were described as medium to medium dense fine sand; and medium-dense fine to medium sand. Figure 4.99 shows an approximate profile representing the depth of soil cover over the pipeline.

Construction of the pipeline began on May 6, 1995 and was completed on May 16, 1995. Table 4.25 shows the daily and cumulative production on the tunnel and provides notes of significance as recorded by the operator.

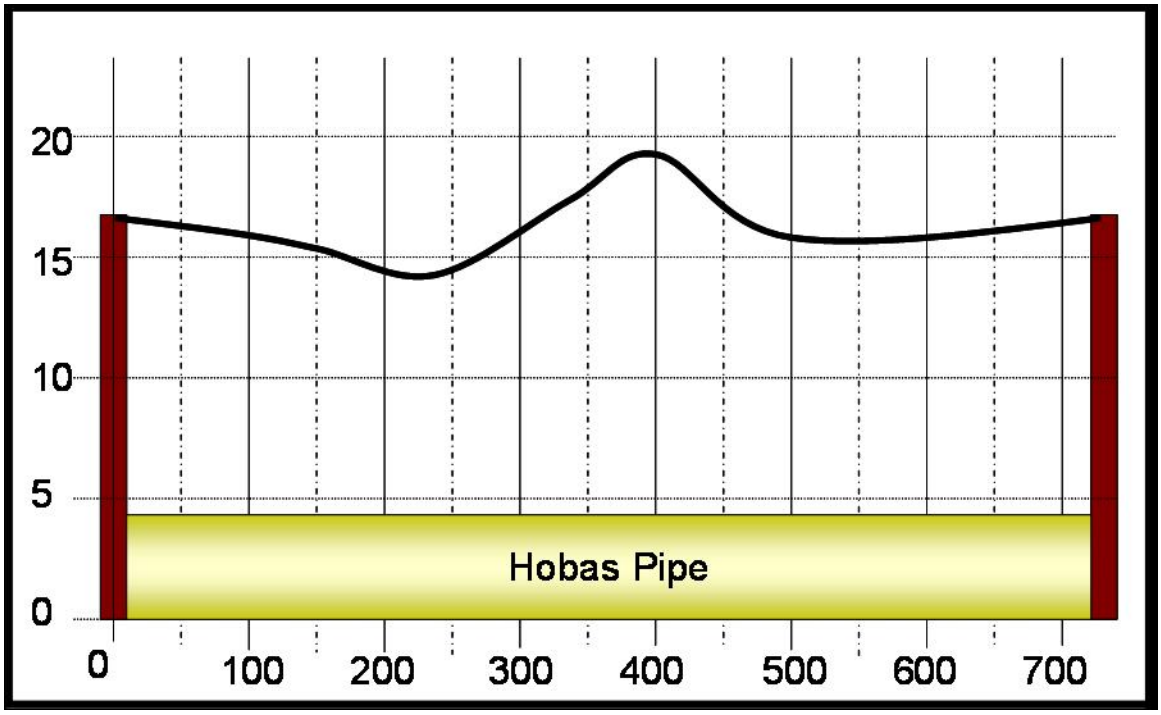

Figure 4.99. Profile of Newark Subbasin Drive 6.

Table 4.25. Daily and Cumulative Production Rates for Drive 6 of the Newark Subbasin 36-inch Diameter Microtunneling.

Date	Pipes Tunneled	Length [ft]	Cumulative Length [ft]	Notes
5/6/95	Machine, Pipe 1, 2	20+10 +10	40	Mixed clay and sand for pipe #2
5/8/95	Pipes 3, 4, 5, 6, 7, 8, 9, 10, 11, 12	100	140	Clay on pipe 4, Silty sand and clay on pipe 9.
5/9/95	Pipes 13, 14, 15, 16, 17, 18, 19, 20, 21, 22	100	240	Fine to coarse sand on Pipe 14. Clay on Pipe 16.
5/10/95	Pipes 23, 24, 25, 26, 27, 28, 29, 30, 31, 32, 33, 34	120	360	Fine dense sand on Pipe 29.
5/11/95	Pipes 35, 36, 37, 38, 39, 40, 41, 42, 43, 44, 45	110	470	Silt and Clay at Pipe 42.
5/12/95	Pipes 46, 47, 48, 49, 50, 51, 52, 53	80	550	Silty sand on pipe 53
5/13/95	Pipes 54, 55, 56, 57, 58, 59, 50, 61, 62	90	640	Coarse sand and Gravel on Pipe 61
5/14/95	Pipes 63, 64, 65, 66	40	680	
5/15/95	Pipes 67, 68, 69, 70, 71, 72	60	740	
5/16/95	Pipes 73, 74	18	758	Hit reception pit 8 feet into pipe #74

4.11.4.1 Jacking Forces on Drive 6

The frictional component of the jacking forces on Drive 6 ranged from 30 to 126 tons. Figure 4.100 shows the frictional component of the jacking forces over the entire drive length.

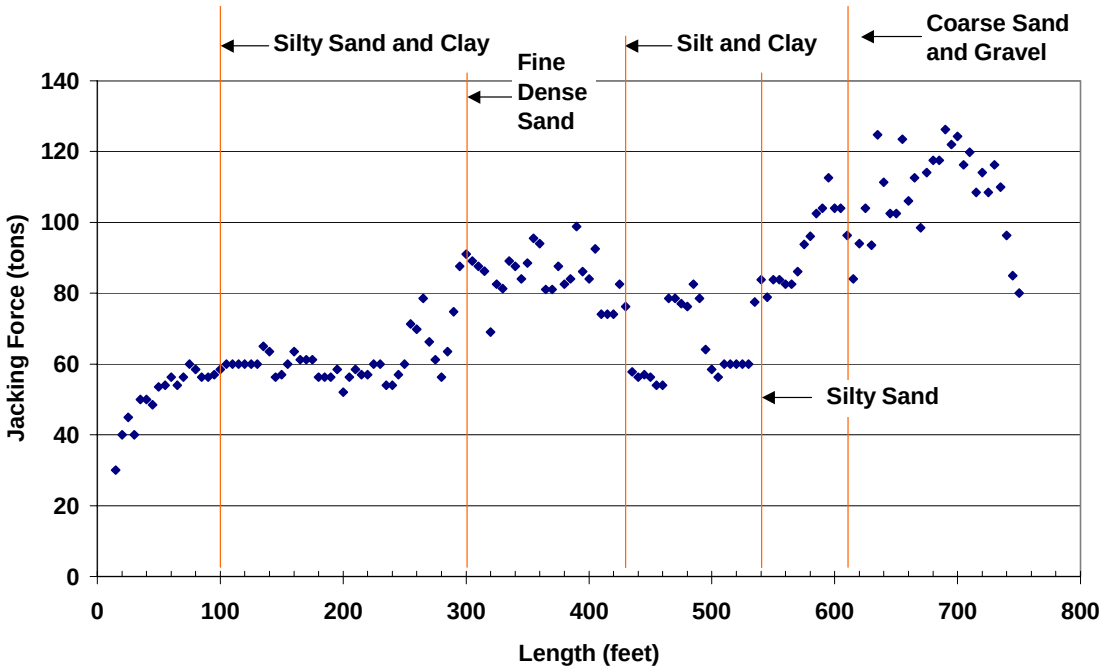

Figure 4.100. Length vs. Jacking Force for the Newark Subbasin Drive 6.

4.11.4.2. Lubrication on Drive 6

Lubrication was applied to the pipeline at approximately 100 feet into the drive and was applied at only one port at the tail shield of the machine. Due to the small diameter of the machine, ports along the pipeline were not connected. Throughout the entire tunnel drive, lubrication was pumped; however, the lubrication was only pumped from the single port at the tail of the tunneling machine approximately 20 feet from the face of the cutter.

4.11.4.3 Isolation of Jacking Force Segments of Drive 6 for Specific Analysis

The first segment for specific analysis is from the launch of the tunnel machine through 55 feet. Through this segment, the jacking stress was 0.51 tons/ft^2. Figure 4.101 shows the frictional component of the jacking force throughout this segment.

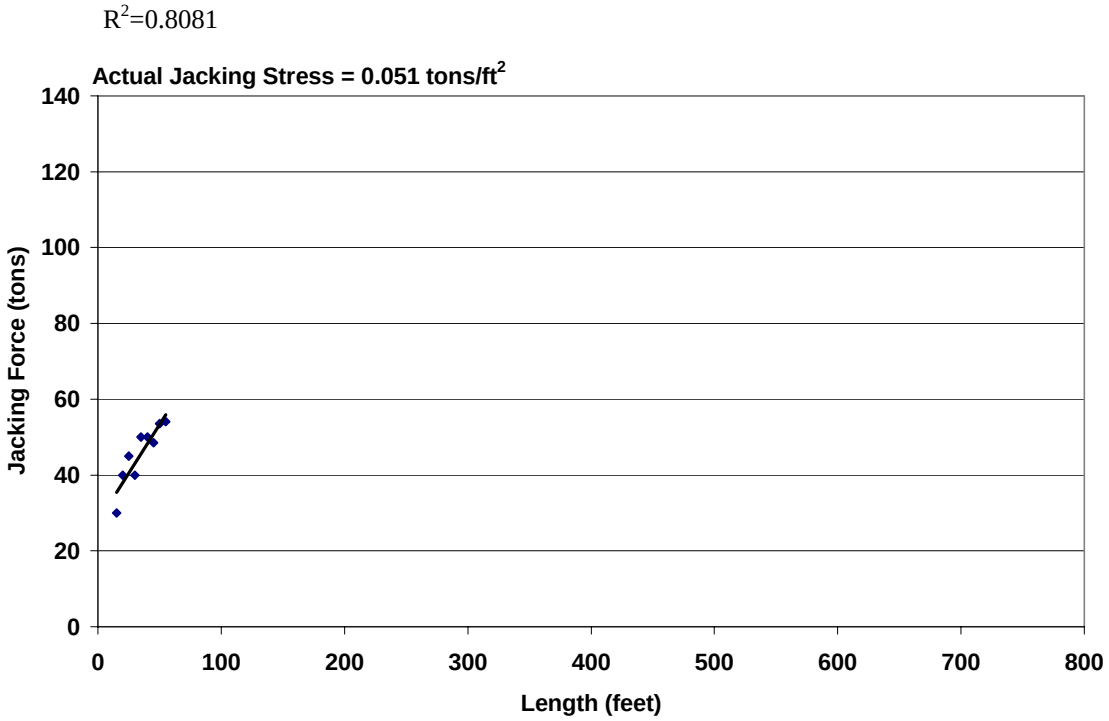

Figure 4.101. Length vs. Jacking Force for the Newark Subbasin Project Drive 6 from 15 to 55 feet.

From 240 to 390 feet there is the first increase in jacking force after the initial lubrication has been applied to the pipeline. Through this segment, the jacking force increases at a jacking stress of 0.021 tons/ft^2. Figure 4.102 shows the frictional component of the jacking force through this segment.

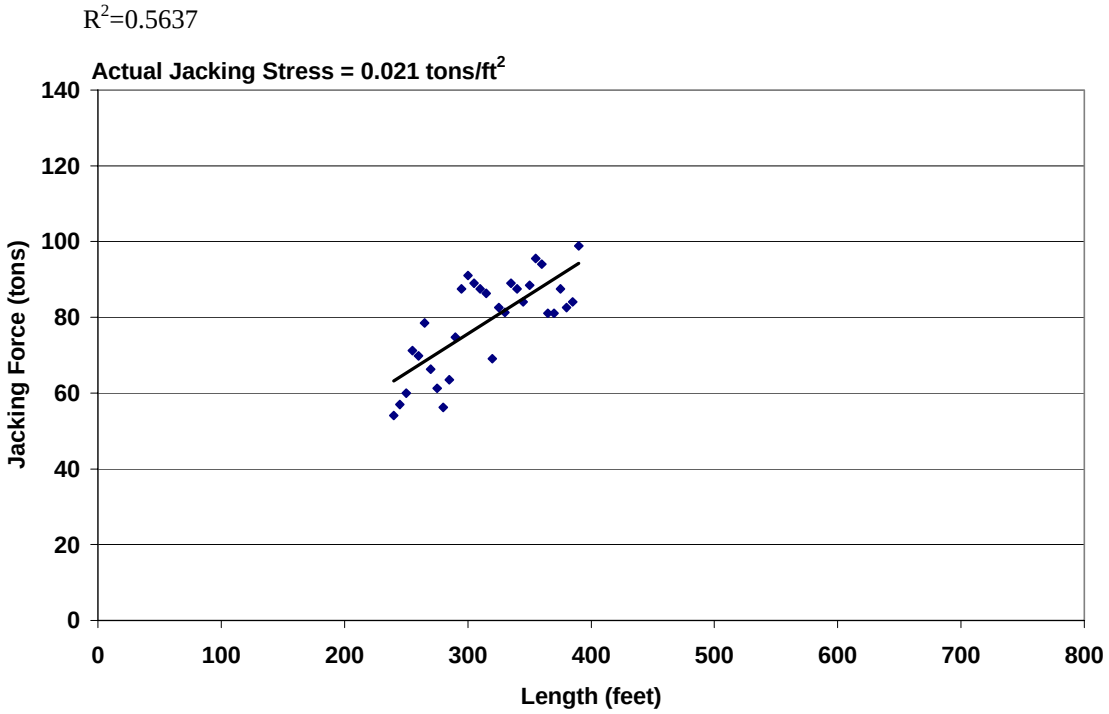

Figure 4.102. Length vs. Jacking Force for the Newark Subbasin Project Drive 6 from 240 to 390 feet.

The final segment for analysis is from 560 to 700 feet where the operator notes that the machine has entered silty sand and coarse sand with some gravel. In this zone, the jacking forces again begin to increase at a steady rate. Throughout this region the jacking stress is 0.023 tons/ft^2. Figure 4.103 shows the frictional component of the jacking forces in this segment.

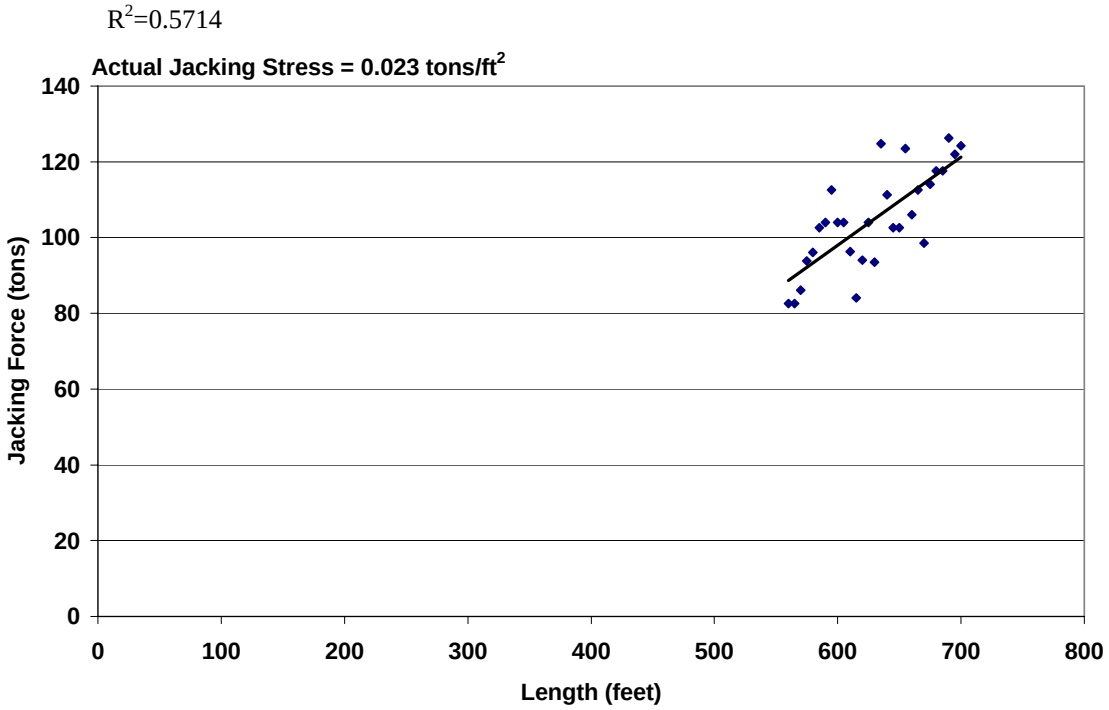

Figure 4.103. Length vs. Jacking Force for the Newark Subbasin Project Drive 6 from 560 to 700 feet.

4.11.5 Construction of Drive 12

Drive 12 was approximately 310 feet in length. One boring was drilled for Drive 12 and the soils in the pipe zone were described as medium dense silty sands. The depth of soil cover over the crown ranged from 15.5 to 16 feet. Figure 4.104 shows a profile of the pipeline.

The microtunnel pipeline was constructed between July 27, 1995 and August 1, 1995. Table 4.26 gives the daily and cumulative production for the tunnel construction and provides notes of significance as recorded by the microtunneling operator.

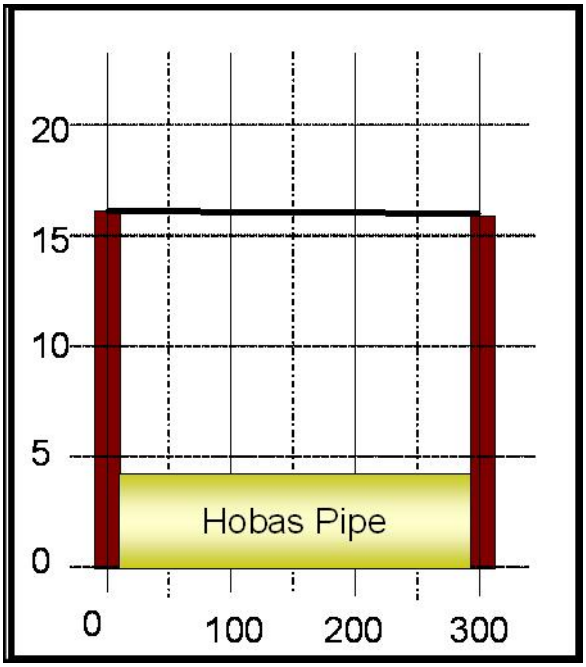

Figure 4.104. Profile of Newark Subbasin Drive 12.

Table 4.26. Daily and Cumulative Production Rates for Drive 12 of the Newark Subbasin 36-inch Diameter Microtunneling.

Date	Pipes Tunneled	Length [ft]	Cumulative Length [ft]	Notes
7/27/95	Machine, Pipe 1, 2, 3	20+30	50	
7/28/95	Pipes 4, 5, 6, 7, 8, 9, 10, 11	80	130	
7/31/95	Pipes 12, 13, 14, 15, 16, 17, 18, 19, 20, 21, 22, 23	120	250	Cleaned slurry tanks on pipe 20
8/1/95	Pipes 24, 25, 26, 27, 28, 29, 30	70	320	Hit exit pit while tunneling Pipe 30

4.11.5.1 Jacking Forces on Drive 12

The frictional component of the jacking forces on Drive 12 ranged from 40 to 90 tons. Figure 4.105 shows the frictional component of the jacking forces for the entire microtunnel drive.

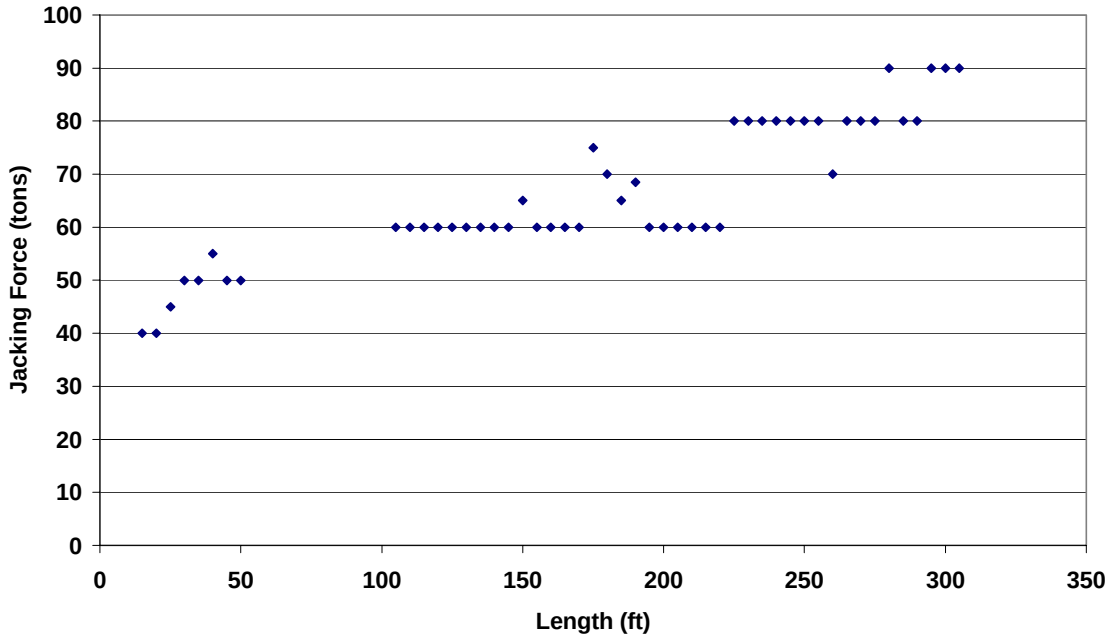

Figure 4.105. Length vs. Jacking Force for the Newark Subbasin Project Drive 12.

4.11.5.2 Lubrication during Drive 12

Lubrication was applied to the microtunnel at approximately 60 feet into the tunnel drive. Lubrication was applied at a single lubrication port located at the tail section of the machine. Lubrication was applied at this port from 60 feet until the termination of the drive at approximately 300 feet.

4.11.5.3 Isolation of Jacking Force Segments of Drive 12 for Specific Analysis

The first segment of the drive for analysis is from the launch to 50 feet. Through this segment, lubrication was not applied to the drive. The jacking stresses in this segment were 0.046 tons/ft^2. Figure 4.106 shows the frictional component of the jacking forces from launch of the machine through 50 feet.

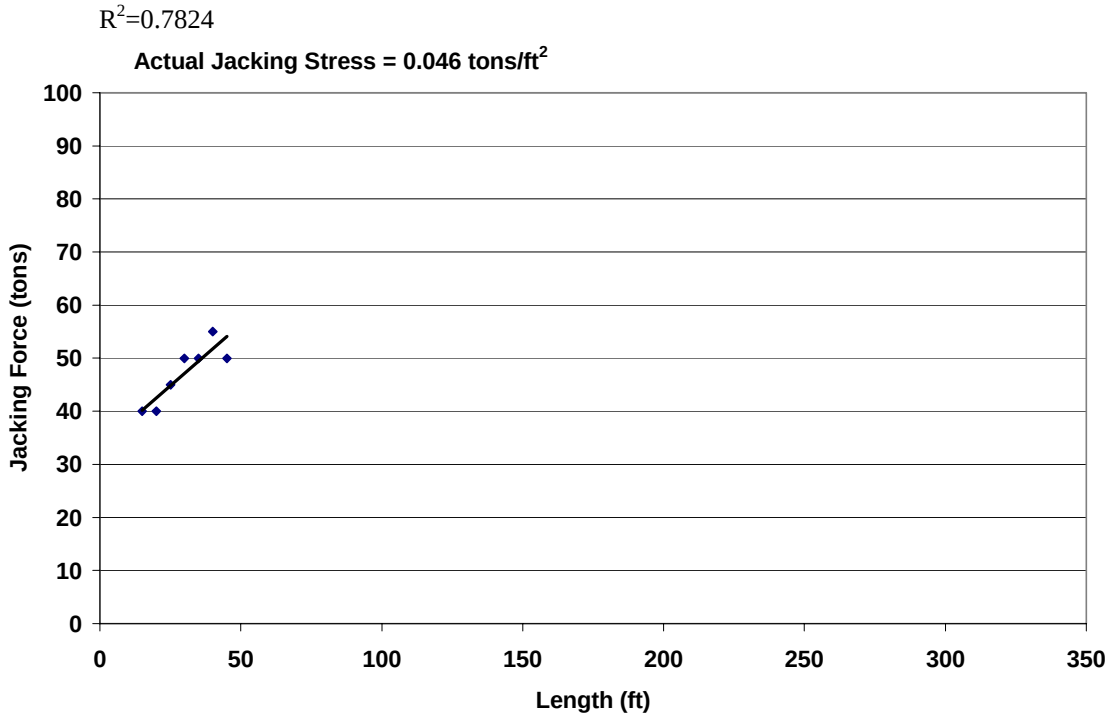

Figure 4.106. Length vs. Jacking Force for the Newark Subbasin Drive 12 from 10 to 50 feet.

The next segment is from 100 feet to the end of the drive at 300 feet. Throughout this segment lubrication was applied and the jacking stress was 0.016 tons/ft^2. Figure 4.107 shows the frictional component of the jacking forces from 100 to 300 feet.

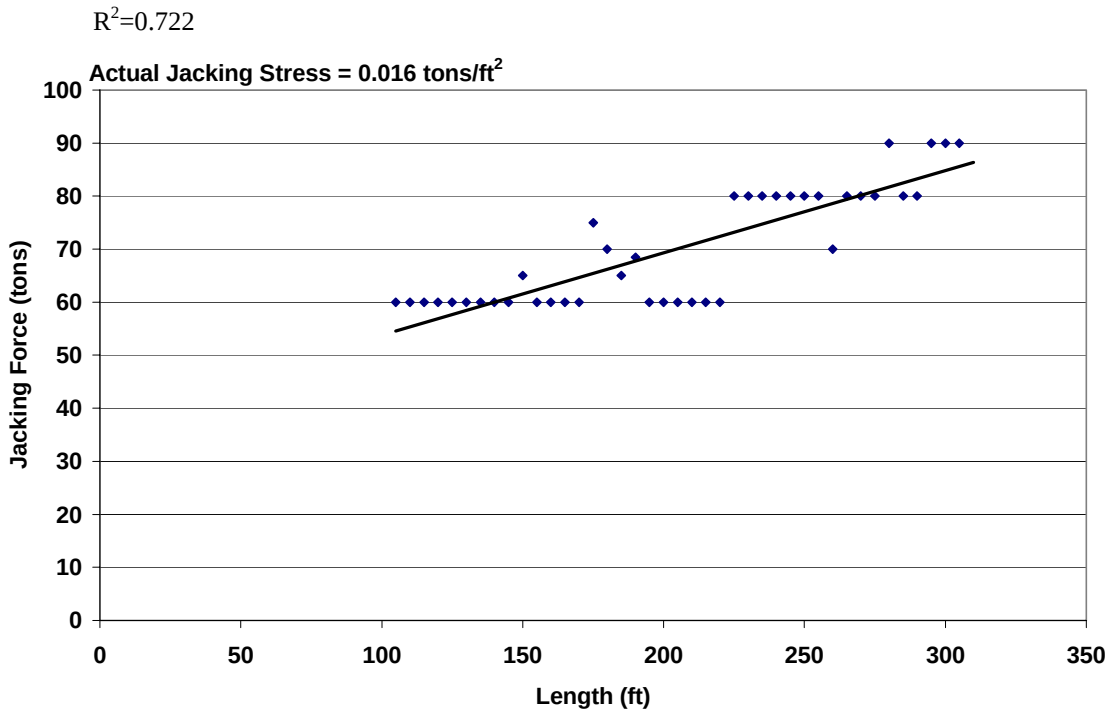

Figure 4.107. Length vs. Jacking Force for the Newark Subbasin Project Drive 12 from 100 to 300 feet.

4.11.6 Construction of Drive 1-24

Drive 1-24 was approximately 340 feet in length and was constructed with 24-inch nominal ID Hobas pipe that had a 25.8 inch outer diameter. The depth of soil cover over the crown of the pipeline was approximately 12 feet. One boring was completed for the design of the microtunnel and the soil in the pipe zone was described as clayey sand. The microtunnel pipeline was constructed between August 24, 1995 and August 30, 1995. Table 4.27 provides the daily and cumulative production rates for the microtunnel drive and any notes of significance provided by the operator.

Table 4.27. Daily and Cumulative Production Rates for Drive 1-24 of the Newark Subbasin 24-inch Diameter Microtunneling.

Date	Pipes Tunneled	Length [ft]	Cumulative Length [ft]	Notes
8/24/95	Machine, Pipe 1, 2, 3, 4	9+40	49	
8/25/95	Pipes 5, 6, 7, 8, 9, 10, 11	60	109	Soil consistently silty sand
8/28/95	Pipes 12, 13, 14, 15, 16, 17, 18, 19, 20, 21, 22, 23	120	229	Very silty sand
8/29/95	Pipes 24, 25, 26, 27, 28, 29, 30, 31, 32, 33, 34, 35	115	344	Reached the exit shaft during tunneling of pipe 35. Very silty sand

4.11.6.1 Jacking Forces on Drive 1-24

Jacking Forces on Drive 1-24 ranged from 9 to 28 tons. Figure 4.108 shows the frictional component of the jacking forces throughout the entire drive.

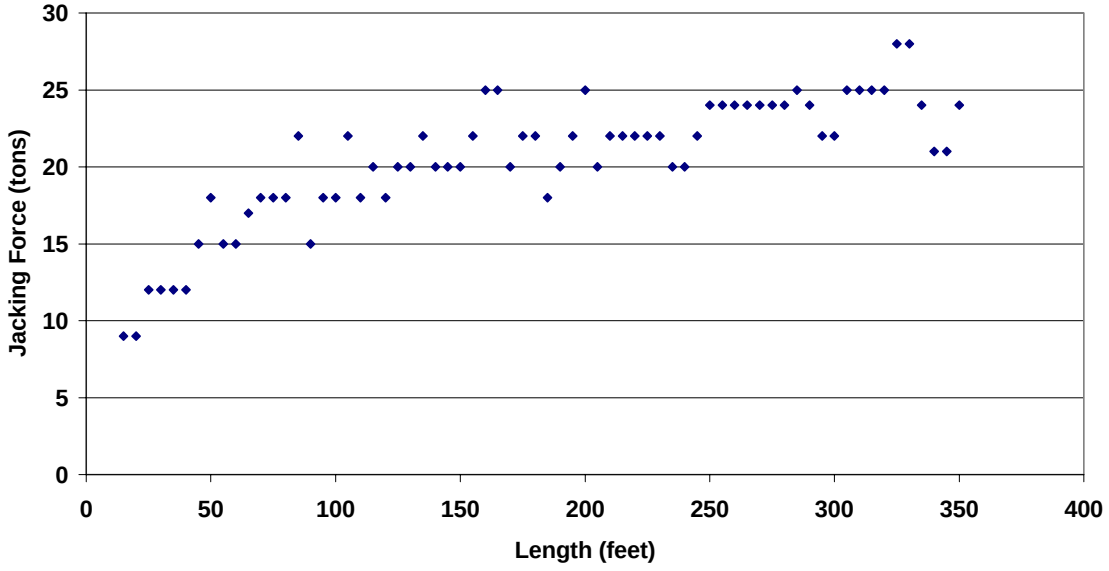

Figure 4.108. Length vs. Jacking Force on the Newark Subbasin Project Drive 1-24.

4.11.6.2 Lubrication along Drive 1-24

Lubrication was applied to the pipeline at approximately 50 feet into the tunnel through a single port in the tail section of the machine, located approximately eight (8) feet behind the face of the microtunneling machine. Due to the small diameter of the machine, no lubrication ports were located along the pipeline. Lubrication was applied from 50 feet into the tunnel drive to the termination of the tunnel.

4.11.6.3 Isolation of Jacking Force Segments of Drive 1-24 for Specific Analysis

The first segment of the tunnel for analysis is from launch to 50 feet. In this zone, no lubrication was applied to the pipeline and the jacking stress was 0.033 tons/ft^2. Figure 4.109 shows the frictional component of the jacking force from launch to 50 feet.

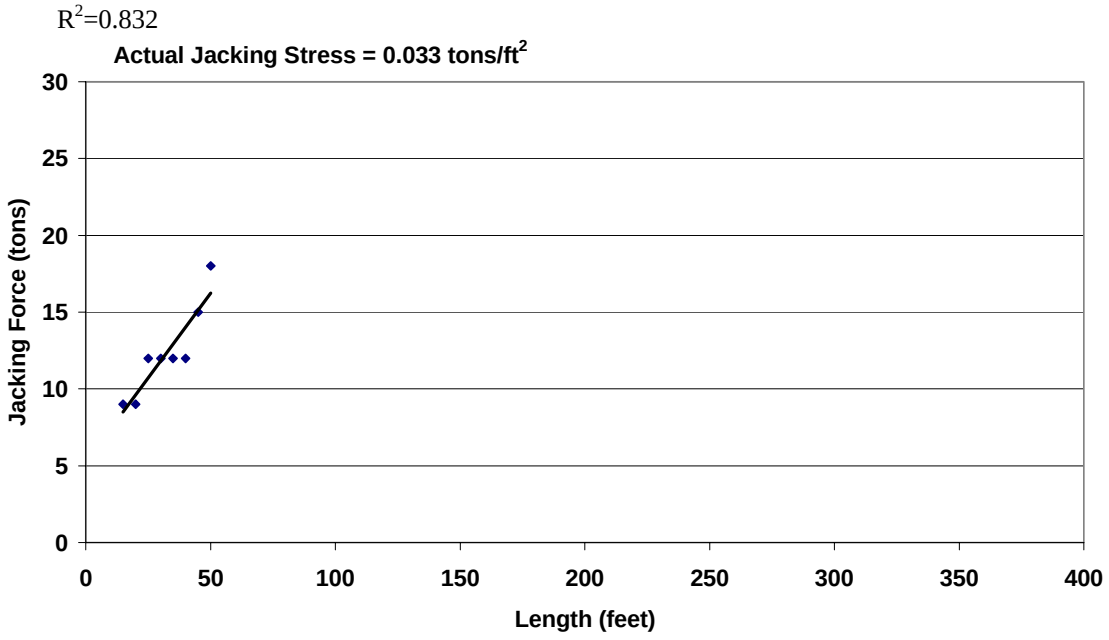

Figure 4.109. Length vs. Jacking Force for the Newark Subbasin Project Drive 1-24 from 15 to 50 feet.

The next segment for analysis is from 65 feet until 320 feet of the tunnel. Throughout this zone the jacking forces are increasing under the effects of lubrication at the tail section of the machine. The jacking stress in this segment is 0.004 tons/ft^2. Figure 4.110 shows the frictional component of the jacking force through this segment.

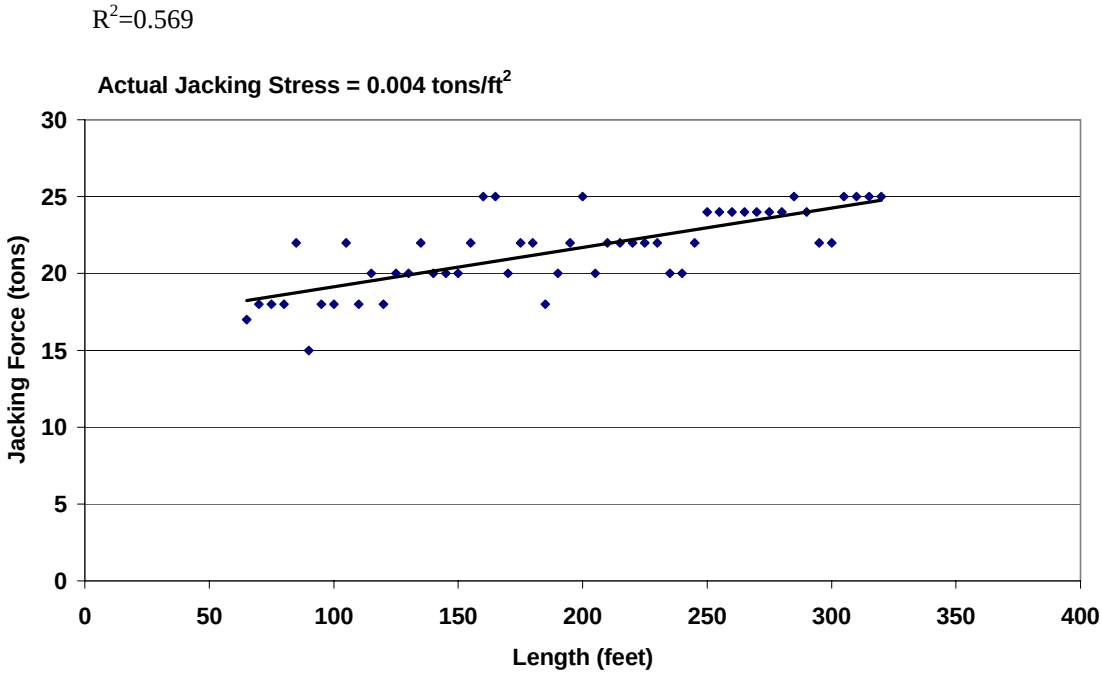

Figure 4.110. Length vs. Jacking Force for the Newark Subbasin Project Drive 1-24 from 65 to 320 feet.

4.11.7 Summary of Jacking Stresses along Isolated Tunneling Segments

Table 4.28 summarizes jacking stresses over all of the isolated segments for specific analysis on the microtunnel drives of the Newark Subbasin Lower Level Relief Sewer Project.

Table 4.28. Jacking Stresses on Isolated Segments of Tunnel Drives on the Newark Subbasin Project.

Drive	Segment Along Tunnel [ft]	Jacking Stress [tons/ft^2]	R^2 Value [-]	Notes
Drive 3	15-100	0.051	0.7959	No Lubrication
Drive 3	100-240	0.051	0.8278	Parallel segment – no lubrication
Drive 3	240-635	0.011	0.7869	Lubricated
Drive 6	15-55	0.051	0.8081	No Lubrication
Drive 6	240-390	0.021	0.5637	Lubricated
Drive 6	560-700	0.023	0.5714	Lubricated
Drive 12	15-50	0.046	0.7824	No Lubrication
Drive 12	100-300	0.016	0.722	Lubricated
Drive1-24	15-50	0.033	0.832	No Lubrication
Drive 1-24	65-320	0.004	0.5685	Lubricated

4.12 Summary

Project details of thirteen microtunnels and one open-shield pipe jacking projects were presented in this chapter. Jacking force records were presented and jacking stresses for segments of tunneling drives were compared. Jacking force records were separated into lubricated and unlubricated segments for further analysis. The frictional component of the jacking force in the unlubricated sections of each tunnel segment can now be compared to the interface frictional values that were measured in the laboratory to develop correlations between field and laboratory data.

CHAPTER 5

ANALYSIS OF JACKING FORCES IN UNLUBRICATED CONDITIONS

Details of interface shear tests between soils and jacking pipes were presented in Chapter 3. Results of these tests showed that pipe surface roughness had an effect on the interface friction coefficient between the pipe material and soil. Chapter 4 presented a number of case histories that contained portions of the microtunnel drive that had unlubricated segments. Within these unlubricated segments, the soil shearing against the jacking pipe was analogous to the laboratory tests. In this chapter, interface friction coefficients will be developed for granular soils with a range of residual friction angles. A model for predicting the normal stresses based on Terzaghi's arching theory will be presented and a jacking force predictive model will be developed. The actual jacking forces from field projects will be compared with predicted jacking forces generated from the model using the interface friction values measured in the laboratory.

5.1 Development of Interface Friction Values for a Broad Range of Granular Soils

The interface friction coefficient between Ottawa 20/30 sand and Atlanta Blasting sand at a normal stress of 80 kPa was determined for each pipe material, as detailed in Chapter 3. Table 5.1 summarizes the residual interface friction coefficients between these two sands and each pipe material at 80 kPa.

Table 5.1 Pipe-Soil Interface Friction Coefficients for Ottawa 20/30 Sand and Atlanta Blasting Sand

Ottawa 20/30			**Atlanta Blasting Sand**	
Peak Friction Angle	38.9°		Peak Friction Angle	43.1°
Residual Friction Angle	27.9°		Residual Friction Angle	34.6°
Pipe Material	Residual Interface Friction Coefficient		Pipe Material	Residual Interface Friction Coefficient
Hobas	0.43		Hobas	0.56
Polycrete	0.43		Polycrete	0.49
Permalok Steel	0.44		Permalok Steel	0.58
Wet Cast Concrete	0.48		Wet Cast Concrete	0.59
Vitrified Clay	0.48		Vitrified Clay	0.61
Packerhead Concrete	0.53		Packerhead Concrete	0.62

Interface friction values were then interpolated between and extrapolated from the residual friction angles of the Ottawa 20/30 (27.9 degrees) and Atlanta Blasting sand (34.6 degrees) to develop a full range of interface friction values for each pipe material and residual friction angles of a variety of granular soils with residual friction angles ranging from 25 to 40 degrees. The resulting values for pipe-residual soil interface friction are shown in Table 5.2

These values can be used to determine the interface friction coefficient between different types of jacking pipe and site soils if the residual friction angle of the soil at the site is known from laboratory testing or can be estimated.

Table 5.2 Pipe-Soil Interface Friction Coefficients for Residual Soil Friction Angles from 25 to 40 degrees on All Pipe Materials

Soil at Interface	**Interface Friction Coefficient between Soil and Pipe**					
Residual Friction Angles	**Hobas**	**Polycrete**	**Permalok Steel**	**Wet Cast Concrete**	**Vitrified Clay pipe**	**Packerhead Concrete**
25	0.37	0.40	0.38	0.43	0.42	0.49
26	0.39	0.41	0.40	0.45	0.44	0.50
27	0.41	0.42	0.42	0.47	0.46	0.52
27.9 **Ottawa 20/30**	**0.43**	**0.43**	**0.44**	**0.48**	**0.48**	**0.53**
28	0.43	0.43	0.44	0.48	0.48	0.53
29	0.45	0.44	0.46	0.50	0.50	0.55
30	0.47	0.45	0.48	0.51	0.52	0.56
31	0.49	0.46	0.51	0.53	0.54	0.57
32	0.51	0.47	0.53	0.55	0.56	0.59
33	0.53	0.48	0.55	0.56	0.58	0.60
34	0.55	0.49	0.57	0.58	0.60	0.61
34.6 **Atlanta Blasting**	**0.56**	**0.49**	**0.58**	**0.59**	**0.61**	**0.62**
35	0.57	0.49	0.59	0.60	0.62	0.63
36	0.59	0.50	0.61	0.61	0.64	0.64
37	0.61	0.51	0.63	0.63	0.66	0.65
38	0.62	0.52	0.65	0.65	0.68	0.67
39	0.64	0.53	0.67	0.66	0.70	0.68
40	0.66	0.54	0.69	0.68	0.72	0.69

5.2 Calculation of Normal Stresses

A total of thirteen (13) case histories were chosen with unlubricated segments that were suitable for comparison with laboratory data. These case histories included Hobas, Polycrete, Permalok Steel, Wet Cast Concrete, and Packerhead Concrete ranging in diameter from 25.8 to 87.5 inches. Using the values for the interface friction coefficient in Table 5.2, based on pipe material and residual soil friction angle of the soil at the project site, the estimated normal stress was calculated for each project. The results of this calculation are shown in Table 5.3, showing that the estimated normal stress was relatively low, ranging from 118 psf to 399 psf. In addition, the estimated normal stresses indicated that the normal stresses were independent of depth, as suggested by

Terzaghi (1943) as the depths of the projects in Table 5.3 ranged from 8 to 85 feet with no correlation between depth and normal stress.

Table 5.3. Projects Showing Parameters Used to Estimated Actual Normal Stresses on the Pipeline Based on Laboratory Values for Interface Friction

Project	**Pipe**	**Pipe Diameter [in]**	**Est. ϕ_r [°]**	**Est. γ_{total} [pcf]**	**μ_{int} [-]**	**Actual Jacking Stress [tsf]**	**Estimated σ_n [psf]**
Newark - 3	Hobas	38.3	26	126	0.39	0.051	260
Newark- 6	Hobas	38.3	26	126	0.39	0.051	260
Newark- 12	Hobas	38.3	26	126	0.39	0.046	229
Newark Drive 1-24	Hobas	25.8	26	126	0.39	0.033	186
Alvarado JP3-RP4	Polycrete	46.6	31	131	0.46	0.045	197
Alvarado JP4-RP4	Polycrete	46.6	30	129	0.45	0.051	227
Alvarado Drive 17	Polycrete	25.9	29	126	0.44	0.026	118
Clearview 2001	Permalok	60	35	135	0.59	0.074	252
Sacramento North	Permalok	72	27	108	0.42	0.070	333
Sacramento South	Permalok	72	27	108	0.42	0.084	399
Highway 50 Crossing	Wet Cast Concrete	59.5	35	140	0.60	0.074	248
ESI Morris Ave	Packer-head Concrete	87.5	32	110	0.58	0.090	308
ESI Houser Way	Packer-head Concrete	87.5	32	110	0.58	0.084	288

Evaluation of the normal stresses indicated that predictive models previously proposed by Auld (1982), ATV A161 (Stein, 1989) Scherle (1977), and Körner, as outlined in Chapter 2, dramatically over-predict normal stresses acting on the pipeline.

Development of a model for calculating the normal stress above the pipeline focused on the redistribution of stresses around the pipeline as the microtunneling machine excavates through the soil. It is important to recognize that the microtunneling

process involves excavating with a pressurized slurry and is cutting a hole with a cutter wheel that is slightly larger in diameter than the machine, typically on the order of three quarters (0.75) to one (1.0) inch larger. As a result, granular soil above the pipeline is allowed to move toward the machine and the pipeline, allowing redistribution of the stresses around the machine.

In large diameter tunneling with a slurry shield, the cavity contraction model has been used to model the behavior of the soil at the face and above the machine during excavation to estimate surface settlements above the tunnel (Atkinson and Potts, 1977; Jacobsz, 2004). The cavity collapse model is also applicable to microtunneling because excavation takes place with a slurry shield. All of the microtunneling case histories listed in Table 5.3 were constructed below the water table. In every case, the jacking records reveal that the pressure within the slurry chamber was maintained below that of the groundwater pressure, indicating that when excavation would begin there was, in fact, an area of lower pressure toward the machine, lending credence to the use of a cavity collapse model. In addition, the low pressure within the tunnel shield would cause granular soils in the immediate vicinity of the machine to drain.

Centrifuge modeling performed by Jacobsz et al (2004) on granular soils above a tunnel, as outlined in Chapter 2, found that the failure envelope agreed well with that defined by Atkinson and Potts (1977) based on the cavity collapse model. Atkinson and Potts related this area to the dilation angle of the soil, as shown in Figure 2.11. However, due to the fact that the soil is collapsing onto the pipeline, it appeared that the soil that would likely remain intact above the pipeline would be above the shear plane of failure.

According to the Mohr-Coulomb failure criteria, shear strength on the failure plane (as seen in Figure 5.1) is defined as

$$\tau_f = \sigma_n \tan\phi + c \tag{5.1}$$

where σ_n = normal stress

ϕ, c = shear strength parameters of soil (where ϕ and c in the above equations are drained strengths for long-term analysis and undrained (ϕ = o and c = Su) for short-term analysis of cohesive materials)

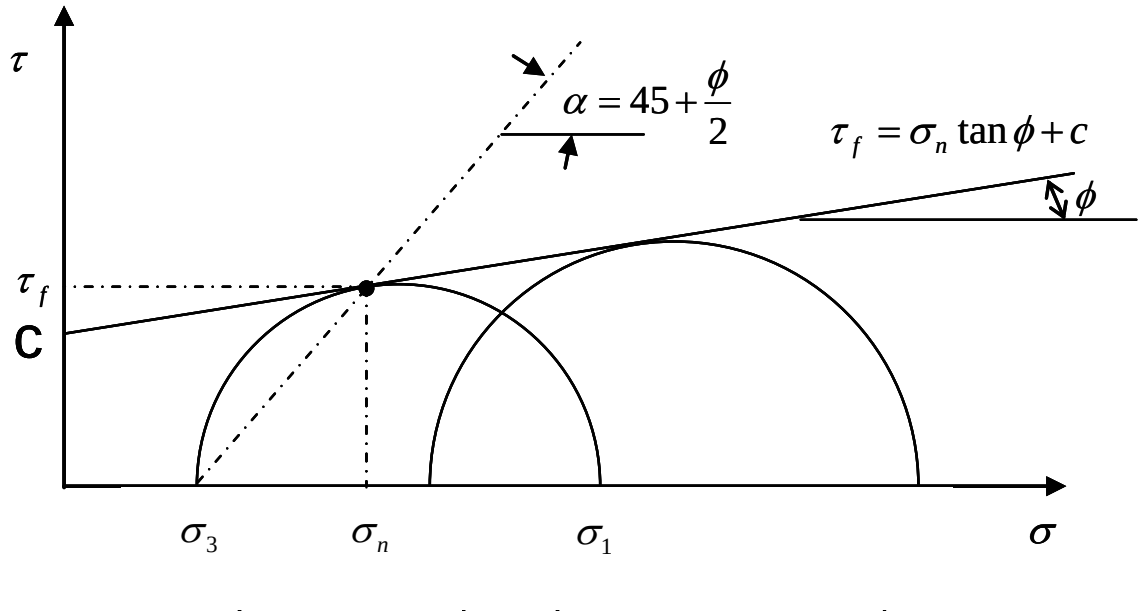

Figure 5.1 Mohr-Coulomb Failure Criterion (from EM1110-2-2502)

The failure plane is inclined at $45 + \frac{\phi}{2}$ degrees from the plane of the major principal stress. For limit-equilibrium analyses to be valid, the assumed slip surface must be inclined at this angle relative to the principal stresses. Discontinuities in the soil, surcharges, and wall friction all cause variation in the principal stress directions and induce curvature in the slip surfaces. (EM 1110-2-2502).

The failure planes, as presented in the Mohr-Coulomb failure criterion, inclined at an angle $45+\frac{\phi}{2}$ present an interesting comparison when one considers the shape of a localized over-excavation over the crown of a tunneling machine. When over-excavation occurs at the face of a tunneling or pipe jacking operation in granular soils, the shape of the void that develops over the tunnel crown manifests as shown in Figure 5.2. The shape of the void presents with the failure planes inclined at a slope normal to the principal stresses and variations in the materials induce the curvature in the slip surfaces, as presented in the Mohr-Coulomb theory.

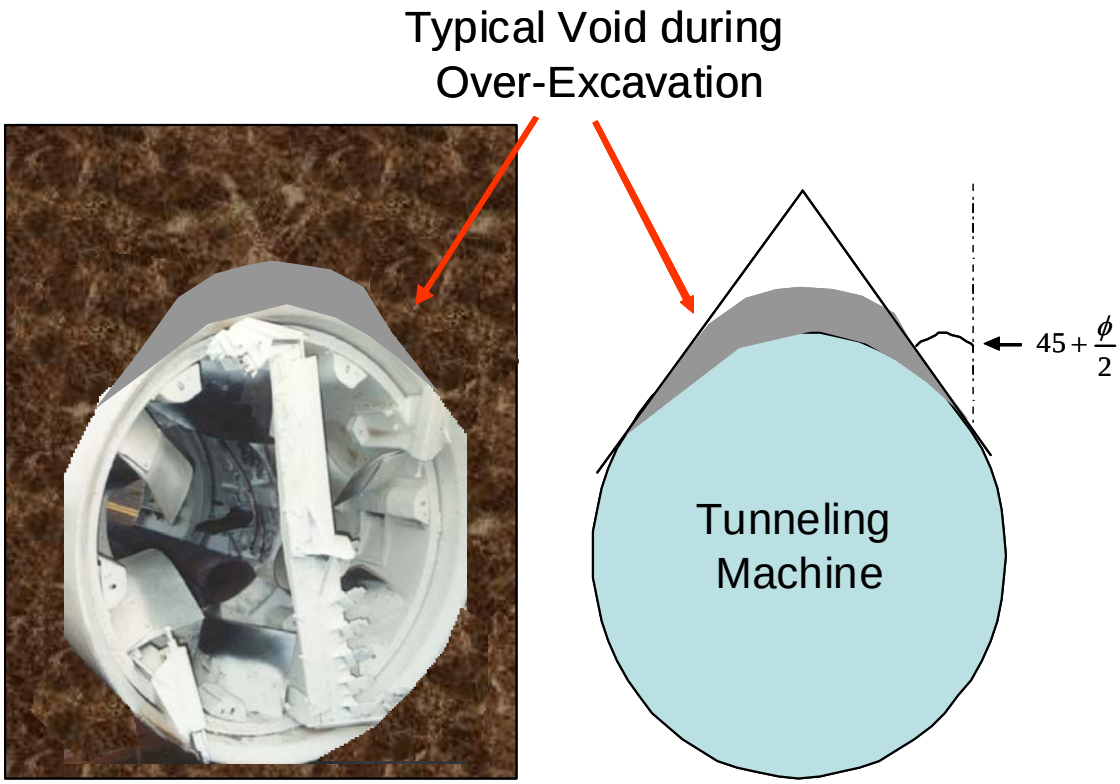

Figure 5.2. Typical Void Development over Tunneling Machine with Over-Excavation

When considering this in conjunction with Terzaghi's Arching Theory, there is reason to reconsider some of the previous interpretations on how Terzaghi's soil arching

experiments, which were conducted on a flat trap door, have been applied to a rounded pipe surface (by Auld, Scherle, ATV A 161, etc).

The creation of the overcut also induces a state analogous to the trap door simulations conducted by Terzaghi. When the gage cutters on the tunneling machine remove the soil at the crown, for example, it induces a state of stress analogous to when the trap door was displaced vertically, inducing arching in the overlying soils. Terzaghi found that for a cohesionless soil, the vertical stress was independent of depth, and presented the following equation, as detailed in Chapter 2:

$$\sigma_v = \sigma_{v\infty} = \frac{\gamma B}{K \tan \phi} \tag{5.2}$$

Terzaghi found K=1 for soils above the yielding trap door, analogous to the soils in the zone above the pipe where the material is moving into the space cleared by the gage cutters; into the overcut.

Based on the observations of the shear planes of failure above the pipeline during over excavations and Morh-Coulomb failure criteria, Figure 5.3 is proposed as the interpretation of the area over the pipeline over which the vertical loading is developed. From Figure 5.3, the factor B* is developed and replaces B in Terzaghi's equation 5.2.

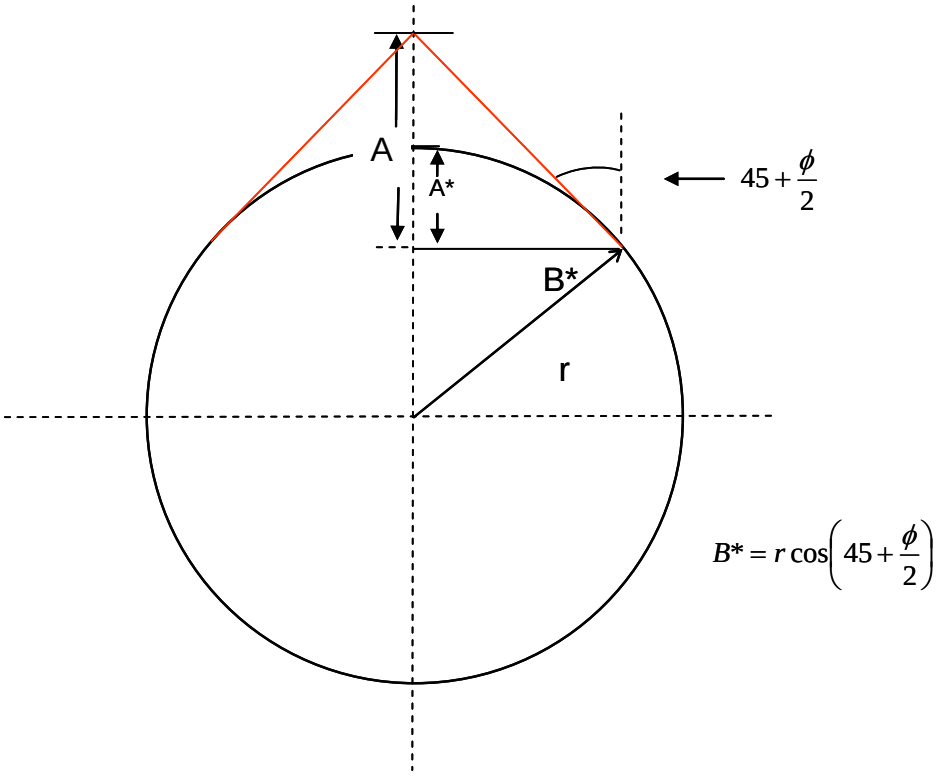

Figure 5.3. B* Factor for use in Vertical Stress Calculations

In Terzaghi's vertical stress calculation, the factor B, representing the width of the trap door, is replaced by B* with is defined by

$$B^* = r \cdot \cos\left(45 + \frac{\phi}{2}\right) \tag{5.3}$$

where r = pipe radius and ϕ = soil internal friction angle.

Therefore, substituting B* into Terzaghi's equation for vertical stress results in the following equation:

$$\sigma_v = \sigma_{v\infty} = \frac{\gamma \cdot r \cdot \cos\left(45 + \frac{\phi}{2}\right)}{\tan\phi} \tag{5.4}$$

Field investigations by Milligan, Norris (1992), and Marshall (1998), included jacking an instrumented pipe equipped with sensors to measure normal stresses around the circumference of the pipe on nine projects, as detailed in Chapter 2. Results of the investigations show that average normal stresses are fairly constant and generally evenly distributed around the pipeline, unless sharp steering corrections are made or the machine encounters material on one side of the pipe that is harder than on the other. They also showed that using the self-weight of the pipe on concrete pipe projects typically grossly over-estimates normal stresses. Zhou (1998) performed numerical modeling studies on interface stresses between pipes and soils during jacking and found the jacking stresses to be evenly dispersed around the jacking pipe, except at areas of stress concentration at the joint where misalignment occurred due to steering corrections.

With the findings of the distributions of normal stresses based on Milligan, Norris, Marshall, and Zhou, the interface friction coefficients as presented in Table 5.2, and the proposed model for predicting normal stress as presented in equation 5.4, the following predictive model for calculating the frictional component of jacking forces is proposed:

$$JF_{frict} = \mu_{\text{int}} \frac{\gamma \cdot r \cdot \cos\left(45 + \frac{\phi_r}{2}\right)}{\tan \phi_r} \cdot \pi \cdot d \cdot l \qquad (5.5)$$

Where JF_{frict} = Frictional Component of Jacking Force [tons force]
μ_{int} = Pipe-Soil Residual Interface Friction Coefficient [unit-less]
γ = Total Unit Weight of the Soil [tons/ft^3]
ϕ_r = Residual Friction Angle of the Soil [degrees]
d = Pipe Diameter [feet]
r = Pipe Radius [feet]
l = Length of the Pipe [feet]

5.3 Comparing Estimated Jacking Forces to Case History Data

Using Equation 5.5, jacking forces were predicted on a number of case histories for unlubricated portions of the microtunnel drives. These unlubricated segments typically corresponded to areas near the tunneling shaft at the beginning of the tunneling drive. By examining unlubricated portions of the case history data, the laboratory data for pipe-soil interface friction coefficients could be used to predict the interface friction behavior between the pipe and the soil at the project sites.

5.3.1 Actual and Predicted Jacking Forces with Hobas Pipe

Four microtunnel drives using Hobas pipe contained unlubricated segments that were suitable for comparing laboratory and field data. The first Hobas drive was Drive 3 on the Newark Subbasin Lower Relief Interceptor Sewer Project which was constructed with 36-inch Hobas pipe and is described in detail in Section 4.11. This drive was not lubricated until approximately 110 feet into the drive. Vertical borings were drilled for the project and can be found in section 4.11.2. For drive 3, at the depth of the microtunnel, the soil was classified as medium-dense silty sand with blow counts ranging from 21 to 25 blows per foot. The dry density of the soil was 101.5 pcf with a moisture content of 24 percent, allowing the calculation of total unit weight of 126 pcf. The soil residual friction angle was estimated from the information contained in the borings. Table 5.4 shows the parameters used to predict the frictional component of the jacking forces over the interval from 20 to 90 feet.

Table 5.4. Parameters used to Predict Jacking Forces for Drive 3 of the Newark Subbasin Lower Level Relief Sewer Project.

Project Name	**Newark – Drive 3**	**Remarks**
Pipe Material	Hobas	
Pipe Diameter [inches]	38.3	
Soil Residual Friction Angle [degrees] (estimated)	26	Determined from Boring Logs found in Section 4.11.2
Total Soil Unit Weight [pcf] (calculated from geotechnical data)	126	See note above
Interface Friction Coefficient	0.39	From Table 5.2
Predicted Normal Stress [psf]	218	From Equation 5.5
Predicted Jacking Stress [tons/ft^2]	0.043	From Equation 5.5
Actual Jacking Stress [tons/ft^2]	0.051	From Field Data
Percent Error	15.8%	%Error = (Actual-Predicted)/Actual

Figure 5.4 shows the actual and predicted frictional component of the jacking forces from 20 to 90 feet.

The second Hobas drive was Drive 6 on the Newark Subbasin Project and had similar soil conditions to those of Drive 3 and is described in Section 4.11. Lubrication for Drive 6 was not applied to the pipeline until approximately 55 feet into the drive. The soil properties used to predict the frictional component of the jacking forces are the same as those used for Drive 3. Table 5.5 shows the parameters used to predict the frictional component of the jacking forces over the interval from 15 to 55 feet.

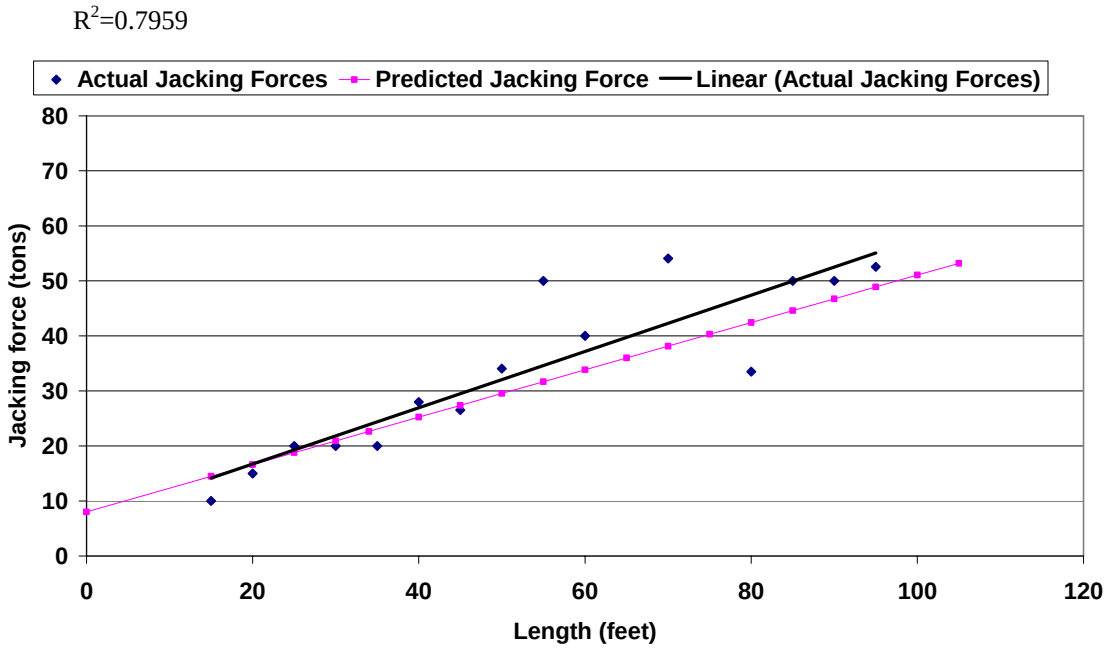

Figure 5.4. Length vs. Actual and Predicted Jacking Forces for the Newark Subbasin Drive 3 from 20 to 90 feet.

Table 5.5. Parameters used to Predict Jacking Forces for Drive 6 of the Newark Subbasin Lower Level Relief Sewer Project.

Project Name	**Newark – Drive 6**	**Remarks**
Pipe Material	Hobas	
Pipe Diameter [inches]	38.3	
Soil Residual Friction Angle [degrees] (estimated)	26	Determined from Boring Logs found in Section 4.11.2
Total Soil Unit Weight [pcf] (calculated from geotechnical data)	126	See note above
Interface Friction Coefficient	0.39	From Table 5.2
Predicted Normal Stress [psf]	218	From Equation 5.5
Predicted Jacking Stress [tons/ft^2]	0.043	From Equation 5.5
Actual Jacking Stress [tons/ft^2]	0.051	From Field Data
Percent Error	15.8%	%Error = (Actual-Predicted)/Actual

Figure 5.5 shows the actual and predicted frictional component of the jacking force from 15 to 55 feet into the drive.

R^2=0.8081

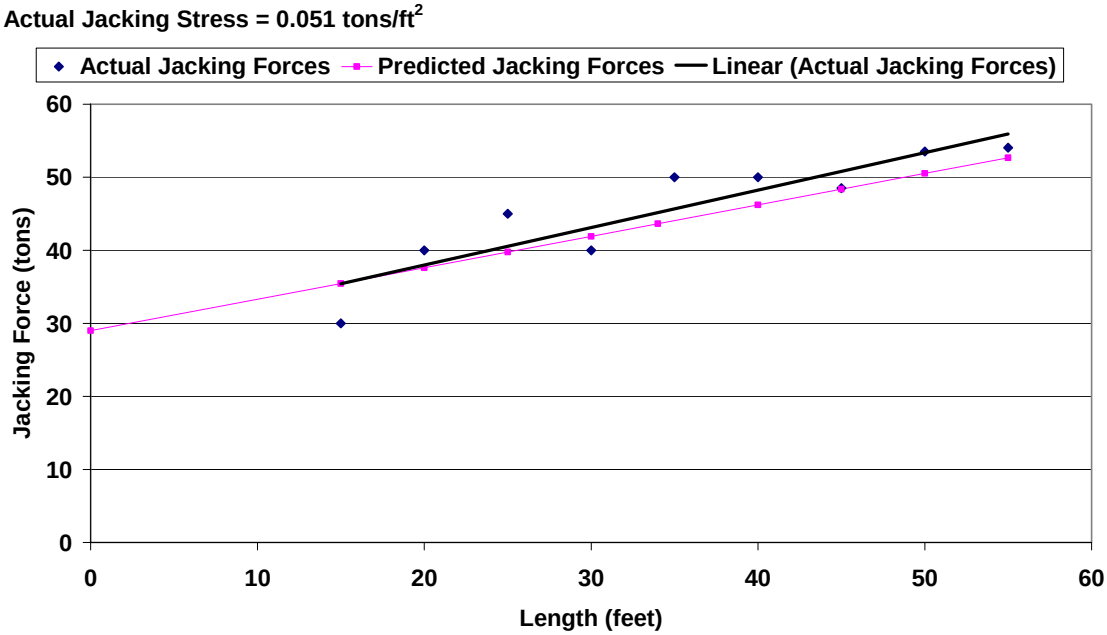

Figure 5.5. Length vs. Actual and Predicted Jacking Force for the Newark Subbasin Drive 6 from 15 to 55 feet.

The third Hobas drive was Drive 12 of the Newark Subbasin Project and had similar soil conditions to those found on Drives 3 and 6 and is described in Section 4.11. Lubrication was not applied to Drive 12 until approximately 45 feet into the drive. Soil properties used to predict the frictional component of the jacking forces were the same as those used on Drive 3 and 6. Table 5.6 shows the parameters used to predict the frictional component of the jacking forces over the first 45 feet of the drive.

Table 5.6. Parameters used to Predict Jacking Forces for Drive 12 of the Newark Subbasin Lower Level Relief Sewer Project.

Project Name	**Newark – Drive 12**	**Remarks**
Pipe Material	Hobas	
Pipe Diameter [inches]	38.3	
Soil Residual Friction Angle [degrees] (estimated)	26	Determined from Boring Logs found in Section 4.11.2
Total Soil Unit Weight [pcf] (calculated from geotechnical data)	126	See note above
Interface Friction Coefficient	0.39	From Table 5.2
Predicted Normal Stress [psf]	218	From Equation 5.5
Predicted Jacking Stress [tons/ft^2]	0.043	From Equation 5.5
Actual Jacking Stress [tons/ft^2]	0.046	From Field Data
Percent Error	6.7%	%Error = (Actual-Predicted)/Actual

Figure 5.6 shows the actual and predicted jacking forces from 15 to 45 feet along the drive.

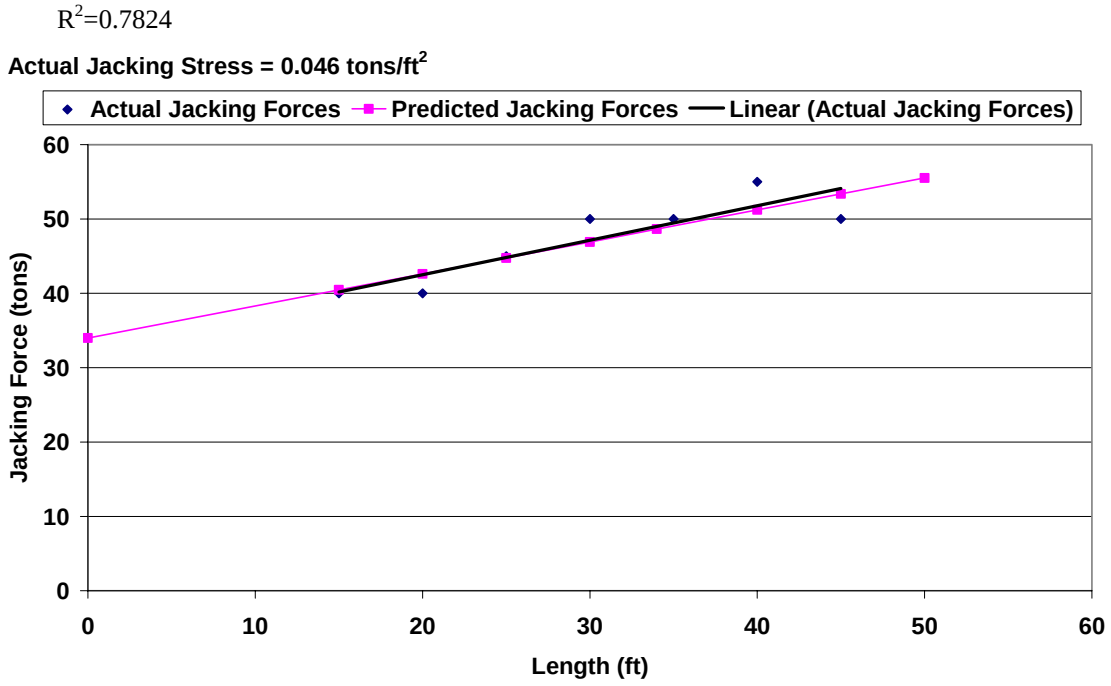

Figure 5.6. Actual and Predicted Jacking Forces for Drive 12 of the Newark Subbasin Project from 15 to 45 feet.

The fourth Hobas drive was Drive 1-24 of the Newark project where 24-inch nominal diameter pipe was used, as described in Section 4.11. This portion of the project was not located in the immediate vicinity of the 36-inch diameter pipelines but the soils encountered on the tunnel drives were very similar. As a result, the same soil parameters were used in the predictive model for the 24-inch diameter as were used for the 36-inch diameter Hobas. Lubrication was not applied to the drive until 50 feet after tunneling began. Table 5.7 shows the parameters used to predict the frictional component of the jacking forces.

Table 5.7. Parameters used to Predict Jacking Forces for Drive 1-24 of the Newark Subbasin Lower Level Relief Sewer Project.

Project Name	**Newark Drive 1-24**	**Remarks**
Pipe Material	Hobas	
Pipe Diameter [inches]	25.8	
Soil Residual Friction Angle [degrees] (estimated)	26	Determined from Boring Logs found in Section 4.11.2
Total Soil Unit Weight [pcf] (calculated from geotechnical data)	126	See note above
Interface Friction Coefficient	0.39	From Table 5.2
Predicted Normal Stress [psf]	144	From Equation 5.5
Predicted Jacking Stress [tons/ft^2]	0.028	From Equation 5.5
Actual Jacking Stress [tons/ft^2]	0.033	From Field Data
Percent Error	14.1%	%Error = (Actual-Predicted)/Actual

Figure 5.7 shows the actual and predicted jacking forces from 15 to 50 feet along the tunnel drive.

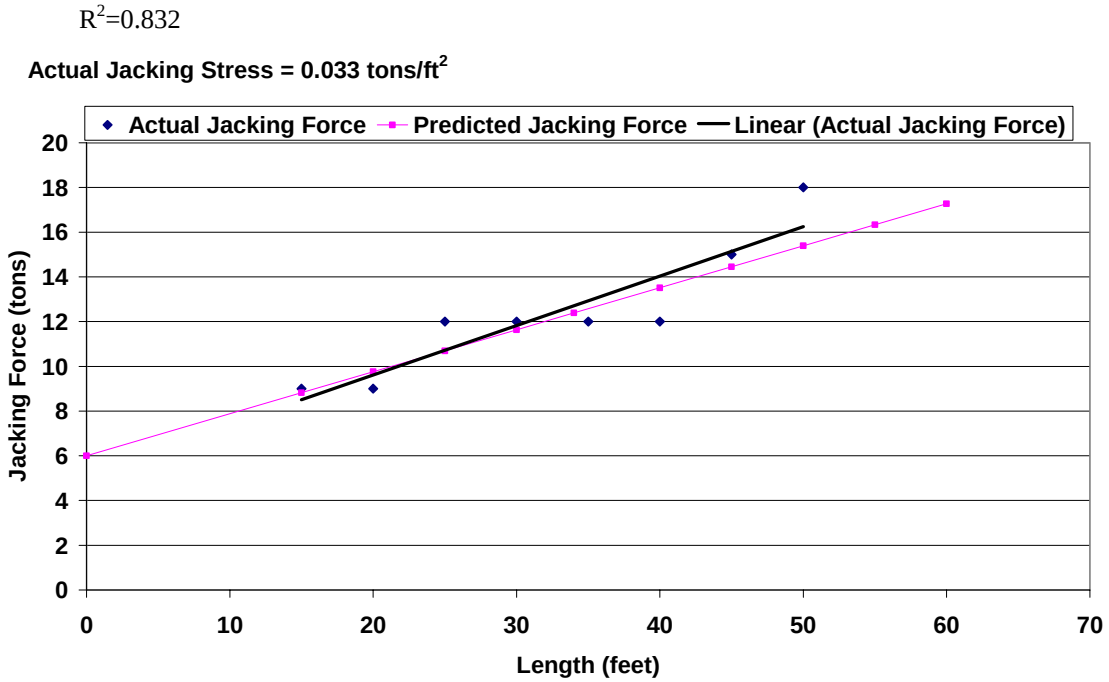

Figure 5.7. Length vs. Actual and Predicted Jacking Force for Newark Subbasin Drive 1 – 24-inch from 15 to 50 feet.

Table 5.8 summarizes the actual and predicted jacking forces for all drives constructed with Hobas pipe.

Table 5.8. Summary of Actual Jacking Stresses, Predicted Jacking Stresses, and Parameters used for Predictive Model for all Microtunnel Drives with Hobas Pipe.

Project	Pipe Diameter [in]	Estimated Friction Angle [°]	Soil Unit Weight [pcf]	Predicted Normal Stress [psf]	Interface Friction Coefficient [-]	Predicted Jacking Stress [tsf]	Actual Jacking Stress [tsf]	Percent Error [%]
Newark Drive 3	38.3	26	126	218	0.39	0.043	0.051	15.8
Newark Drive 6	38.3	26	126	218	0.39	0.043	0.051	15.8
Newark Drive 12	38.3	26	126	218	0.39	0.043	0.046	6.7
Newark Drive 1-24	25.8	26	126	144	0.39	0.028	0.033	14.1

5.3.2 Actual and Predicted Jacking Forces with Polycrete Pipe

Three microtunnel drives with Polycrete pipe contained unlubricated segments suitable for comparing laboratory and field data. The first was on the Alvarado Boulevard project Jacking Pit 3 to Reception pit 4, as described in Section 4.8. The first 85 feet of the microtunnel drive was not lubricated. To predict the jacking forces with Equation 5.5, the residual friction angle and total soil unit weight had to be estimated from the geotechnical information known about the Alvarado site. Geotechnical data were presented in Section 4.8.2. At the elevation of the pipeline, the soil was classified as medium-dense silty sand (SM) with blow counts of 40 blows per foot. The sample collected at the pipeline elevation graded at six (6) percent gravel, 51% sand, 30% silt and 13% clay. A moisture content of 21 percent was measured and a dry density of 108 pcf was provided, allowing the calculation of a total unit weight of 131 pcf. The residual soil friction angle was estimated to be 31 degrees.

Table 5.9 contains the parameters used in the prediction of the frictional component of the jacking forces over the segment from 20 to 85 feet of the drive.

Table 5.9 Parameters used to Predict Jacking Forces for Alvarado JP3 to RP4

Project Name	**Alvarado – JP3 to RP4**	**Remarks**
Pipe Material	Polycrete	
Pipe Diameter [inches]	46.6	
Soil Residual Friction Angle [degrees] (estimated)	31	Determined from boring logs found in Section 4.8.2
Total Soil Unit Weight [pcf] Calculated from Geotechnical Data	131	See note above
Interface Friction Coefficient	0.49	From Table 5.2
Predicted Normal Stress [psf]	209	
Predicted Jacking Stress [ton/ft^2]	0.048	From Equation 5.5
Actual Jacking Stress [ton/ft^2]	0.045	From Field Data
Percent Error	-6.1%	%Error = (Actual-Predicted)/Actual

Figure 5.8 shows the actual and predicted jacking forces for the non-lubricated segment between 20 and 85 feet for the Alvarado Boulevard drive between Jacking Pit 3 and Reception Pit 4.

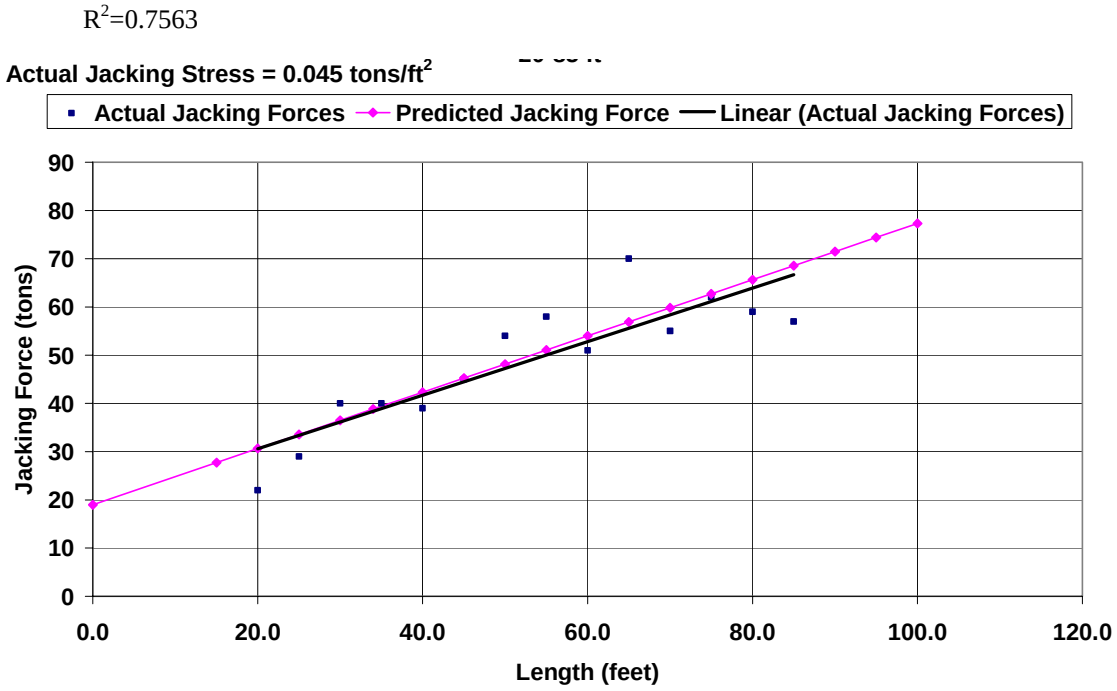

Figure 5.8. Length vs. Actual and Predicted Jacking Forces for Alvarado Blvd Project Jacking Pit 3 to Reception Pit 4 from 20 to 80 feet.

The second Polycrete pipe drive was on the Alvarado Boulevard Project from Jacking Pit 4 to Reception Pit 4, as described in Section 4.9. This drive included a non-lubricated section near the jacking shaft location from 10 to 75 feet into the tunnel drive. A vertical boring was drilled at the jacking shaft and is shown in section 4.9.2. At the elevation of the pipeline, the soil is classified as a medium-dense silty sand with blow counts of 22 blows per foot. The moisture content of the soil is given at 22 percent and the dry density is 106 pounds per cubic foot, allowing the calculation of the total unit

weight of 129 pcf. The residual friction angle of the soil was estimated at 30 degrees. Table 5.10 details the parameters used to predict the jacking forces for this segment of the drive.

Table 5.10 Parameters used to Predict Jacking Forces for Alvarado JP4 to RP4

Project Name	**Alvarado – JP4 to RP4**	**Remarks**
Pipe Material	Polycrete	
Pipe Diameter [inches]	46.6	
Soil Residual Friction Angle [degrees] (estimated)	30	Determined from boring logs found in Section 4.9.2
Total Soil Unit Weight [pcf] (calculated from geotechnical data)	129	See note above
Interface Friction Coefficient	0.45	From Table 5.2
Predicted Normal Stress [psf]	217	From Equation 5.5
Predicted Jacking Stress [tons/ft^2]	0.049	From Equation 5.5
Actual Jacking Stress [tons/ft^2]	0.051	From Field Data
Percent Error	4.5%	%Error = (Actual-Predicted)/Actual

Figure 5.9 shows the actual and predicted jacking forces for the non-lubricated section between 10 and 75 feet on the drive between JP4 and RP 4.

The third Polycrete pipe drive was on Drive 17 of the Alvarado project, as described in Section 4.10. This drive was constructed with 26 inch Polycrete. This drive had a non-lubricated segment from 20 to 90 feet along the drive. A vertical boring was drilled at the jacking shaft and is shown in section 4.10.2. The soil conditions at the elevation of the pipeline were classified as medium-dense silty/clayey sand (SM/SC) with blow counts of 29 blows per foot. The moisture content of the soil was 25 percent and the dry density was given as 101 pcf, allowing the calculation of the total unit weight of 126 pcf. A soil residual friction angle of 29 degrees was estimated for this soil. Table 5.11 contains the parameters used to predict the jacking forces throughout the non-lubricated segment.

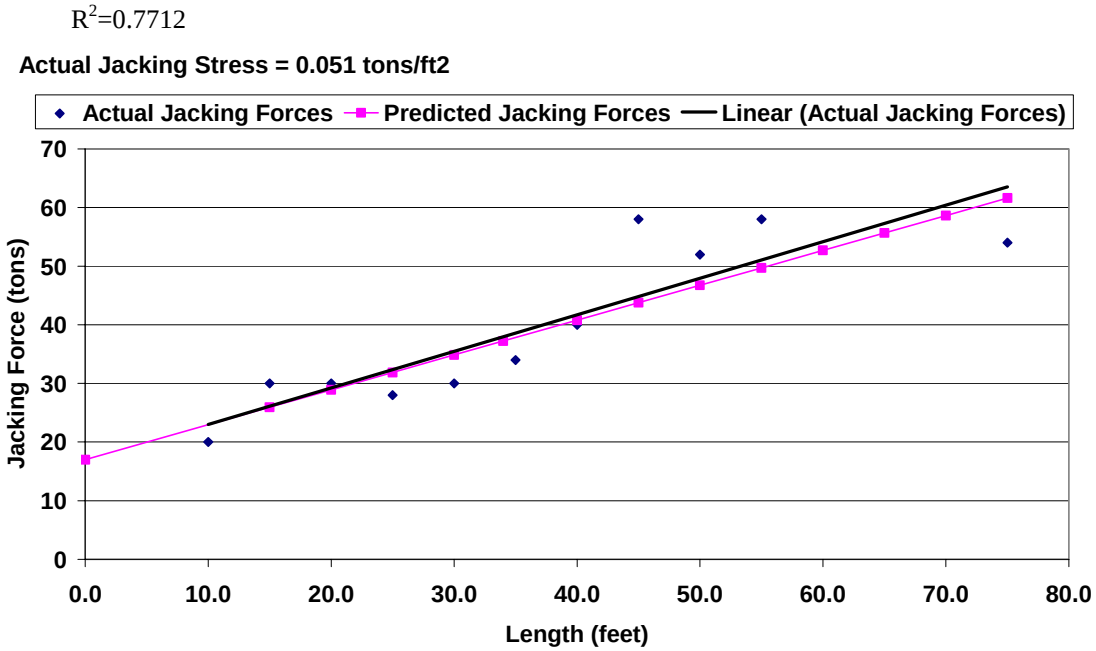

Figure 5.9. Length vs. Actual and Predicted Jacking Force for Alvarado Blvd from Jacking Pit 4 to Reception Pit 4 from 15 to 75 feet.

Table 5.11 Parameters used to Predict Jacking Forces for Alvarado Drive 17 – 26 inch

Project Name	**Alvarado – Drive 17 – 26 inch**	**Remarks**
Pipe Material	Polycrete	
Pipe Diameter [inches]	25.92	
Soil Residual Friction Angle [degrees] (estimated)	29	Determined from boring logs found in Section 4.10.2
Total Soil Unit Weight [pcf] (calculated from geotechnical data)	126	See Note Above
Interface Friction Coefficient	0.44	From Table 5.2
Predicted Normal Stress [psf]	125	From Equation 5.5
Predicted Jacking Stress [tons/ft^2]	0.027	From Equation 5.5
Actual Jacking Stress [tons/ft^2]	0.026	From Field Data
Percent Error	-5.8%	%Error = (Actual-Predicted)/Actual

Figure 5.10 shows the actual and predicted jacking forces on Drive 17 of the Alvarado project.

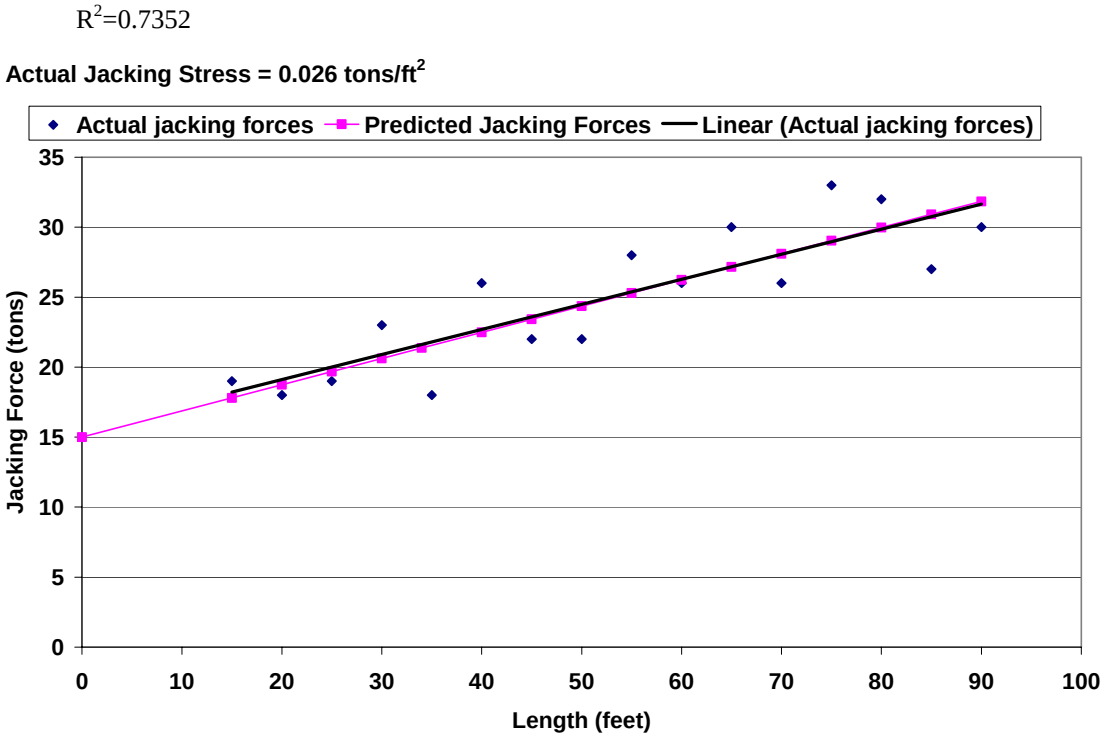

Figure 5.10. Length vs. Actual and Predicted Jacking Forces for Alvarado Blvd Drive 17 from 15 to 90 feet

Table 5.12 provides a summary of the actual and predicted jacking force predictions for Polycrete pipe.

Table 5.12 Summary of Actual Jacking Stresses, Predicted Jacking Stresses, and Parameters used for Predictive Model for all Microtunnel Drives with Polycrete Pipe

Project	Pipe Diameter [in]	Estimated Friction Angle [°]	Soil Unit Weight [pcf]	Predicted Normal Stress [psf]	Interface Friction Coefficient [-]	Predicted Jacking Stress [tsf]	Actual Jacking Stress [tsf]	Percent Error [%]
Alvarado JP3-RP4	46.6	31	131	209	0.46	0.048	0.045	-6.1
JP4-RP4	46.6	30	129	217	0.45	0.049	0.051	4.5
Drive 17	25.9	29	126	125	0.44	0.027	0.026	-5.8

5.3.3 Actual and Predicted Jacking Forces with Permalok Steel Pipe

Three microtunneling drives with Permalok Steel pipe contained unlubricated segments suitable for comparing laboratory and field data. The first was the Snohomish River Crossing 2001 project that is described in detail in Section 4.3. On this drive, lubrication was not applied until 90 feet into the microtunnel drive. To use the model to predict the jacking forces, values for the residual friction angle of the soil and the total unit weight of the soil had to be chosen. Borings along the alignment are shown in section 4.3.2. Soil at the depth of the tunnel was classified by the USCS as a well-graded gravel with sand having blow counts of 41 blows per foot. Another sample along the alignment was classified as a poorly-graded gravel with silt and sand. This sample was 59% gravel, 35% sand, and contained 6% fines. This sample had blow counts of 23 blows per foot. The Geotechnical Investigation Report (CH2M Hill, 2001) did not provide unit weights for the soil; therefore, unit weights had to be estimated. Based on the soils information provided in the Geotechnical Report (CH2M Hill, 2001), the jacking forces for the tunnel segment between 20 and 90 feet were predicted with the parameters listed in Table 5.13.

Table 5.13 Parameters used to Predict Jacking Forces for Clearview Snohomish River Crossing 2001

Project Name	**Clearview Snohomish River Crossing 2001**	**Remarks**
Pipe Material	Permalok Steel	
Pipe Diameter [inches]	60	
Soil Residual Friction Angle [degrees] (estimated)	35	Determined from Boring Logs found in Section 4.3.2
Total Soil Unit Weight [pcf] (estimated)	135	See note above
Interface Friction Coefficient	0.59	From Table 5.2
Predicted Normal Stress [psf]	223	From Equation 5.5
Predicted Jacking Stress [tons/ft^2]	0.065	From Equation 5.5
Actual Jacking Stress [tons/ft^2]	0.074	From Field Data
Percent Error	11.6%	%Error = (Actual-Predicted)/Actual

Figure 5.11 shows the actual and predicted frictional component of the jacking forces from 20 to 90 feet for the Clearview Snohomish River Crossing 2001.

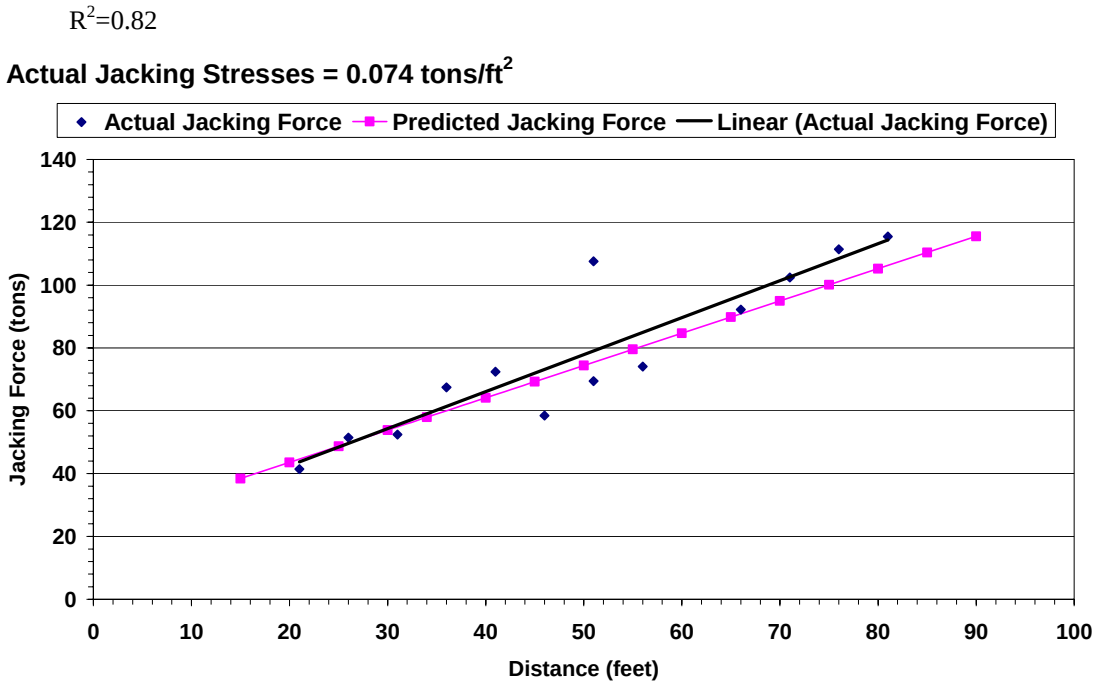

Figure 5.11. Length vs. Actual and Predicted Jacking Forces for Clearview Snohomish River Crossing 2001 from 20 to 90 feet.

The second microtunneling drive with Permalok Steel Pipe was the North Bore of the Sacramento River Intake Project and is described in detail in Section 4.1. Lubrication was not applied until approximately 100 feet into the bore. The jacking segment from 50 to 100 feet represents the length in which the pipe was in contact with the native soils because of localized grouting at the launch shaft and the entrance can that was used to launch the machine. A vertical boring was drilled in the vicinity of the jacking shaft and can be found in section 4.1.2. Soil at the depth of the tunnel is described as medium-dense poorly-graded sand with silt (SP-SM) with blow counts of 18 blows per foot. The moisture content of the soil was 24 percent and the dry density of the soil was 87 pcf,

allowing the calculation of the total unit weight of the soil of 108 pcf. The residual friction angle of the soil was estimated to be 27 degrees based on the information contained in the boring log. The frictional component of the jacking force was predicted using the parameters shown in Table 5.14.

Table 5.14. Parameters used to Predict Jacking Forces for the North Microtunnel of the Sacramento River Intake Project.

Project Name	**Sacramento Intake – North Microtunnel**	**Remarks**
Pipe Material	Permalok Steel	
Pipe Diameter [inches]	72	
Soil Residual Friction Angle [degrees] (estimated)	27	Determined from Boring Logs found in Section 4.1.2
Total Soil Unit Weight [pcf] (calculated from geotechnical data	108	See note above
Interface Friction Coefficient	0.42	From Table 5.2
Predicted Normal Stress [psf]	332	From Equation 5.5
Predicted Jacking Stress [tons/ft^2]	0.071	From Equation 5.5
Actual Jacking Stress [tons/ft^2]	0.070	From Field Data
Percent Error	0.09%	%Error = (Actual-Predicted)/Actual

Figure 5.12 shows the actual and predicted frictional component of the jacking force from 50 to 100 feet along the North Microtunnel of the Sacramento River Intake project.

R^2=0.5151

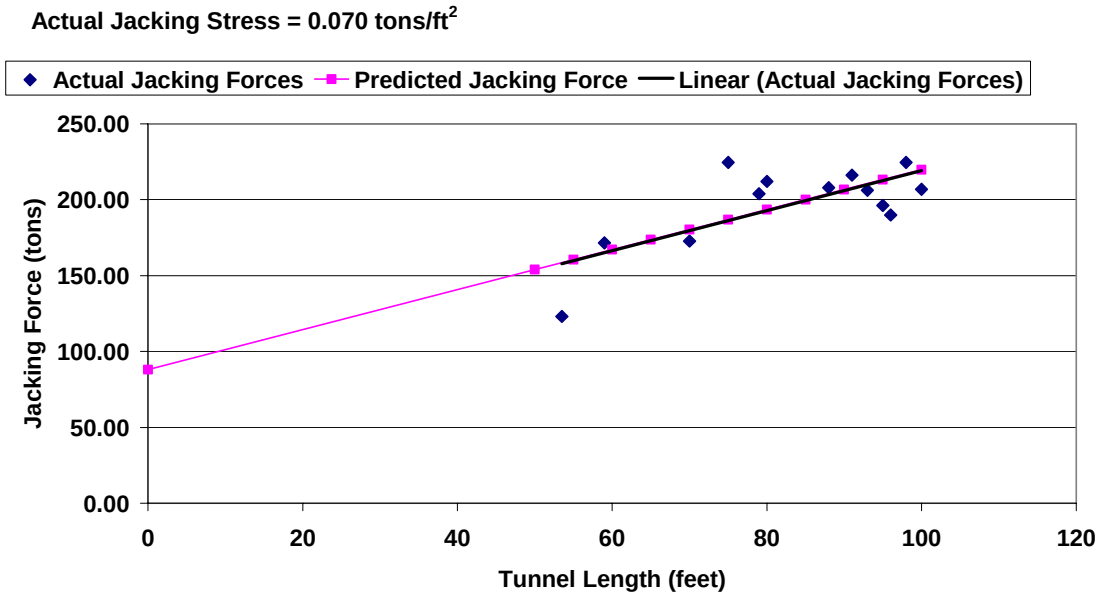

Figure 5.12. Length vs. Actual and Predicted Jacking Forces for the Sacramento Intake North Microtunnel from 50 to 100 feet.

The third Permalok Steel Pipe microtunnel drive was the South Microtunnel of the Sacramento River Intake Project and is described in detail in Section 4.1. Lubrication was not applied until 75 feet into the microtunnel drive. The North and South microtunnels were parallel bores and separated by approximately 20 feet. Only one boring was completed at the jacking shaft for both the North and the South microtunnel. Therefore, the same soil parameters were used to predict the frictional component of the jacking forces for both tunnels. Table 5.15 shows the parameters used to predict the jacking forces for the South microtunnel of the Sacramento River Intake tunnels.

Table 5.15. Parameters used to Predict Jacking Forces for the South Microtunnel of the Sacramento River Intake Project.

Project Name	**Sacramento Intake – South Microtunnel**	**Remarks**
Pipe Material	Permalok Steel	
Pipe Diameter [inches]	72	
Soil Residual Friction Angle [degrees] (estimated)	27	Determined from Boring Logs found in Section 4.1.2
Total Soil Unit Weight [pcf] (calculated from geotechnical data)	108	See note above
Interface Friction Coefficient	0.42	From Table 5.2
Predicted Normal Stress [psf]	332	From Equation 5.5
Predicted Jacking Stress [tons/ft^2]	0.07	From Equation 5.5
Actual Jacking Stress [tons/ft^2]	0.084	From Field Data
Percent Error	16.7%	%Error = (Actual-Predicted)/Actual

Figure 5.13 shows the actual and predicted jacking forces for the South Bore of the Sacramento River Intake project from 20 to 75 feet.

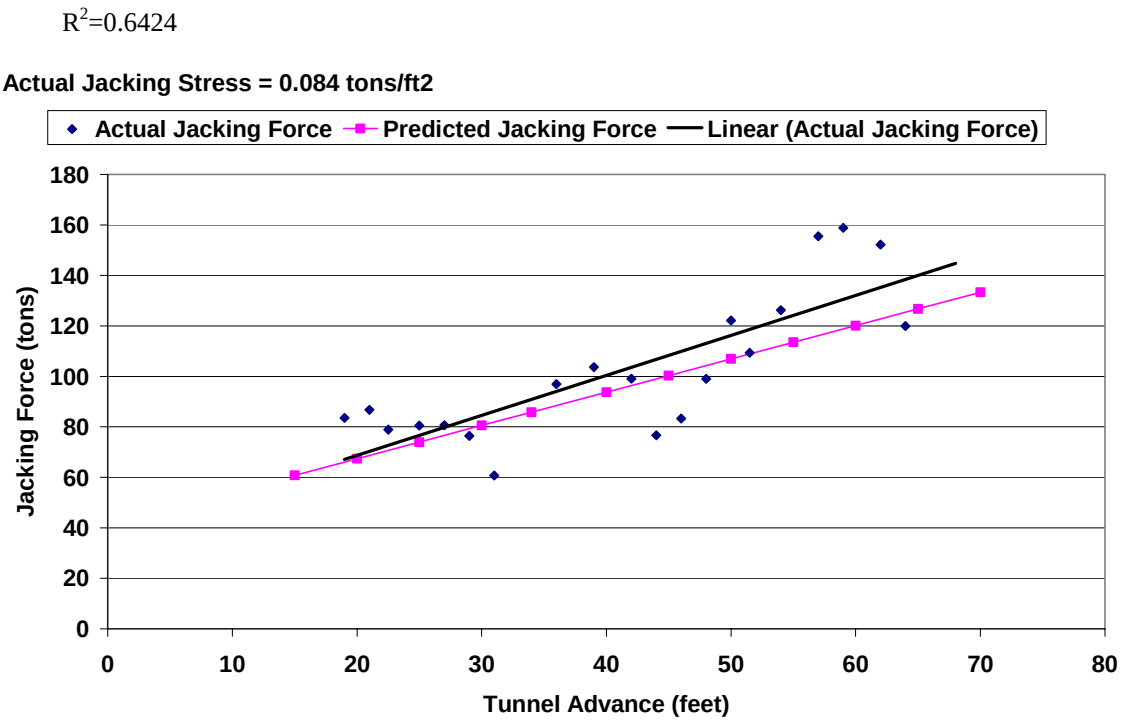

Figure 5.13. Length vs. Actual and Predicted Jacking Forces for the Sacramento Intake South Bore from 20 to 75 feet.

Table 5.16 summarizes the actual and predicted jacking forces for all drives constructed with Permalok Steel pipe.

Table 5.16. Summary of Actual Jacking Stresses, Predicted Jacking Stresses, and Parameters used for Predictive Model for all Microtunnel Drives with Permalok Steel Pipe

Project	**Pipe Diameter [in]**	**Estimated Friction Angle [°]**	**Soil Unit Weight [pcf]**	**Predicted Normal Stress [psf]**	**Interface Friction Coefficient [-]**	**Predicted Jacking Stress [tsf]**	**Actual Jacking Stress [tsf]**	**Percent Error [%]**
Clearview 2001	60	35	135	223	0.59	0.065	0.074	11.6
Sacramento North Bore	72	27	108	332	0.42	0.071	0.070	0.09
Sacramento South Bore	72	27	108	332	0.42	0.070	0.084	16.7

5.3.4 Actual and Predicted Jacking Forces with Wet Cast Concrete

One microtunnel drive constructed with Wet Cast Concrete pipe contained an unlubricated section suitable for comparing laboratory and field data. This was the Highway 50 Crossing on the South Lake Tahoe Rocky Point Project and is described in detail in Section 4.5. This drive was not lubricated until approximately 150 feet into the drive. No borings were completed for the project. The soils were described in the contract as very dense, heavily glaciated well-graded sands with blow counts ranging from 50 blows per foot to 50 blows for 6-inches. Estimates of both the unit weight and the residual friction angle were used in the predictive model because of the lack of field testing and laboratory data. Table 5.17 shows the parameters used to predict the frictional component of the jacking forces.

Table 5.17. Parameters used to Predict Jacking Forces for the Highway 50 Crossing of the South Lake Tahoe Rocky Point Project

Project Name	**Highway 50 Crossing**	**Remarks**
Pipe Material	Wet Cast Concrete	
Pipe Diameter [inches]	59.5	
Soil Residual Friction Angle [degrees] (estimated)	35	Determined from description of soil in contract documents
Total Soil Unit Weight [pcf] (estimated)	140	See note above
Interface Friction Coefficient	0.60	From Table 5.2
Predicted Normal Stress [psf]	229	From Equation 5.5
Predicted Jacking Stress [tons/ft^2]	0.068	From Equation 5.5
Actual Jacking Stress [tons/ft^2]	0.074	From Field Data
Percent Error	7.7%	%Error = (Actual-Predicted)/Actual

Figure 5.14 shows the actual and predicted frictional component of the jacking forces from 40 to 150 feet.

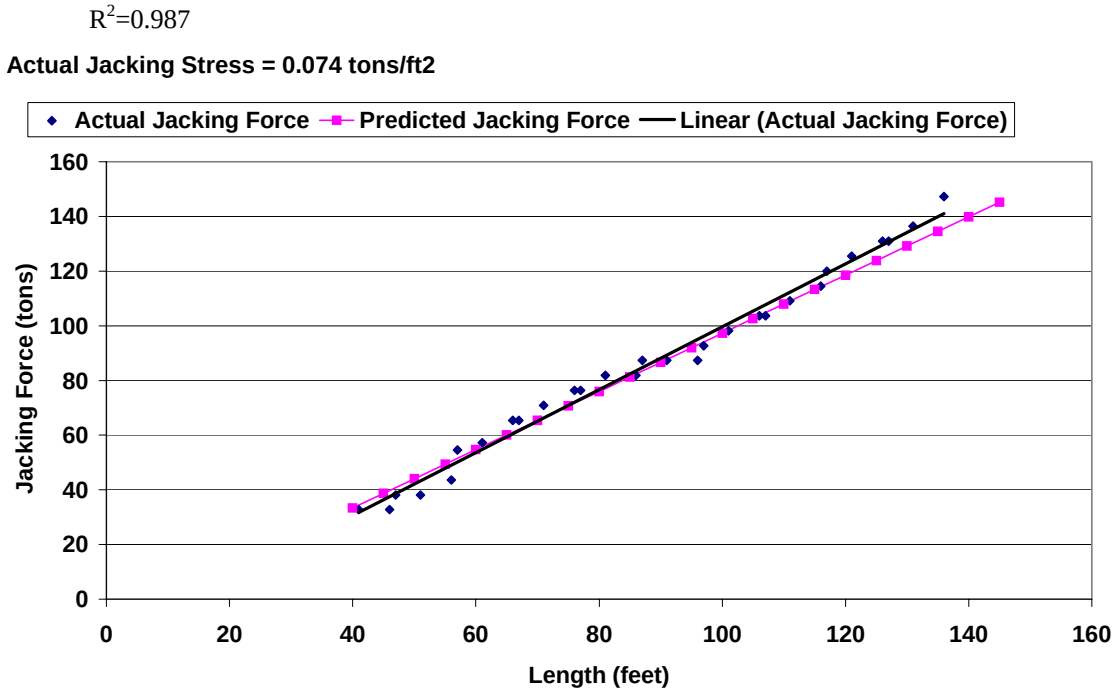

Figure 5.14. Length vs. Actual and Predicted Jacking Forces for the South Tahoe Rocky Point Highway 50 Crossing from 40 to 150 feet.

Table 5.18 summarizes the actual and predicted jacking forces for the drive constructed with Wet Cast Concrete pipe.

Table 5.18. Summary of Actual Jacking Stresses, Predicted Jacking Stresses, and Parameters used for Predictive Model for all Microtunnel Drives with Wet Cast Concrete Pipe.

Project	Pipe Dia-meter [in]	Est. Friction Angle [°]	Soil Unit Weight [pcf]	Predicted Normal Stress [psf]	Interface Friction Coefficient [-]	Predicted Jacking Stress [tsf]	Actual Jacking Stress [tsf]	Percent Error [%]
Highway 50 Crossing	59.5	35	140	229	0.60	0.068	0.074	7.7

5.3.5 Actual and Predicted Jacking Forces with Packerhead Concrete

Two microtunnel drives constructed with Packerhead Concrete contained unlubricated segments suitable for comparison between laboratory and field data. The first was the Morris Avenue drive of the Eastside Interceptor Restoration Project and is described in detail in Section 4.6. Lubrication was not applied to the pipeline until approximately 175 feet into the drive. A vertical boring was drilled at the jacking shaft and can be found in section 4.6.2. Soil at the depth of the tunnel was classified as a loose to medium-dense silty fine to medium sand. Blow counts ranged from three to18 blows per foot. A moisture content of 30 percent was given but dry densities for the soil were not provided; therefore, soil unit weights had to be estimated. The soil residual friction angle was estimated from the information contained in the geotechnical report. Table 5.19 shows the parameters that were used to predict the frictional component of the jacking forces along the drive.

Table 5.19 Parameters used to Predict Jacking Forces for the Morris Avenue Drive of the Eastside Interceptor Project.

Project Name	**Morris Avenue Drive**	**Remarks**
Pipe Material	Packerhead Concrete	
Pipe Diameter [inches]	87.5	
Soil Residual Friction Angle [degrees] (estimated)	32	Determined from Boring Logs found in Section 4.6.2
Total Soil Unit Weight [pcf] (estimated)	110	See note above
Interface Friction Coefficient	0.59	From Table 5.2
Predicted Normal Stress [psf]	311	From Equation 5.5
Predicted Jacking Stress [tons/ft^2]	0.091	From Equation 5.5
Actual Jacking Stress [tons/ft^2]	0.090	From Field Data
Percent Error	-1.0%	%Error = (Actual-Predicted)/Actual

Figure 5.15 shows the actual and predicted jacking force from 30 to 175 feet into the microtunnel drive.

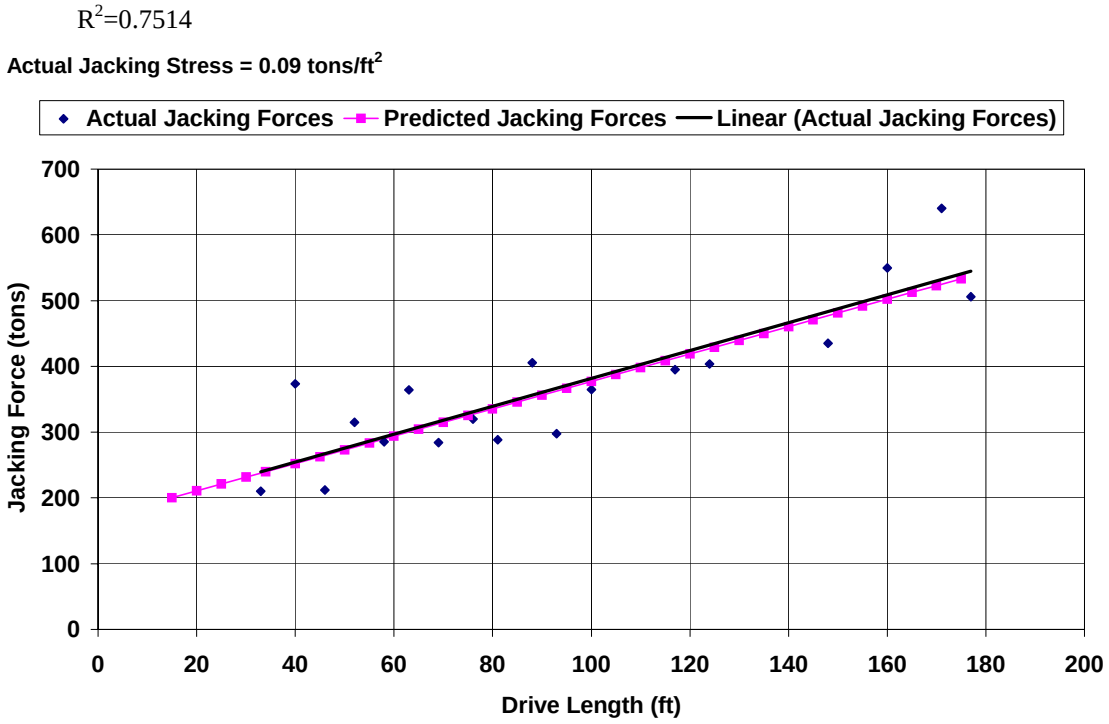

Figure 5.15. Length vs. Actual and Predicted Jacking Force for the Eastside Interceptor Morris Avenue Drive from 30 to 175 feet.

The second drive constructed with Packerhead Concrete was the Houser Way Drive of the Eastside Interceptor Project and is described in detail in Section 4.7. Lubrication was not applied to the pipeline until approximately 120 feet into the drive. Individual borings were conducted for the Morris and Houser drives; however, the borings did not provide friction angles or unit weights for the soils. Since the soils in the area were similar, and these parameters had to be estimated to use in the predictive model, the parameters used in both the Morris and Houser predictions were the same. Table 5.20 shows the parameters used to predict the frictional component of the jacking forces for the Houser Way drive.

Table 5.20. Parameters used to Predict Jacking Forces for the Houser Way Drive of the Eastside Interceptor Project.

Project Name	**Houser Way Drive**	**Remarks**
Pipe Material	Packerhead Concrete	
Pipe Diameter [inches]	87.5	
Soil Residual Friction Angle [degrees] (estimated)	32	Determined from Boring Logs found in Section 4.6.2
Total Soil Unit Weight [pcf] (estimated)	110	See note above
Interface Friction Coefficient	0.59	From Table 5.2
Predicted Normal Stress [psf]	311	From Equation 5.5
Predicted Jacking Stress [tons/ft^2]	0.091	From Equation 5.5
Actual Jacking Stress [tons/ft^2]	0.082	From Field Data
Percent Error	-10.8%	%Error = (Actual-Predicted)/Actual

Figure 5.16 shows the actual and predicted jacking force as a function of length on the Houser Way Drive of the Eastside Interceptor project.

R^2=0.6951

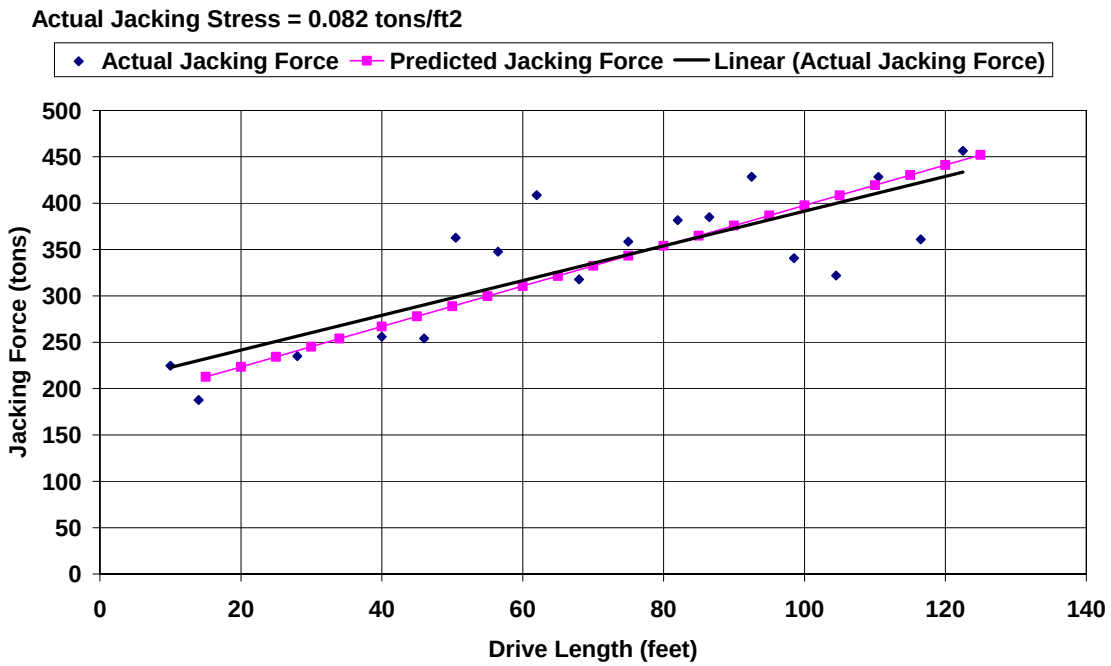

Figure 5.16. Length vs. Actual and Predicted Jacking Force for the Eastside Interceptor Houser Way Drive from 15 to 125 feet.

Table 5.21 summarizes the actual and predicted jacking forces for all drives constructed with Packerhead Concrete pipe.

Table 5.21. Summary of Actual Jacking Stresses, Predicted Jacking Stresses, and Parameters used for Predictive Model for all Microtunnel Drives with Packerhead Concrete Pipe.

Project	Pipe Diameter [in]	Estimated Friction Angle [°]	Soil Unit Weight [pcf]	Predicted Normal Stress [psf]	Interface Friction Coefficient [-]	Predicted Jacking Stress [tsf]	Actual Jacking Stress [tsf]	Percent Error [%]
Morris Ave	87.5	32	110	311	0.58	0.091	0.090	-1.0
Houser Way	87.5	32	110	311	0.58	0.091	0.084	-10.8

5.3.6 Summary of all Actual and Predicted Jacking Forces

Table 5.22 provides a summary of all of the projects on which the predictive model was used to estimate the jacking forces on the non-lubricated sections of the drive. The table shows the parameters that were used in the model for the predictions. Soil parameters used in the model were obtained from soils testing performed for the field projects, or based on estimates made from the boring information for each project. Interface friction coefficients were obtained from Table 5.2 contained herein.

Table 5.22. Summary of All Projects Actual Jacking Stresses, Predicted Jacking Stresses, and Parameters used for Predictive Model for all Microtunnel Drives.

Project	**Pipe**	**Pipe Dia-meter [in]**	**Est. ϕ_r [°]**	**Est. γ_{total} [pcf]**	**Predicted σ_n [psf]**	**μ_{int} [-]**	**Predicted Jacking Stress [tsf]**	**Actual Jacking Stress [tsf]**	**Percent Error [%]**
Newark-3	Hobas	38.3	26	126	218	0.39	0.043	0.051	15.8
Newark-6	Hobas	38.3	26	126	218	0.39	0.043	0.051	15.8
Newark-12	Hobas	38.3	26	126	218	0.39	0.043	0.046	6.7
Newark Drive 1-24	Hobas	25.8	26	126	218	0.39	0.028	0.033	14.1
Alvarado JP3-RP4	Polycrete	46.6	31	131	209	0.46	0.048	0.045	-6.1
Alvarado JP4-RP4	Polycrete	46.6	30	129	217	0.45	0.049	0.051	4.5
Alvarado Drive 17	Polycrete	25.9	29	126	125	0.44	0.027	0.026	-5.8
Clearview 2001	Permalok	60	35	135	223	0.59	0.065	0.074	11.6
Sacramento North	Permalok	72	27	108	332	0.42	0.070	0.070	0.09
Sacramento South	Permalok	72	27	108	332	0.42	0.070	0.084	16.7
Highway 50	Wet Cast Concrete	59.5	35	140	229	0.60	0.068	0.074	7.7
ESI Morris Ave	Packer-head Concrete	87.5	32	110	311	0.58	0.091	0.090	-1.0
ESI Houser Way	Packer-head Concrete	87.5	32	110	311	0.58	0.091	0.084	-10.8

5.4 Comparison of Predictive Model with Models Developed by Others.

The model used to predict the frictional component of the jacking force as shown in equation 5.5 was compared to models developed by Bennett (1998), Chapman (1999), and Scherle (as summarized in Stein, 2005). The predictive models of Bennett, Chapman and Scherle are described in detail in Chapter 2. Scherle's model was chosen for comparison because it provides the basis for much of the German international construction standards for microtunneling contained in, ATV A 161. Chapman's model was chosen because it is a follow-on product of the work performed by the ISTT Working Group No.3 from Japan that evaluated a tremendous amount of case history data. Chapman's work, although published in 1999, has not been widely disseminated in the United States and is relatively "unknown" to the industry. Bennett's model was chosen as his work has received much attention in the microtunneling industry and is often used for prediction of jacking forces by engineers.

It is important to note that in each case, only the frictional components of the jacking force were compared. Both Bennett and Chapman give guidelines for the face pressure force as the machine enters the ground but both recognize that the face pressure force is highly dependent on the operation of the machine. Scherle gives a much more prescriptive model for the face pressure force. For comparative purposes, the frictional component for all of the models was compared to the actual jacking forces on a particular drive. The face pressure force or force at which the tunnel machine entered the ground used for each model was the actual face pressure force measured as the tunneling machine exited the jacking shaft. Jacking force predictions for each model were then additive frictional components of each model. This method "normalized" the

comparisons and allowed an unbiased comparison of the frictional component of each model with the frictional component of the actual jacking forces.

When comparing the actual and predicted jacking forces with the various predicted models it is important to keep the following factors in mind. The actual forces presented are for unlubricated portions of the tunnel. Bennett's model is the only model that distinguishes between lubricated and non-lubricated sections. Bennett's model predicts both higher normal stressses and higher frictional forces in the non-lubricated sections, resulting in dramatically higher predictions of jacking forces in the non-lubricated zones than in the lubricated zones. Scherle's predictive model provides some guidance for interface friction coefficients to be used in lubricated and non-lubricated segments. However, Scherle uses the full column soil loading over the pipeline to determine the normal stress, taking no account for soil arching in granular soils. As a result, with microtunneling installations of any significant depth (over 15 feet), Scherle's predictive model typically gives very high predictions of jacking forces regardless of whether the user chooses the lubricated or non-lubricated interface friction coefficients recommended by Scherle. Chapman's model provides a frictional jacking stress that is a function of diameter, based on the soil types that are very generic (clay, sand, sand/gravel). Therefore, the results of Chapman's model can deviate from actual jacking forces if the diameter gets too big or small, or if the soil conditions are non-homogeneous.

5.4.1 Predicted Jacking Forces with Various Models on the Clearview Snohomish River Crossing 2001 Project (Permalok Steel Pipe)

For the predictive analysis of the Clearview Snohomish River Crossing 2001 Project, the first 100 feet of the tunnel drive was used for the prediction, as it was an un-lubricated section of the drive. Table 5.23 presents the parameters that were used in the predictive models.

Table 5.23. Properties used in Various Jacking Force Predictive Models for the Clearview Snohomish River Crossing 2001.

Parameters Used in Predictive Models							
Pipe Material	Permalok Steel		Soil Type	Sandy Gravel		Depth to Crown	65 feet
Pipe Diameter	60-inch		Residual Friction Angle	35 degrees		Depth to Water	15 feet
Pipe Weight	556 lbs/ft		Soil Unit Weight	135 pcf		Interface Friction Coefficient (Scherle)	0.20
Interface Friction Coefficient (Staheli)	0.59		Bennett Arching Factor, C_a (unlubed)	0.75 (Lower) 1.0 (Best) 1.5 (Upper)		Bennett Friction Factor, C_f (unlubed)	1.0

Figure 5.17 shows the actual and predictive jacking force for the first 100 feet of the Snohomish River Crossing. For the unlubricated zone, Bennett's model presents a lower-bound, a best-fit, and an upper-bound model, all of which are shown on the graph. Chapman and Scherle each give only one predictive model. The linear interpolation and the R^2 value shown on Figure 5.17 is for the actual jacking force data throughout this interval.

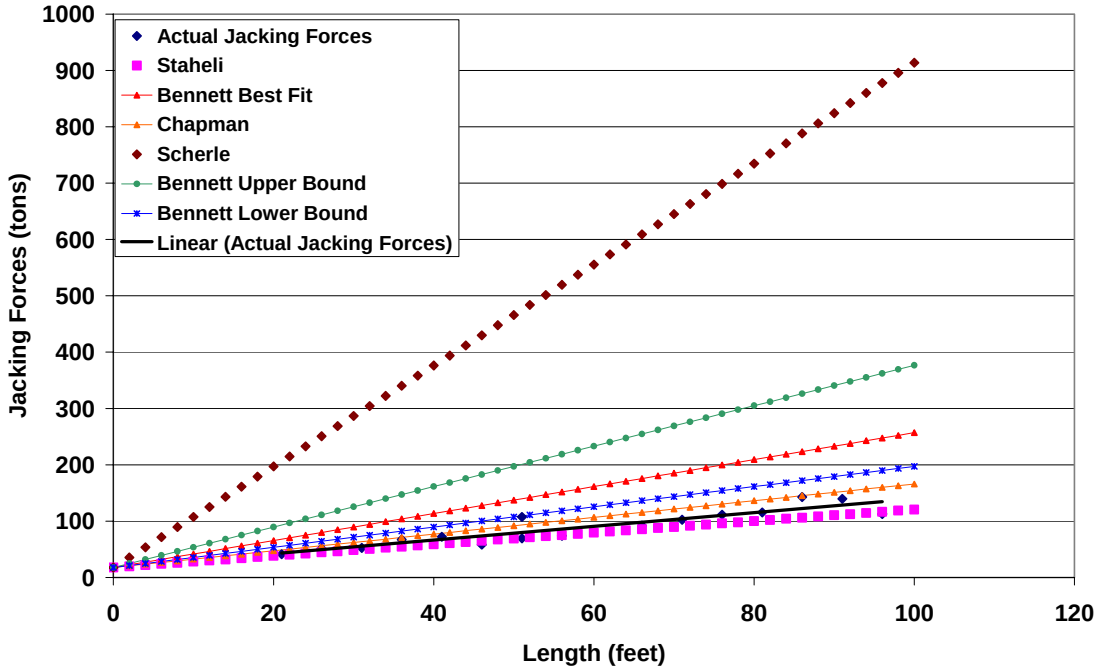

Figure 5.17. Length versus Actual and Predicted Jacking Force for a Variety of Predictive Models on the Snohomish River Crossing 2001 from 0 to 100 feet.

Table 5.24 presents the actual jacking stresses and the jacking stresses predicted by each of the predictive models, along with the percent error as a function of the actual jacking stress.

Table 5.24 Comparison of Actual and Predicted Jacking Stresses and Percent Error for the Clearview Snohomish River Crossing 2001.

Model	Jacking Stress [tons/ft^2]	Percent Error [%]
Actual	0.077	-
Staheli	0.072	15.5
Chapman	0.094	-21.8
Bennett, Lower Bound	0.123	-47.6
Bennett, Best Fit	0.164	-96.74
Bennett, Upper Bound	0.245	-195.1
Scherle	0.635	-636.8

Note: % Error= (Actual Stress – Predicted Stress) / Actual Stress. Positive Value is indicative of under-prediction. Negative Value indicative of over-prediction.

Bennett's model tends to predict higher loads in the unlubricated zones as it does not recognize any reduction in the internal friction angle of the soil at the interface in the unlubricated zone, and accounts for arching in his lower-bound and best-fit models to a

limited extent only. While Scherle's method allows for a reduction in the friction angle at the interface, the model vastly over-predicts the jacking forces in deep installations due to the fact that the predictive model does not account for any soil arching, and considers full soil column load above the pipe that is equal to the full depth of burial.

5.4.2 Predicted Jacking Forces with Various Models on the Eastside Interceptor – Morris Avenue Drive (Permalok Steel Pipe)

For the Eastside Interceptor Project – Morris Avenue Drive, the first 180 feet of the actual jacking forces were compared to jacking force predictions, because this section of the drive was not lubricated. Table 5.25 shows the parameters that were used in the predictive models.

Table 5.25. Properties used in Various Jacking Force Predictive Models for the Eastside Interceptor – Morris Avenue Crossing.

Parameters Used in Predictive Models							
Pipe Material	Packerhead Concrete		Soil Type	Loose Sands		Depth to Crown	17 feet
Pipe Diameter	87-5-inch		Residual Friction Angle	32 degrees		Depth to Water	6 feet
Pipe Weight	2,138 lbs/ft		Soil Unit Weight	110 pcf		Interface Friction Coefficient (Scherle)	0.25
Interface Friction Coefficient (Staheli)	0.58		Bennett Arching Factor, C_a (unlubricated)	0.75 (Lower) 1.0 (Best) 1.5 (Upper)		Bennett Friction Factor, C_f (unlubricated)	1.0

Bennett's lower- and upper- bound and best-fit models were predicted, along with the Chapman and Scherle model. Figure 5.18 shows the actual and predicted jacking force for the first 180 feet of the tunnel drive.

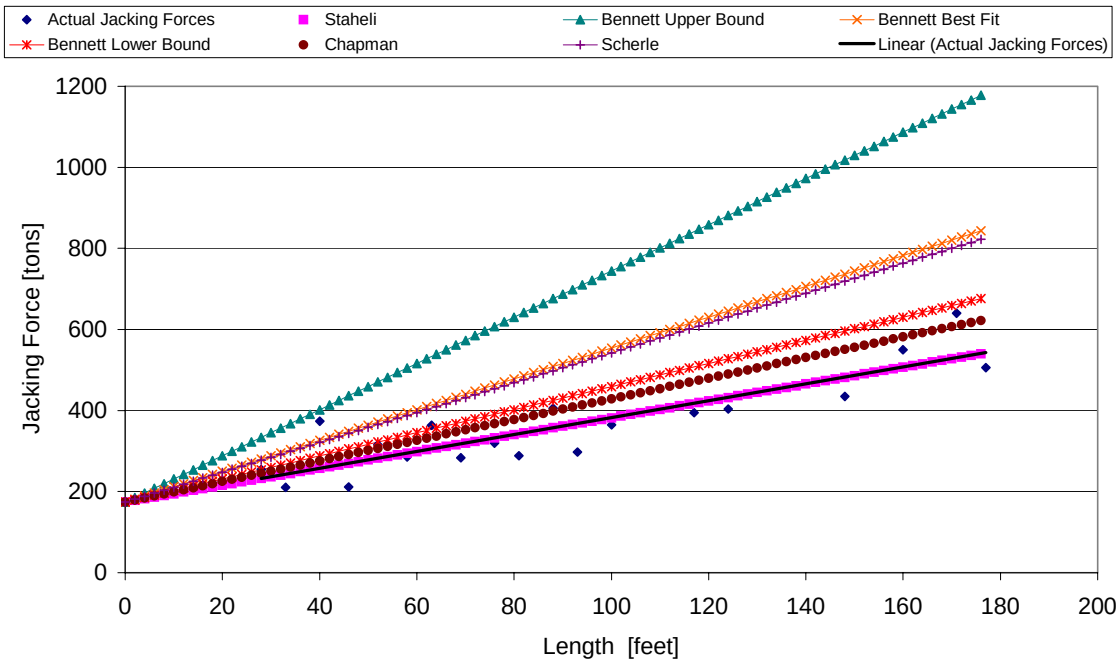

Figure 5.18. Length versus Actual and Predicted Jacking Forces with a Variety of Predictive Models for the Eastside Interceptor – Morris Avenue Drive.

The linear curve fit and the R^2 value is for the actual jacking force data for the microtunnel drive. Table 5.26 presents the actual jacking stresses and the jacking stresses predicted by each of the predictive models, along with the percent error as a function of the actual jacking stress.

Table 5.26. Comparison of Actual and Predicted Jacking Stresses and Percent Error for the Eastside Interceptor – Morris Avenue Drive.

Model	Jacking Stress [tons/ft^2]	Percent Error [%]
Actual	0.091	-
Staheli	0.091	0.03
Chapman	0.111	22.4
Bennett, Lower Bound	0.124	37.0
Scherle	0.161	76.8
Bennett, Best Fit	0.167	82.6
Bennett, Upper Bound	0.249	173.9

Note: % Error= (Actual Stress – Predicted Stress) / Actual Stress. Positive Value is indicative of under-prediction. Negative Value indicative of over-prediction.

Bennett's model provides a better prediction with a rougher pipe because the actual interface friction coefficient between the soil and the pipe is closer to the actual residual friction angle of the soil, which Bennett uses in his model. His lower-bound estimate provides the best solution as it accounts for soil arching that most accurately represents the state of stress in the soil.

Although still relatively high, Scherle's predictions with concrete pipe are closer to the actual jacking forces than with smoother pipe surfaces since Scherle developed interface friction coefficients for his model based on field experiments with concrete pipe. Therefore, Scherle's predictions with concrete pipe tend to be more accurate than for other pipe materials, as long as the installation depth is shallow. If the installation depth is significant, Scherle's prediction of normal stress will result in a very high estimate of jacking force even with concrete pipe.

Chapman's model is within 22.4 percent on the Eastside Interceptor projects when using his recommended jacking stress for sand.

5.4.3 Predicted Jacking Forces with Various Models on the Alvarado Trunk Sewer Project – Drive 17 (Polycrete Pipe)

On the Alvarado Project – Drive 17, the first 100 feet of the microtunnel drive jacking forces were compared to predicted jacking forces for the various models because that section of the drive was not lubricated. Table 5.27 shows the parameters that were used in the predictive models.

Table 5.27. Properties used in Various Jacking Force Predictive Models for the Alvarado Project – Drive 17

Parameters Used in Predictive Models						
Pipe Material	Polycrete	Soil Type	Medium Dense Sands	Depth to Crown	18 feet
Pipe Diameter	26-inch	Residual Friction Angle	29 degrees	Depth to Water	15 feet
Pipe Weight	185 lbs/ft	Soil Unit Weight	126 pcf	Interface Friction Coefficient (Scherle)	0.20
Interface Friction Coefficient (Staheli)	0.44	Bennett Arching Factor, C_a (unlubricated)	0.75 (Lower) 1.0 (Best) 1.5 (Upper)	Bennett Friction Factor, C_f (unlubricated)	1.0

Figure 5.19 shows the actual and predicted jacking forces for the first 100 feet of Drive 17 of the Alvarado tunnel project.

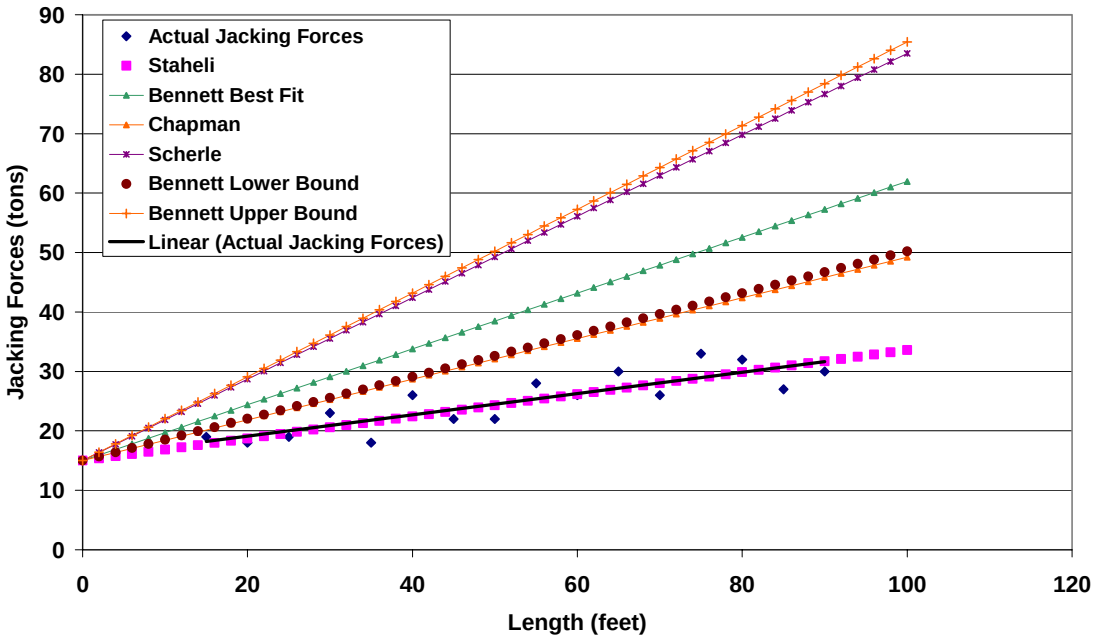

Figure 5.19. Length vs. Actual and Predicted Jacking Forces with a Variety of Predictive Models for the Alvarado Trunk Sewer – Drive 17.

Bennett's model has a high deviation because the interface friction coefficient between the site soil and the relatively smooth Polycrete Pipe is much lower than the internal angle of friction of the site soil used in his model.

Chapman's model significantly deviates from the actual jacking forces. Chapman correlates the overall jacking stress to the pipe diameter. This case history has a smaller diameter, and although the soils fall within his description of "sands," the diameter appears to be problematic for the model.

Scherle's predictive model yields high results due to the depth of burial of the microtunnel, resulting in high normal stress in Scherle's model and interface friction coefficients based on concrete pipe as opposed to the relatively smooth Polycrete pipe.

Table 5.28 presents the actual jacking stresses, and the jacking stresses predicted by each of the predictive models, along with the percent error as a function of the actual jacking stress.

Table 5.28. Comparison of Actual and Predicted Jacking Stresses and Percent Error for the Alvarado Trunk Sewer – Drive 17.

Model	Jacking Stress [tons/ft^2]	Percent Error [%]
Actual	0.026	-
Staheli	0.025	-3.9
Chapman	0.050	91.1
Bennett, Lower Bound	0.051	96.7
Bennett, Best Fit	0.069	161.2
Scherle	0.096	282.5
Bennett, Upper Bound	0.103	293.3

Note: % Error= (Actual Stress – Predicted Stress) / Actual Stress. Positive Value is indicative of under-prediction. Negative Value indicative of over-prediction.

5.4.4 Predicted Jacking Force with Varying Models on the Newark Subbasin Project – Drive 6 (Hobas Pipe)

On the Newark Subbasin Project – Drive 6, the first 55 feet of the microtunnel drive actual jacking forces were compared to the predicted jacking forces because that section of the drive was not lubricated. Table 5.29 shows the parameters that were used in the predictive models.

Table 5.29. Properties used in Various Jacking Force Predictive Models for the Newark Subbasin Project – Drive 6.

Parameters Used in Predictive Models							
Pipe Material	Hobas – CCFRPM		Soil Type	Dense Silty Sands		Depth to Crown	13 feet
Pipe Diameter	38.3-inch		Residual Friction Angle	26 degrees		Depth to Water	17 feet
Pipe Weight	208 lbs/ft		Soil Unit Weight	126 pcf		Interface Friction Coefficient (Scherle)	0.20
Interface Friction Coefficient (Staheli)	0.39		Bennett Arching Factor, C_a (unlubricated)	0.75 (Lower) 1.0 (Best) 1.5 (Upper)		Bennett Friction Factor, C_f (unlubricated)	1.0

Figure 5.20 shows the actual and predicted jacking forces on the first 55 feet of Drive 6 of the Newark Subbasin project.

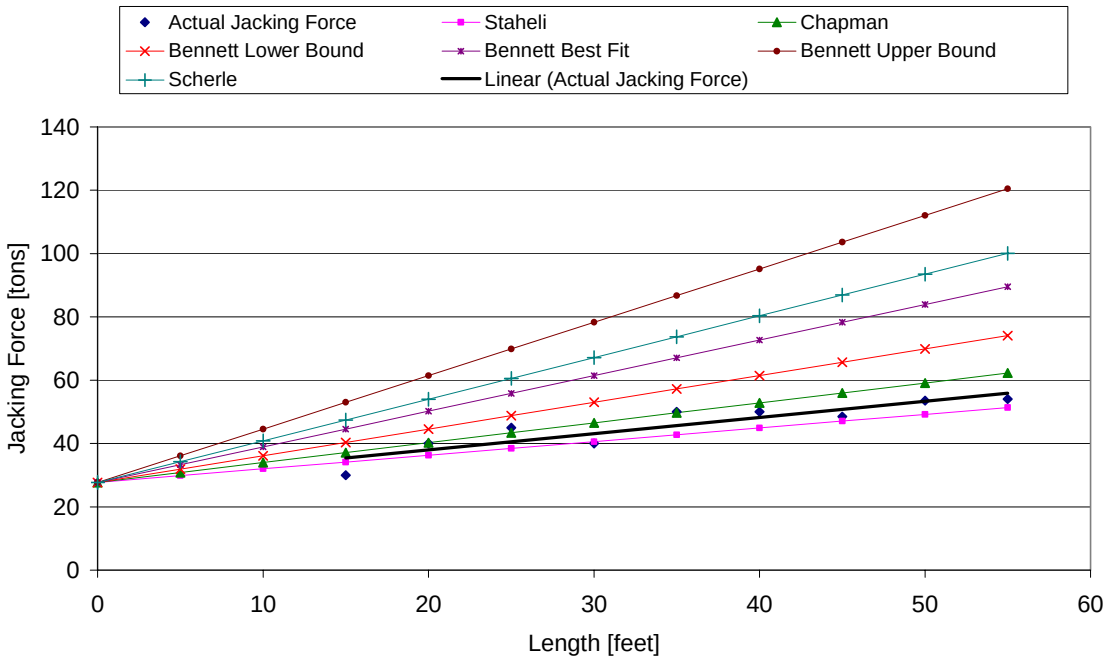

Figure 5.20. Length versus Actual and Predicted Jacking Forces with a Variety of Predictive Models for the Newark Subbasin Project – Drive 6.

The linear regression and the R^2 value shown in Figure 5.20 is for the actual jacking force data gathered during construction of the microtunnel. Bennett's model over-predicts because it uses the full friction angle of the soil to determine the interface frictional coefficient with the very smooth Hobas pipe. It should be noted that for Chapman's model, although within 23 percent, was predicted for "sand" where the site soil was highly silty sand and clayey sand, which might tend to lead to some confusion on the values for jacking stress that the user must choose. Sherle's model suffers from both the frictional component, as he uses interface frictional values indicative of concrete rather than the much smoother Hobas pipe, and the normal stress component due to the depth of burial of the pipe, resulting in a large over-prediction of jacking force.

Table 5.30 shows the actual jacking stresses on the drive, the jacking stresses predicted by each of the predictive models, and the percent error of each of the models as a function of the actual jacking stresses.

Table 5.30 Comparison of Actual and Predicted Jacking Stresses and Percent Error for the Newark Subbasin – Drive 6.

Model	Jacking Stress [tons/ft^2]	Percent Error [%]
Actual	0.051	-
Staheli	0.048	-16.0
Chapman	0.063	22.6
Bennett, Lower Bound	0.119	64.5
Scherle	0.156	119.3
Bennett, Best Fit	0.159	156.6
Bennett, Upper Bound	0.238	229.1

Note: % Error= (Actual Stress – Predicted Stress) / Actual Stress. Positive Value is indicative of under-prediction. Negative Value indicative of over-prediction.

5.5 Parametric Analysis of Predictive Model

A parametric analysis was performed on Equation 5.5 to determine which input parameter had the greatest impact on the calculated jacking force. Equation 5.5 is shown below:

$$JF_{frict} = \mu_{\text{int}} \frac{\gamma \cdot r \cdot \cos\left(45 + \frac{\phi_r}{2}\right)}{\tan \phi_r} \cdot \pi \cdot d \cdot l \qquad (5.5)$$

Where JF_{frict} = Frictional Component of Jacking Force [tons force]
μ_{int} = Pipe- Soil Residual Interface Friction Coefficient [unit-less]
γ = Total Unit Weight of the Soil [tons/ft^3]
ϕ_r = Residual Friction Angle of the Soil [degrees]
d = Pipe Diameter [feet]
l = Length of the Pipe [feet]

The parametric study was conducted on the pipe diameter, d; the total unit weight of the soil, γ; and the residual friction angle of the soil, ϕ_r. The soil residual interface friction coefficient, μ_{int}, is a function of the residual friction angle of the soil and is therefore integrally related to the parametric study of ϕ_r.

5.5.1 The Effect of Pipe Diameter on Frictional Jacking Forces

As one would expect, pipe diameter has the largest overall effect on frictional jacking forces. The frictional force takes place over the surface area of the pipeline, which is directly proportional to the pipe diameter. However, the normal stress is also a function of the pipe diameter, resulting in an overall jacking force that is a function of the diameter squared. A series of curves was generated for Permalok Steel pipe. A sandy soil with a unit weight of 130 pounds per cubic foot and a residual friction angle of 32 degrees was chosen for the analysis. This resulted in an interface friction coefficient of

0.524. Figure 5.21 shows length versus jacking force for pipe diameters ranging from 24 to 84 inches.

This data can then be evaluated at each length along the tunnel drive at the full range of pipe diameter to determine the relationship between the jacking force and the pipe diameter. Figure 5.22 shows the pipe diameter versus the jacking force at specific intervals along given tunnel drives, all tunneled with Permalok Steel pipe in a soil material with a 32-degree residual friction angle.

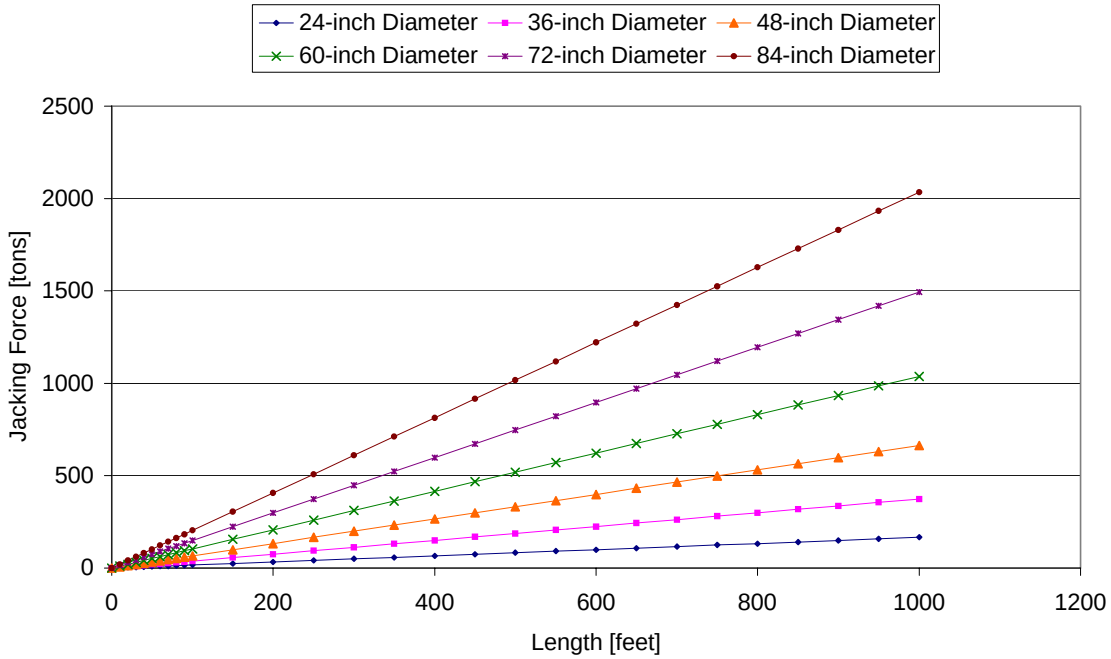

Figure 5.21. Length vs. Jacking Force for Pipe Diameters Ranging from 24 to 84 inches, Permalok Steel Pipe, 32 Degree Residual Friction Angle.

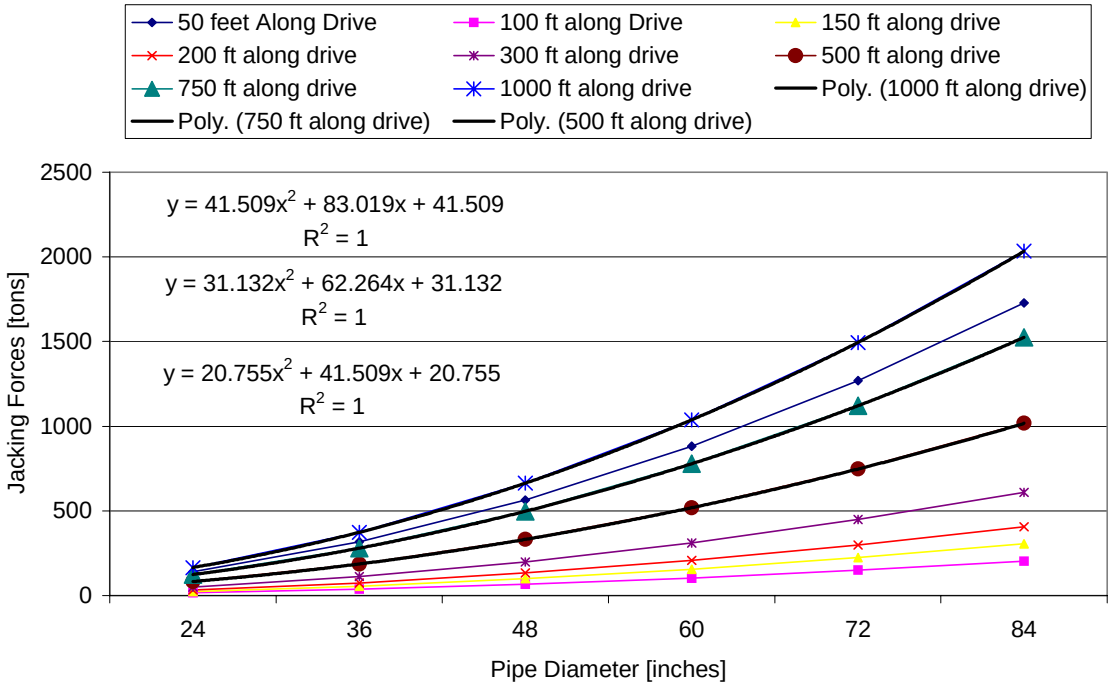

Figure 5.22. Pipe Diameter vs. Jacking Force for Permalok Steel Pipe Jacked in Sand with a 32-Degree Residual Friction Angle.

It is clear from Figure 5.22 that there is a quadratic relationship between the pipe diameter and the jacking force, i.e., the jacking force varies with the square of the diameter. The diameter has the greatest impact on the calculated jacking forces of all input parameters. Fortunately it is a parameter that is typically known and therefore provides little cause for error.

5.5.2 The Effects of Total Soil Unit Weight on Frictional Jacking Forces

The effects of unit soil weight were varied from 105 pcf to 145 pcf in Equation 5.5 to determine the effect on the jacking force. From examination of Equation 5.5, one can see that the jacking force is directly proportional to the total soil unit weight; therefore, as the unit weight is increased, the frictional component of the jacking force is also increased. Figure 5.23 shows the frictional component of the jacking force on a

1,000-foot tunnel drive for a 48-inch Permalok steel pipe in soil with a varying total unit weight from 105 to 145 pcf. For the purposes of the parametric analysis the residual friction angle is held constant at 32 degrees, resulting in a interface residual friction coefficient of 0.524. Figure 5.24 shows the total soil unit weight as a function of the jacking force at different lengths along tunnel drives to determine the total effect of the unit weight.

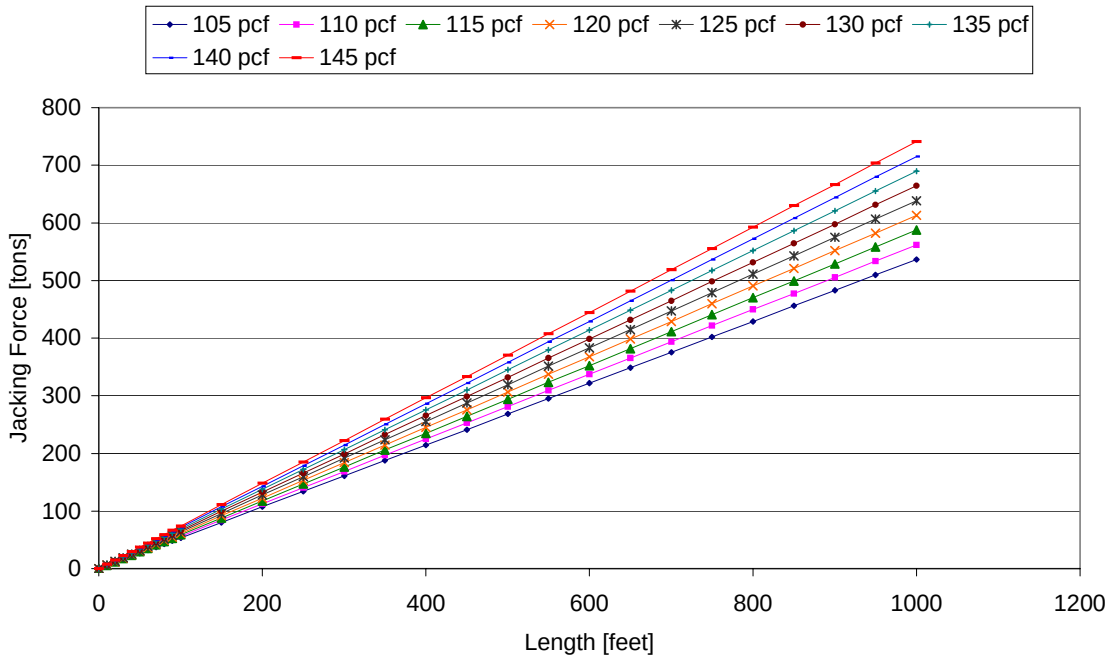

Figure 5.23. Tunnel Length vs. Jacking Force for Varying Total Soil Unit Weight with a 48-inch Permalok Steel Pipe with a 32-Degree Residual Friction Angle.

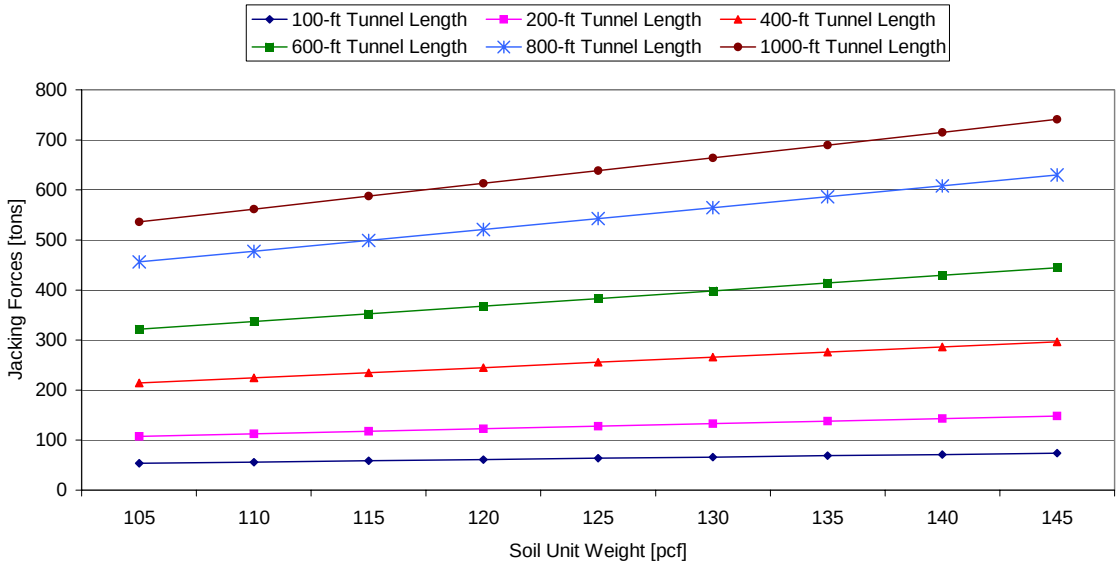

Figure 5.24. Total Soil Unit Weight. Vs. Jacking Force for Varying Lengths along Tunnel Drives.

Figure 5.24 shows that as the soil unit weight increases from 105pcf to 145 pcf, a 38.1% increase, the jacking force increases 38.1%. This variability in this parameter has the potential to introduce error into the calculation of the predicted jacking forces as the soil unit weight will change over the length of the tunnel, and may not be accurately estimated from the geotechnical borings taken at the site. Providing more thorough site investigations that allow the determination of soil unit weights are a key factor in reduction of this error. Site soil investigations may need to include a variety of tools to adequately characterize the site including cone penetration testing, soil sampling with large diameter auger rigs to identify larger particles, and careful sampling, logging, and sample preservation on standard vertical soil boring rigs to collect accurate "undisturbed" samples for laboratory testing.

5.5.3 The Effect of Residual Friction Angle on Frictional Jacking Forces

The effect of the residual friction angle is multifaceted since the residual friction angle is used to determine the normal stress as it contributes to the arching of the soil and as it dictates the interface friction coefficient between the soil and the pipe material. In addition, the relationship between the residual friction angle and the residual friction coefficient was unique for each pipe material. When evaluating this parameter it became clear that it was necessary to evaluate the normal stress and the interface frictional component independently prior to combining the effects to completely understand the effect of the residual friction angle on the frictional component of the jacking force.

5.5.3.1 Residual Friction Angle and Normal Stresses

The jacking force model, Equation 5.5, uses Equation 5.4 for calculating the normal stress as shown below:

$$\sigma_v = \sigma_{v\infty} = \frac{\gamma \cdot r \cdot \cos\left(45 + \frac{\phi}{2}\right)}{\tan\phi} \qquad (5.4)$$

The jacking force model uses the residual friction angle of the soil for the value of ϕ shown in equation 5.4. Normal stresses were calculated using Equation 5.4 for a range of residual friction angles from 25 to 40 degrees. A pipe radius of two (2) feet was used and a soil unit weight of 130 pcf was used for the calculation. Figure 5.25 shows the normal stress as a function of the residual friction angle.

Figure 5.25 shows a clearly decreasing trend in normal stress with increasing residual friction angles. This illustrates Terzaghi's Arching Theory, showing that soils with higher residual friction angles have higher shear strength parameters and are able to

withstand higher shear stresses in the walls above the pipeline, hence exhibiting more arching characteristics resulting in lower normal stresses on the pipeline.

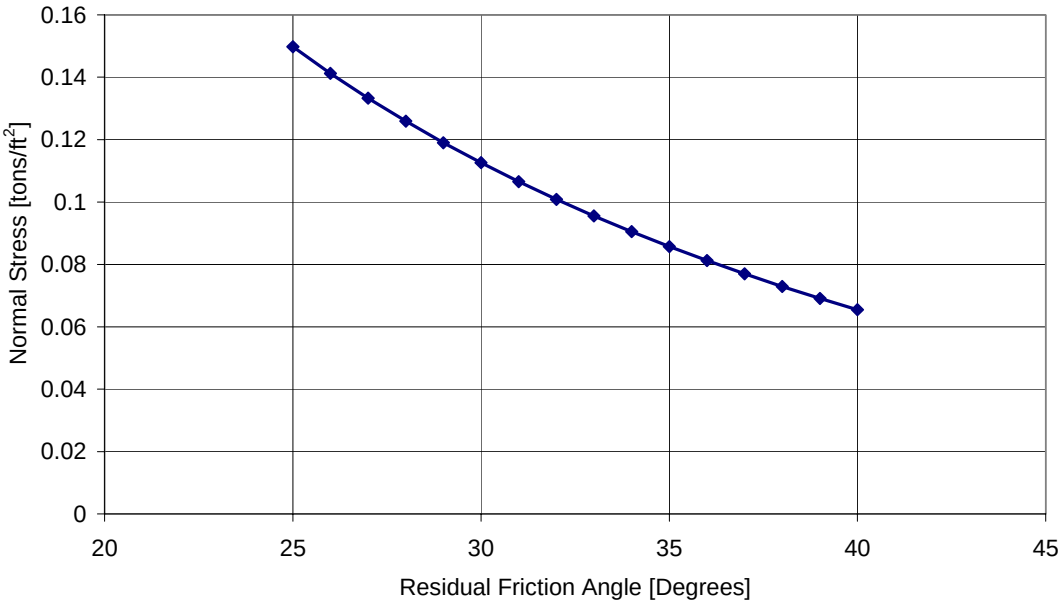

Figure 5.25. Residual Friction Angle vs. Normal Stress

5.5.3.2 Residual Friction Angle and Interface Friction Coefficient

Interface friction coefficients were measured for each pipe material with two types of granular soil with different residual friction angles (refer to Chapter 3). Residual interface friction values were then extrapolated for soils with interface friction angles ranging from 25 to 40 degrees. The difference in the residual friction angles of the soils that were sheared on the pipe materials was 6.7 degrees (34.6 degrees for the residual friction angle of the Atlanta Blasting Sand and 27.9 degrees for the Ottawa 20/30 sand). However, when these sands were sheared at the pipe interfaces with different roughness

values, not only was the friction angle at the interface higher with increasing roughness, but the absolute difference between the friction angle at the interface also varied for different pipe surface roughness characteristics as shown in Table 5.31.

Table 5.31. Variation in Absolute Difference of Interface Friction Coefficients and Angles when Sheared Against Ottawa 2030 and Atlanta Blasting Sand on Pipes with Varying Roughness

Pipe Material	μ_{int}, with Ottawa 20/30	ϕ_{int} with Ottawa 20/30 [°]	μ_{int} with Atlanta Blasting	ϕ_{int} with Atlanta Blasting [°]	Difference in $\mu_{int,}$	Difference in ϕ_{int},
Polycrete	0.43	23.27	0.49	26.10	0.06	2.84
Hobas	0.44	23.75	0.56	29.25	0.12	5.50
Permalok Steel	0.44	23.75	0.58	30.11	0.14	6.36
Wet Cast Concrete	0.48	25.64	0.58	30.11	0.10	4.47
Vitrified Clay	0.48	25.64	0.61	31.38	0.13	5.74
Packerhead Concrete	0.53	27.92	0.62	31.80	0.09	3.88

Once the values for interface friction coefficient are extrapolated over a wider range of soil residual friction values, these trends can be seen more clearly, as shown in Figure 5.26.

Figure 5.26 shows that it is not only the absolute value of the interface friction coefficient that is different for pipes with varying surface roughness characteristics, but also the rate of change of the interface friction coefficient with the residual friction angle that impacts the overall jacking force, based on the residual friction angle used in the model.

5.5.3.3 Residual Friction Angle and the Coupled Impacts of Normal Stress and Interface Friction Coefficients

When the combined effects of soil residual friction angle on the normal stress and the interface friction coefficient are considered it is noteworthy that as the soil residual friction coefficient increases the normal stress decreases while the interface friction coefficient increases, thus creating a canceling effect in the lower values of soil

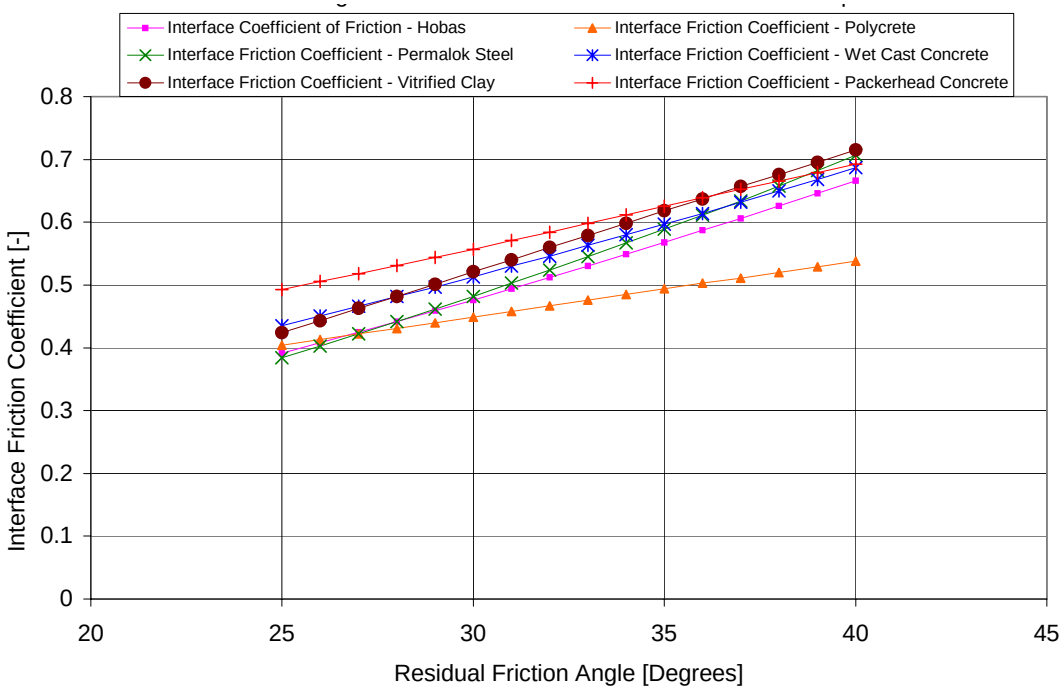

Figure 5.26. Residual Friction Angle vs. Interface Friction Coefficient for Different Pipe Materials.

residual friction angle. However, at higher values of soil residual friction angle, the normal stress decreases faster than the interface friction coefficient decreases, resulting in an overall decrease in jacking force with increasing soil residual friction angles. Figure 5.27 shows length versus jacking force for 48-inch Permalok Steel pipe on a variety of 1000-foot tunnel drives with soil having a unit weight of 130 pcf and varying residual friction angles ranging from 25 to 40 degrees. The effect of the decreasing normal stress

and the increasing interface friction coefficient can be seen if the jacking forces for the series of curves in Figure 5.27 are evaluated at specific lengths along the tunnel drives.

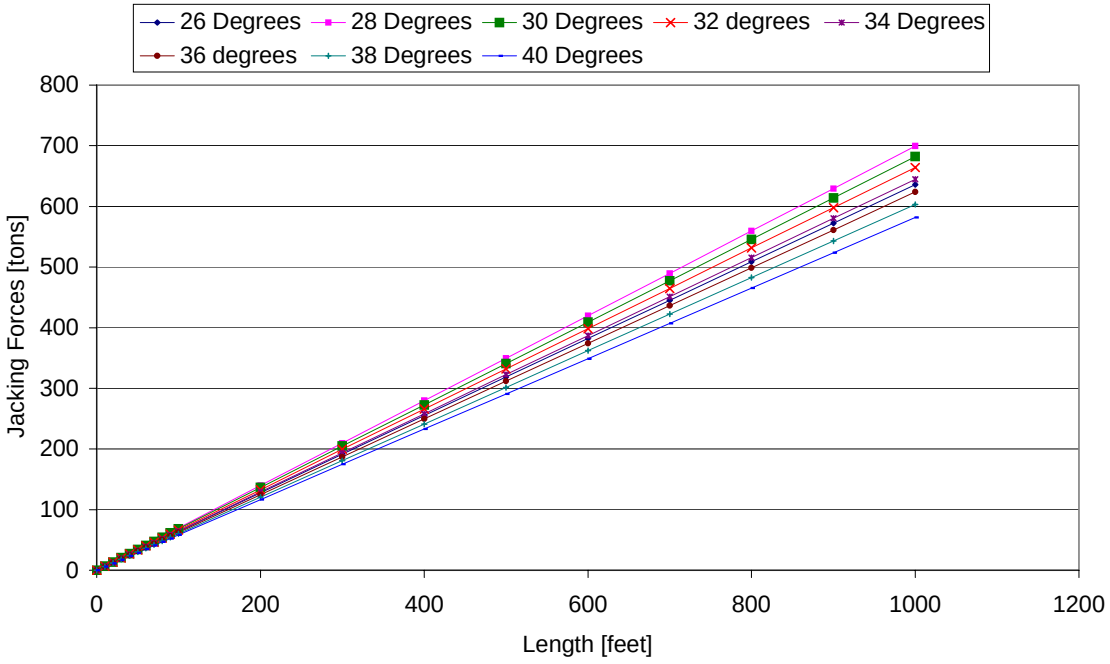

Figure 5.27. Length vs. Jacking Force for a variety of Residual Friction Angles.

Figure 5.28 shows the jacking force as a function of the soil residual friction angle at various lengths along the tunnel drives.

When all pipe materials are shown at a distance of 500 feet into a tunnel drive, a plot can be generated that shows residual friction angle versus jacking force, as seen in Figure 5.29. Figure 5.29 shows the predicted jacking force for a 48-inch pipe for a variety of pipe materials if the tunnel length were 500-feet and the soil unit weight were 130 pcf.

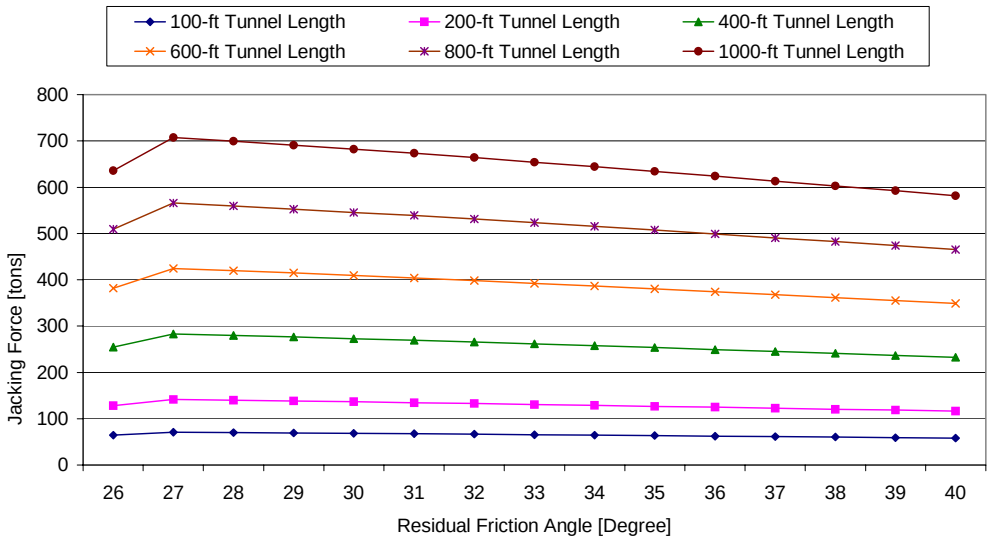

Figure 5.28. Residual Friction Angle vs. Jacking Force at Various Lengths along Tunnel Drives.

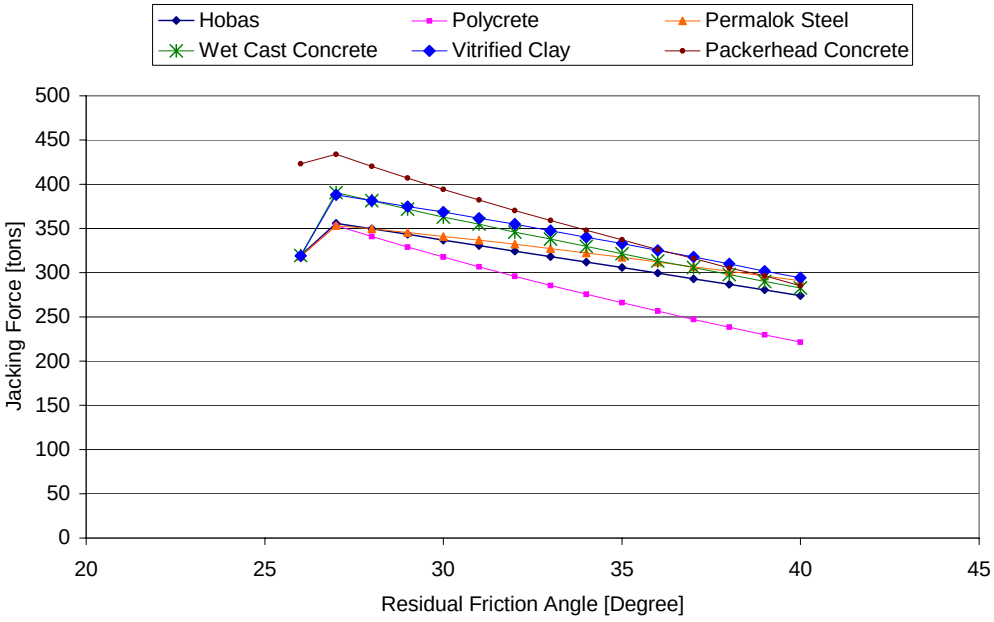

Figure 5.29. Residual Friction Angle vs. Jacking Force for a Variety of Pipe Materials on a Tunnel Drive 500 feet in Length.

It is apparent from the graph that the effect of the residual friction angle on the jacking force will be different for each pipe material. Table 5.32 details the absolute deviation in jacking force that can result as an effect of changing the residual friction angle in the model between 25 and 40 degrees for each pipe material.

Table 5.32. Sensitivity of Jacking Force Model to Soil Residual Friction Angle by Pipe Material.

Pipe Material	Absolute Change in Frictional Jacking Force by Changing Residual Friction Angle between 25 and 40 Degrees [%]
Hobas	21.7
Polycrete	35.1
Permalok Steel	16.8
Wet Cast Concrete	25.9
Vitrified Clay	22.9
Packerhead Concrete	32.1

5.5.4 Overview of Parametric Analysis

The parametric analysis of the predictive model revealed that the frictional component of the jacking force is a function of the square of the pipe diameter. This is because the normal stresses are independent of depth and based on Terzaghi's Arching Theory, with the calculated soil arching as a function of the pipe radius. The normal stress then multiplied over the pipe surface area, also a function of the diameter.

The frictional component of the jacking force is combined to be directly proportional to the total unit weight of the soil; therefore, it is important to collect accurate geotechnical information or base estimates of unit weights on accurate soil descriptions. Tables providing guidance on selection of unit weights based on soil descriptions and other parameters can be found in Appendix A. Based on a unit weight

range of 105 to 145 pounds per cubic foot, the estimate of frictional jacking force would be impacted up to 38%.

The residual interface friction angle of the soil affects both the normal stress and the interface friction coefficient component of the frictional jacking force. As the residual internal friction angle of the soil increases, the normal stress decreases while the interface friction coefficient between the soil and the pipe increases. These phenomena have a counter-balancing effect. In addition, the overall magnitude of the effect is different for each pipe material, depending on material roughness. As a result, over the range of residual internal friction angles of 25 to 40 degrees, the impact on the frictional jacking force ranges from 17 to 35 percent, depending on pipe material.

5.6 Summary

Interface friction coefficients have been established for a variety of pipe materials and granular soil conditions, and a model for predicting jacking forces in unlubricated ground has been presented. In reality, many microtunneling projects have lubrication applied to the pipeline at some stage in the pipe jacking process. Therefore, it is necessary to understand the effects of lubrication to account for these effects in the jacking force model.

CHAPTER 6

EFFECTS OF LUBRICATION ON JACKING FORCES

The prediction and analysis of jacking forces thus far has been focused on non-lubricated jacking forces. This allowed the identification of the mechanisms controlling jacking forces, as well as correlation between interface friction values measured in the laboratory environment and jacking forces measured in the field. However, in practice, lubrication is commonly used to decrease and/or control jacking forces within a manageable range, as seen in the case histories presented in Chapter 4.

6.1 Lubrication Equipment, Materials, and Application Strategies

While the practice of using lubrication is fairly standard, lubrication practices are far from standard. There are a number of lubrication strategies that can be used with pipe jacking. These include lubricating from the beginning of the tunnel to maintain lower overall jacking forces, applying larger volumes of lubrication should jacking forces increase. Other strategies include pumping minimal amounts of bentonite, ensuring the capacity of the pipe or equipment are not exceeded. With this strategy small batching plants that hold only a few hundred gallons of bentonite are used to mix the lubrication, such as the plant shown in Figure 6.1. Still another strategy is to pump significantly high volumes of lubrication to ensure that jacking forces remain low throughout the entire drive to mitigate any potential problems that could occur due to elevated jacking forces. Large bentonite plants capable of mixing thousands of gallons, such as the plant shown in Figure 6.2 are used for such a strategy.

Figure 6.1. Small Bentonite Lubrication Batching Plant.

Figure 6.2. Fully Contained, Dual Mixer/Pump Bentonite System.

In addition to the several bentonite batching systems available, there are a number of lubrication materials that are available for use with microtunneling and pipe jacking systems, including polymers and bentonite mixed with a variety of polymer additives. However, bentonite is the most commonly used material due to proven effectiveness, ease of availability, and low cost.

There is also a variety of ways to configure the pipeline with lubrication ports for effective delivery of bentonite to the annular space. The annular space is defined as the space between the largest diameter excavated and the machine and/or pipe. Lubrication ports are typically one (1) to two (2) inches in diameter and are drilled through the pipe wall. They are fitted with a one-way check valve to allow lubrication to be pumped to the outside of the pipe while keeping groundwater from outside the pipeline from flowing into the pipeline. Figure 6.3 shows a typical lubrication port in a Hobas pipe.

Figure 6.3. Lubrication Port in Hobas Pipe.

Lubrication ports are typically located at 10-to 20-foot linear spacing along the pipe string and can be inserted along the pipeline at any circumferential location. Contractors most commonly insert the lubrication ports between the 10-o'clock and 2-o'clock positions around the circumference of the pipeline. However, occasionally contractors will place lubrication ports between the 4-o'clock and 8-o'clock positions. Because the lubrication systems are typically operated from a manifold system, most contractors do not place lubrication ports on the bottom 1/3 of the pipeline because they believe that lubrication will not pump to those ports due to the weight of the pipe. It is, therefore, very rare to see lubrication ports on the bottom of the pipeline during pipe jacking operations.

6.2 Evaluation of Case Histories with Lubricated Segments

A number of the case histories presented in Chapter 4 contained unlubricated intervals immediately followed by lubricated segments. This allowed a comparison of the behavior of the non-lubricated interface frictional characteristics with those of the lubricated sections of the pipeline. While some of the case histories provided excellent information on the locations and volumes of lubrication pumped, others provided only limited information. However, there were some compelling trends in the data between case histories with similar soil conditions and lubrication histories.

6.2.1 South Tahoe Highway 50 Crossing Lubrication Analysis

The South Lake Tahoe Highway 50 Crossing was a 59.5-inch O.D. Wet Cast Concrete pipe that was installed with open shield pipe jacking for approximately 250 feet beneath Highway 50. The project is described in detail in Section 4.5. The first approximately 150 feet of the drive was not lubricated and the jacking forces increased in

a linear fashion to approximately 170 tons. At 150 feet into the drive, the contractor realized that the jacking forces would soon exceed the available capacity of the jacking frame. Thus, a 2-inch lubrication line was attached to each lubrication port in the pipeline. Lubrication ports were located in each pipeline (20-feet apart) at the 12-o'clock position. Bentonite lubrication was pumped during pipe jacking. Subsequent pipe sections were connected to the lubrication system as pipe jacking continued. Figure 6.4 shows the jacking forces for the drive.

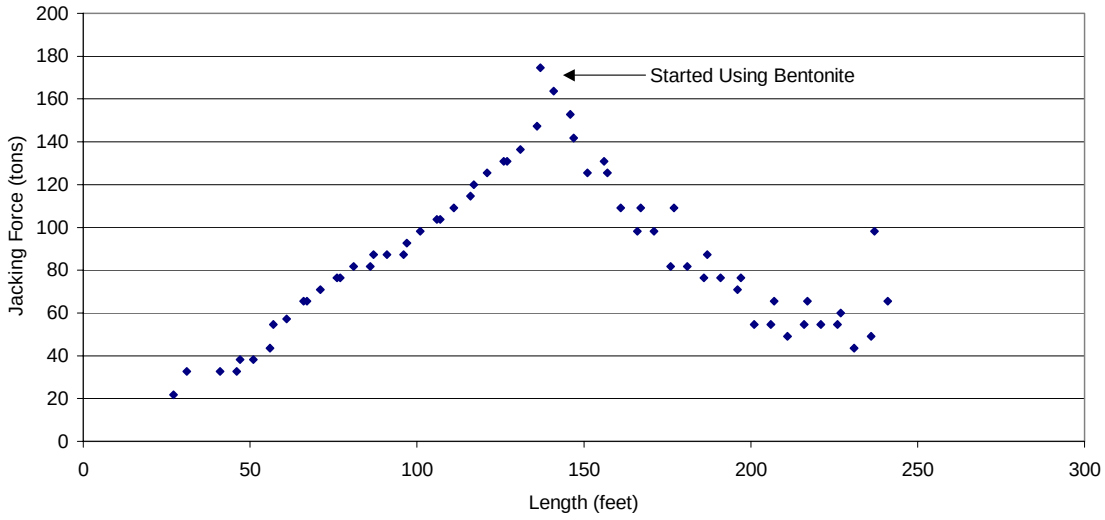

Figure 6.4. Length vs. Jacking Force for the South Lake Tahoe Highway 50 Crossing.

The interface friction coefficient between the wet cast concrete and the dense sand at the site was calculated to be 0.60 (see Section 5.3.4) after accounting for the model error. When the lubrication begins, lubrication is pumped from the tail section of the open-shield tunneling machine, and from each 20-foot pipe segment back to the pipe. Therefore, the distribution of lubrication over the pipeline is gradual as the pipe jacking

process is continuing forward. Figure 6.5 shows a schematic representation of lubrication distribution as the pipeline is jacked forward on the South Tahoe Project.

From the onset of lubrication injection, jacking forces began decreasing over the next 50 feet. Analysis of Figure 6.4 shows that the decrease in jacking forces is uniform in the zone from 150 to 200 feet, after which the jacking forces then remain constant or show a slight increase with length. The linear decrease in jacking force between 150 and 200 feet indicates that the lubrication is distributed over the pipeline in a uniform fashion. The pipeline is assumed to be fully lubricated at 200 feet. The lubricated interface friction coefficient, $\mu_{int.lube}$, is 0.06 or 10% of the non-lubricated interface friction coefficient.

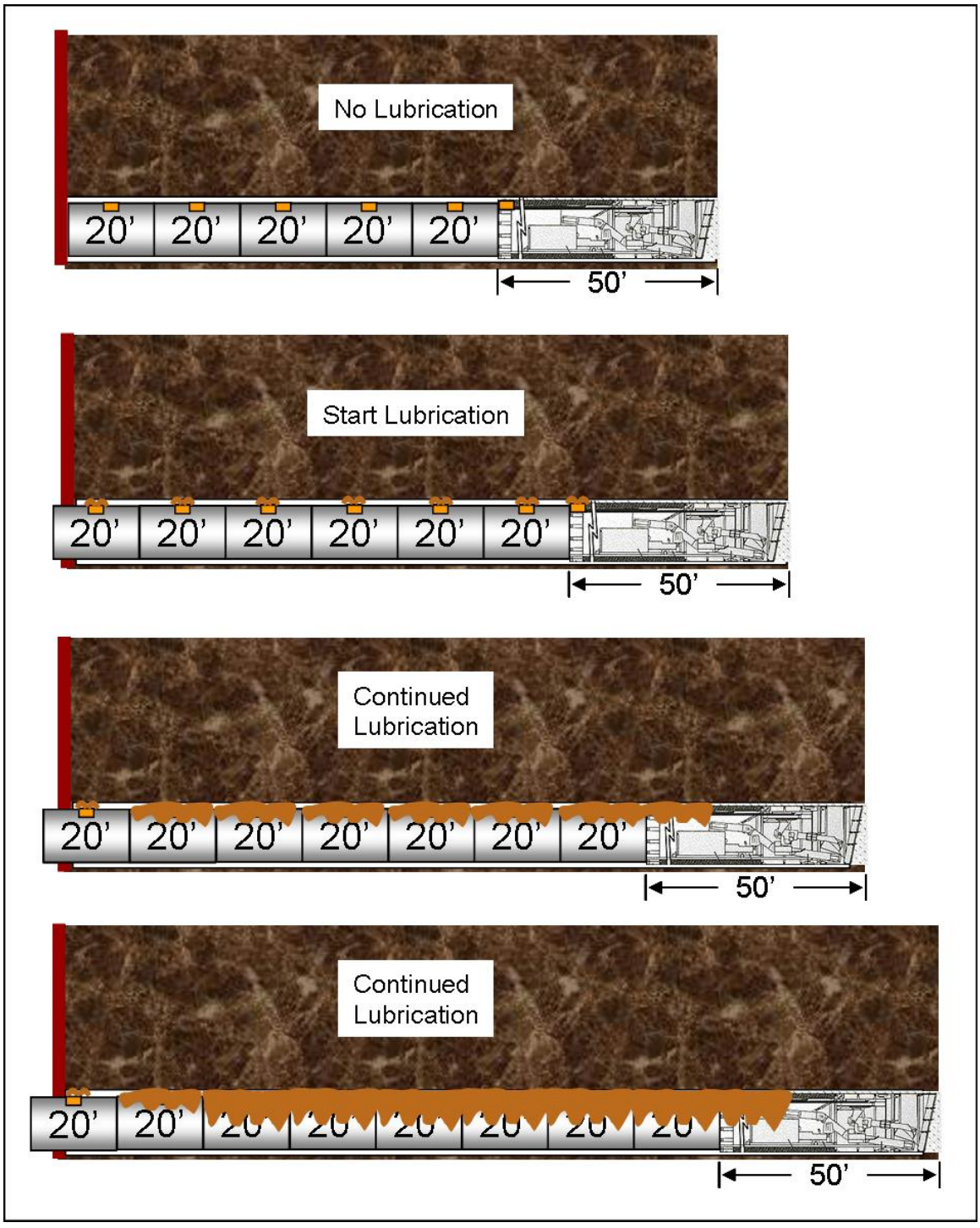

Figure 6.5. Schematic of Lubrication Sequence as Pipeline Progresses Forward during Pipe Jacking Operations.

Figure 6.6 shows the actual and predicted jacking forces using a non-lubricated interface friction coefficient of 0.6, and a lubricated interface friction coefficient of 0.06.

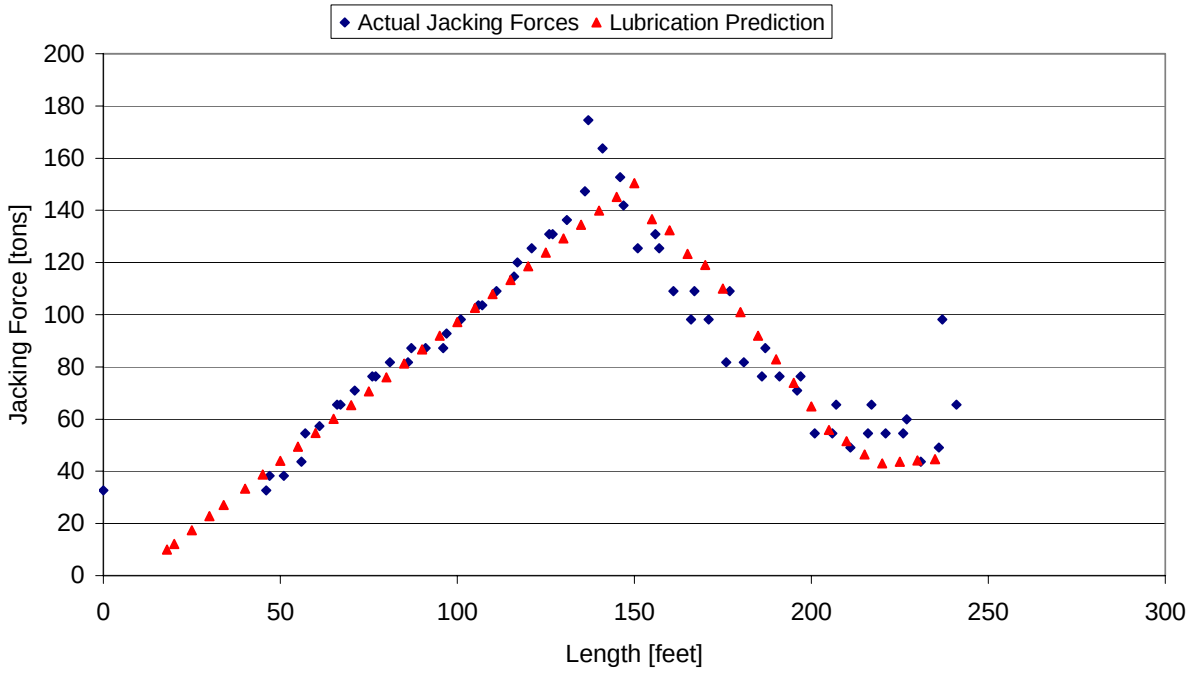

Figure 6.6. Length vs. Actual Jacking Forces and Predicted Lubricated Jacking Forces for the South Tahoe Highway 50 Crossing.

6.2.2 Eastside Interceptor- Houser Way Lubrication Analysis

The Houser Way drive of the Eastside Interceptor Project was an 87.5-inch Packerhead Concrete microtunneling drive approximately 675 feet long. The project is described in detail in Section 4.7. The first 120 feet of the pipeline was not lubricated and the jacking forces increased quickly to approximately 450 tons. The bentonite system was then activated and pumped liberally throughout the remainder of the microtunneling. The microtunneling system used on the project had a highly

sophisticated automated bentonite system that allowed pumping from several ports in the pipeline at different pressures and different rates. As a result, a tremendous amount of detailed lubrication information was gathered during tunneling. Details of the lubrication implementation are included in Section 4.7.5. It is important to note that very large quantities of bentonite were pumped on this project. The contractor had a bentonite tank with a capacity of several thousand gallons of bentonite. On more than one occasion, bentonite migrated from the pipeline to the street and into other neighboring sewers in the immediate vicinity of the pipeline.

Figure 6.7 shows the jacking forces as a function of length along the Houser Way alignment. Once the pumping of bentonite commenced, it is clear from the graph that jacking forces decreased in a uniform fashion until approximately 200 feet in the alignment, after which the jacking forces are then seen to gradually increase over the remainder of the drive. When lubrication commenced, lubrication ports were connected at the tail section of the machine, 25 feet from the cutting edge of the machine; in the first pipe section, 31 feet from the cutting edge of the machine; and in the fifth pipe section, 78 feet from the cutting edge of the machine.

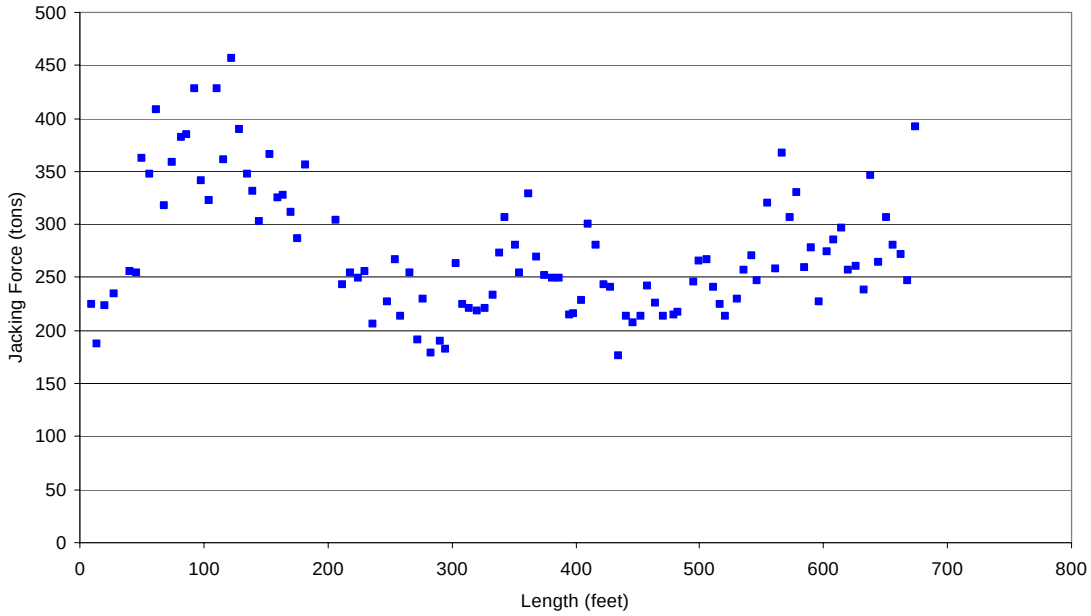

Figure 6.7. Length vs. Jacking Forces for the Eastside Interceptor Houser Way Drive.

The actual unlubricated interface friction coefficient, μ_{int}, between the packerhead concrete and the sand at the site is 0.53 (see Section 5.3.5) in the first 120 feet of the drive after accounting for the model arror. Assuming that the lubrication is distributed uniformly over the pipe surface area throughout the zone between 120 and 200 feet, the lubricated interface friction coefficient becomes 0.05 or 10% of the non-lubricated interface friction coefficient. Figure 6.8 show the actual jacking forces, the predicted jacking forces through the unlubricated zone, and the lubricated prediction for the jacking forces using 10% of the unlubricated interface friction coefficient.

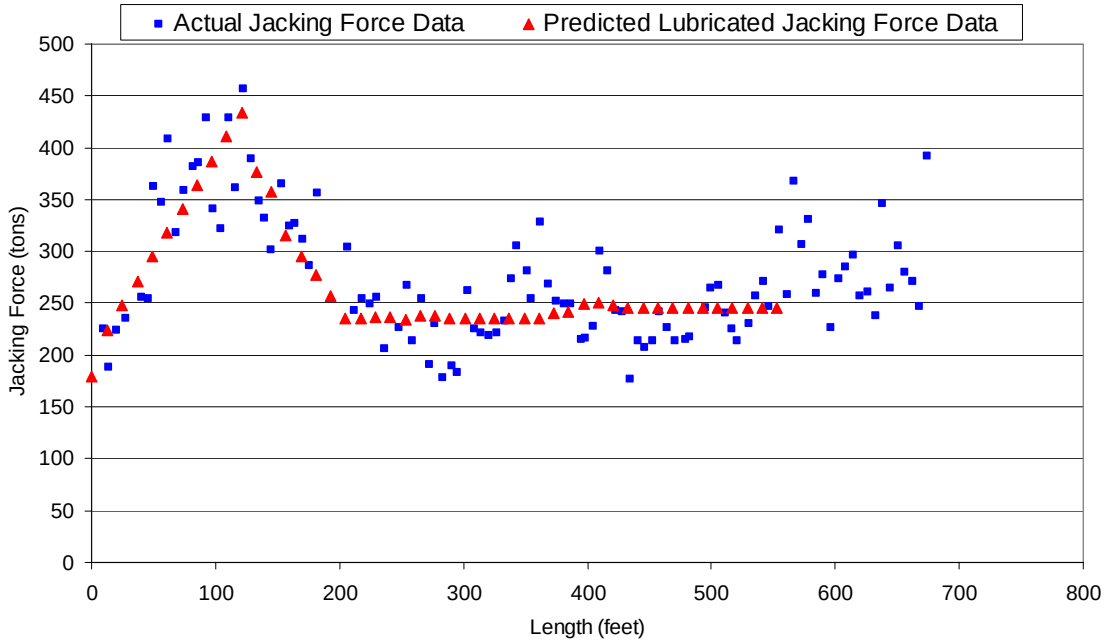

Figure 6.8. Length vs. Actual Jacking Forces and Predicted Lubricated Jacking Forces for the Eastside Interceptor Project – Houser Way Drive.

6.2.3 Clearview Snohomish River Crossing 2001 Lubrication Analysis

The Clearview Snohomish River Crossing 2001 Project was a 60-inch Permalok Steel Pipe that was microtunneled approximately 550 feet beneath the Snohomish River. The project is described in detail in Section 4.3. The first 90 feet of the microtunnel was not lubricated. The jacking forces over the first 90 feet quickly increased to approximately 120 tons. Lubrication ports were connected to a 2-inch lubrication hose at the tail section of the microtunneling machine, 20 feet from the cutting edge of the machine; and in the first pipe section, 35 feet from the cutting edge of the machine, and bentonite was pumped thorough the ports.

This project did not have a large bentonite system or an automated bentonite system but instead has a small batching plant as shown in Figure 6.1. Towards the

beginning of the drive when many construction activities were simultaneously occurring, labor personnel were extremely busy and the bentonite system was not a priority. As a result, the bentonite lubrication was not applied continuously to the pipeline. From 90 feet to 150 feet into the drive the bentonite system completely drained while the lubrication was pumping and the system was not replenished. From 150 to 240 feet into the drive, bentonite was not pumped along the pipeline. Bentonite pumping resumed at 240 feet and was pumped from 240 feet until approximately 275 feet into the drive. At 275 feet into the drive, the bentonite system once again ran dry and bentonite was not flowing to the pipeline between 275 and 340 feet. Figure 6.9 shows the jacking forces between the launch and 350 feet into the drive.

The actual non-lubricated interface friction coefficient, μ_{int} , between the Permalok Steel pipe and the silty sand with gravel at the site over the first 90 feet of the microtunnel drive is 0.6 (See Section 5.3.3) after accounting for the model error. Once the lubrication is applied to the pipeline at 90 feet into the drive, the jacking forces begin to decrease in a uniform fashion until the lubrication is stopped at 150 feet into the drive. Assuming that the lubrication is distributed uniformly over the pipeline between the interval between 90 and 150 feet, the lubricated interface friction coefficient, $\mu_{int.lube}$, is 0.06, or 10% of the non-lubricated interface friction coefficient. Figure 6.10 shows the non-lubricated prediction of jacking force, followed by the lubricated prediction through the first lubricated segment between 90 and 150 feet of the drive.

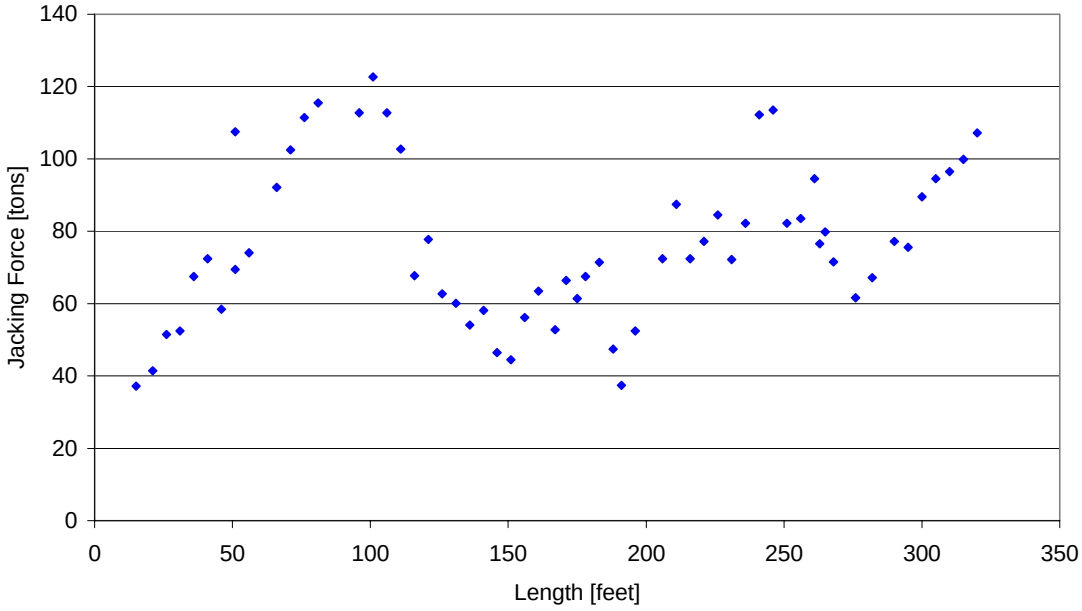

.

Figure 6.9. Length vs. Jacking Forces for the first 350 feet of the Clearview Snohomish River Crossing 2001.

Once lubrication stopped after 150 feet into the drive, jacking forces began to increase. This segment between 150 and 240 feet has both lubricated and unlubricated portions. The interface friction coefficient is therefore an effective value accounting for both lubricated and unlubricated zones. The calculated effective interface friction coefficient in this zone is 0.35, as shown in Figure 6.11.

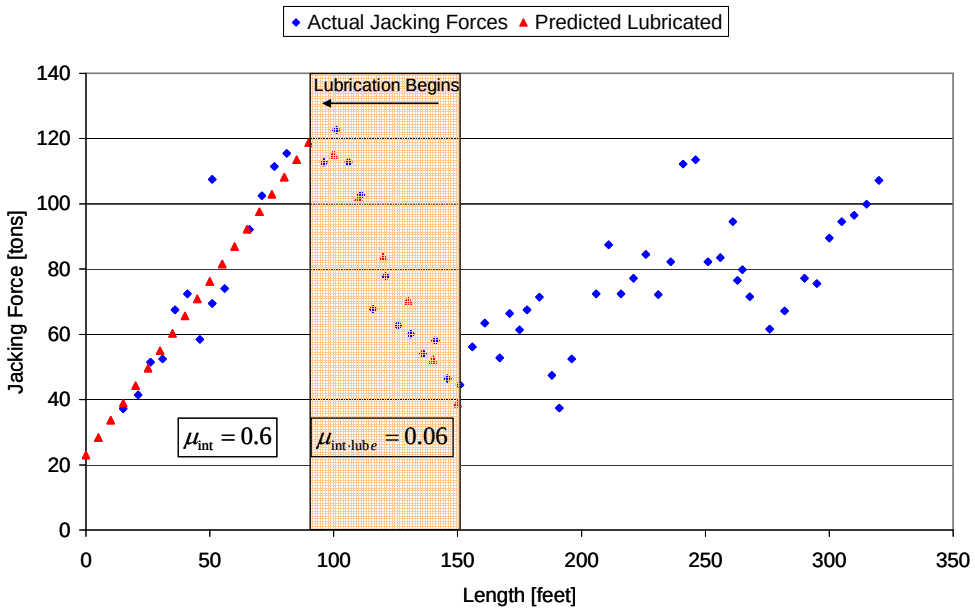

Figure 6.10. Length vs. Actual Jacking Forces and Predicted Lubricated Jacking Forces for the first 150 feet of the Clearview Snohomish River Crossing 2001.

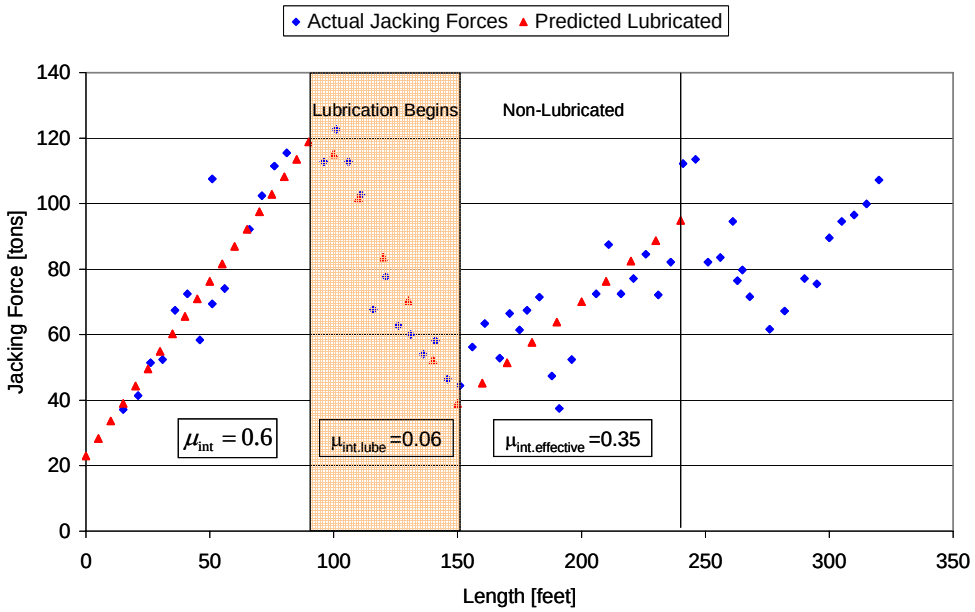

Figure 6.11. Length vs. Actual Jacking Forces and Predicted Lubricated Jacking Forces for the first 240 feet of the Clearview Snohomish River Crossing 2001.

At 240 feet into the drive, lubrication is again pumped at the port in the tail section of the machine; in the lubrication port in the first pipe section, in the lubrication port in the third pipe section, 70 feet behind the cutting edge of the machine; and in the seventh pipe section, 110 feet behind the cutting edge of the machine. Again, the jacking forces decrease in a uniform fashion in the distance between 240 and 275 feet where lubrication is once again stopped. Assuming that the lubrication is uniformly distributed over the surface area of the pipeline, the lubricated interface friction coefficient between 240 and 275 feet along the drive is 0.06 or 10% of the non-lubricated interface friction coefficient. Figure 6.12 shows the actual jacking forces and the predicted lubricated jacking forces from the beginning of the drive through 275 feet with the lubricated interface friction coefficients.

At 275 feet into the drive, lubrication was stopped once again until 340 feet. The jacking forces increase throughout this segment; however, the interface friction coefficient is a combination of two unlubricated segments and two lubricated segments. At the beginning of this segment, the overall non-lubricated length is 230 feet (0 to 140 feet and 150 to 240 feet) and the lubricated length is 95 feet. The jacking forces throughout this segment increase with an effective interface friction coefficient, $\mu_{int.effective}$, of 0.5. Figure 6.13 shows the actual jacking force and the predicted lubricated jacking force from the beginning of the drive through 340 feet with the lubricated and non-lubricated interface friction coefficients.

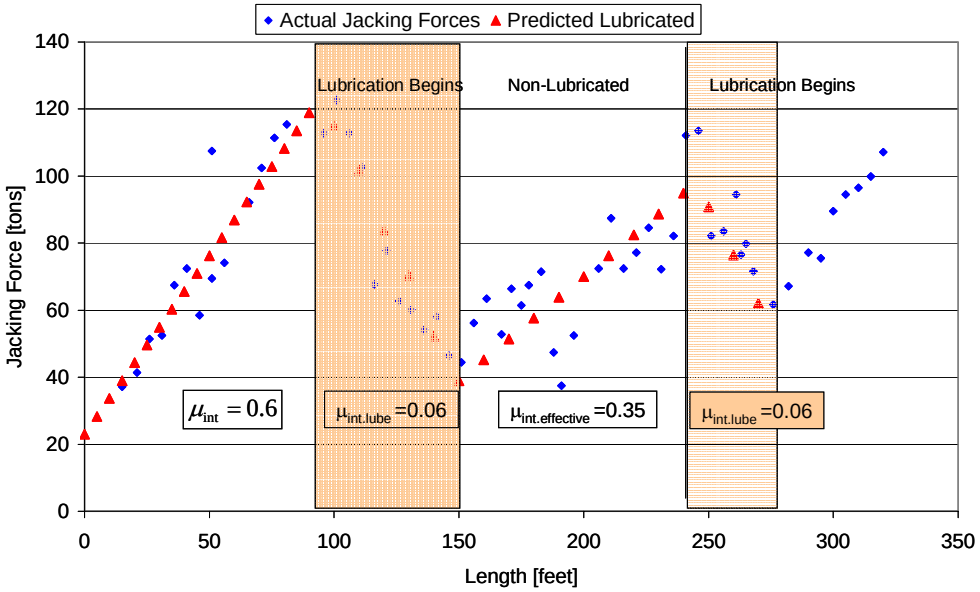

Figure 6.12. Length vs. Actual and Predicted Lubricated Jacking Forces through 275 feet for the Clearview Snohomish River Crossing 2001.

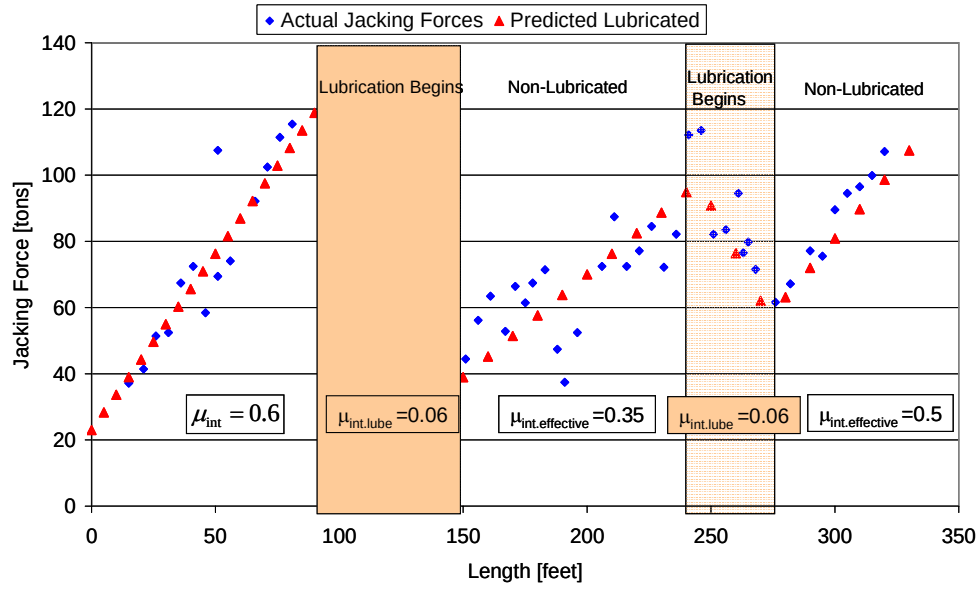

Figure 6.13. Length vs. Actual and Predicted Lubricated Jacking Forces through 340 feet for the Clearview Snohomish River Crossing 2001.

6.2.4. Clearview Snohomish River Crossing 2002 Lubrication Analysis

The Clearview Snohomish River Crossing 2002 was constructed nearly parallel to the 2001 crossing, starting at a depth of 85 feet, which is 20-feet deeper than the 2001 crossing. The microtunnel was constructed with 60-inch Permalok Steel pipe on a tunnel drive that was approximately 1,100 feet in length. A detailed description of the project can be found in Section 4.4. Unlike the 2001 Crossing, the 2002 Snohomish River Crossing used an automated bentonite lubrication system that was capable of pumping bentonite to the pipeline through several ports along the pipeline. However, the automated system was new to the contractor who experienced some technical difficulty with the system. As a result, the application of bentonite was less than optimum and the reduction in the interface friction coefficient did not reach the full potential. Figure 6.14 shows the jacking forces throughout the microtunnel drive.

Lubrication was applied between 50 and 110 feet within the tunnel drive. Within this segment, the jacking stress was 0.056 tons/ft^2. This jacking stress is equal to a lubricated interface friction coefficient, $\mu_{int.lube}$, of 0.5. From the Snohomish River Crossing 2001 Project, the non-lubricated interface friction coefficient, μ_{int}, through this segment was found to be 0.6. Therefore, the lubrication through this segment reduced the interface friction coefficient by 17%. Between 110 feet and 810 feet into the drive the lubrication was pumped in every other pipe at varying intervals and in varying amounts. Although the records of the exact locations and amounts are not available, gross volumes of bentonite were recorded. It was verified that in the segment between 110 and 810 feet, the total volume of bentonite pumped exceed the annular volume by 5.2 times. This

massive volume of bentonite kept the jacking forces below 200 tons over the 800 feet of length.

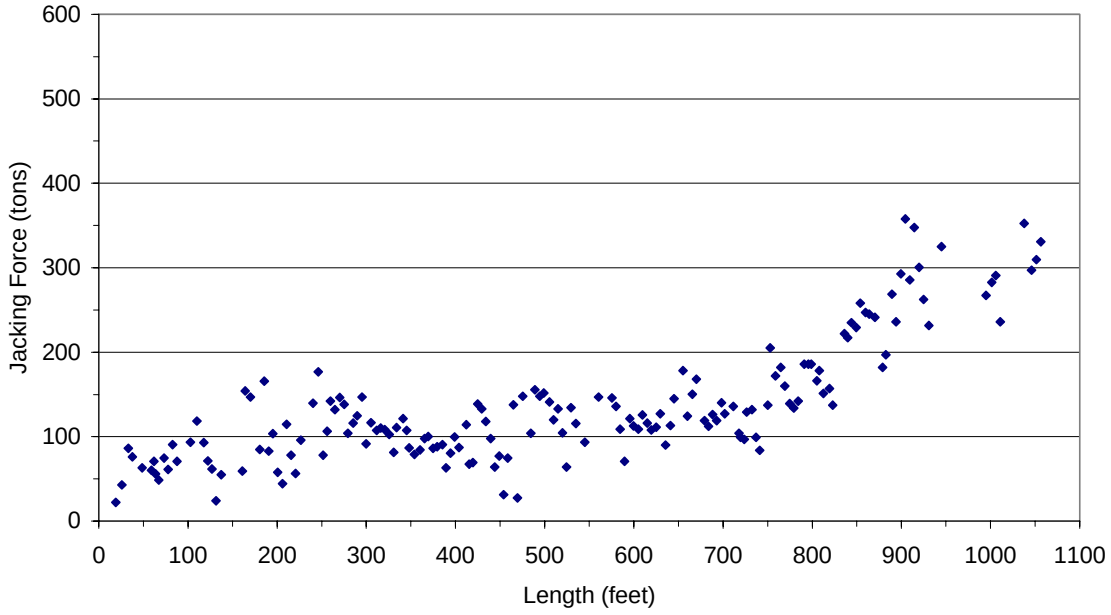

Figure 6.14. Length vs. Jacking Forces for the Clearview Snohomish River Crossing 2002.

Figure 6.15 shows the jacking forces between 110 and 810 feet into the drive. Throughout this segment, the jacking stress was 0.005 tons/ft^2.Throughout this segment where heavy lubrication was applied, the lubricated interface friction coefficient, $\mu_{int.lube}$, was 0.05 or 8.3% of the non-lubricated interface friction coefficient.

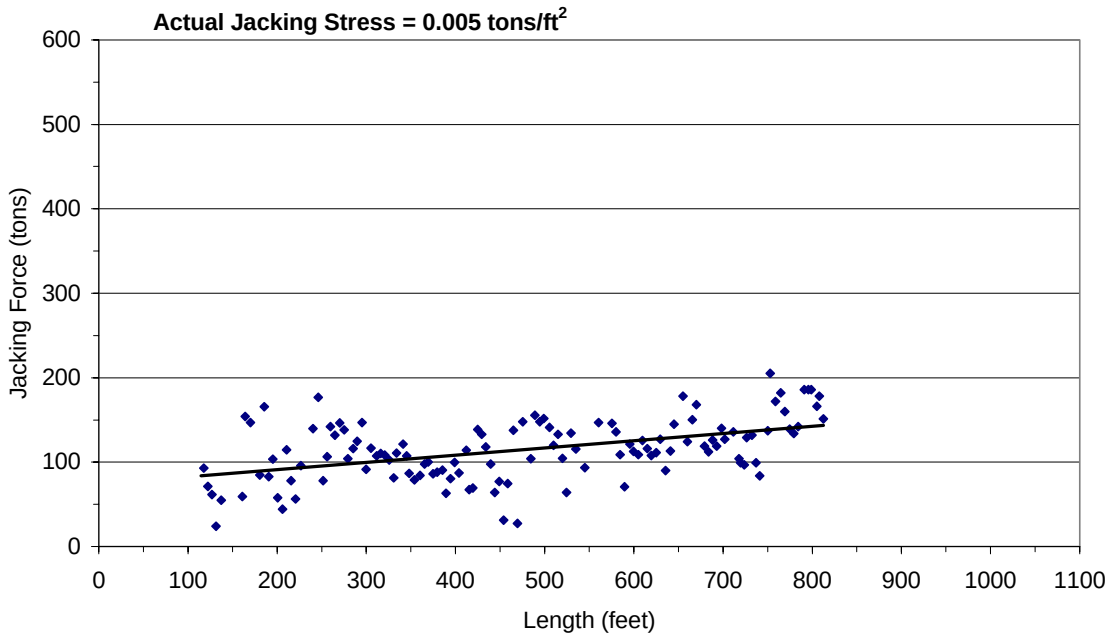

Figure 6.15. Length vs. Jacking Force for the Clearview Snohomish River Crossing from 110 to 810 feet.

At 810 feet into the tunnel drive, lubrication was stopped. There is a corresponding increase in jacking force from the point where the lubrication stopped until the end of the drive. Figure 6.16 shows the jacking force from 810 to 950 feet. The jacking stress through this segment is 0.05 tons/ft^2. This represents an effective interface friction coefficient of 0.5, equal to that of the zone between 50 and 100 feet where lubrication was minimally applied.

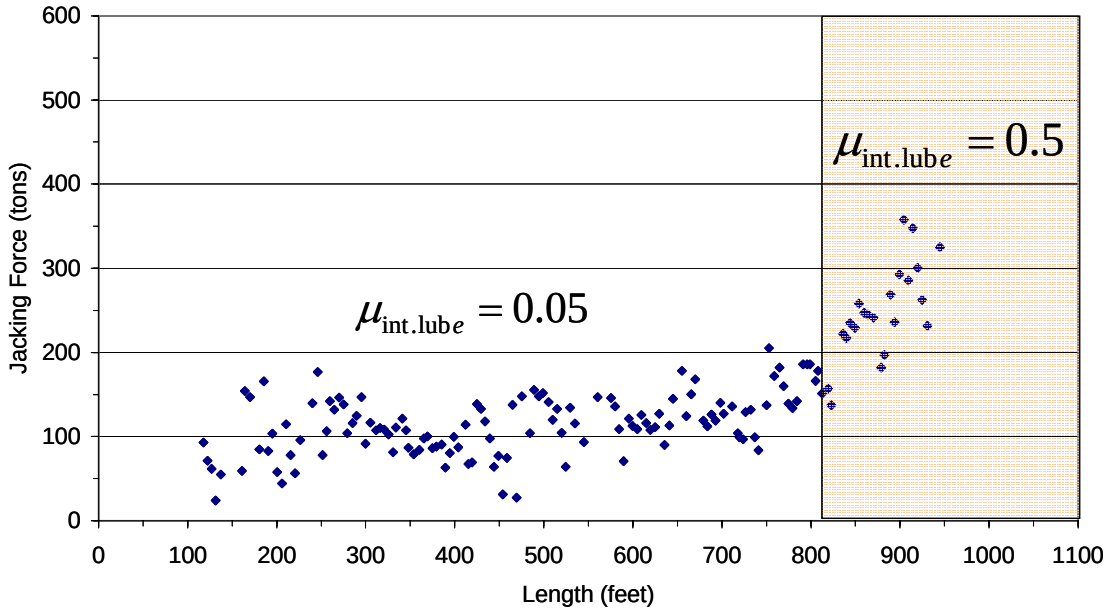

Figure 6.16. Length vs. Jacking Force for the Clearview Snohomish River Crossing 2002 from 110 to 950 feet.

6.2.5 Lowell Snohomish River Road-- Burlington Northern Railroad Crossing Lubrication Analysis

The Lowell Snohomish River Road – Burlington Northern Railroad Crossing was a 60-inch Permalok Steel Pipe microtunnel crossing approximately 210 feet long. A detailed description of the project is contained in Section 4.2. A small bentonite lubrication system as shown in Figure 6.1 was used on the project. Bentonite was pumped continuously from the bentonite port located at the end of the tail section of the machine, approximately 20 feet behind the cutting edge of the machine from the beginning of the drive through 120 feet. Figure 6.17 shows the jacking forces as a function of length throughout the tunnel drive.

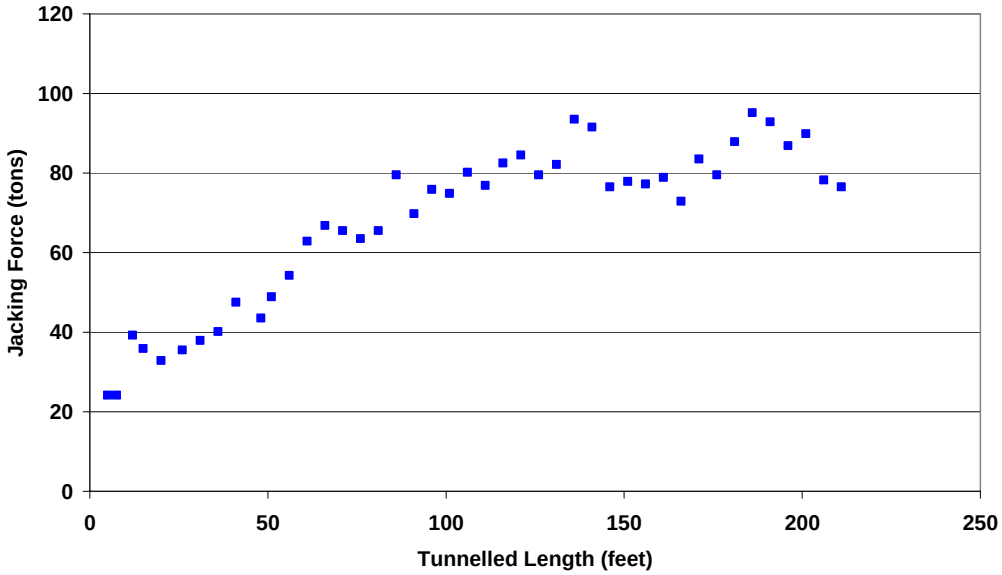

Figure 6.17. Length vs. Jacking Forces for the Lowell Snohomish River Road – Burlington Northern Railroad Crossing.

Through the first 120 feet, the non-lubricated jacking force prediction yields a jacking stress of 0.058 tons/ft^2. The actual jacking stress through this segment is 0.03 tons/ft^2, or 50% of the predicted non-lubricated jacking stress. These values correspond to an interface friction coefficient between the Permalok Steel pipe and the site sand with an estimated residual friction angle of 26-degrees, μ_{int}, of 0.40 and a lubricated interface friction coefficient, $\mu_{int.lube}$, of 0.20. Figure 6.18 shows the actual and predicted non-lubricated jacking forces from launch to 120 feet into the drive.

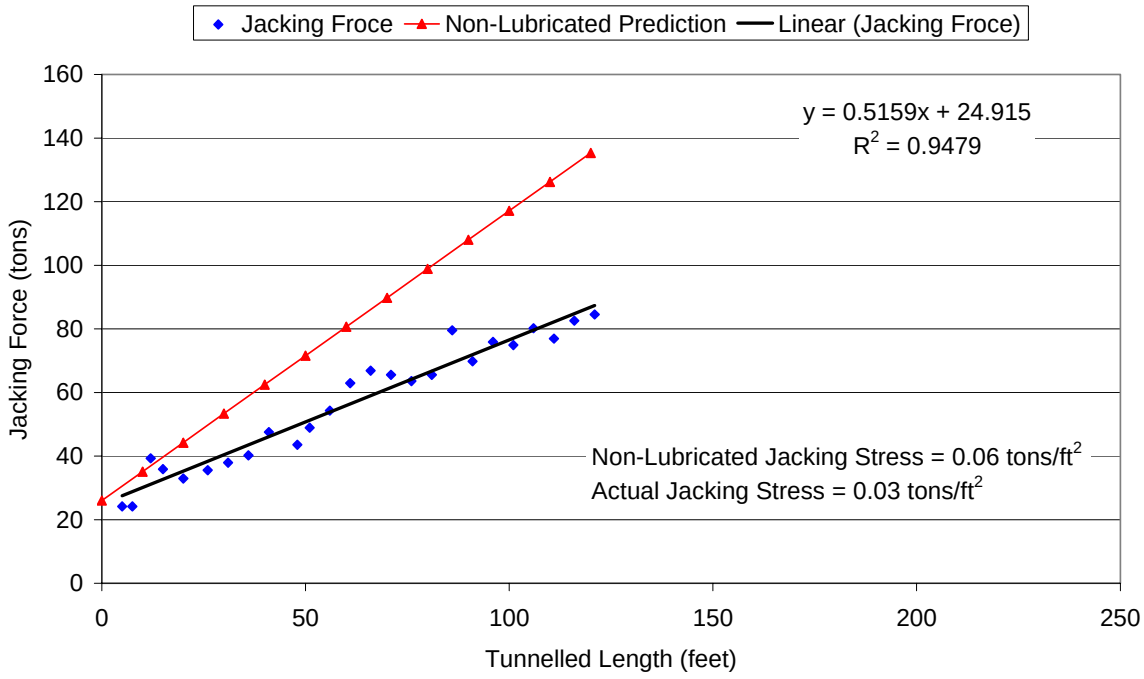

Figure 6.18. Length vs. Actual and Predicted Non-Lubricated Jacking Forces for the Lowell Snohomish River Road – Burlington Northern Railroad from 0 to 120 feet.

At 120 feet into the drive, a second lubrication port was connected approximately 60 feet behind the head, and lubrication was pumped from this lubrication port and the tail shield port. Lubrication was pumped at a higher volume from both ports after 120 feet into the drive than previously during tunneling. Figure 6.19 shows the actual jacking forces for the entire drive and the predicted lubricated jacking forces. At 120 feet into the drive, the predicted lubricated coefficient of friction decrease from 50% of the non-lubricated interface friction coefficient to 10% of the non-lubricated interface friction coefficient.

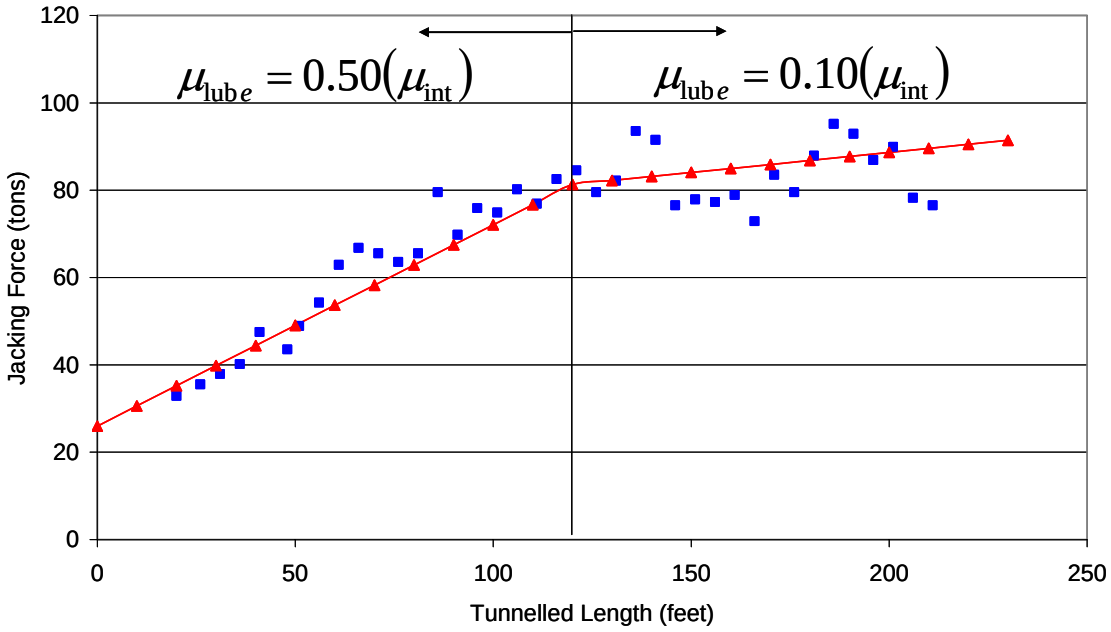

Figure 6.19. Length vs. Actual and Predicted Lubricated Jacking Forces for the Lowell Snohomish River Road- Burlington Northern Railroad Crossing from 0 to 210 feet.

6.3 Summary

From the case history back-analysis, there appear to be two distinct types of lubrication: mass application, where jacking forces are rising rapidly and may be considered "out of control", and controlled lubrication, where lubrication is pumped continuously in lower volumes from the beginning of the drive to keep jacking forces relatively low throughout a microtunneling drive. During mass application lubrication, many ports are connected at one time and the volumes of lubrication pumped often far exceed the volume of the annular space. This results in a sudden decrease in jacking forces as the interface friction coefficient along the pipeline is reduced in areas that were previously tunneled at a higher interface friction coefficient. In the case histories

examined, the lubricated interface friction coefficient was approximately 10% of the non-lubricated interface friction coefficient.

With controlled lubrication, the contractor may not be receiving the full potential benefit of the lubrication; however, the jacking forces are maintained within a lower range and are not allowed to rise out of a controlled limit. Should the jacking forces increase beyond the established "comfort level" of the contractor, lubrication volumes and pumping locations can be increased. Table 6.1 summarizes the lubricated case histories, the type of lubrication, and the interface friction coefficients for each segment of the tunnel drives.

Table 6.1. Summary of Lubricated Segments and Interface Friction Coefficients.

Project	Segment [feet]	Description	Type of Lubrication	Interface Friction Coefficient [-]
South Lake Tahoe Highway 50 Crossing	0-150	Non-Lubricated	None	0.6
	150-240	Lubricated	Mass Application	0.06
Eastside Interceptor Houser Way	0-120	Non-Lubricated	None	0.53
	120-550	Lubricated	Mass Application	0.05
Snohomish River Crossing 2001	0-90	Non-Lubricated	None	0.6
	90-150	Lubricated	Mass Application	0.06
	150-240	Non-Lubricated	None	0.35 (effective)
	240-275	Lubricated	Mass Application	0.06
	275-340	Non-Lubricated	None	0.5 (effective)
Snohomish River Crossing 2002	50-110	Lubricated	Controlled	0.5
	110-810	Lubricated	Mass Application	0.05
	810-950	Non-Lubricated	None	0.5 (effective)
Lowell Snohomish River Road - BNRR	0-120	Lubricated	Controlled	0.2
	120-240	Lubricated	Mass Application	0.04

CHAPTER 7

CONCLUSIONS AND RECOMMENDATIONS

7.1 Introduction

This dissertation presents the results of a study focused on the interface shearing behavior between pipes and soils and the effects on jacking forces. Understanding the mechanisms that govern the shearing behavior at the pipe-soil interface is crucial for the prediction and control of jacking forces. Six (6) jacking pipe materials including Centrifugally Cast Fiber Reinforced Mortar Pipe (Hobas), Polymer Concrete (Polycrete), Permalok Steel, Wet Cast Concrete, Packerhead Concrete, and Vitrified Clay, were characterized to determine their average surface roughness and the effect of surface roughness on interface strength. Each pipe material was sheared against two characteristically different sands in the laboratory: Ottawa 20/30 sand, a sub-rounded quarts sand and Atlanta Blasting sand, an angular quartz sand. Interface friction coefficients between each sand and pipe material were determined by performing shear tests with a modified shearing apparatus. A family of interface friction coefficients was developed for each pipe material over a range of residual soil friction coefficients.

A method for predicting jacking forces was proposed based on an adaptation of Terzaghi's Arching Theory for the prediction of normal stresses and interface friction coefficients measured in the laboratory.

Field research was conducted on fifteen microtunneling and open shield pipe jacking projects where data were collected on a myriad of tunneling parameters to capture events impacting jacking forces. Non-lubricated segments of jacking force

records collected on the projects were analyzed. The jacking force model was used to predict jacking unlubricated jacking forces and compared to case history data.

Records of lubricated segments of jacking forces were also analyzed and lubricated interface friction coefficients were back-calculated to determine the overall impact of lubrication on jacking forces. This chapter summarizes the results of these investigations, presents a step-by-step process for using the jacking force model to predict jacking forces on projects, and provides recommendations for further research on the prediction and control of jacking forces.

7.2 Conclusions

Though jacking forces have previously been studied by others, these studies have largely focused on empirical analyses, and few have investigated the mechanisms of shearing at the pipe-soil interface. The results have been the development of models that predict jacking forces to some degree of accuracy in site-specific environments, but do not predict jacking forces well when site parameters change, such as pipe material, soils, depth of burial, pipe diameter, etc. The focus of the study contained herein is to identify the mechanism of shearing at the interface between various jacking pipes and soils and to develop a model that accurately predicts jacking forces for all site parameters. The primary results of the research are summarized herein.

7.2.1 Pipe Surface Roughness Characterization

The surface of six (6) jacking pipe materials was characterized using a Taylor-Hobson Talysurf Series-2 Stylus Profilometer to determine the average roughness, R_a. The jacking pipe materials included Centrifugally Cast Fiber Reinforced Polymer Mortar

pipe (Hobas), Polymer Concrete (Polycrete), Permalok Steel, Concrete manufactured with the Wet Casting method, Concrete manufactured with the Packerhead method, and Vitrified Clay. The surface profiles for the pipe materials tested revealed a range of average roughness values, as well as a range of variations in the average roughness values as shown in Table 7.1.

Table 7.1 Jacking Pipe Materials and Average Roughness

Parameter	Hobas	Polycrete	Permalok	Wet Cast Concrete	Packerhead Concrete	Vitrified Clay
Average R_a	6.5	16.9	18.7	24.8	55.1	93.8
STDEV	1.2	9.4	8.8	19.5	10.6	12.2
%Stdev/Mean	18.3	55.3	47.2	78.5	19.2	13.0
Repeatability	2.7%	1.5%	4.4%	3.7%	2.5%	1.9%

7.2.2 Interface Shear Testing

Interface shear tests were conducted between each pipe material and two types of sand: Ottawa 20/30 and Atlanta Blasting. The Ottawa 20/30 sand was a sub-rounded quarts sand with a peak and residual friction angle of 38.9- and 27.9 degrees. The Atlanta Blasting sand was an angular quartz sand with a peak and residual friction angle of 43.1- and 34.6- degrees, respecitvely. The interface shear tests were conducted in the laboratory on a large-displacement constant-stress shear testing apparatus developed at Georgia Institute of Technology (Zettler, 1999).

As the surface roughness of the pipe increased, the interface friction coefficient increased. The absolute differences between the interface friction coefficient for the roughest pipe material and the smoothest pipe material was more pronounced for the peak interface friction coefficients than for the residual interface friction coefficients. The

peak coefficient of friction was mobilized within a relatively small horizontal displacement, with smoother pipes reaching the peak coefficient of friction within a smaller relative displacement than the rougher pipes.

There was a clear post-peak decrease in interface strengths for pipes with intermediate and high roughness values including Permalok Steel, Wet Cast Concrete, Packerhead Concrete, and Vitrified Clay. However, post-peak softening was not observed in smoother pipes including Hobas and Polycrete. This is attributed to particle sliding at the interface on the smoother pipes versus particle rearrangement at the interface of the rougher pipes. The particle rearrangement occurs until a stable steady state lower bound friction value is reached, representing the residual interface friction value.

Plots of the average roughness versus the peak and residual coefficient of friction for each pipe material revealed a bi-linear relationship and a critical roughness value that approximated the internal friction coefficient of the particulate media that was sheared against the pipe.

Although Polycrete has a higher average roughness value than Hobas, the interface friction coefficient at both the peak and residual state was slightly higher for the Hobas than the Polycrete pipe material at some of the normal loads tested (at other normal loads, the interface friction coefficient for the Hobas and the Polycrete were equal, although the Polycrete had a higher average roughness value). This was attributed to plowing by the soil particles at the interface into the Hobas, which has a lower hardness value than the Polymer Concrete pipe.

Although Vitrified Clay pipe had the highest average roughness value of the jacking pipe materials, the interface friction coefficients measured during shear testing were below those measured for Packerhead Concrete at all normal stress levels. This was attributed to the brittle nature of the pipe surface, making the surface susceptible to plowing, in conjunction with pipe surface characteristics that differ substantially from the other pipe materials. Since the Vitrified Clay pipe surface exhibits large longitudinal distances between the peaks and valleys on the surface, the average roughness parameter may not be representative of the surface nature and may not provide a good comparative parameter to the other pipe materials.

7.2.2.1 Effects of Angularity

The effects of angularity were determined by shearing each pipe material with Ottawa 20/30 sand and Atlanta Blasting sand at equal normal loading conditions. For each pipe material, the interface friction coefficient for Atlanta Blasting Sand was higher than the interface friction coefficient with Ottawa 20/30 sand. This is attributed to particle interlocking with the pipe as well as particle interlocking within the soil mass.

7.2.2.2 Effects of Relative Density

The effects of relative density of the soil was evaluated by performing shear tests on Hobas, Packerhead Concrete and Vitrified Clay pipe with Ottawa 20/30 sand with relative densities ranging from 47% to 98%. Results of these studies showed that the peak interface friction coefficient increased with increasing relative density. This is due to particle interlocking at the interface and within the soil mass at the higher relative densities. This effect was much more pronounced for the rougher pipes, Packerhead

Concrete and Vitrified Clay, than for the Hobas due to the sliding friction on the Hobas surface.

7.2.2.3 Effects of Normal Stress

Trends in the interface shearing behavior were the same for all values of normal stress; however, the post-peak softening on the rougher pipes was more pronounced at the lower normal stress levels where particles were under less stress and allowed to move more freely into the steady state residual friction arrangement.

As normal stresses were increased, the interface coefficient of friction decreased to a value of 80 kPa, at which point the interface friction coefficient became constant, absent the effects of plowing. The magnitude of the decrease was higher in the peak interface friction coefficient than in the residual interface friction coefficient. A log-log plot of the normal stress vs. the coefficient of friction revealed that for normal stresses less than 80 kPa, the interface friction coefficient increases linearly with a decrease in normal load. This can be attributed to a non-linear decrease in contact area of the soil particles to the surface with the normal load. Because the contact area is not decreasing at the same rate as the normal load, the coefficient of friction tends to increase.

7.2.3 Development of Interface Friction Coefficients

Values for the interface friction coefficient between Ottawa 20/30 sand, with a residual friction angle of 27.9 degrees, and each of the pipe materials was determined in the laboratory. Values for the interface friction coefficient between Atlanta Blasting sand, with a residual friction angle of 34.6 degrees, and each of the pipe materials was determined in the laboratory. From those values, which are uniquely related by the bi-

linear average surface roughness versus residual interface friction coefficient curve, Table 5.2 was developed for a range of residual friction coefficients between 25 and 40 degrees.

Table 5.2 Interface Friction Coefficients for a Variety of Residual Friction Angles and Jacking Pipe Materials

Soil at Interface	Interface Friction Coefficient between Soil and Pipe					
Residual Friction Angles	Hobas	Polycrete	Permalok Steel	Wet Cast Concrete	Vitrified Clay pipe	Packerhead Concrete
25	0.37	0.40	0.38	0.43	0.42	0.49
26	0.39	0.41	0.40	0.45	0.44	0.50
27	0.41	0.42	0.42	0.47	0.46	0.52
27.9 Ottawa 20/30	0.43	0.43	0.44	0.48	0.48	0.53
28	0.43	0.43	0.44	0.48	0.48	0.53
29	0.45	0.44	0.46	0.50	0.50	0.55
30	0.47	0.45	0.48	0.51	0.52	0.56
31	0.49	0.46	0.51	0.53	0.54	0.57
32	0.51	0.47	0.53	0.55	0.56	0.59
33	0.53	0.48	0.54	0.56	0.58	0.60
34	0.55	0.49	0.57	0.58	0.60	0.61
34.6 Atlanta Blasting	0.56	0.49	0.58	0.59	0.61	0.62
35	0.57	0.49	0.59	0.60	0.62	0.63
36	0.59	0.50	0.61	0.61	0.64	0.64
37	0.61	0.51	0.63	0.63	0.66	0.65
38	0.62	0.52	0.65	0.65	0.68	0.67
39	0.64	0.53	0.67	0.66	0.70	0.68
40	0.66	0.54	0.69	0.68	0.72	0.69

7.2.4 Development of a Jacking Force Prediction Model

A predictive model was developed for determining the frictional component of jacking forces using the interface friction coefficient developed in Table 5.2 and normal forces based on Terzaghi's Arching Theory. The proposed predictive model was shown as Equation 5.5.

$$JF_{frict} = \mu_{\text{int}} \frac{\gamma \cdot r \cdot \cos\left(45 + \frac{\phi_r}{2}\right)}{\tan \phi_r} \cdot \pi \cdot d \cdot l \qquad (5.5)$$

Where JF_{frict} = Frictional Component of Jacking Force [tons force]
μ_{int} = Pipe-Soil Residual Interface Friction Coefficient (from Table 5.2)
γ = Total Unit Weight of the Soil [tons/ft^3]
ϕ_r = Residual Friction Angle of the Soil [degrees]
d = Pipe Diameter [feet]
r = Pipe Radius [feet]
l = Length of the Pipe [feet]

The predictive model was compared with non-lubricated segments on thirteen microtunneling and open shield pipe jacking projects to determine the accuracy of the predictive model. Table 7.2 provides a summary of the projects, the pipe material, pipe diameter, soil properties, interface friction coefficient, jacking stresses calculated by the model, actual jacking stresses on the project, and percent error between the actual jacking stresses and the predicted jacking stresses.

7.2.5 Comparison of Predictive Model with Jacking Force Models developed by Others

A host of other authors have developed jacking force models to predict jacking forces. The jacking force model developed herein was compared to models developed by Bennett (1998), Chapman (1999), and Scherle (as summarized in Stein, 2005). Each of the models was compared to actual jacking force data from four field case histories with different pipe materials: Permalok steel, Packerhead Concrete, Polycrete, and Hobas. In addition, the pipe diameters ranged from 25.8 to 87.5 inches. Table 7.3 summarizes and compares the predictive models.

Table 7.2 Comparison of Actual and Predicted Jacking Stresses on Non-Lubricated Segments of Pipe Jacking Projects

Project	Pipe	Pipe Dia-meter [in]	Est. ϕ_r [°]	Est. γ_{total} [pcf]	Predicted σ_n [psf]	μ_{int} [-]	Predicted Jacking Stress [tsf]	Actual Jacking Stress [tsf]	Percent Error [%]
Newark Drive 3	Hobas	38.3	26	126	218	0.393	0.043	0.051	15.8
Newark Drive 6	Hobas	38.3	26	126	218	0.393	0.043	0.051	15.8
Newark Drive 12	Hobas	38.3	26	126	218	0.393	0.043	0.046	6.7
Newark Drive 1-24	Hobas	25.8	26	126	218	0.393	0.028	0.033	14.1
Alvarado JP3-RP4	Polycrete	46.6	31	131	209	0.458	0.048	0.045	-6.1
Alvarado JP4-RP4	Polycrete	46.6	30	129	217	0.449	0.049	0.051	4.5
Alvarado Drive 17	Polycrete	25.9	29	126	125	0.440	0.027	0.026	-5.8
Clearview 2001	Permalok	60	35	135	223	0.588	0.065	0.074	11.6
Sacramento North Bore	Permalok	72	27	108	332	0.421	0.070	0.070	0.09
Sacramento South Bore	Permalok	72	27	108	332	0.421	0.070	0.084	16.7
Highway 50 Crossing	Wet Cast Concrete	59.5	35	140	229	0.597	0.068	0.074	7.7
ESI Morris Ave	Packer-head Concrete	87.5	32	110	311	0.584	0.091	0.090	-1.0
ESI Houser Way	Packer-head Concrete	87.5	32	110	311	0.584	0.091	0.084	-10.8

Table 7.3 Comparison of Actual Jacking Forces and Models by Staheli, Bennett (1998), Chapman (1999) and Scherle (1977)

	Clearview 2001		ESI- Morris Avenue		Alvarado Dr 17		Newark Drive 6	
	60-inch	Permalok	87.5-inch	Packer-head	25.8 inch	Poly-crete	38.3-inch	Hobas
	65 ft	Deep	17 ft	Deep	18 ft	Deep	13 ft	Deep
	$\phi_r = 35°$	$\gamma = 135$ [pcf]	$\phi_r = 32°$	$\gamma = 110$ [pcf]	$\phi_r = 29°$	$\gamma = 126$ [pcf]	$\phi_r = 26°$	$\gamma = 126$ [pcf]
	μ_{int}= 0.588	Sandy Gravel	μ_{int}= 0.584	Loose Sand	μ_{int}= 0.440	MD Sands	μ_{int}= 0.393	Silty Sands
Actual Jacking Stress	0.077	% Error	0.091	% Error	0.026	% Error	0.051	% Error
Staheli	0.072	15.5	0.091	0.03	0.025	3.9	0.048	16.0
Chapman	0.094	-21.8	0.111	-22.4	0.050	-91.1	0.063	-22.6
Bennett-Lower Bound	0.123	-47.6	0.124	-37.0	0.051	-96.7	0.119	-64.5
Bennett - Best Fit	0.164	-96.7	0.167	-82.6	0.069	-161.2	0.159	-156.6
Bennett-Upper Bound	0.254	-195.1	0.249	-173.6	0.096	-282.5	0.238	-229.1
Scherle	0.635	-636.8	0.161	-76.8	0.103	-293.3	0.156	-119.3

Note: % Error = (Actual – Predicted)/Actual. Positive Value = Under-Prediction. Negative Value = Over-Prediction.

7.2.6 Effects of Lubrication on Jacking Forces

The effects of lubrication on jacking forces was investigated by critically examining case histories where bentonite lubrication was applied to the pipeline, and evaluating the effect on the interface friction coefficient. Two types of lubrication strategies were identified: "mass application" and "controlled lubrication". Mass application lubrication refers to lubrication implementation when jacking forces were allowed to increase without the use of lubrication and then lubrication is applied in large volumes along the pipe string throughout areas that had been previously tunneled. Controlled lubrication refers to the use of smaller volumes of lubrication throughout tunneling operations, often from only a

single lubrication port that serves to keep jacking forces within a lower range throughout tunneling operations.

When mass lubrication operations were applied, lubricated interface friction coefficients were back-calculated to be approximately 10% of non-lubricated interface friction coefficients. The lubricated interface friction coefficients were maintained at 10% of the non-lubricated interface friction coefficient as long as mass lubrication practices were maintained. However, if mass lubrication was employed only for a short period to reduce jacking forces, followed by pumping smaller volumes of lubrication, the interface friction coefficient was found to increase to an effective value, between the non-lubricated and 10% of the non-lubricated interface friction coefficient value, depending on the proportional length of the pipeline that was lubricated. If mass lubricated was then resumed, the interface friction coefficient would reduce, once again, to approximately 10% of the non-lubricated interface friction coefficient.

When controlled lubrication practices were employed, the lubricated interface friction coefficient was found to be higher than the mass lubricated interface friction coefficient, but still significantly lower than the non-lubricated interface friction coefficient. Two case histories involved tunnels that utilized controlled lubrication techniques, lubricating from launch of the machine throughout the tunnel drive. On one of the projects, lubrication was pumped sparingly and reduced the non-lubricated interface friction coefficient by 17%. On the other project, lubrication was pumped liberally from the single lubrication port in the tail section and reduced the non-lubricated interface friction coefficient by 50%. With the controlled lubrication strategy, the benefits of the lubrication were directly related to the amount of bentonite distributed

over the pipeline through the single port in the tail section of the machine. In both cases, the analysis evaluated the overall jacking force decrease; therefore, the distribution of lubrication around the pipeline within the soil mass could play an equal or greater role than the volume of bentonite pumped.

7.2.7 Importance of Quality Geotechnical Data

The predictive model relies on two geotechnical parameters for the calculation of jacking forces: residual friction angle and total unit weight. The model relies on quality geotechnical information from the microtunneling or pipe-jacking site to produce estimates of jacking forces that will be reflective of the actual site conditions. It is critical to urge project owners and representatives to invest in the necessary geotechnical investigation and testing programs to determine these critical soils parameters. By determining actual site soil parameters, errors due to the estimation of soil parameters by using general correlations can be eliminated from jacking force estimates.

7.3 Guide for Using Jacking Force Prediction Model

The proposed model for predicting jacking forces, originally presented as equation 5.5 and repeated below for ease of the reader has input variables five (5) input variables.

$$JF_{frict} = \mu_{\text{int}} \frac{\gamma \cdot r \cdot \cos\left(45 + \frac{\phi_r}{2}\right)}{\tan \phi_r} \cdot \pi \cdot d \cdot l \qquad (5.5)$$

Where JF_{frict} = Frictional Component of Jacking Force [tons force]
μ_{int} = Pipe-Soil Residual Interface Friction Coefficient (from Table 5.2)
γ = Total Unit Weight of the Soil [tons/ft^3]
ϕ_r = Residual Friction Angle of the Soil [degrees]
d = Pipe Diameter [feet]
r = Pipe Radius [feet]
l = Length of the Pipe [feet]

Two of the variables are a function of the tunnel geometry: tunnel diameter, d, which should always be entered as the outer diameter of the pipe; and length of the pipe, l, which should be entered as the full length of the tunnel, shaft-to-shaft.

Two soil parameters are required to use the proposed model to predict jacking forces: soil total unit weight, γ, and residual internal friction angle of the soil, ϕ_r. Often a geotechnical investigation is conducted for the design of a microtunnel or pipe jacking project, the results of which are contained in a geotechnical investigation report. These parameters may be provided in a geotechnical investigation report prepared for the specific tunnel or pipe jacking operation for which jacking force predictions are sought. However, if laboratory data for these parameters is not available, it is necessary for the user to estimate these values for use in the model. Tables providing correlations between

some commonly measured soil parameters and total unit weight and residual friction angle are presented in Appendix A.

Once the residual internal angle of friction is determined, the last remaining variable, the interface friction coefficient, μ_{int}, can be determined by referring to Table 7.2. Table 7.2 provides interface friction coefficients for six (6) different jacking pipe materials and a range of interface friction coefficients.

7.3.1 Step-by-Step Process for Using the Predictive Model

The following step-by-step process is provided for using the jacking force predictive model to for non-lubricated jacking force predictions:

1. Determine the pipe outer diameter and radius. The user should make sure these parameters are in units of [feet].
2. Determine the length of the tunnel or segment of tunnel over which jacking force predictions are sought. This length should be in units of [feet].
3. Determine the total unit weight of the soil. This parameter may be provided in the geotechnical report prepared for the project. Some geotechnical reports provide information on the dry density of the soil and the moisture content, w, from which the total unit weight can be calculated (See Appendix A). Parameters developed from soil samples at the pipe elevation are the preferred input information. If appropriate soil parameters are not provided (γ_{total}, γ_{dry}, and w), guidance on estimating values for total unit weight are provided in Appendix A. It should be noted that soil unit weights are commonly given in units of pounds/ft^3. For

consistency in units, the total soil unit weight must be in units of tons/ft3, therefore, typical soil unit weights should be divided by 2000.

4. Determine the residual friction angle of the soil. This parameter may be provided in the geotechnical investigation report for the project if direct shear tests were performed on soil samples at the elevation of the pipeline; however, if values for the residual friction angle are not provided, guidance on estimating values for the residual friction angle of different soil types are provided in Appendix A. The residual friction angle is in units of [degrees].
5. Determine the interface friction coefficient by using Table 7.2 with the appropriate pipe material and residual friction angle of the soil. The interface coefficient of friction is a unit-less value [-].
6. The parameters determined above can be substituted into Equation 7.1 to determine the estimated jacking forces in units of tons. It should be noted that the jacking force prediction is for non-lubricated pipe jacking and, therefore, should be considered an upper-bound solution.

7.4 Recommendations For Further Research

With the important insights and developments discovered in this research, a number of interesting subjects arose that warrant additional study and are summarized below.

7.4.1 Expanding the Range of Soils for the Determination of Interface Friction Coefficients

The interface shear testing was performed on the jacking pipes with two uniform soils: Ottawa 20/30 sand and Atlanta Blasting sand. However, it is rare to encounter such uniform soils in the field. Clearly additional insight could be gained by examining the interface frictional behavior of well-graded soils.

In addition, the Ottawa 20/30 sand had a D_{50} value of 0.64 mm and the Atlanta Blasting sand had a D_{50} value of 0.82 mm. Further interface shearing tests should be conducted to determine if altering the D_{50} value has an impact on the interface friction coefficient between the jacking pipe material and the soil.

7.4.2 Extrapolated Interface Friction Coefficients

Interface friction coefficients were determined for each pipe material for residual soil coefficients of 27.9 degrees (Ottawa 20/30 sand) and 34.6 degrees (Atlanta Blasting sand). Values for interface friction coefficients were then interpolated between 27.9 and 34.6 degrees for each pipe material. The change in interface friction coefficient was unique for each pipe material. However, the absolute value of the change did not vary with pipe roughness. The smallest change in the interface friction coefficient was found in the Polycrete pipe, where sliding friction occurred at the interface and no plowing

effects were observed. In the Polycrete pipe, the absolute change in the interface friction coefficient between the residual friction angles of 27.9 degrees and 34.6 degrees was 0.06. Although smoother than the Polycrete, the Hobas pipe had a wider range of interface friction coefficients between 27.9 and 34.6 degrees with an absolute difference of 0.13. This was due to higher values of interface friction with the Atlanta Blasting sand due to plowing. Permalok steel pipe had the widest range of interface friction coefficients between 27.9 degrees and 34.6 degrees with an absolute difference of 0.14. This compared to 0.11 for Wet Cast Concrete and 0.13 for Vitrified Clay pipe. Packerhead Concrete had a small range of interface friction coefficients with an absolute difference of only 0.09 between 27.9 and 34.6 degrees. When sheared against the Ottawa 20/30 sand, the interface friction coefficient was equal to the tangent of the internal friction angle of the Ottawa 20/30 sand (tangent 27.9 degrees) or 0.53. However, this was not the case for the Atlanta Blasting sand which had an interface friction of 0.62 against the Packerhead Concrete, compared to an internal friction coefficient of 0.69 (tangent 34.6 degrees). This deserves some further investigation to develop a full range of interface friction coefficients between the various jacking pipe materials and a variety of soils with a broad range of residual friction angles.

In addition, the interface friction coefficients were extrapolated outside of the data tested in the laboratory as Table 5.2 provides interface friction coefficients for residual soil friction angles ranging from 25 to 40 degrees. Until further work has been completed to verify interface friction values outside of the range tested in the laboratory, the user should be cautious of these values when using them in this or any other predictive model.

7.4.3 Interface Shear at Lower Normal Stress Levels

Interface shear testing was performed at normal stress levels ranging from 40 kPa to 200 kPa on the Ottawa 20/30 sands. The extrapolated interface friction coefficients in Table 7.2 were based on interface shear tests conducted at 80 kPa because shear tests were conducted on both Ottawa 20/30 sand and Atlanta Blasting sand at this normal stress level. However, once the laboratory testing was completed, allowing analysis of the field jacking force data, it was discovered that actual normal stresses acting on the pipelines were lower than the normal stresses at which the shear tests were conducted. Normal stresses in the field were common back-calculated to be in the range of 10 to 15 kPa. When evaluated on a log-log scale, interface friction coefficients have been shown to increase linearly with decreasing normal stress below 60 kPa (as shown in Chapter 5). Therefore, performing interface shear tests on the pipe materials at lower normal stress values may prove to be valuable to determine interface friction coefficients that more clearly reflect values representative of those in the field. Table 7.4 compares the interface friction coefficients measured for Ottawa 20/30 sand sheared against each pipe material at normal stress values of 80 and 40 kPa.

Table 7.4 Changes in Interface Friction Coefficient with Changes in Normal Stress for Pipe Materials Sheared Against Ottawa 20/30 Sand

Pipe Material	Interface Friction Coefficient Tested at 80 kPa	Interface Friction Coefficient Tested at 40 kPa
Hobas	0.43	0.43
Polycrete	0.43	0.42
Permalok Steel	0.44	0.49
Wet Cast Concrete	0.48	0.49
Packerhead Concrete	0.53	0.54
Vitrified Clay	0.48	0.50

Hobas and Polycrete do not show any increase in friction coefficient when the normal stress decreases from 80 kPa to 40 kPa which is attributed the smooth surface and the sliding at the interface. However, pipes with rougher surfaces did show some increase in friction coefficient with decreasing normal stresses, further showing the need to perform additional shear testing at lower normal stresses indicative of normal stresses in the field.

7.4.4 Normal Stress Distribution around the Pipe

The predictive model uses a modified interpretation of Terzaghi's Trap Door model and relates the vertical stress acting on the top of the pipe to the radius of the pipe by the following equation originally presented as:

$$\sigma_v = \frac{\gamma \cdot r \cdot \cos\left(45 + \frac{\phi_r}{2}\right)}{\tan \phi_r} \qquad (5.4)$$

where γ = Soil Total Unit Weight
ϕ_r = Residual Friction Angle of the Soil
r = Pipe Radius

Although this is the vertical stress acting on the crown of the pipeline, the model assumes that this stress is uniformly distributed around the circumference of the pipeline. The model, therefore, does not account for the varying weights of the different jacking pipes or add the weight of the jacking pipe to the vertical stress of the soil at the crown. It is therefore valuable to evaluate the component of the pipe weight and compare the weight of the pipe to the calculated normal stress acting circumferentially around the pipeline. Assuming that the pipe weight acts over only the bottom one-fifth of the pipe surface area, Table 7.5 compares the distribution of the pipe weight compared to the calculated

normal stresses predicted by the model for Polycrete, Permalok Steel, Hobas, and Packerhead Concrete on selected case histories.

Table 7.5 Distribution of Pipe Weight Compared to Normal Stresses Calculated with Predictive Model

Project Name	Pipe	Pipe Weight [lbs/ft]	Predicted Normal Stress (with Model) [lbs/ft^2]	Stress due to Pipe Weight (acting on bottom 1/5 of pipeline) [lbs/ft^2]	Difference %
Alvarado JP3-RP4	Polycrete- 46”	470	208	192	8.3%
Alvarado Drive 17	Polycrete- 26”	185	125	136	8.1%
Clearview 2001	Permalok- 60”	556	242	177	26.9%
Eastside Interceptor - Morris	Packerhead Concrete – 87.5”	2138	311	467	36.7%
Newark – Drive 3	Hobas – 38.3”	208	218	103	112%

Due to the variations in the pipe weights compared to the stresses estimated in the model, further research in the area of stress distributions around the pipeline during pipe jacking is necessary to refine the normal forces in the model. Numerical modeling would be beneficial to develop insight to questions surrounding the stress distributions around the pipeline during jacking operations.

7.4.5 Effects of Lubrication

The effects of lubrication were examined on a limited basis within this thesis. Laboratory testing between pipe and lubricated soils would further the development of interface friction coefficients for determining jacking forces in lubricated environments.

Interface friction coefficients could be developed for pipe/bentonite interfaces, along with pipe/soil-bentonite mixtures to simulate a variety of field lubrication environments as described herein. In addition to a variety of lubrication mixtures, the effects of pumping pressurized lubrication on the outside of the pipeline requires further examination to determine the effects on the normal stress distribution around the pipeline and the contribution to the jacking forces.

APPENDIX A

REFERENCES FOR SELECTING SOIL PROPERTIES FOR USE IN PREDICTIVE JACKING FORCE CALCULATION MODEL

Tables and Figures are provided within this appendix to assist in the selection of soil properties for use in the predictive jacking force calculation model. No correlation or table of values can substitute for site-specific field data. Whenever possible, a thorough geotechnical investigation should be conducted in order to obtain accurate values for the unit weight of the soil and the residual friction angle of the soil. However, for the cases where this information is not available, Tables and Figures have been provided to help the user establish reasonable values of soil properties that best represent actual soil conditions at the site.

Table A.1. Correlations for Cohesionless Soils between Compactness, Relative Density and SPT-N-Value. From Gibbs and Holtz (Hunt, 2005).

Compactness	Relative Density	SPT N-Value
Very Loose	<0.15	<4
Loose	0.15-0.35	4-10
Medium Dense	0.35-0.65	10-30
Dense (compact)	0.65-0.85	30-50
Very Dense	0.85-1.0	>50

Unified Soil Classification System (ASTM D-2487)

Major Division			Group Symbols		Typical Names	Laboratory Classification Criteria
Coarse-grained soils (more than half of material is larger than no. 200 sieve size)	Gravels (more than half of coarse fraction is larger than No. 4 sieve size)	Clean gravels (little or no fines)	GW		Well-graded gravels, gravel-sand mixtrues, little or no fines	$Cu = \frac{D_{60}}{D_{10}}$ greater than 4: $C_c = \frac{(D_{30})^2}{D_{10} \times D_{60}}$ between 1 and 3
			GP		Poorly graded gravels, gravel-sand mixtures, little or no fines	Not meeting all gradation requirement for GW
		Gravels with fines (appreciable amount of fines)	GM	d u	Silty gravels, gravel-sand clay mixtures	Atterberg limits below " A " line or PI less than 4 — Above " A " line with PI between 4 and 7 are border line cases requiring use of dual symbols
			GC		Clay gravels, gravel sands, little or no fines	Atterberg limits below " A " line or PI greater than 7
	Sands (more than half of coarse fraction is smaller than no. 4 sieve size)	Clean sands (little or no fines)	SW		Well-graded sands, gravelly sands, little or no fines	$Cu = \frac{D_{60}}{D_{10}}$ greater than 4: $C_c = \frac{(D_{30})^2}{D_{10} \times D_{60}}$ between 1 and 3
			SP		Poorly graded sands, gravelly sands, little or no fines	Not meeting all gradation requirements for SW
		Sands with fines (appreciable amount of fines)	SM[a]	d u	Silty sands, sand-silt mixtures	Atterberg limits above " A " line or PI less than 4 — Limits plotting in hatched zone with PI between 4 and 7 are borderline caes requiring use of dual symbols
			SC		Clayey sands, sand-clay mixtures	Atterberg limits above " A " line with PI greater than 7
Fine-grained soils (more than half material is smaller than no. 200 sieve)	Silts and clays (liquid limit less than 50)		ML		Inorganic silts and very fine, rock flour, silty or clayey fine sands, or clayey silts with slight plasticity	
			CL		Inorganic clays of low to mediem plasiticity, gravelly clays, sandy clays, silty clays, lean clays	
			OL		Organic silts and organic silty clays of low plasticity	
	Silts and clays (liquid limit greater than 50)		MH		Inorganic silts, micaceous or diatomaceous fine sandy or silty soils, elasticsilts	
			CH		Inorganic clays of high plasticity, fat clays	
	Highly organic soils		Pt		Peat and other highly organic soils	

Determine percentages of sand gravel from grain-size curve. Depending on percentage of fines (fraction smaller than No. 200 sieve size), coarse-organised soils are classified as follows:
Less than 5 % — GW, GP, SW, SP
More than 12 % — GM, GC, SM, SC
5 to 12 % — Borderline cases requiring dual symbols

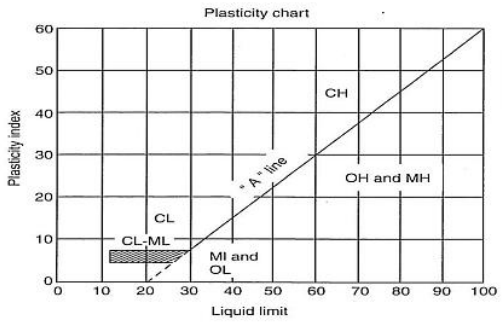

Figure A.1 Unified Soil /classification System (Hunt, 2005).

Common Properties of Cohesionless Soils

Material	Compactness	D_R (%)	N[a]	γdry (g/cm^3)[b]	γdry (pcf)[b]	Void ratio e	Strength[c] ϕ
GW:well-graded gravels, gravel-sand mixtures	Dense	75	90	2.21	138	0.22	40
	Medium dense	50	55	2.08	130	0.28	36
	Loose	25	<28	1.97	123	0.36	32
GP: poorly graded gravels, gravel-sand mixtures	Dense	75	70	2.04	127	0.33	38
	Medium dense	50	50	1.92	120	0.39	35
	Loose	25	<20	1.83	114	0.47	32
SW: well-graded sands, gravelly sands	Dense	75	65	1.89	118	0.43	37
	Medium dense	50	35	1.79	112	0.49	34
	Loose	25	<15	1.70	106	0.57	30
SP: poorly graded sands, gravelly sands	Dense	75	50	1.76	110	0.52	36
	Medium dense	50	30	1.67	104	0.60	33
	Loose	25	<10	1.59	99	0.65	29
SM: silty sands	Dense	75	45	1.65	103	0.62	35
	Medium dense	50	25	1.55	97	0.74	32
	Loose	25	<8	1.49	93	0.80	29
ML: inorganic silts, very fine sands	Dense	75	35	1.49	93	0.80	33
	Medium dense	50	20	1.41	88	0.90	31
	Loose	25	<4	1.35	84	1.0	27

Figure A.2. Common Properties of Cohesionless Soils (Hunt, 2005).

Typical Properties of Compacted Soils[a]

Group Symbol	Soil Type	Range of Maximum Dry Unit Weight (pcf)	Range of Optimum Moisture (%)	Typical Value of Compression: Percent of Original Height: At 1.4 tsf (20 psi)	Typical Value of Compression: Percent of Original Height: At 3.6 tsf (50 psi)	Typical Strength Characteristics: Cohesion as Compacted (psf)	Typical Strength Characteristics: Cohesion (Saturated) (psf)	Typical Strength Characteristics: Effective Stress Envelope ϕ (deg)	Typical Strength Characteristics: tan ϕ	Typical Coefficient of Permeability (ft/min)	Range of CBR Values	Range of Subgrade Modulus k_s (lb/in.^{3})
GW	Well-graded clean gravels, gravel–sand mixtures	125–135	11–8	0.3	0.6	0	0	>38	>0.79	5×10^{-2x}	40–80	300–500
GP	Poorly graded clean gravels, gravel–sand mix	115–125	14–11	0.4	0.9	0	0	>37	>0.74	10^{-1}	30–60	250–400
GM	Silty gravels, poorly graded gravel–sand silt	120–135	12–8	0.5	1.1	–	–	>34	>0.67	$>10^{-6}$	20–60	100–400
GC	Clayey gravels, poorly graded gravel-sand–clay	115–130	14–9	0.7	1.6	–	–	>31	>0.60	$>10^{-7}$	20–40	100–300
SW	Well-graded clean sands, gravelly sands	110–130	18–9	0.6	1.2	0	0	38	0.79	$>10^{-3}$	20–40	200–300
SP	Poorly-graded clean sands, sand–gravel mix	100–120	21–12	0.8	1.4	0	0	37	0.74	$>10^{-3}$	10–40	200–300
SM	Silty sands, poorly graded sand–silt mix	110–125	16–11	0.8	1.6	1050	420	34	0.67	5×10^{-5}	10–40	100–300
SM-SC	Sand–silt clay mix with slightly plastic fines	110–130	15–11	0.8	1.4	1050	300	33	0.66	2×10^{-6}	–	

Figure A.3. Typical Properties of Compacted Soils (Hunt, 2005).

Typical Engineering Properties of Residual Soils of Basalt and Gneiss

Parent Rock	Zone	Location	*N* Value (SPT)	LL	PI	*e*	ϕ (deg)	*c* (kg/cm^2)	Ref.[a]
Granite gneiss	Upper	Georgia	10–25	30–50	9–25	0.7–0.8			(*a*)
Granite gneiss	Intermediate	Georgia	5–10	20–40	0–5	0.8–1.2			
Granite gneiss	Saprolite	Georgia	17–70			0.8–0.4			
Gneiss		Brazil (coastal mountains)		20–70	0–35	1.4–1.0	25–31	0.4–0.6	(*b*)
Basalt (porous clays)	Upper	Brazil		35–75	15–40	1.1–1.0	27–31	0.1–0.2	
Gneiss[b,c]	Upper	Rio de Janeiro	5–10						(*c*)
Gneiss[b,c]	Intermediate	Rio de Janeiro	10–30	20–55	5–25	2.3–0.8	23–43	0–0.4	
Gneiss[b,c]	Saprolite	Rio de Janeiro	30–50				23–38	0.2–0.5	
Gneiss	Upper	São Paulo	8–28	50–70	30–35				(*d*)
Gneiss	Intermediate	São Paulo	7–10	40–50	30–20				
Gneiss	Saprolite	São Paulo	10–30	48–50	20–25				
Basalt	Upper	Parana, Brazil		53–60	26–18				
Basalt	Intermediate	Parana, Brazil		65–45	17–10		24–31	0.1–0.7	

[a] References: (*a*) Sowers (1954); (*b*) Vargas (1974); (*c*) data courtesy of Tecnosolo S.A.; (*d*) Medina (1970).

[b] Strength tests performed at natural moisture; not necessarily saturated.

[c] Natural density range: 1.6–1.8 g/cm^3: saturated, 1.8–2.0 g/cm^3.

Figure A.4. Engineering Properties of Residual Soils of Basalt and Gneiss (Hunt, 2005).

Identification Properties of the Tertiary Formations in the Los Angeles Area[a]

Material Activity	Description	Dry Unit Weight (pcf)	Natural Water Content (%)	Liquid Limit	Plastic Index	Plastic Limit	% Smaller Than 0.002 mm	% Smaller Than 200 Sieve	Activity
Weathered clayey Modelo	Stiff brown and gray silty clay thin bedded with some light-gray fine sand	89.8	28.7	66	31	35	34	85	0.91
Unweathered clayey Modelo	Hard, dark-gray silty clay thin bedded with some light gray fine sand	98.2	23.3	69	37	32	31	84	1.19
Sandy Modelo	Compact, light gray and tan, fine to medium sand, some silt, occasional seams	110.4	16.5	NP	—	NP	6	26	—
Weathered clayey Martinez	Soft to medium stiff, brown clayey silt and silty clay	103.6	22.1	62	38	24	30	73	1.26
Weathered sandy Martinez	Medium compact, rust brown and yellow silty fine to medium sand	108.2	17.6	NP	—	NP	14	42	—
Unweathered sandy Martinez	Very compact, gray-green clayey fine lo medium sand with calcareous concretions	120.7	12.8	NP	—	NP	16	38	—
Unweathered clayey Martinez	Hard, dark gray-green clay with some pockets of gray medium to fine sand, occasional shale fragments	105.6	19.2	68	40	28	30	80	1.33

[a] From Gould, T.P., *Proceedings of ASCE, Research Conference on Shear Strength of Cohesive Soils*, Boulder, CO, June 1960. With permission.

Figure A.5. Engineering Properties of Soils in the Los Angeles Area (Hunt, 2005).

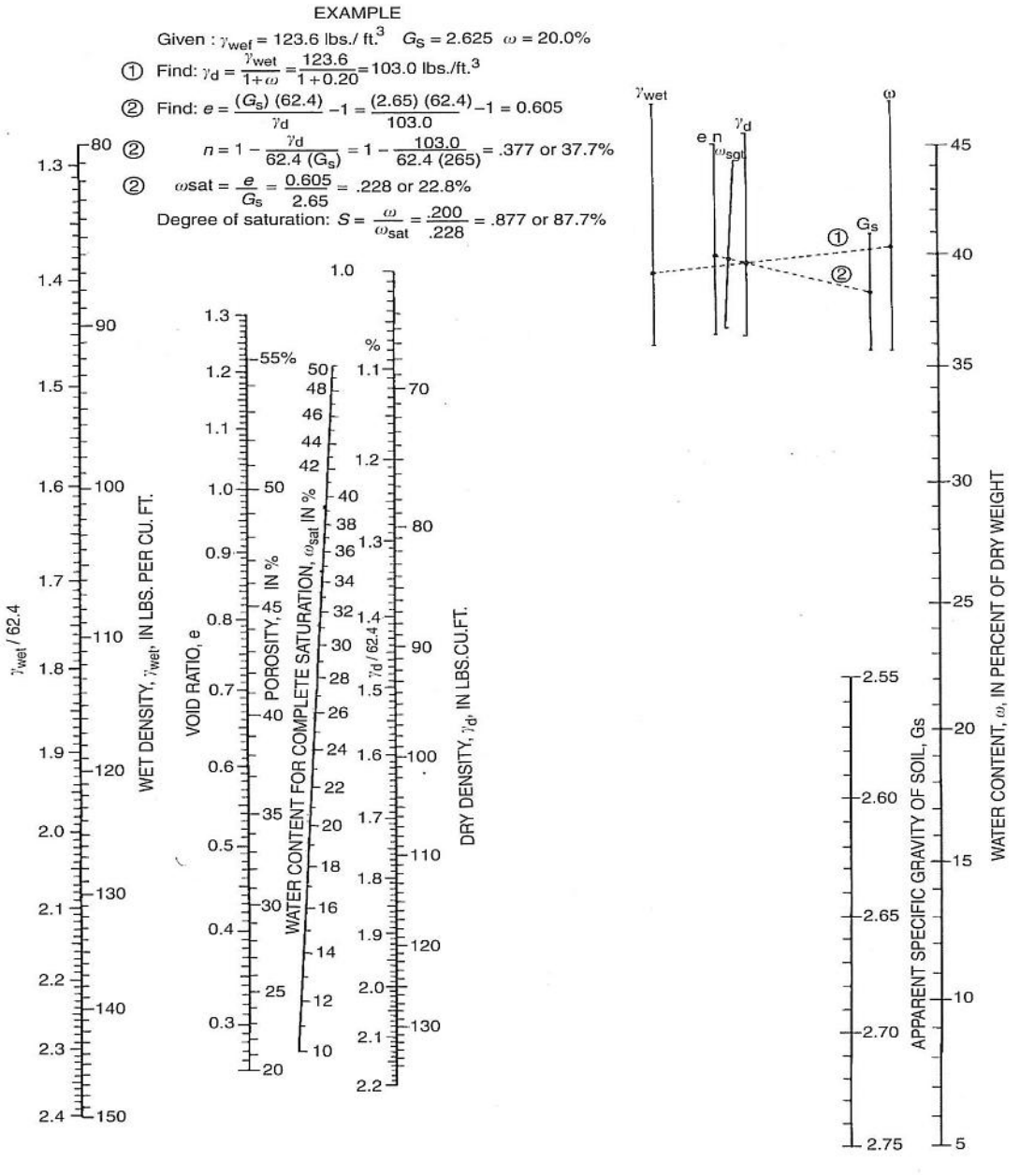

Figure A.6. Nomograph to Determine Basic Soil Properties Developed by the USBR, Earth Manual, Bureau of Reclamation, Denver, CO, 1974 (Hunt, 2005).

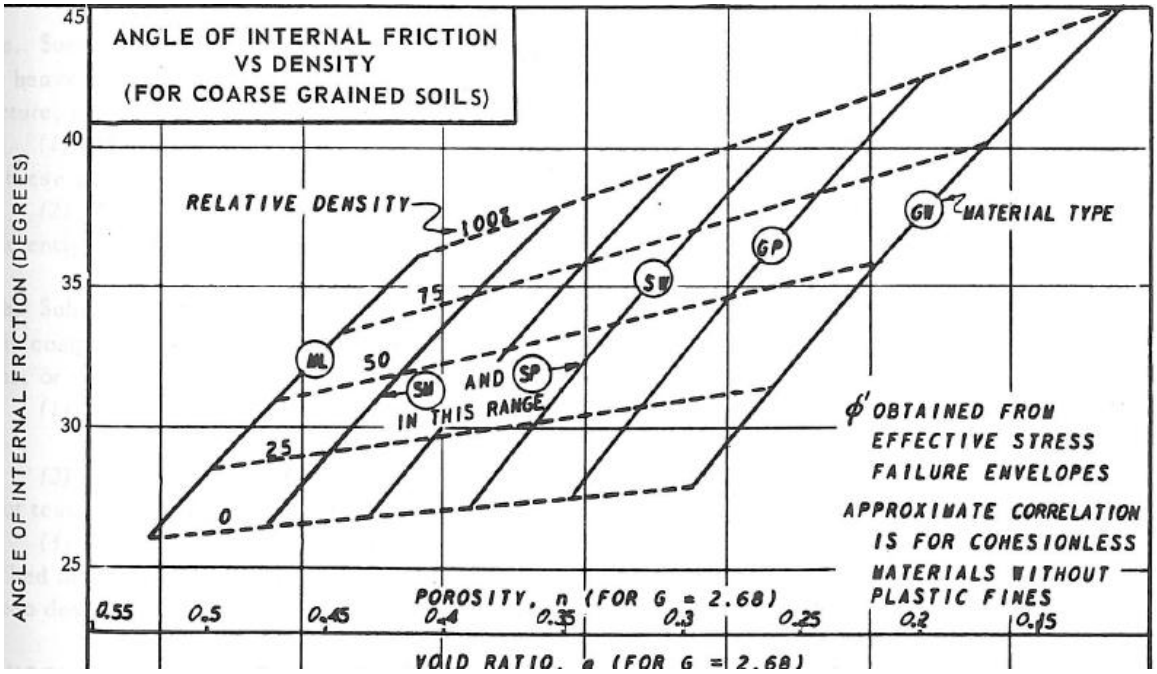

Figure A.7. Angle of Internal Friction and Density for Coarse Grained Soils (NAVFAC DM7, 1971)

REFERENCES

American Geological Society. (2000). Sacramento River Water Treatment Plant Proposed Intake Structure and Pipelines. Final Report. Geotechnical Study. Prepared for CH2M Hill. Sacramento, CA.

Amiantit Pipe Systems and Amitech USA. (2005). Polymer Concrete Pipe Product Guide. Zachary, LA.

Archard, J.F. (1957). Elastic Deformation and The Laws of Friction. *Proceedings of the Royal Society of London, Series A, Mathematical and Physical Science*. Vol 243. Issue 1233. pp. 190-205.

Atkinson, J.H, and Potts, D.M. (1977). Subsidence Above Shallow Tunnels in Soft Ground. *Journal of Geotechnical Engineering*. ASCE. Vol. 103. GT4, pp. 203-215.

ATV Working Sheet A 161E. (1990). Structural Calculation of Driven Pipes (01.1991) (Identical with DVGW Working Sheet GW312: Statische Berechnung von Vortriebsrohren (01.1990)).

Auld, F.A. (1982). Determination of pipe jacking loads. *Proceedings of the Pipe Jacking Association*. Manchester.

Bennett, R. D. (1998). Jacking Forces and Ground Deformations Associated with Microtunneling. Dissertation in Partial Fulfillment of the Requirements for the Degree of Doctor of Philosophy in Civil Engineering. University of Illinois at Urbana-Champaign, Illinois.

Brown and Caldwell. (1993). Plans and Specifications for the Newark Subbasin Lower Level Relief Interceptor Sewer Project. Newark, California.

Brumund, W.F., and Leonards, G.A. (1973). Experimental Study of Static and Dynamic Friction Between Sand and Typical Construction Materials. Journal of Testing and Evaluation. JTEVA. Vol. 1. No.2. pp. 162-165.

Calderwood, Kevin. (2002). Plans and Specifications for the Construction of the Alvarado Boulevard Trunk Sewer Project, Phase 1. Brown and Caldwell, Walnut Creek, CA.

Calderwood, Kevin. (2004). Plans and Specifications for the Construction of the Alvarado Boulevard Trunk Sewer Project, Phase 2. Brown and Caldwell, Walnut Creek, CA.

CH2M Hill. (2000). Plans and Specifications for the Sacramento River Raw Water Treatment Plant Replacement Intake Project. Sacramento and Redding, CA.

CH2M Hill. (2001). Geotechnical Baseline Report – March 2001, Supplemental Geotechnical Data Report-- October 1999, and Geotechnical Data Report—May 1998 for the Clearview Water Supply Project. Prepared for the Clearview Group. Bellevue, WA.

Chapman, D.N., and Ichioka, Y. (1999). Prediction of Jacking Forces for Microtunneling Operations. Trenchless Technology Research. Vol. 14. No. 1. International Society of Trenchless Technology. pp. 31-41.

Dove, J.E., and Frost, J.D. (1999). Peak Friction Behavior of Smooth Geomembrane-Particle Interfaces. *Journal of Geotechnical and Geoenvironmental Engineering.* ASCE. Vol.125. No. 7, pp. 544-555.

Ebert, I. (1990). Erfassung und Berechnung der Vortriebswiderstände unter Beachtung der Speziellen Bedingungen des Stahlbetonvortriebs. Dissertation. TH liepzig.

Frost, J.D., and Park, J.-Y. (2003). A Critical Assessment of the Moist Tamping Technique. *Geotechnical Testing Journal*, ASTM. Vol.26. No.1. pp. 57-70.

Hasan, M. (1996). Abschätzung der Eindring—und Reibungswiderstände beim unterirdischen Rohrvortrieb. Dissertation. IGBE. Universität Hannover.

Helm, H. (1964). Bau eines Abwasserdükers unter dem Neckar und dem Schifffahrtskanal in Heidelberg. Straßen- und Tiefbau. Issue 2.

Herrenknecht (2006). www.herrenknecht.com. April, 2006.

Herzog, M. (1985). Die Pressenkräfte bei Schildvortreib und Rohrvorpressungen im Lockergestein. BMT.

Hobas USA. (2005). Large Diameter Centrifugally Cast Fiberglass Reinforced Polymer Mortar Pipe Product Brochure. Revision 10. Houston, TX. June, 2005.

Hunt, Roy E. (2005). Geotechnical Engineering Investigation Handbook. 2nd Edition, Taylor and Francis, Boca Raton, Florida.

HWA, Hong West and Associates. (2000). Geotechnical Report Eastside Interceptor Section 1, Capacity Restoration Project. HWA Project NO. 98148. Prepared for Tetra Tech/KCM, Inc. Renton, WA.

International Society for Trenchless Technology. (1994). Working Group No. 3. Microtunneling Jacking Forces. Report from the Working Group No. 3 (Microtunneling). Presented to ISTT, May 1994.

Jacobsz, S.W., Standing J.R. and Mair,R.J. (2004). Tunneling Effects on Pile Groups in Sand. Proceedings of the International Conference on Advances in Geotechnical Engineering. The Skempton Conference. Jardine, R.J., Potts D.M. and Higgins K.G. (Eds). Thomas Telford. London. pp1056-1067.

Marshall, Mark. (1998). Pipe-Jacked Tunneling: Jacking Loads and Ground Movements. Thesis submitted for the Degree of Doctor of Philosophy. Magdalen College. University of Oxford. Trinity Term.

Mathy, D, Gelinas, M, and Nielson, D. (2002). Geotechnical Engineering Investigation Report, Alvarado Boulevard Trunk Sewer Project, Phase 1. DCM/Joyal Engineering, Inc. Walnut Creek, CA.

Mathy, D, Gelinas, M, and Nielson, D. (2004). Geotechnical Engineering Investigation Report, Alvarado Boulevard Trunk Sewer Project, Phase 2. DCM/Joyal Engineering, Inc. Walnut Creek, CA.

Milligan, G. W. and Norris, P. (1999) Pipe-Soil Interaction During Pipe Jacking. Proceedings of the Institution of Civil Engineers. Geotechnical Engineering. January, 1999. Vol. 137. pp 27-44.

Montgomery Watson. (2000). Plans and Specifications for the Alderwood Water District for the Clearview Group. Clearview Snohomish River Crossing. February, 2000. Bellevue, WA.

NAVFAC DM-7. (1971). Soil Mechanics, Foundations, and Earth Structures, Naval Facilities Engineering Command Publications Transmittal. January, 1971.

Norris, Paul. (1992). The Behavior of Jacked Concrete Pipes during site Installation. Thesis Submitted for the Degree of Doctor of Philosophy. Pembrook College. University of Oxford. Trinity Term.

Norris, P. and Milligan, G. (1991). Field Instrumentation for Monitoring the Performance of Jacked Concrete Pipes. Field Measurements in Geotechnics. Norwegian Geotechnical Institute. Oslo, Norway. Sorum (Ed.). Balkema. Rotterdam. Volume 1.

National Clay Pipe Institute. (1998). Engineering Manual. Modified April 1, 1998.

Ontario Concrete Pipe Association. (2004). Concrete Pipe Materials. www.ocpa.com, February, 2006.

Osumi, Toru. (2000), Calculating Jacking Forces for Pipe Jacking Methods. No-Dig International Research. October, 2000. pp. 40-42.

Paul, O. Versagen eines Widerlagers bei der Durchörterung eines Bahndammes. Bauplanung-Bautechnik. Volume 28.

Potyondy, J. G. (1961). Skin Friction Between Various Soils and Construction Materials. Geotechnique. Vol. 11. pp. 339-355.

Radhakrishnan, V. (1970). Effect of Stylus Radius on the Roughness Values Measured with Tracing Stylus Instruments. Wear. Volume 16. pp 325-335.

Rinker. (2006). www.rinker.com/hydroconduit. Concrete Pipe Manual. Microtunneling and Jacking Pipe. pp. 36-43.

Salomo, K.P. (1979). Experimentelle und theoretische Bestimmung der Pressenkräfte und der Bodenverformun beim Vortrieb eines Vortriebsrohres in rolligen Böden. Dissertation. TU Berlin. Berlin.

Scherle, M. (1977). Rohrvotrieb- Part 2. Bauverlag. Wiesbaden/Berlin.

Stein, Dietrich. (2005) Trenchless Technology for Installation of Cables and Pipelines. Stein and Partner. Arnsberg, Germany.

Stein, D, Möllers, K, and Bielecki, R. (1989). Microtunneling-- Installation and Renewal of Nonman-Size Supply and Sewage Lines by the Trenchless Construction Method. Ernst & Sohn. Berlin.

Szentandrasi, K. (1981). Vorpresswiderstände und Vorpresskräfte sowie deren Beeinflussung durch Stütz- und Gleitmittel. Lecture at the Technische Akademie Wuppertal, July, 1981.

Terzaghi, Karl. (1943). Theoretical Soil Mechanics. Wiley and Sons. New York, New York.

Uesugi, M. and Kishida, H. (1986)-a. Frictional Resistance at Yield Between Dry Sand and Mild Steel. Soils and Foundations. Vol. 26. No. 4. pp. 139-149.

Uesugi, M. and Kishida, H. (1986)-b. Influential Factors of Friction Between Steel and Dry Sands", Soils and Foundations. Vol. 26. No. 2. pp.33-46.

Walensky, G., and Möcke, H. (1970). Erfahrungen mit Horizongal-Pressbohrverfahren. Bauplanung- Bautechnik. Issue 6.

Ward, H.C. (1999). Rough Surfaces. Thomas, T.R. Ed., Longman, London. pp.278.

Weber, W. (1981). Experimentelle Untersuchungen in rolligen Böden zur Dimensionierung von Preβbohranlagen. Dissertation. Wissenschaftlicher Bericht aus der Arbeit des Institutes für Baumaschinen und Baubetrieb der Rheinisch-Westfälisch Technischen Hochschule Aachen. RWTH Aachen.

Weber, W., and Hurtz, G. (1981). Ermittlung der Rohrreibung und Entwicklung eines Bohrgerätes. TIS (1981). Issue 8.

Zettler, T.E. (1999) Operational Induced Changes in Geomembrane Surface Topography. M.S. Theses, School of Civil and Environmental Engineering. Georgia Institute of Technology. Atlanta, Georgia.

Zhou, J.Q. (1998). Numerical Analysis and Laboratory Test of Concrete Jacking Pipes. Thesis submitted for the Degree of Doctor of Philosophy. Linacre College. University of Oxford. Trinity Term.